



**This electronic thesis or dissertation has been
downloaded from Explore Bristol Research,
<http://research-information.bristol.ac.uk>**

Author:

Pradeilles, Johan

Title:

Boron-Assisted Synthesis of Conformationally Controlled Hydrocarbons

General rights

Access to the thesis is subject to the Creative Commons Attribution - NonCommercial-No Derivatives 4.0 International Public License. A copy of this may be found at <https://creativecommons.org/licenses/by-nc-nd/4.0/legalcode>. This license sets out your rights and the restrictions that apply to your access to the thesis so it is important you read this before proceeding.

Take down policy

Some pages of this thesis may have been removed for copyright restrictions prior to having it been deposited in Explore Bristol Research. However, if you have discovered material within the thesis that you consider to be unlawful e.g. breaches of copyright (either yours or that of a third party) or any other law, including but not limited to those relating to patent, trademark, confidentiality, data protection, obscenity, defamation, libel, then please contact collections-metadata@bristol.ac.uk and include the following information in your message:

- Your contact details
- Bibliographic details for the item, including a URL
- An outline nature of the complaint

Your claim will be investigated and, where appropriate, the item in question will be removed from public view as soon as possible.



University of
BRISTOL

Boron-Assisted Synthesis of Conformationally Controlled Hydrocarbons

Johan A. Pradeilles

Supervisor: Prof. Varinder K. Aggarwal, FRS

A dissertation submitted to the University of Bristol in accordance with the requirements for award of the degree of Doctor of Philosophy in the Faculty of Science.

University of Bristol, School of Chemistry

March 2019

Word count: 64680

ABSTRACT

This thesis is composed of two chapters reporting contributions to two different projects.

The first chapter presents a research project aiming to develop a new class of helical molecules which, upon activation from an external stimulus, would be able to reversibly switch from one screw-sense to the other. All-*syn* methyl-substituted hydrocarbons, as described by Aggarwal¹ in 2014, were shown to adopt helical conformations with very high levels of control. More importantly, one of these unique molecules could access either the *M* or the *P* screw-sense, depending on its physical state. Therefore, all-*syn* methyl-substituted hydrocarbons seemed to be promising candidates for the design of a new class of molecular switches. A diamond lattice-based analysis revealed that the number of *syn*-pentane and *gauche* interactions in the chain was one of the key parameters that dictated its conformational preference. A series of six compounds of different chain lengths was designed and synthesised using an efficient bidirectional iterative homologation of *C*₂-symmetric boronic esters. A QM/NMR approach was employed to quantitatively describe the conformational landscape of these molecules and confirmed the diamond lattice-based model with a good degree of confidence. A screening of different substituents at the termini revealed that alkyne, hydroxyl, amino or aromatic groups could be considered as ‘small’ groups, favouring the helical conformer with both terminal dihedral angles in a *gauche* conformation. However, the combined effects of two *tert*-butyl groups might force both terminal dihedral angles to adopt an antiperiplanar conformation, thus favouring the opposite screw-sense. These findings set the experimental basis to design a new molecular switch.

The first part of the second chapter describes the development of a new decarboxylative borylation methodology² and its application to the synthesis of α -amino boronic esters. Some medicinal chemistry-type examples and three additional natural products have been added to the substrate scope. Key mechanistic experiments were conducted to prove the radical pathway and provide support for an outer sphere radical trapping process. In the second part, a study on the decarboxylative borylation of amino acids was conducted. First, the reaction conditions were optimised on a proline derivative. With these new conditions in hand, other activated amino acids were tested. However, most of them did not afford the desired products. To identify the cause of failure, a number of parameters were investigated (the effects of free N–H bonds, redox potentials and protecting groups). A different mode of activation involving the use of hypervalent iodine derivatives was attempted but failed to provide the desired products. Finally, a limited substrate scope composed of proline derivatives was subjected to the reaction conditions. Unfortunately, none of these examples gave the desired product.

ACKNOWLEDGEMENTS

First, I wish to express my deepest gratitude to my supervisor, Professor Varinder K. Aggarwal. His unfailing support over my entire Ph.D. has made me more confident, both in the lab and as a person. These four years in his research group have been an extraordinary experience. I have learned a lot and met amazing scientists.

Secondly, I would like to thank Dr. Eddie L. Myers for his wise patience and invaluable advice. My Ph.D. would not have been the same without his guidance and suggestions. I am indebted to his enthusiasm and support.

My sincere acknowledgements also go to Dr. Siying Zhong. I have been very lucky to share a research project with such a great chemist and friend. I have been amazed by the amount and the diversity of work that she was able to carry out. I am sure that she will have a brilliant career.

During the course of my Ph.D., I have met amazing friends who made my life in the lab such an enjoyable experience. In particular, I wish to thank Joseph Batemen (my brother-in-chemistry), Dr. Teerawut Bootwicha (who taught me how to perform assembly-line synthesis and how to cook Pad-Thai), Lorenz Löffler (The Prince of Denmark), Dr. Damien Mailhol (¡ gracias hombre !), Dr. Alba Millán Delgado, Dr. Ana Varela, Dr. Cristina García Ruiz, Dr. Daniel Pflästerer, Dr. Giorgia Casoni, Dr. Murat Kucukdisli, Dr. Nandakumar Meganathan, Dr. Olivier Wagnières and the many others who I have failed to mention here. Special thanks to Dr. Alexander Fawcett who trusted me and gave me the opportunity to work on an exciting project.

I am deeply grateful to all the people who helped me by proofreading this thesis: Dr. Adam Noble, Dr. Andreas Lerchen, Dr. Beatrice Lefanu Collins, Dr. Belén Rubial, Charlotte Gregson, Dr. Daniel Kaiser, Dr. Durga Prasad Hari, Dr. Felix Pape, James Fordham, Lydia Dewis, Dr. Mattia Silvi, Dr. Nils Winter, Oliver Dutton, Pradip Songara, Dr. Raffael Schrof, Riccardo Mega, Rory Cameron Mykura, Sheenagh Aiken, Steven Bennett and Dr. Valerio Fasano.

I also owe my deepest gratitude to Laura, Morgane, Julie P., Julie M. and Benjamin who have always been present despite the distance.

Finally, my warmest thank goes to my family. I am eternally indebted for your help and support, and everything you do. Thomas, nothing would have been possible without you.

AUTHOR'S DECLARATION

I declare that the work in this dissertation was carried out in accordance with the requirements of the University's *Regulations and Code of Practice for Research Degree Programmes* and that it has not been submitted for any other academic award. Except where indicated by specific reference in the text, the work is the candidate's own work. Work done in collaboration with, or with the assistance of, others, is indicated as such. Any views expressed in the dissertation are those of the author.

SIGNED: DATE:

ACRONYMS AND ABBREVIATIONS

4-AcPy	4-acetylpyridine
4-MeOPy	4-methoxypyridine
4-MePy	4-methylpyridine
4-NCPy	4-cyanopyridine
4- <i>tert</i> -BuPy	4- <i>tert</i> -butylpyridine
9-BBN-H	9-borabicyclo[3.3.1]nonane
Ac	acetyl
acac	acetylacetonate
<i>app.</i>	apparent
aq.	aqueous
Ar	aryl
b.p.	boiling point
B3LYP	Becke exchange with Lee-Yang-Parr correlation
B3LYP-D2	B3LYP with Grimme's D2 dispersion correction
Bn	benzyl
Boc	<i>tert</i> -butoxycarbonyl
br.	broad
Bu	butyl
cat	catecholato
cat.	catalytic amount
Cb	diisopropylcarbamoyl
Cbz	benzyloxycarbonyl
CD	circular dichroism
COSY	homonuclear correlation spectroscopy
CPBA	chloroperbenzoic acid
Cy	cyclohexyl
d	doublet
<i>d.r.</i>	diastereoisomeric ratio
DABCO	1,4-diazabicyclo[2.2.2]octane
dba	dibenzylideneacetone
DCC	dicyclohexylcarbodiimide
DFT	density functional theory
DIAD	diisopropyl azadicarboxylate
DIC	diisopropylcarbodiimide
DIPEA	<i>N,N</i> -diisopropylethylamine
DMAc	<i>N,N</i> -dimethylacetamide
DMAP	<i>N,N</i> -dimethylaminopyridine
DMF	<i>N,N</i> -dimethylformamide
DMI	1,3-dimethyl-2-imidazolidinone
DMPU	<i>N,N'</i> -dimethylpropyleneurea
DMSO	dimethylsulfoxide
DMTrocCl	1,1,1-trichloro-2-methylpropan-2-yl carbonochloridate
DTBM-SEGPPOS	1,1'-[4,4'-bi-1,3-benzodioxole]-5,5'-diylbis[1,1-bis[3,5-bis(1,1-dimethylethyl)-4-methoxyphenyl]phosphine
<i>e.r.</i>	enantiomeric ratio
EDA	electron donor-acceptor
EI	electron ionisation
equiv.	equivalent(s)
ESI	electrospray ionisation
Et	ethyl
<i>et al.</i>	<i>et alia</i>
FID	flame ionisation detector

FT	Fourier transform
<i>g</i>	<i>gauche</i>
GC	gas chromatography
GP	general procedure
hept	heptet
HMBC	heteronuclear multiple-bond correlation spectroscopy
HMDS	hexamethyldisilazane
HPLC	high performance liquid chromatography
HRMS	high resolution mass spectroscopy
HSQC	heteronuclear single-quantum correlation spectroscopy
<i>i-</i>	iso
<i>i.e.</i>	<i>id est</i>
IEFPCM	integral equation formalism polarisable continuum model
IR	infrared
IUPAC	International Union of Pure and Applied Chemistry
L	ligand
LDA	lithium diisopropylamide
LED	light-emitting diode
LG	leaving group
m	multiplet
<i>M</i>	left-handed
<i>m-</i>	<i>meta-</i>
m.p.	melting point
MAD	mean absolute deviation
MALDI	matrix-assisted laser desorption/ionisation
Me	methyl
MM	molecular mechanics
MMFF	Merck molecular force field
MS	mass spectroscopy
<i>n-</i>	<i>normal-</i>
nbd	2,5-norbornadiene
NBS	<i>N</i> -bromosuccinimide
NHPI	<i>N</i> -hydroxyphthalimide
NMR	nuclear magnetic resonance
NOE	nuclear Overhauser effect
Nu	nucleophile
<i>P</i>	right-handed
<i>p-</i>	<i>para-</i>
pent	pentet
pin	pinacolato
Piv	pivaloyl
PMP	<i>para</i> -methoxyphenyl
Pr	propyl
q	quartet
QM	quantum mechanics
quant.	quantitative
QUINAP	1-(2-diphenylphosphino-1-naphthyl)isoquinoline
r.t.	room temperature
s	singlet
<i>s-</i>	<i>sec-</i>
SAR	structure–activity relationship
SCE	saturated calomel electrode
SET	single-electron transfer
sext	sextet
SFC	supercritical fluid chromatography

sp	sparteine
StDev	standard deviation
t	triplet
<i>t</i>	<i>trans</i>
TBAF	terabutylammonium fluoride
TBS	<i>tertio</i> -butyldimethylsilyl
<i>tert</i> -	<i>tertio</i> -
THF	tetrahydrofuran
TIB	2,4,6-triisopropylbenzoyl
TIPS	triisopropylsilyl
TLC	thin layer chromatography
TMS	trimethylsilyl
TMU	tetramethylurea
Tol	tolyl
Tr	trityl
TSA	toluenesulfonic acid
UV	ultraviolet
v/v	volume per volume
VCD	vibrational circular dichroism
w/w	weight per weight
μ.w.	microwave

CONTENTS

CHAPTER 1 – TOWARDS THE SYNTHESIS OF NEW MOLECULAR SWITCHES..... 1

1.1. Introduction 1

1.1.1. Reactivity of organoboron compounds..... 1

1.1.2. Functionalisation of boronic esters 2

1.1.3. Homologation of boronic esters 5

1.1.4. Conformational analysis of flexible molecules 11

1.1.5. Definition and applications of molecular switches..... 14

1.1.6. Research proposal..... 18

1.2. Results and discussion 23

1.2.1. Synthesis of the first targets 23

1.2.2. Preliminary NMR analysis and Molecular Mechanics 30

1.2.3. Towards a new stereochemical model..... 33

1.2.4. Design of new targets 36

1.2.5. Synthesis and preliminary NMR results 37

1.2.6. Application of the QM/NMR approach 42

1.2.7. Vibrational Circular Dichroism analysis 47

1.2.8. Influence of the end-groups on the conformation..... 48

1.2.9. Towards a new helical switch..... 55

1.3. Conclusion..... 62

CHAPTER 2 – DECARBOXYLATIVE BORYLATION METHODOLOGY AND ITS APPLICATION TO α -AMINO BORONIC ESTERS 65

2.1. Introduction 65

2.1.1. Applications and synthesis of α -amino boronates..... 65

2.1.2. Development of a new decarboxylative borylation methodology 68

2.1.3. Other decarboxylative borylation methodologies..... 74

2.1.4. Research proposal..... 76

2.2. Results and discussion 77

2.2.1. Improvement of the substrate scope 77

2.2.2. Unsuccessful substrates 78

2.2.3. Optimisation study on cyclopropane derivatives 80

2.2.4. Further mechanistic investigations 81

2.2.5. Decarboxylative borylation of proline..... 82

2.2.6. Effect of N–H bonds..... 83

2.2.7. Effect of redox potentials 85

2.2.8. Optimisation study on activated glycine..... 87

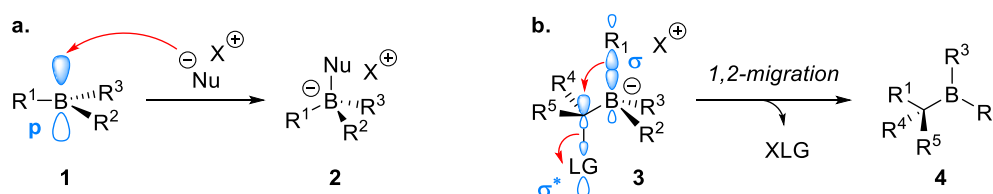
2.2.9. Hypervalent iodine derivatives	88
2.2.10. Limited substrate scope	92
2.3. Conclusion.....	93
 EXPERIMENTAL SECTION.....	 95
3.1. General experimental.....	95
3.1.1. Computation	95
3.1.2. Solvents and reagents	95
3.1.3. Chromatography and data analysis	96
3.1.4. Naming of compounds	97
3.1.5. Photoreactor.....	97
3.2. Supplementary materials – Chapter 1.....	98
3.2.1. General procedures	98
3.2.2. Experimental procedures and characterisation data.....	100
3.3. Supplementary materials – Chapter 2.....	165
3.3.1. General procedures	165
3.3.2. Experimental procedures and characterisation data.....	166
 REFERENCES.....	 205

CHAPTER 1 – TOWARDS THE SYNTHESIS OF NEW MOLECULAR SWITCHES

1.1. Introduction

1.1.1. Reactivity of organoboron compounds

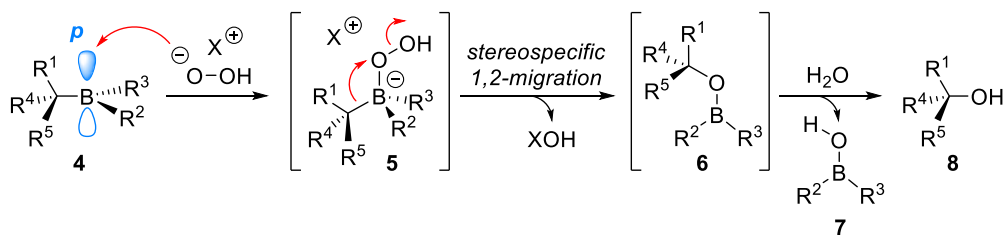
The history of asymmetric synthesis is indubitably linked to the development of organoboron chemistry. After the publication of the first example of enantioselective hydroboration of alkenes by Brown in 1961,³ a variety of methods have been explored to introduce boron atoms into organic molecules in a stereocontrolled manner.⁴ These efforts find their justification in that the boryl functional group can serve as a useful handle to further functionalise a molecule through stereospecific carbon–boron bond transformations.⁵ Most of these stereospecific reactions rely on the ability of organoborons to accept a nucleophilic electron pair into their boron-centred empty p-orbital to form boronate complexes⁶ (**Scheme 1a**).



Scheme 1. **a.** Boronate complex formation. **b.** Stereospecific 1,2-metallate rearrangement. Nu = nucleophile; LG = Leaving group.

If a leaving group is geminal to the negatively-charged boron atom, the boronate complex can undergo a 1,2-metallate rearrangement, which is defined as the 1,2-migration of a boron-bound substituent to the adjacent atom, with concomitant release of the leaving group (**Scheme 1b**). The migration only proceeds when the σ -orbital of the migrating group is aligned with the σ^* -orbital of the leaving group (*i.e.*, when the migrating and leaving groups adopt an antiperiplanar relationship).⁷ Such a concerted mechanism usually leads to the complete inversion of configuration at the α -boryl carbon centre, and retention of configuration of the migrating group.⁸

This mechanism is encountered in the hydrogen peroxide-mediated stereospecific oxidation of organoboron derivatives.⁹ Here, an organoboron species (**4**) reacts with a peroxide anion to form boronate complex **5**, which undergoes 1,2-metallate rearrangement to deliver the corresponding alcohol **8**, after hydrolysis of the boron–oxygen bond (**Scheme 2**). Through this concerted process, the chiral information is transferred from organoboron species **4** to alcohol **8** with the highest degree of fidelity.



Scheme 2. Hydrogen peroxide-mediated oxidation of organoboron compounds.

At its early stage, organoboron chemistry focussed mainly on organoboranes (**9**). These species, composed of a boron atom linked to three carbon atoms, are highly electrophilic and can react with a wide range of nucleophiles; however, such reactivity comes with disadvantages in terms of air and moisture sensitivity. In fact, boranes are generally unstable compounds, prone to oxidation and cannot be isolated by column chromatography. To circumvent this problem, new methodologies involving boronic esters such as **10** (*i.e.*, a boron atom bound to one carbon and two oxygen substituents) have been developed during recent decades. In particular, due to their higher stability, pinacol boronic esters (RBpin) have become the functional group of choice in modern organoboron chemistry.^{10,11} Indeed, π -donation from the lone pair of an oxygen atom into the empty p-orbital of the boron centre (**Chart 1**) reduces its electrophilic character with respect to boranes and renders pinacol boronic esters stable at room temperature, under air and compatible with silica gel purification.

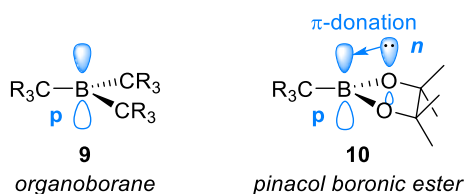
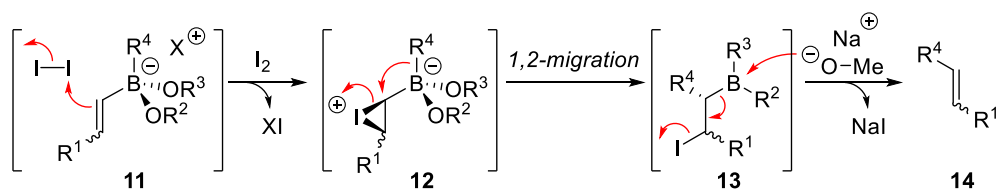


Chart 1. Boronic esters are less electrophilic than organoboranes due to π -donation from a lone-pair of one oxygen to the empty p-orbital on boron.

1.1.2. Functionalisation of boronic esters

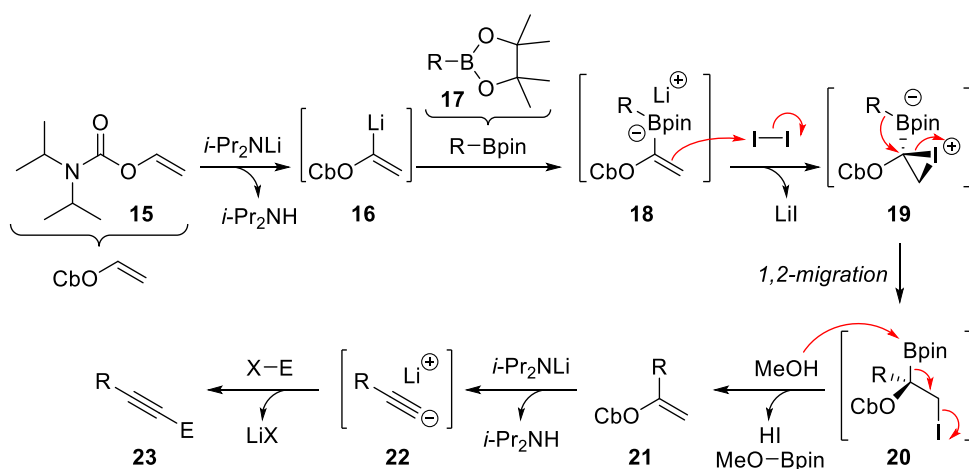
Although boronic esters are less electrophilic than boranes, they still exhibit the same type of reactivity towards nucleophiles. Not only can they easily be derivatised to their corresponding alcohols using basic peroxide, they also give access to other classes of molecules, such as alkene derivatives. Inspired by seminal work by Zweifel on organoboranes,¹² Matteson and Evans independently showed that boronic esters could successfully be converted to *E*- or *Z*-alkenes.^{13–16} In this transformation (**Scheme 3**), negatively-charged vinyl boronate complex **11** reacts with iodine to form iodonium intermediate **12**. Both charges are neutralised when the alkyl group attached to

boron migrates, with concomitant ring-opening of the iodonium moiety. The resulting β -iodoboronic ester **13** undergoes *anti*-elimination upon treatment with sodium methoxide to deliver the corresponding alkene **14**.



Scheme 3. Mechanism of Zweifel olefination using boronic esters as substrates.

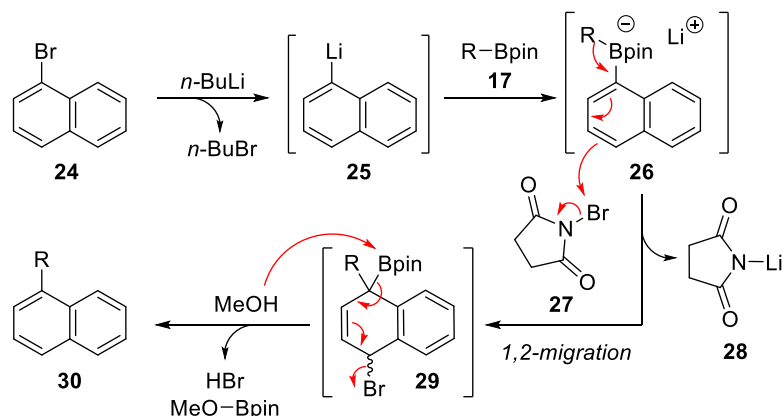
Recently, Aggarwal and co-workers developed a related methodology¹⁷ to synthesise alkyne derivatives from boronic esters (**Scheme 4**). They reacted boronic esters **17** with α -lithiated vinyl carbamate **16** to form vinyl boronate complex **18**. When treated with iodine and methanol, these species undergo a Zweifel olefination-type iodination/elimination sequence to give the corresponding 1,1-disubstituted alkene **21**. Addition of a base (*tert*-BuLi or LDA) leads to elimination of the leaving group and gives rise to alkyne anion **22**. These nucleophiles can be quenched by addition of electrophiles to give corresponding internal alkynes **23** or with water to obtain terminal alkynes.



Scheme 4. Mechanism of Aggarwal alkynylation.

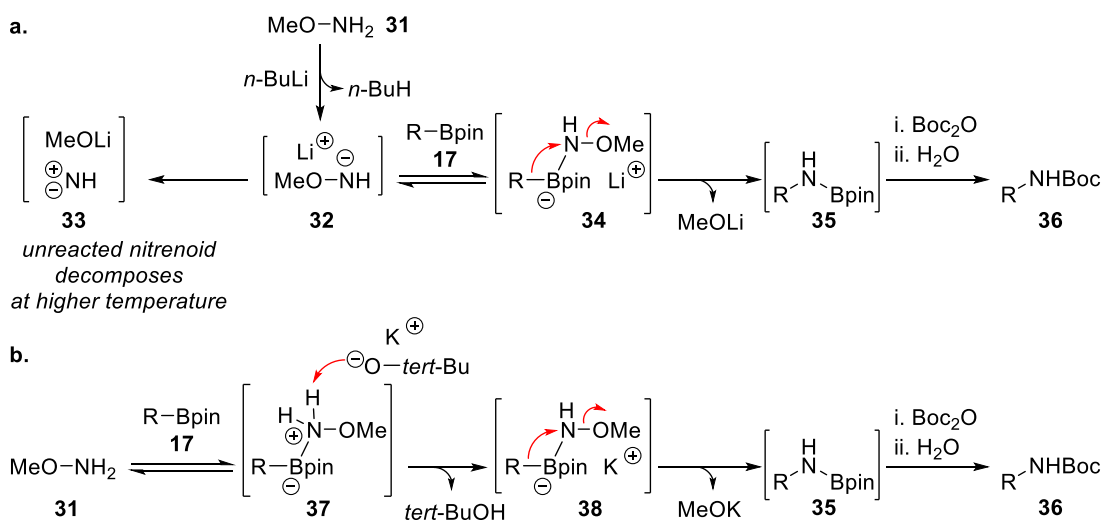
The concept of electrophile-triggered 1,2-metallate rearrangement observed in the Zweifel olefination has been extended to aryl boronate complexes by Aggarwal,^{18–26} who engaged lithiated (hetero)aryl derivatives and boronic esters in a successful enantiospecific sp^2 – sp^3 cross-coupling to obtain substituted (hetero)aryl compounds in good to excellent yields and perfect enantiospecificity. In the proposed mechanism, 1-naphthyl lithium **25** attacks boronic ester **17** to generate boronate complex **26**. Upon addition of *N*-bromosuccinimide **27**, the electron-rich aromatic group undergoes a bromination reaction with concomitant 1,2-migration of the alkyl substituent from

the boron centre to the aromatic moiety. A subsequent nucleophile-assisted elimination leads to the re-aromatisation of the system and delivers cross-coupling product **30** (**Scheme 5**).



Scheme 5. Mechanism of Aggarwal's transition metal-free cross-coupling.

Another example of useful derivatisation of boronic esters was proposed by Morken and co-workers in 2012,²⁷ who reported a stereospecific amination methodology. Specifically, boronic ester **17** is treated with methoxyamine-derived lithium nitrenoid **32** to form a boronate complex. Then, a stereospecific 1,2-metallate rearrangement occurs at 60 °C to give, after addition of Boc_2O , protected amine **36** (**Scheme 6a**). However, this methodology was limited to primary and secondary boronic esters. Presumably, in the case of more sterically-demanding tertiary boronic esters, lithiated methoxyamine **32** fails to efficiently bind the boron centre and undergoes decomposition to nitrene **33** upon heating.



Scheme 6. a. Morken stereospecific amination using first-generation conditions. **b.** Morken stereospecific amination using second-generation conditions.

The same research group reported alternative conditions²⁸ which involved mixing boronic ester **17**, methoxyamine **31** and potassium *tert*-butoxide in toluene at 80 °C. Under these conditions,

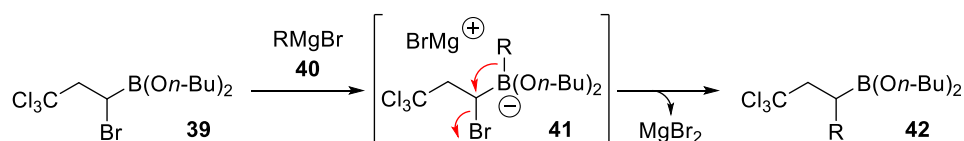
methoxyamine is deprotonated after coordination to the organoboron substrate (**Scheme 6b**). Hence, the formation of highly unstable nitrenoid is avoided and the desired product is formed in good yield with excellent enantiospecificity.

In all these previous examples (**Schemes 2–6**), the initial boronic ester moiety is not present in the final molecule (cleavage by hydrolysis or by nucleophile-triggered elimination). A different approach consists of utilising the boronic ester functional group to form new carbon–carbon bonds while maintaining the boryl moiety in the final product for further functionalisation. This process is commonly referred to as homologation of boronic esters.

1.1.3. Homologation of boronic esters

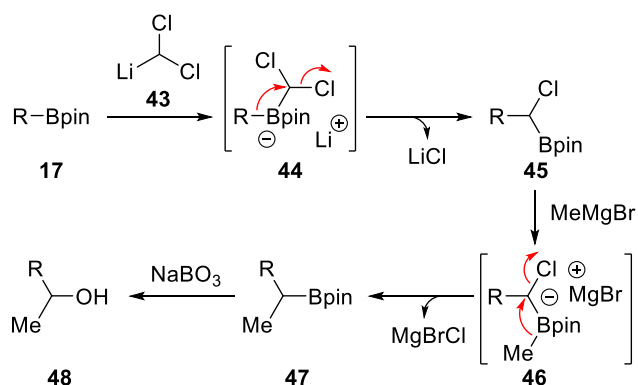
1.1.3.1. Seminal studies

In 1963, Matteson and co-workers reported an unusual nucleophilic substitution.²⁹ In this experiment (**Scheme 7**), they reacted α -bromoboronic ester **39** with different Grignard reagents (**40**), forming boronate complex (**41**) that rearranged upon warming to room temperature to displace the α -halogen and generate a new boronic ester (**42**).



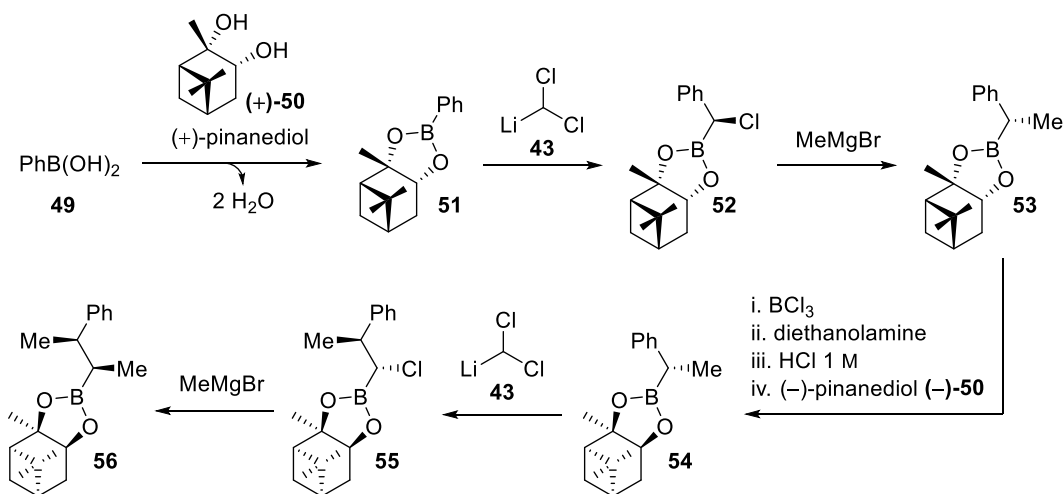
Scheme 7. Boron-assisted nucleophilic substitution reaction.

Twenty years later, drawing on this observation, Matteson developed a new methodology for carbon–carbon bond formation, involving sp^3 carbenoids such as **43**.³⁰ Due to their nucleophilicity, they can react with boronic esters at low temperature to form boronate complexes. As described above, these boronates can undergo stereospecific 1,2-migration, with concomitant displacement of the chloride leaving group.⁸ The product is an α -chloroboronic ester that can be further elaborated through addition of a Grignard reagent (**Scheme 8**). By treating boronic ester **17** with (dichloromethyl)lithium **43**, Matteson and co-workers could form boronate complex **44** that underwent 1,2-migration to give homologated α -chloroboronic ester **45**. Subsequently, another nucleophile could be added, forming a new boronate (**46**) that rearranged upon warming, displacing the second chloride. Finally, oxidation of the C–B bond revealed alcohol **48** in good yield.³¹



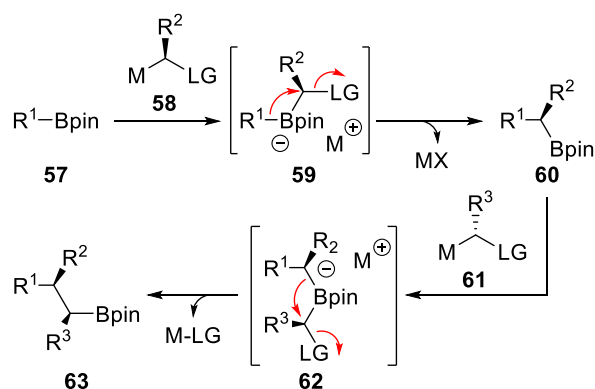
Scheme 8. First examples of homologation of boronic esters by Matteson.

Matteson also showed that this method can be rendered asymmetric by using chiral boronic esters such as **51** (**Scheme 9**), which allowed the formation of contiguous stereocentres with high levels of stereocontrol when performed iteratively.³² As this method operates under substrate control, there are associated drawbacks. The main drawback of this methodology appears when one wishes to create two stereocentres with opposite chirality: before the second homologation, a ligand-exchange sequence is necessary to remove the chiral diol ligand on the boronic ester and replace it with its opposite enantiomer.³³



Scheme 9. First example of substrate-controlled asymmetric homologation of boronic esters.

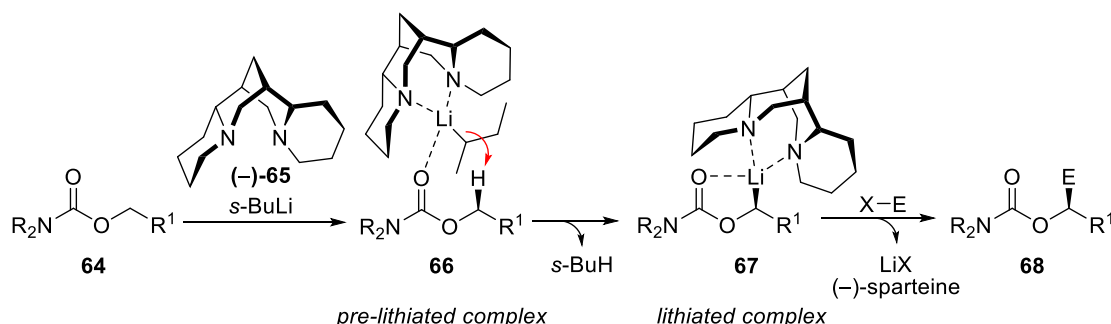
This problem can be overcome by employing a reagent-controlled approach, where the stereochemical information is transferred through the use of a chiral reagent (**Scheme 10**). A variety of methods can be used to generate chiral carbenoids, such as deprotonation of sulfonium salts^{34–36} or sulfoxide-metal exchange of α -sulfinyl chlorides.^{37,38}



Scheme 10. Example of homologation by reagent control. M = Metal; LG = Leaving group.

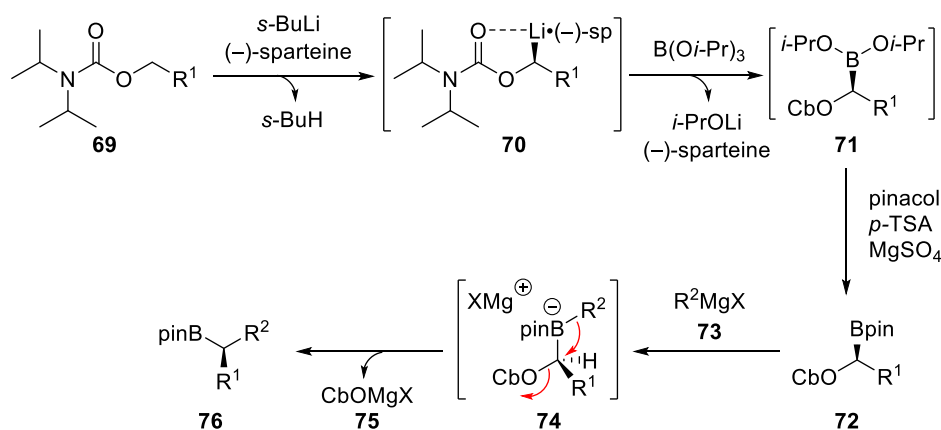
1.1.3.2. Sparteine-mediated asymmetric deprotonation

Selective deprotonation of *O*-alkyl carbamates **64** has been widely explored by Hoppe and co-workers.^{39–42} In the presence of (–)-sparteine, *s*-BuLi could generate enantioenriched α -lithiated carbamates (**67**), which were found to be chemically and configurationally stable at $-78\text{ }^{\circ}\text{C}$. These chiral organolithium compounds then react with electrophiles with retention of configuration⁴⁰ (**Scheme 11**).



Scheme 11. (–)-Sparteine-mediated asymmetric deprotonation of *O*-alkyl carbamates, followed by stereoretentive electrophilic trapping. Brackets have been omitted for clarity.

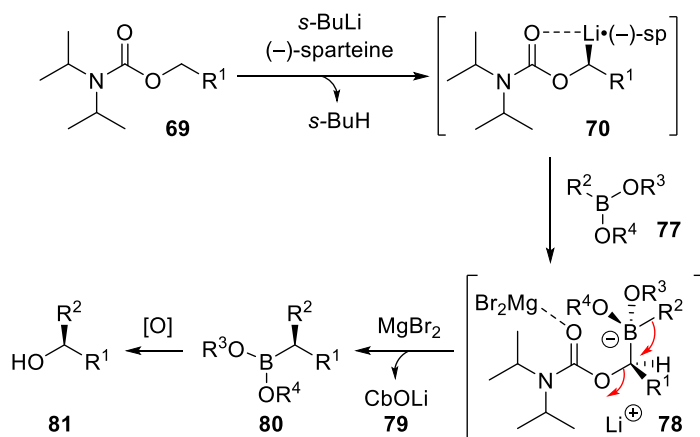
Later, Hoppe and co-workers described the electrophilic trapping of their lithiated carbamates **70** with triisopropyl borate to generate boronic ester intermediate **71**, which was transesterified with pinacol under acidic conditions.⁷ The resulting pinacol boronic ester **72** was then treated with a Grignard reagent (**73**) at low temperature to form boronate complex **74**. Upon warming to room temperature, the 1,2-metallate rearrangement took place to deliver homologated boronic ester **76** and released the carbamate moiety (**Scheme 12**). In this particular case, the carbamate plays two crucial roles: first, it acts as a directing group in the deprotonation step, forming a pre-lithiated species with *s*-BuLi, and then as a leaving group in the migration step.



Scheme 12. Asymmetric synthesis of boronic esters developed by Hoppe and co-workers.

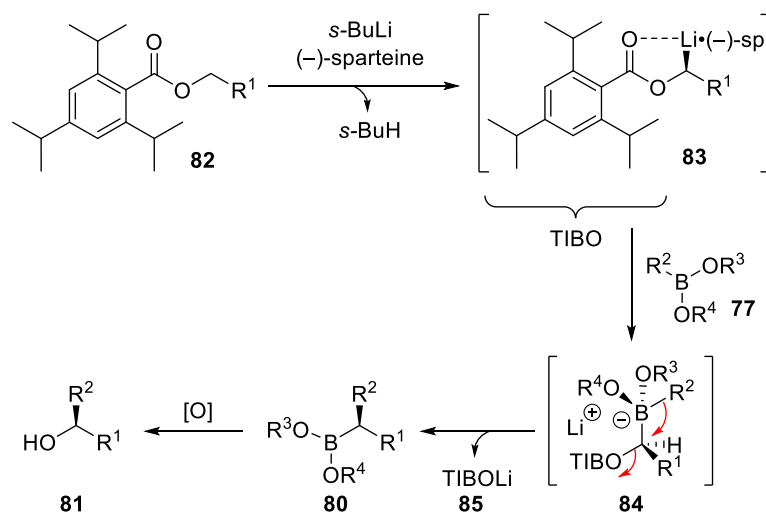
1.1.3.3. Homologations using α -lithiated carbamates or benzoates

In 2006, Kociensky and co-workers reported the first one-step homologation of a boronic ester, using Hoppe's lithiated carbamates in the synthesis of (*S*)-(-)-*N*-acetylcolchicol. ⁴³ More generally, this method was found to be an efficient way to access chiral secondary alcohols **81**, as proven by Aggarwal and co-workers shortly afterwards ⁴⁴ (**Scheme 13**).



Scheme 13. Synthesis of chiral secondary alcohols using Hoppe's lithiated carbamates.

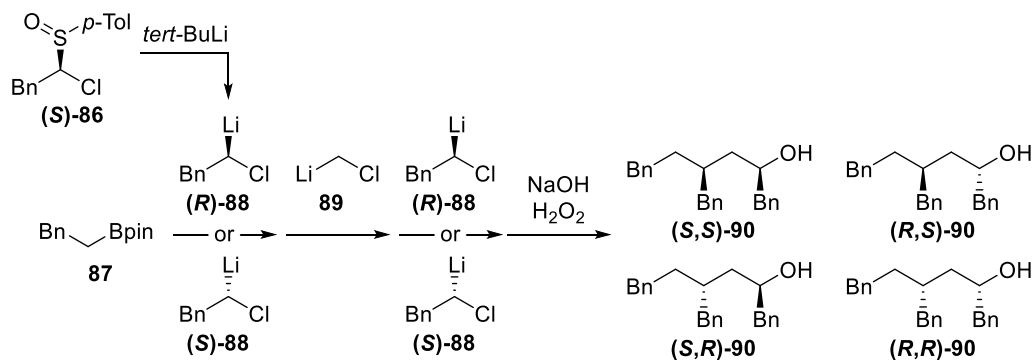
The presence of weak Lewis acids, such as MgBr_2 , can promote this 1,2-migration, and are sometimes added when this process is slow. ⁴⁵ Inspired by the work of Hammerschmidt, ⁴⁶ Aggarwal also showed that sparteine-mediated deprotonation of *O*-alkyl 2,4,6-triisopropylbenzoates (*O*-alkyl TIB) **82**, as described by Beak and co-workers, ⁴⁷ leads to suitable carbenoids **83** for the homologation of boronic esters. ⁴⁸ As the benzoate moiety is a better leaving group than the carbamate, no Lewis acid is needed to promote the 1,2-migration (**Scheme 14**).



Scheme 14. Synthesis of chiral secondary alcohols using Beak's lithiated benzoates.

1.1.3.4. Iterative homologation of boronic esters

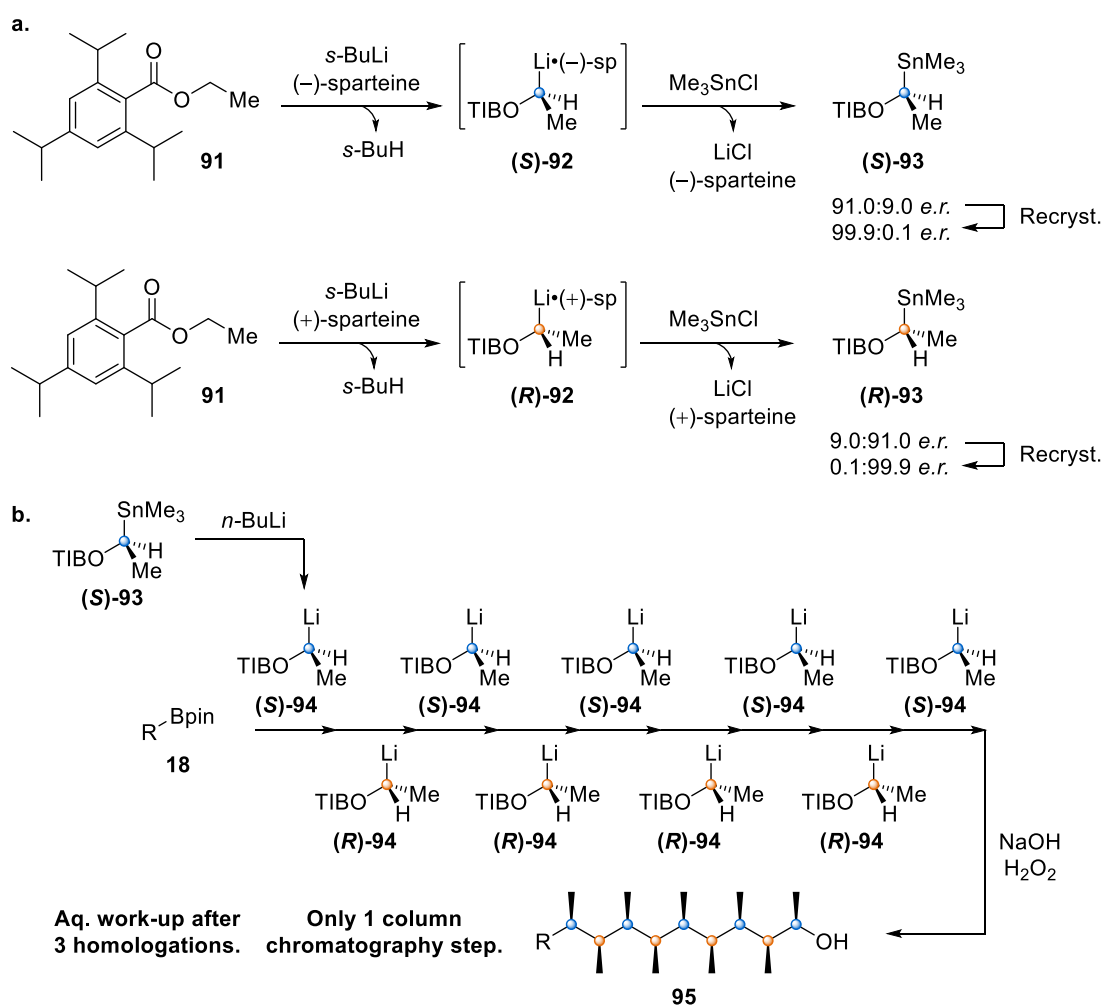
In 2007, Blakemore and co-workers used sulfoxide-derived enantioenriched carbenoids **88** to homologate boronic ester **87** three times³⁸ (**Scheme 15**). Depending on the configuration of the carbenoid used, they could selectively synthesise four diastereoisomers of alcohol **90** in excellent enantiomeric ratio (*e.r.*) and low diastereoisomeric ratio (*d.r.*) due to chiral amplification. Notably, in this sequence, each intermediate was purified by column chromatography.



Scheme 15. Iterative reagent-controlled homologation using sulfoxide-derived carbenoids.

The first example of fully stereocontrolled iterative homologation of boronic esters was reported by Aggarwal and co-workers.¹ In this report, nine iterative homologations were performed by using enantiopure carbenoids derived from corresponding α -stannyl benzoates **93**, which were synthesised by sparteine-mediated asymmetric deprotonation of *O*-ethyl benzoate **91**, electrophilic trapping with trimethyltin chloride and recrystallisation in methanol. (**Scheme 16a**).

This process thereby converts a simple boronic ester into a highly complex molecule with just a single purification step and can be assimilated to a molecular assembly line (**Scheme 16b**). Practically, α -stannyl methyl benzoate **93** is subjected to tin–lithium exchange, using *n*-BuLi, to reveal carbenoid **94**. Boronic ester **17** is then added and quickly forms a boronate complex. Upon warming to room temperature, the 1,2-migration occurs, releasing the benzoate moiety and generating a new boronic ester that can be engaged in the next homologation. Very high levels of purity were observed because each homologation reaction occurs with >99% efficiency and with >99% stereocontrol.



Scheme 16. **a.** Synthesis of enantiopure (*S*)- and (*R*)- α -stannyl benzoates **93**. **b.** ‘Assembly-line synthesis’ as described by Aggarwal and co-workers in 2014.

Interestingly, the conformation of the final molecules was found to be highly dependent on the relative configuration of the methyl substituents along their main carbon chains. These compounds are therefore typical examples of fully-flexible molecules with controlled conformations.

1.1.4. Conformational analysis of flexible molecules

1.1.4.1. *Syn*-pentane interactions and conformational control

Hoffmann devoted an important part of his career to the study of flexible molecules with defined shape.^{49–69} Considering that the conformation of a molecule is closely related to its function in biological systems, his research contribution aimed to understand and rationalise the rules that nature employs to confer specific spatial arrangements on active compounds. He articulated a useful description of the conformation of hydrocarbons as being defined by a sequence of dihedral angles involving the carbon atoms of the principal chain, with the terms g^+ , g^- , and t , denoting dihedral angles of about $+60^\circ$, -60° , and 180° , respectively (**Figure 1a**).

According to this notation, a *syn*-pentane interaction appears when a g^+ dihedral angle is directly followed by a g^- dihedral angle. In this case, the distance between both groups of atoms is about 2.5 Å and the resulting steric penalty can reach 3.5 kcal mol⁻¹.⁷⁰ An emblematic example of *syn*-pentane interactions is encountered between two axial methyl groups in cyclohexane chair-type structures.^{58,71}

The energy cost associated with such interactions is high enough to constrain flexible molecules to avoid *syn*-pentane-containing conformations. For example, in the case of *n*-pentane (**Figure 1b**), the only conformer bearing a *syn*-pentane interaction represents 0.5% of the overall conformational landscape at room temperature.⁷⁰ This general principle found applications in conformational analysis and molecular design.

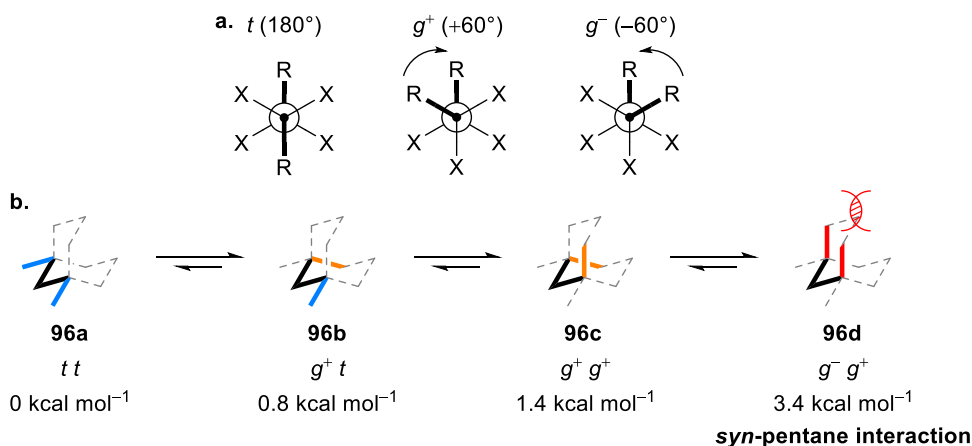


Figure 1. a. Hoffmann's description of dihedral angles. b. Analysis of steric interactions in *n*-pentane. MP4SDQ 6-31G(d) level of theory was used to calculate the relative energies.⁷⁰

A thorough theoretical analysis brought Hoffmann and co-workers to predict that a disyndiotactic (alternating *syn*–*anti*) hydrocarbon such as **97** would adopt a $(t)_n$ dihedral angle sequence (*i.e.*, a

linear conformation) to avoid *syn*-pentane interactions. For the same reason, the researchers suggested that the lowest-energy conformer of *threo*-diisotactic (all-*syn*) isomer **98** would be helical with a $(t\ g^+)_n$ dihedral angle sequence (**Chart 2**).

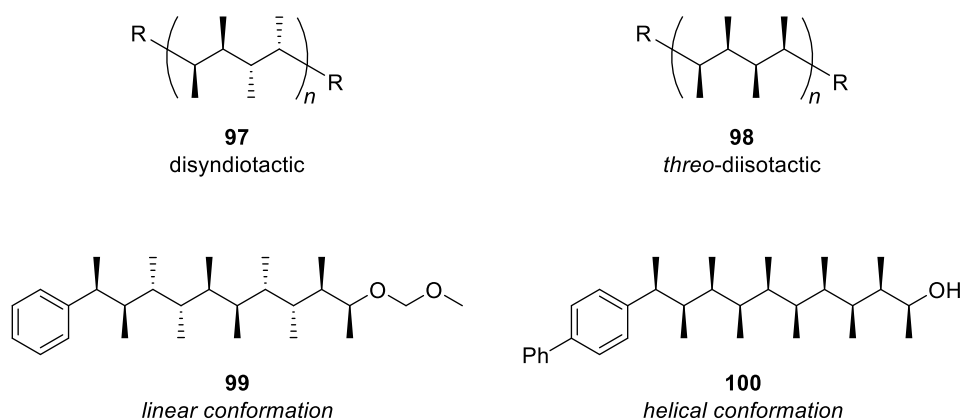


Chart 2. As predicted by Hoffmann and proved by Aggarwal, the substitution pattern of contiguously methyl-substituted hydrocarbons dictates the conformational behaviour of these molecules in solution and solid state.

Based on this seminal work, Aggarwal and co-workers predicted that the avoidance of *syn*-pentane interactions would force alternating *syn-anti* diastereoisomer **99** to display a linear shape in solution, and all-*syn* isomer **100** to adopt a helical conformation. The authors could confirm Hoffmann's predictions by synthesising both molecules and analysing them using a combined experimental and computational approach.

1.1.4.2. Quantum Mechanics/Nuclear Magnetic Resonance approach

The rate of conformational interconversion of a small flexible molecule is generally faster than the nuclear magnetic resonance (NMR) timescale. As a consequence, only time-average signals can be observed by NMR spectroscopy. Due to this limitation, it is not trivial to quantify conformer populations of a given flexible molecule by NMR analysis. Such a precise conformational description would require information about NMR parameters (chemical shifts (δ), scalar coupling constants (J) and inter-nuclear distances) of individual conformers.

To estimate these NMR parameters, theoretical values can be generated using quantum mechanical calculations for each conformer. One of the quickest ways to find low-energy conformers is to perform a molecular mechanics (MM) conformational search calculation. In this 'ball and spring' model, the overall energy of a molecule is defined by the sum of bond stretching energy (E_{stretch}), bond angle bending energy (E_{bend}), torsional angle rotations energy (E_{torsion}), electrostatic interactions energy (E_{coulomb}) and van der Waals interactions energy (E_{vdW}).⁷² This steps finds the local minima and the global minimum within a given energy threshold.

Once low-energy conformers have been generated, quantum mechanics (QM), and more specifically density functional theory (DFT), is employed to optimise their geometries and estimate their Gibbs free energies (considering zero-point energy correction, entropy and solvation),⁷³ which are used to calculate the Boltzmann-averaged populations of conformers at room temperature. These DFT-computed geometries are then used to calculate NMR parameters (δ , J and NOE-derived interproton distances) of each individual conformer. These values are subsequently Boltzmann-averaged to access the ensemble-averaged NMR properties of the compound. Finally, this theoretical picture is quantitatively compared to the experimental data to establish the conformational landscape of the molecule. This methodology was called Quantum Mechanics/Nuclear Magnetic Resonance (QM/NMR) approach (**Figure 2**).

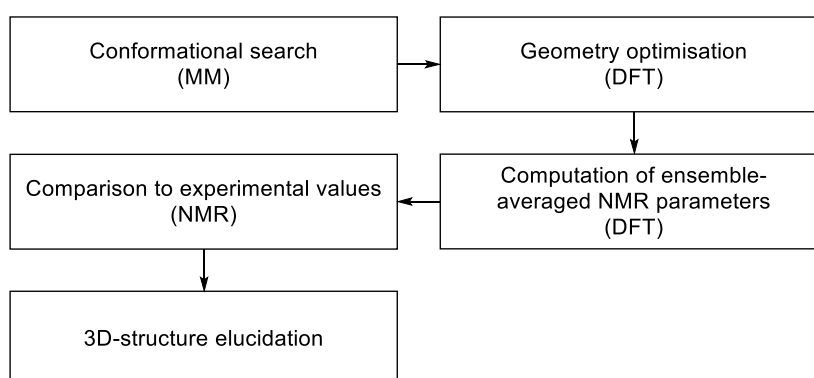


Figure 2. Workflow of QM/NMR approach for the conformational analysis of molecules in solution.

As mentioned above, Aggarwal and co-workers successfully applied this method to contiguously methyl-substituted hydrocarbons (**99** and **100**).¹ They used molecular mechanics (MM3 force field), followed by DFT calculations (DF-LMP2-F12 VDZ-F12//B3LYP-D2 6-311+G(d)) to generate the optimised conformers. The Boltzmann-averaged population of isomer **99** showed that 95% of the conformers would adopt a linear conformation, while 74% of the conformers of isomer **100** would adopt a helical conformation (**Chart 2**). J_{H-H} , J_{H-C} and NOE-derived distances were calculated by DFT (mPW1PW91 6-311G(d,p)//B3LYP-D2 6-311+G(d)), Boltzmann-averaged, and compared to experimental data. In both cases, computed values were in good agreement with measured parameters, with 1 Hz error in the comparison of coupling constant values and 5% error in the comparison of NOE-derived distances.

1.1.4.3. Vibrational Circular Dichroism

The QM/NMR approach is not the only methodology available to obtain information about the structural features of a flexible molecule. Conformational behaviour of foldamers is generally determined by a complementary set of analytical techniques, such as NMR,^{74–78} single crystal X-

ray crystallography^{79–82} or circular dichroism (CD).^{83–85} Although less frequently employed, vibrational circular dichroism (VCD) has also been found to be very useful to probe the conformation of organic compounds.

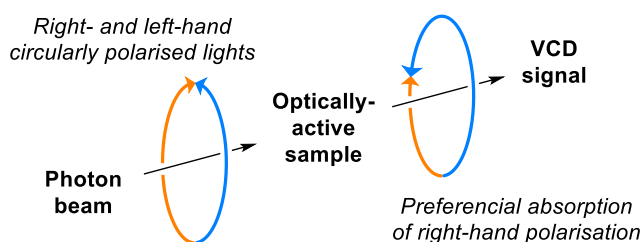


Figure 3. Concept of VCD analysis. In this example, an optically-active molecule absorbs preferentially right-hand polarised light.

This technique measures the differential absorption of left- and right-handed circularly polarised radiation (**Figure 3**) in the infrared region,⁸⁶ where vibrational transitions occur in the ground electronic state of a molecule. The combination of measured vibrational spectra and theoretical calculations provides unambiguous insights on the absolute configuration and the conformation of the compound of interest.^{87–89} For example, this method was used to determine the major conformation of dialkyl tartrates in different solvents,^{89–91} in complexation equilibrium with cyclodextrins⁹² or confined in micelles.⁹³ One could imagine that VCD analysis could give additional evidence for the conformational control observed by Aggarwal and co-workers in the case of methyl-substituted hydrocarbons.¹

1.1.5. Definition and applications of molecular switches

Miniaturisation appears to be one of the main challenges for future technology.^{94–100} Engineering organic materials at the molecular level benefits from the possibility to adjust a wide range of physical properties by subtle changes in the structure, as well as the opportunity to address fundamental problems through the isolation and full characterisation of single molecular components.^{101–103} Amongst a variety of possible applications, transport systems,^{104–106} control of nanoscale architectures,^{107–109} catalysts,^{110,111} surface properties of materials,^{106,112–118} mechanical devices,^{119–128} target-directed delivery systems¹²⁹ or nano-sensors^{130–132} can be envisioned.

As an illustration of the potential of organic materials for miniaturisation purposes, the Nobel Prize in Chemistry was jointly awarded to Feringa, Sauvage and Stoddart in 2016 for the design and synthesis of molecular machines. In parallel to their contributions, key discoveries in the fields of nano-structures^{133–135} and patterned surfaces^{136–142} with defined organisation of discrete entities, according to the principles of self-assembly phenomena,^{143–151} have also emerged.

A compound can be defined as a molecular switch if it can exist in two different forms, which can be interconverted. This unusual feature is called bistability and finds its origin in a range of physical properties such as complexation affinities, rate of isomerisations or electron transfers. The interconversion process can be triggered by a change in pH, pressure, temperature, light irradiation, magnetic or electric fields, or by chemical modification of the molecular structure.^{152–}

157

When the interconversion occurs upon modifications of light irradiation, one can speak of photochromism. Photoreversible molecules usually exist in two different states presenting distinct absorption spectra.^{158–163} The properties of a range of photoreversible compounds have been explored, including azulenes, stilbenes, fulgides, diarylethenes, azobenzenes, spiropyrans, viologens or salicylideneimines (**Chart 3**). The photochromic processes associated with these types of molecules are photocyclisation, isomerisation, keto–enol tautomerism or photoinduced electron transfer.^{150–161}

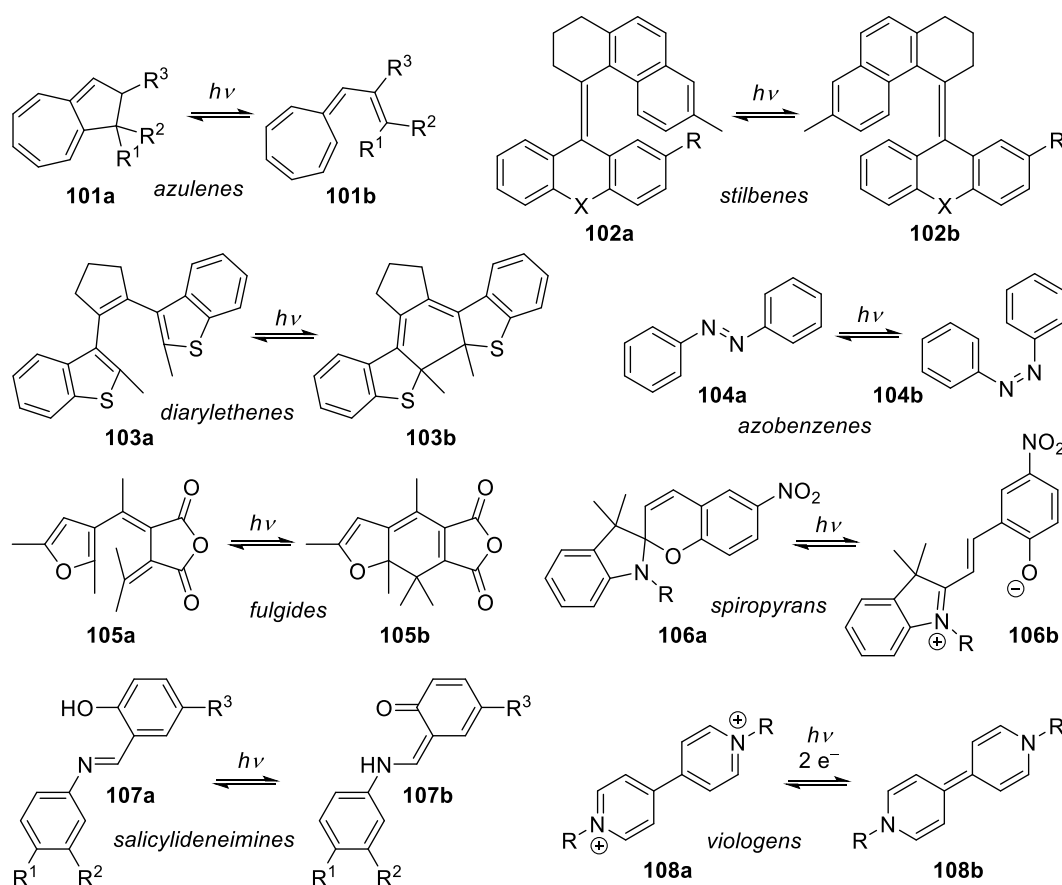


Chart 3. Selection of photoreversible compounds.

A remarkable application of these concepts was reported by Clayden and co-workers in 2016.¹⁶⁴ The control of stereoisomerism by light irradiation, in combination with foldamer chemistry, allowed the authors to synthesise a biomimetic system, bound in a phospholipid bilayer, in which

an azobenzene moiety was attached to a helical peptide. In its *trans* form, the azobenzene group forced the peptide chain to adopt a left-handed (*M*) helical conformation. Upon irradiation at 365 nm, the photoisomerisation of the N=N double bond occurred, switching from *trans* to *cis*, and the conformational control of the helical peptide decreased dramatically (*i.e.*, more equal populations of left- (*M*) and right-handed (*P*) helices were observed). Irradiation at 455 nm caused the azobenzene moiety to switch back to its initial state (*trans*), restricting the peptide oligomer in its *M* form (**Figure 4**). As shown by this example, the inherent screw-sense reversibility of helical molecules establishes them as privileged scaffolds for the design of molecular switches.

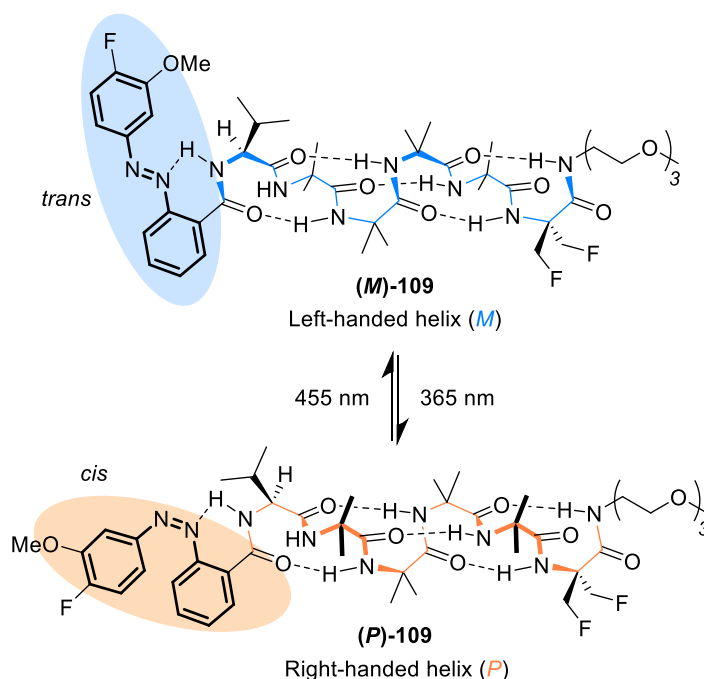


Figure 4. Clayden and co-workers reported that the isomerisation of an azobenzene moiety can induce the helical switch of a synthetic peptide embedded in a phospholipid bilayer.

Among a large variety of geometrically defined molecular shapes, helical structures have been widely studied since the fundamental discoveries of the helical architectures of proteins by Pauling¹⁶⁵ and DNA by Watson and Crick¹⁶⁶ in the early 50's. In the same decade, Natta demonstrated that synthetic polyhydrocarbons could also adopt a helical conformation.¹⁶⁷ Following his pioneering investigations on the synthesis and tacticity of polypropylene, other helical molecular scaffolds, such as annulated arenes, oligoarylamides, polyisocyanates, polyolefins, polyacetylenes, synthetic polypeptides, polysilanes and *para*-terphenyls, have been designed, synthesised and thoroughly studied.¹⁶⁸ These helical macromolecules have become synthetic targets of choice due to their interesting optical and electronic properties,^{169,170} their ability to induce asymmetry in chemical reactions,¹⁷¹ and to display functionality in a predictable pattern.¹⁷² Most of these

valuable properties strongly rely on screw-sense control.^{173,174} Therefore, scientists have developed useful tools to influence the helicity of such molecules. For example, the incorporation of one enantiomeric form of an additional element of chirality either at the termini^{81,175,176} or as part of a repeating substituent along the chain¹⁷⁷ can lead to a preference for either *M* (left-handed) or *P* (right-handed) screw-sense.

Small molecules do not benefit from the same amplification rules observed in polymers¹⁷⁸ and therefore chemists had to adopt different strategies to synthesise smaller helical entities. For instance, hydrogen bond networks in polyamides,¹⁷⁹ salt, disulfide and lactam bridges in oligopeptides¹⁸⁰ or electrostatic interactions in polyfluoroalkanes¹⁸¹ were successfully employed to impart or reinforce the helical conformation of such molecules. Another challenge appears if one wants to design small helical hydrocarbons. The propensity of non-functionalised small chains to fold into helices in a constrained environment has been studied by Rebek and co-workers through the encapsulation-induced folding of *n*-alkanes.^{182,183} In these examples, linear hydrocarbons prefer adopting a helical conformation to fit in the cavity of self-assembled host capsules. However, in the absence of external constraints, conformational control must arise from a subtle combination of steric interactions brought by a precise substitution pattern along the chain, as shown by the invaluable work conducted by Hoffmann and co-workers^{50,55,58,64,184} in the 90's.

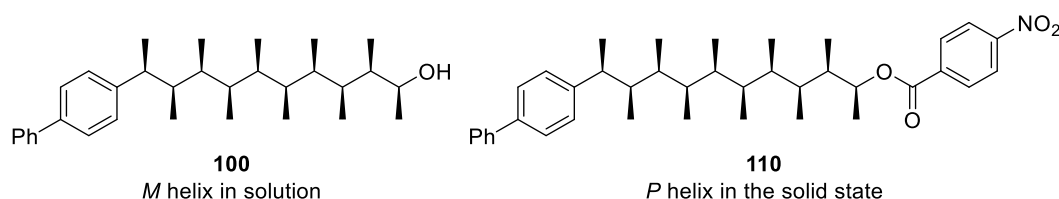


Chart 4. Compounds **100** and **110** have the same absolute configuration. Although they both adopt helical conformations, **100** folds into an *M* helix in solution while **110** crystallises as a *P* helix.

Interestingly, Aggarwal and co-workers observed that all-*syn* isomer **100** with hydroxyl and bi-phenyl terminal groups adopted an *M* helix in solution, while its crystalline benzoate derivative **110** adopted a *P* helix in the solid state¹ (**Chart 4**). This result showed that both *P* and *M* helical forms were accessible to the molecule. Although a single helical form was favoured in solution, this preference could be over-ridden by crystal packing forces in the solid state. This research project is aimed at understanding the origin of the sense of helicity, particularly in solution, and design a new class of molecular helical switches, thereby building a theoretical framework from which technological applications in catalysis, materials, and medicine could arise.

1.1.6. Research proposal

Based on the fact that a single chiral centre at one extremity of a foldamer can induce a strong conformational preference on the whole structure,⁸¹ it has been suggested by Huc and co-workers that, at the stereogenic centre of the end-group, the largest group points away from the helix, the medium group aligns itself with the helical backbone and the small group points towards the helix. Therefore, by assigning a new configuration (R^S and S^S) to the stereogenic centre based on steric hindrance (helix > aryl > methyl > H)—rather than on the classic Cahn–Ingold–Prelog rules—, R^S and S^S chirality favours *M* and *P* helicity, respectively (**Figure 5**).

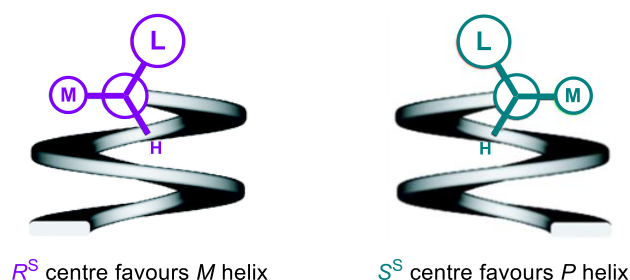


Figure 5. Huc's model: The large group (L) points away from the helix. The medium group (M) aligns itself with the helical backbone. The small group (H) points to the helix.

Such an analysis brings up an important consideration for helical compounds such as **111** and **112** (**Chart 5**). For compounds in which the terminal groups are separated by an even number of methyl-substituted methines, both end-groups will favour the same helical screw-sense and changing the relative size of the end-groups should not induce helical switching. However, for compounds in which the end-groups are separated by an odd number of carbon atoms, the termini will have different configurations (R^S and S^S) and the sense of helicity will presumably depend on which end-group is dominant, thus allowing switching to be possible. As a corollary, molecules with an even number of methine units, should adopt more stable helical forms than those with an odd number of methine units because the termini will have the same configuration and thus will cooperate to enforce the same sense of helicity.

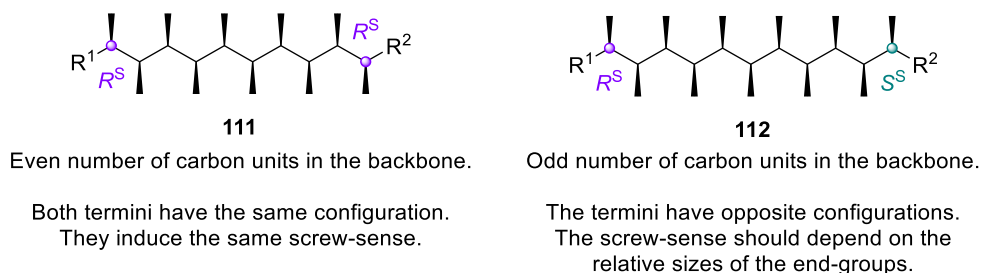
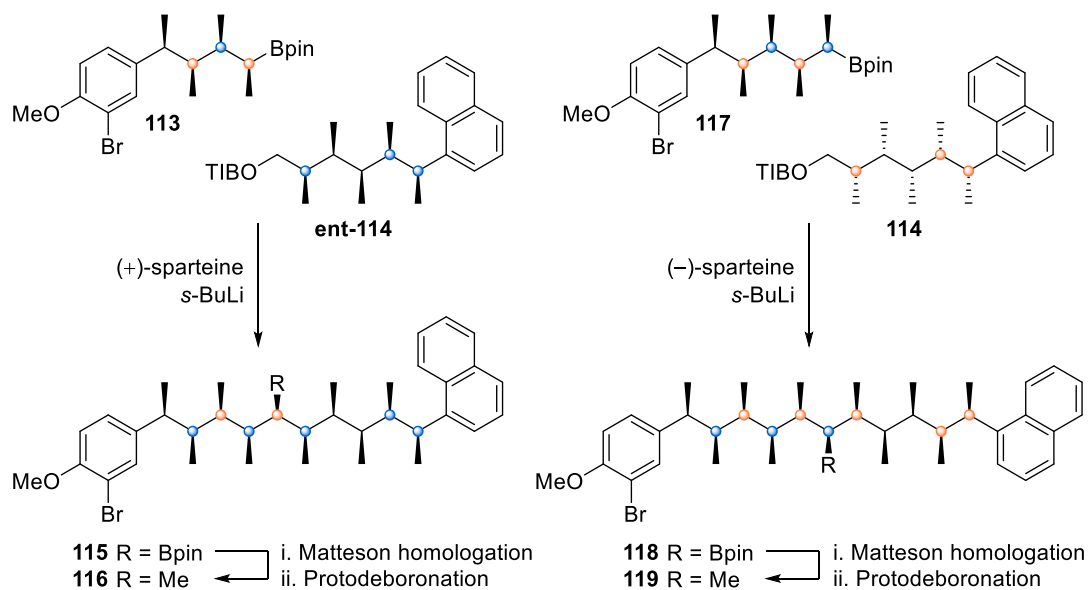


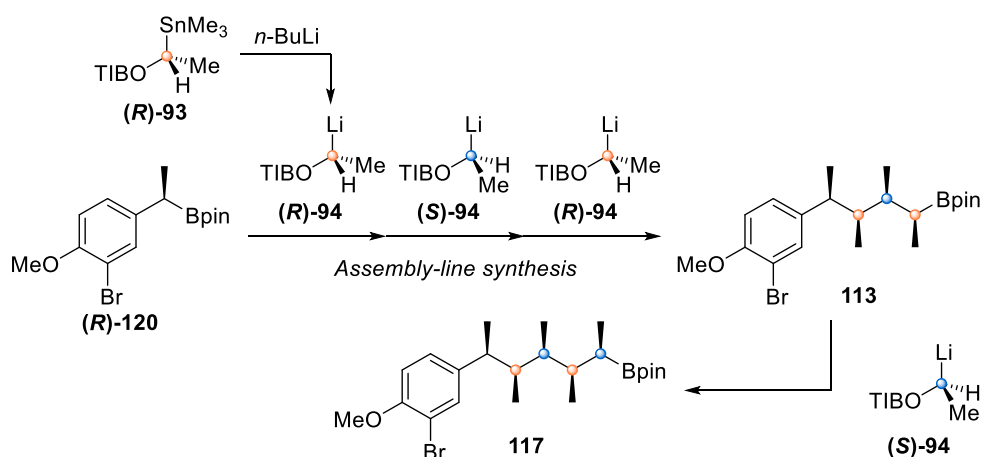
Chart 5. Huc's analysis applied to theoretical model compounds.

To determine whether Huc's model can be used to reliably predict the helical screw-sense of these molecules, compounds **116** and **119** will be prepared (**Scheme 17**). Although these compounds could be prepared by elaborating a precursor one carbon unit at a time, a building-block strategy,¹⁸⁵ which the Aggarwal group has previously employed in the context of the total synthesis of natural products,^{186–189} will be attempted here. Compounds will be prepared by the stitching together, through lithiation–borylation, of advanced intermediates. The boryl group in **115** and **118** will be transformed into a methyl group using the Matteson homologation followed by protodeboration.¹⁹⁰



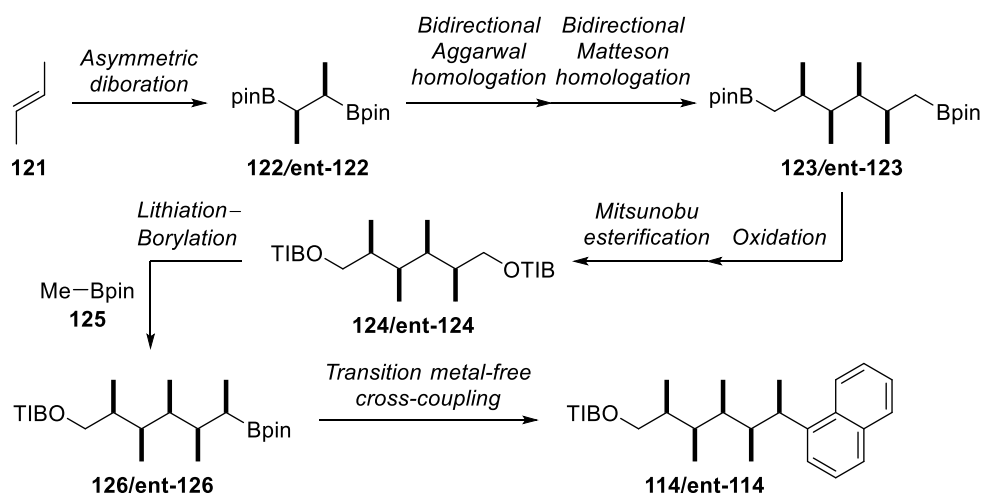
Scheme 17. Building-block strategy to synthesise target compounds **116** and **119**.

Advanced intermediates **113** and **117** will be prepared using iterative reagent-controlled homologation of boronic ester (**R**)-**120** involving enantiopure lithiated benzoates **94** generated through tin–lithium exchange of the corresponding α -stannyl benzoates **93** (**Scheme 18**). The aryl bromide, which will form part of the left-hand end-group, can later be functionalised through Buchwald–Hartwig, Stille, or Suzuki–Miyaura coupling to introduce varying degrees of steric hindrance at this end.



Scheme 18. Synthetic plan to access boronic esters **113** and **117**.

Advanced intermediate **114** (respectively, **ent-114**) will be generated using a novel iterative bi-directional lithiation–borylation¹⁹¹ of C_2 -symmetric bis(boronic ester) **122** (respectively, **ent-122**), which will in turn be prepared through Morken asymmetric diboration^{192,193} of *trans*-butene **121** (**Scheme 19**). C_2 -symmetric bis(boronic ester) intermediate **123** (respectively, **ent-123**) will be oxidized to the corresponding diol and esterified using Mitsunobu conditions. The naphthyl-based right-hand end-group will be introduced through lithiation–borylation using MeBpin **125**, followed by metal-free stereoretentive cross-coupling¹⁸ of boronic ester **126** (respectively, **ent-126**).

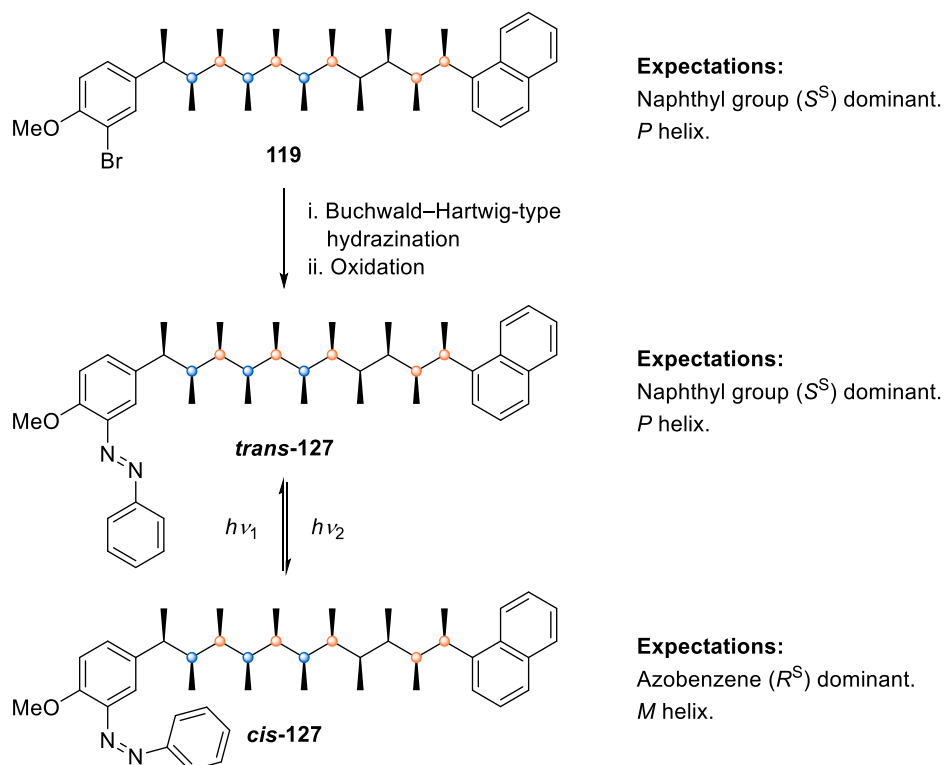


Scheme 19. Synthetic plan to access benzoates **114** or **ent-114**.

The QM/NMR approach (Section 1.1.4.2.) will be used to exhaustively explore the conformational space for all compounds. In parallel, attempts will be made to crystallise the compounds, so that their helical structure and screw-sense can also be determined through X-ray crystallography. The expectation is that **116** should fold into an *M* helix. On the other hand, the naphthyl group in compound **119** is expected to be the dominant group and thus force the molecule to

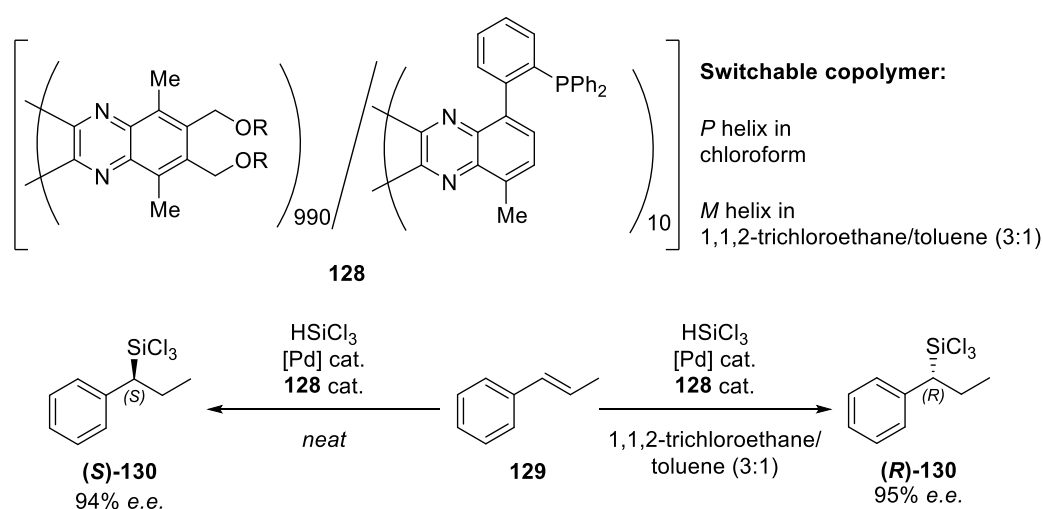
adopt a *P*-helical conformation. The percentage of helical conformers is predicted to be higher for **116**, owing to the end-groups having matched helical preferences.

To confer helical switchability to these molecules, an azobenzene moiety will be introduced (Section 1.1.5.) into the left-hand end-group by using a methodology developed by Cho and co-workers,¹⁹⁴ that is, Buchwald–Hartwig-type hydrazination of aryl bromide **119** to give a diaryl *N*-Boc hydrazine, followed by oxidation to reveal the N=N bond (**Scheme 20**). The conformational space, vicinal coupling constant values, and NOE-derived interproton distances for the *cis* and *trans* azobenzene isomers of **127** will be estimated computationally and compared with experimental values obtained from NMR experiments of the compound kept in the dark (the *trans* isomer) and that exposed to *in situ* laser irradiation¹⁹⁵ (the photostationary *cis* isomer). For the *cis* isomer, the left-hand end-group should have the greater steric impact on the helix, thus enforcing an *M* screw-sense. However, the right-hand naphthyl group should be dominant when the azobenzene is *trans*, thus maintaining a *P* screw-sense.



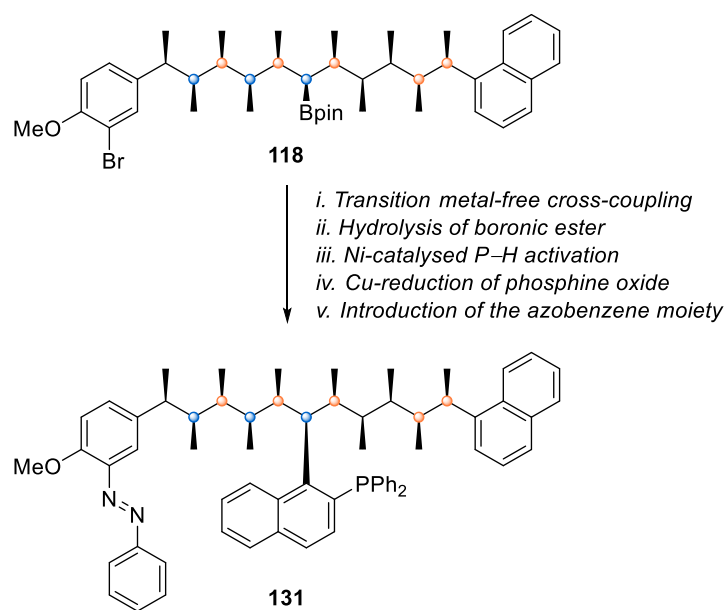
Scheme 20. Synthetic plan for the preparation and isomerisation of compound **127**.

With a design for a polymethylated linear hydrocarbon with switchable helicity that can tolerate at least one large substituent in the middle of the chain in hand, a triarylphosphine derivative will be prepared and tested as a switchable ligand in asymmetric Pd-catalysed hydrosilylation. In a related application,¹⁹⁶ Suginome and co-workers showed that helical poly(quinoxaline-2,3-diyl) copolymers **128**, that contain chiral and achiral units, can switch from one helical form to another by changing the solvent, a characteristic that was exploited in catalysis by incorporating triarylphosphine-appended monomers.¹⁹⁷ In one helical form, the polymer mediated a palladium-catalysed hydrosilylation of styrenes to give the desired product with very high levels of enantioselectivity. In the other helical form, the product of opposite configuration was obtained (**Scheme 21**) with similar selectivity.



Scheme 21. By introducing triarylphosphine moieties to a switchable polymer, Suginome and co-workers developed a switchable ligand for palladium-catalysed asymmetric hydrosilylation of styrenes.

The phosphine moiety at C6 will be introduced through stereoretentive cross-coupling: the Aggarwal group has recently developed conditions allowing the boryl group to be retained in such a process through its migration into an *ortho* position.²⁰ The boryl group will then be hydrolysed to the boronic acid and transformed into a triaryl phosphine moiety using a nickel-catalysed P–H activation of a secondary phosphine oxide,¹⁹⁸ followed by copper-catalysed reduction¹⁹⁹ (**Scheme 22**). The azobenzene moiety will be introduced as outlined above (**Scheme 20**).



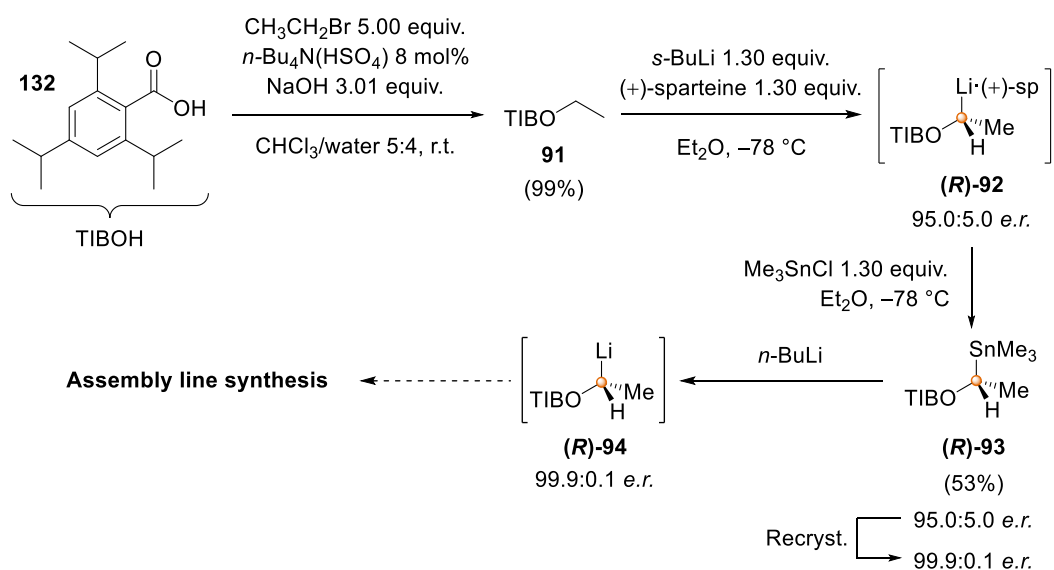
Scheme 22. Synthetic plan for the preparation of a new photo-responsive ligand for the asymmetric hydrosilylation of styrenes.

The conformation and switching behaviour of **131** will be analysed by computation and NMR analysis. Once the helicity switching is confirmed, the compound will be ligated to a palladium centre and the resulting complex analysed. The Pd–**131** complex will then be tested for its ability to asymmetrically catalyse the hydrosilylation of styrene **129**, both in the dark and under UV light irradiation. The sense of enantioinduction in the dark and under UV light will be determined through chiral HPLC analysis of the corresponding silanes (*S*)-**130**.

1.2. Results and discussion

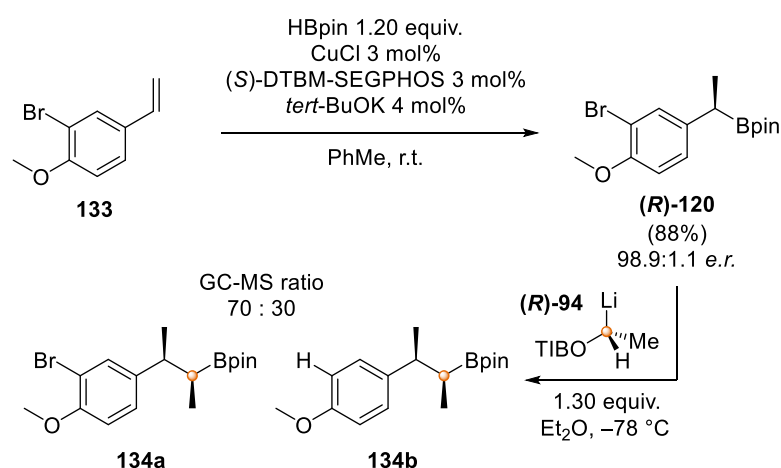
1.2.1. Synthesis of the first targets

The first task of this project was to prepare both enantiomers of stannane **93** to serve as building blocks for the iterative homologation of boronic esters.¹ Benzoate **91** was successfully synthesised using a known phase-transfer catalysis method (**Scheme 23**). Pleasingly, increasing the scale of this reaction up to 40 grams of starting material did not affect the yield, which remained quantitative. This material was subsequently engaged in asymmetric stannylation reactions, on large scales (*i.e.*, 10.00 g of starting material), using (+)- or (–)-sparteine **65** as chirality inducers to generate (*R*)- or (*S*)-**93**, respectively. Both species were recrystallised from methanol to improve their enantiomeric ratios up to 99.9:0.1. These masked carbenoids can then be stored, or treated with *n*-butyllithium to undergo a stereospecific tin–lithium exchange reaction, revealing the lithium carbenoid building blocks (*R*)- or (*S*)-**94** for the assembly-line synthesis.



Scheme 23. Preparation of enantiopure building block (**R**)-**93** for the iterative homologation of boronic esters. The enantiomer (**S**)-**93** was synthesised using (–)-sparteine instead of (+)-sparteine.

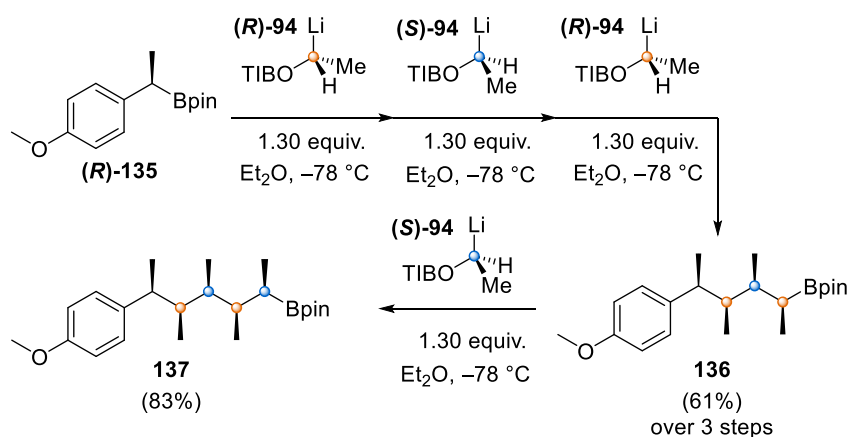
To test whether secondary benzylic boronate complex formation was faster than an aromatic bromine–lithium exchange reaction, boronic ester (**R**)-**120** was synthesised in two steps from commercially available 3-bromo-4-methoxystyrene. First, a Wittig reaction gave alkene **133**, which was successfully converted to enantioenriched boronic ester (**R**)-**120**, using an efficient asymmetric hydroboration methodology developed by Yun and co-workers.²⁰⁰ It is important to emphasise that a thorough purification of all the reagents involved in this chemical reaction was key to obtain the desired product with the required enantiomeric ratio (*i.e.*, >98:2 *e.r.*). The first attempt of the homologation reaction on (**R**)-**120** gave an inseparable mixture of extended boronic esters **134a** and **134b** in a 70:30 ratio (**Scheme 24**).



Scheme 24. Yun's asymmetric hydroboration applied to 3-bromo-4-methoxystyrene.

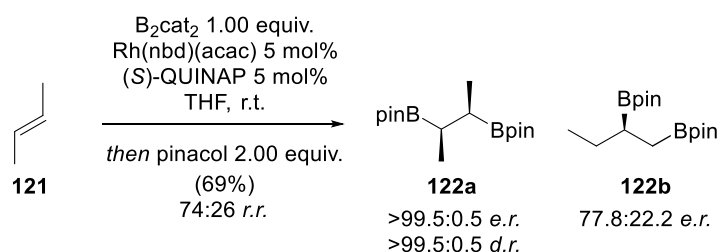
These results suggested that the boronate complex formation was the first reaction to take place, but the excess of lithium carbenoid (**R**)-**94** used (+0.30 equiv.) was subsequently engaged in a

bromine–lithium exchange process to generate the de-halogenated product **134b**. An easy way to circumvent this problem would be to reduce the number of carbenoid equivalents (*i.e.*, from 1.30 to 1.00 equiv.). However, it has been reported that an excess of lithiated benzoate was crucial to obtain a full conversion of the starting material.¹ Another synthetic plan was therefore envisioned, where the bromine atom would be introduced at a later stage.



Scheme 25. Preparation of fragments **136** and **137** using Aggarwal's iterative homology methodology.

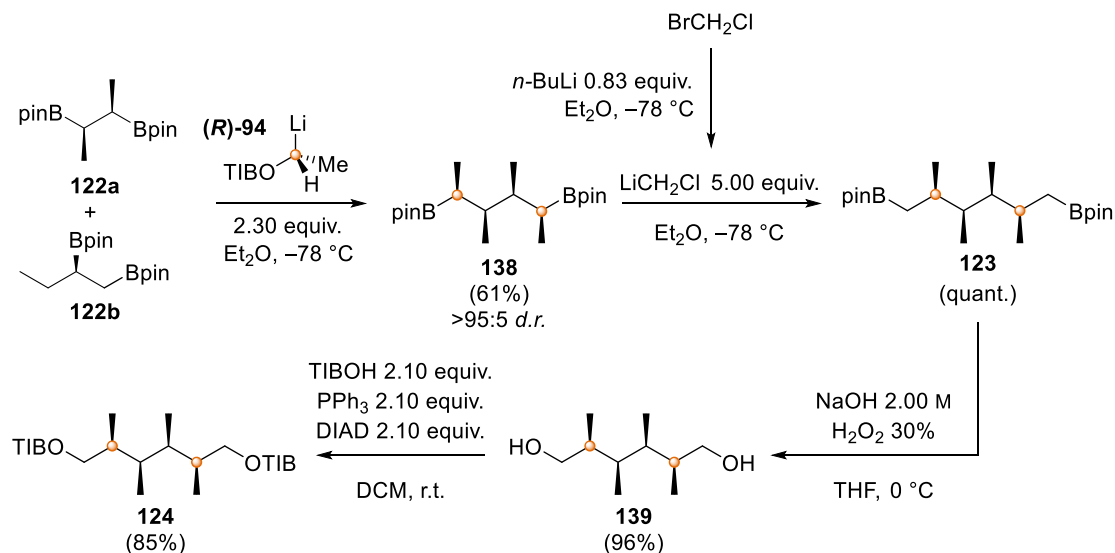
Yun's asymmetric hydroboration procedure was applied to 4-methoxystyrene to generate boronic ester (**R**)-**135** in 99.4:0.6 *e.r.* This molecule served as a starting point for a three-round iterative homology sequence, using (**R**)-, (**S**)- and (**R**)-**94** successively, to deliver boronic ester **136** in 61% yield over three homologies without intermediate purification (**Scheme 25**). Part of this material was then converted to fragment **137**, using the same homology methodology.



Scheme 26. Morken's asymmetric diboration methodology applied to *trans*-butene.

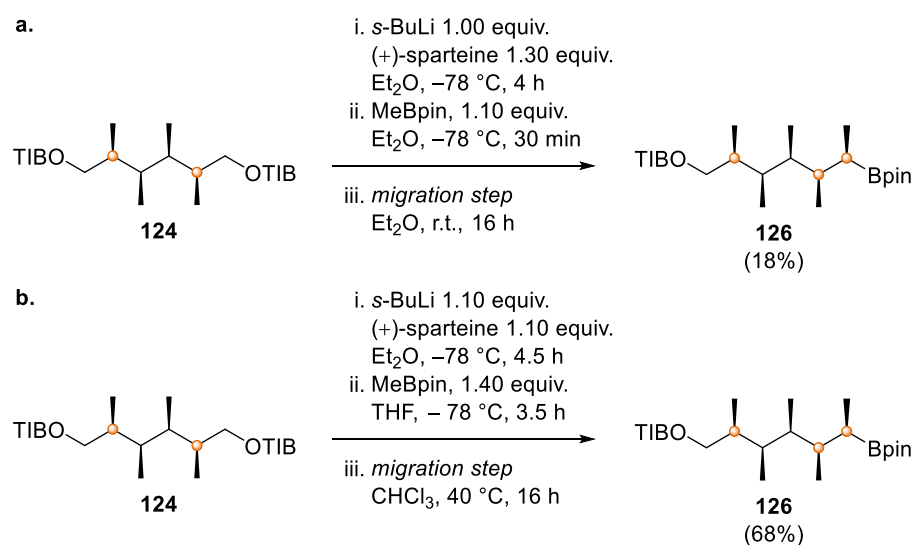
A unidirectional assembly-line synthesis was required to obtain fragments **136** and **137** as the 4-methoxyphenyl moiety could not be installed in a stereospecific manner at a later stage. However, a more efficient bidirectional chain-extension process was investigated to access fragment **114**. First, *trans*-butene **121** was subjected to Morken's asymmetric diboration methodology.^{192,193} Despite the relatively small size of its substituents, this gaseous substrate gave *C*₂-symmetric boronic ester **122a** in good yield (**Scheme 26**). Interestingly, a substantial amount of isomer **122b** was obtained, however with poor *e.r.* This side product most likely arose from the isomerisation of the double bond in the presence of the rhodium catalyst prior to the diboration

reaction. The lack of stereocontrol around this terminal olefin is in line with Morken's results, when this methodology was applied to monosubstituted alkenes. The mixture of isomers was directly engaged in the next step to give, after recrystallisation, pure boronic ester **138** in perfect *d.r.* The relative configuration of the methyl groups was confirmed by X-ray crystallography.



Scheme 27. Bidirectional synthesis of dibenzoate **124**.

A bidirectional Matteson homologation,²⁰¹ followed by oxidation and double Mitsunobu reaction, delivered benzoate **124** in 82% yield over three steps (**Scheme 27**). Compound **124** was then desymmetrised by (+)-sparteine-mediated asymmetric deprotonation and subsequent trapping of the carbenoid intermediate with methyl boronic ester **125**, which itself was easily synthesised in one step from methyl pinacol boronic acid.²⁰² Unfortunately, the first attempt gave the desired product (**126**) in only 18% yield (**Scheme 28a**).



Scheme 28. Desymmetrisation of dibenzoate **124**. **a.** Conditions and yield before *in situ* IR spectroscopy-assisted optimisation. **b.** Conditions and yield after *in situ* IR spectroscopy-assisted optimisation.

In situ IR spectroscopy was used to monitor and optimise this lithiation–borylation reaction, as the starting material **124**, carbenoid intermediate **Li-124** and boronate-complex **ate-124** have strong and sharp $\nu_{\text{C=O}}$ bands at 1728, 1634 and 1667 cm^{-1} , respectively, which importantly did not overlap with any other signals.²⁰³ The experiment showed that the full deprotonation of benzoate **124** was achieved in only one hour after the addition of *s*-BuLi (1.00 equiv.). However, the boronate-complex formation was found to be slower than the usual borylation reaction times and reached a plateau three hours after the addition of the solution of boronic ester **125** (1.00 equiv.) in diethyl ether (**Figure 6**).

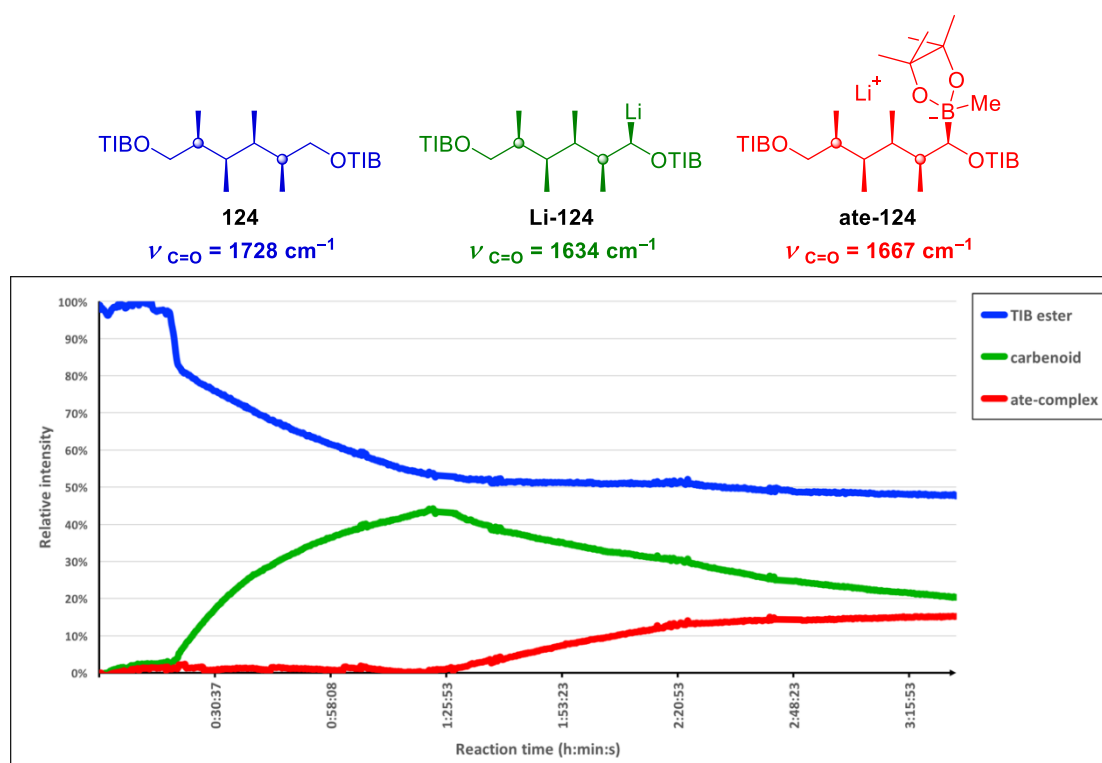


Figure 6. Lithiation–borylation reaction monitored by *in situ* IR spectroscopy. Concentrations of starting material **124** (in blue), carbenoid **Li-124** (in green) and boronate complex **ate-124** (in red) over time.

In their recent study on the borylation of diamine-ligated α -lithiated benzoates,²⁰³ Myers and Aggarwal determined that solvent had a dramatic impact on the borylation reaction time. They showed that by adding the boronic ester in tetrahydrofuran (THF) instead of diethyl ether, they could facilitate the borylation step through displacement of the bulky diamines coordinated to the lithium carbenoid, with no erosion of *e.r.* This solvent effect was successfully employed to shorten the problematic borylation step and promote the formation of boronate-complex **ate-124**. However, in the above case, the migration step seemed to be troublesome too: after sixteen hours at room temperature, ^{11}B NMR analysis revealed that boronate-complex was still present.

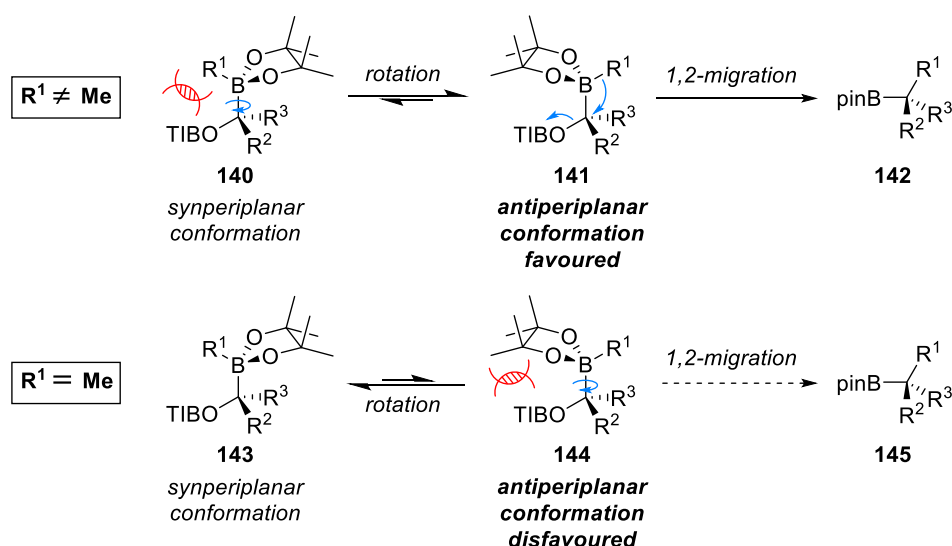
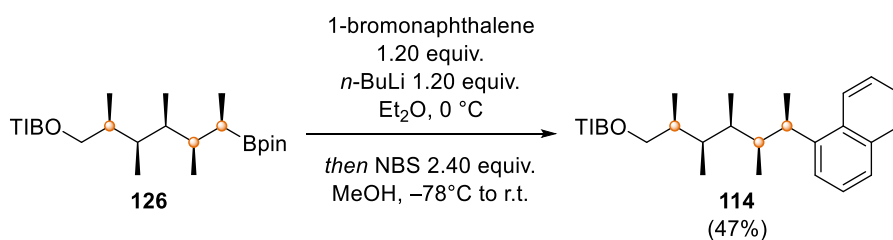


Figure 7. When the migrating group is a methyl group, the required antiperiplanar conformation is disfavoured. Therefore, the migration step becomes slower than usual. Charges have been omitted for clarity.

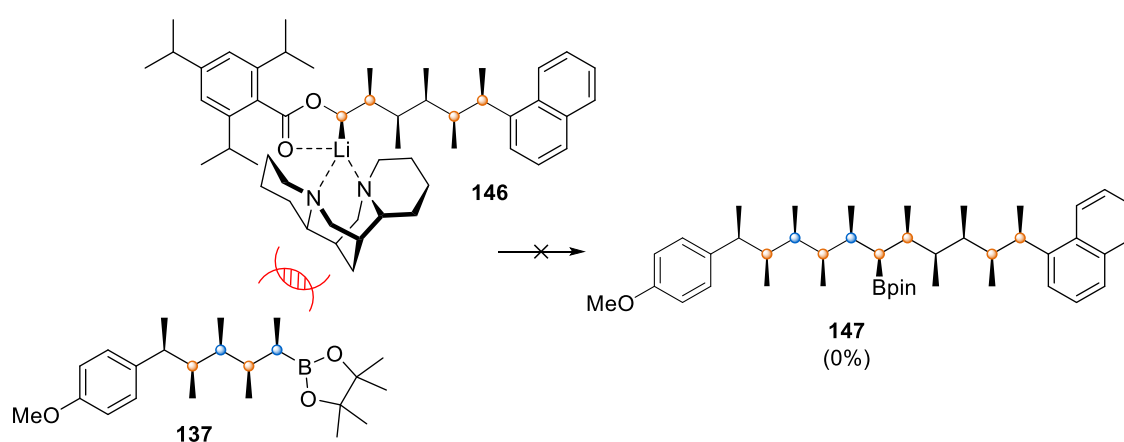
The poor migrating ability of the methyl group can be rationalised by analysing steric interactions within the boronate-complex⁶ (**Figure 7**). In fact, the 1,2-migration only occurs when the migrating group and the leaving group are antiperiplanar. Generally, in the case of large R^1 groups, the migrating group positions itself antiperiplanar to the leaving group to prevent any steric clash between them, thus enhancing the rate of the migration step. However, in the case of the small methyl group, this steric clash is reduced. More importantly, the pinacol moiety, which is now bulkier than the migrating group, sits antiperiplanar to the benzoate moiety, favouring the wrong conformation for alkyl 1,2-migration.²⁰⁴



Scheme 29. Transition metal-free cross-coupling between 1-bromonaphthalene and boronic ester **126**.

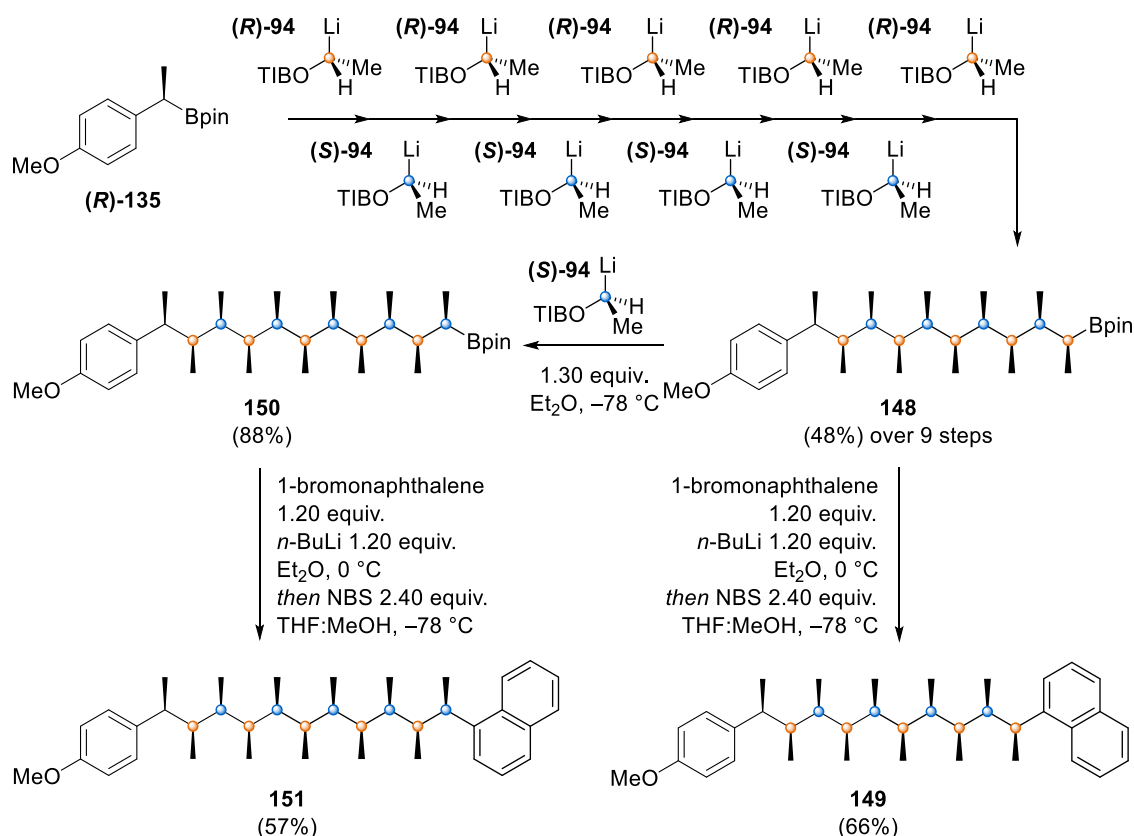
It has been shown that a solvent switch from diethyl ether or tetrahydrofuran to a less coordinating solvent such as chloroform or toluene allows the Lewis acidic lithium counter cation to bind more efficiently to the leaving group and thus increase the effectiveness of the 1,2-metallate rearrangement.¹⁸⁷ This second solvent effect was also used in the above case to increase the rate of the migration. After optimisation, this desymmetrisation reaction delivered boronic ester **126** in 68% yield (**Scheme 28b**). Finally, a transition-metal-free cross-coupling methodology¹⁸ was utilised to obtain fragment **114** (**Scheme 29**).

The coupling reaction between **114** and **137** was expected to be challenging, as lithiation–borylation methodology was sensitive to steric hindrance. For this reason, the reaction was again followed by *in situ* IR spectroscopy. It turned out that the lithiation step was quite slow (seven hours) and the borylation step inefficient (no boronate-complex formation was observed after two hours). These results can easily be understood by looking at the structure of carbenoid/(+)-sparteine complex **146** (**Scheme 30**). The reactive centre is flanked by the triisopropylbenzoate moiety, the methylated backbone and the sparteine ligand. In these conditions, there is no room for a bulky boronic ester such as **137** to approach the carbanion and form a boronate-complex. Adding boronic ester **137** in THF helped to form the desired boronate complex. However, the yield of the reaction remained very low.



Scheme 30. Due to steric hindrance, the coupling reaction between carbenoid **146** and boronic ester **137** was not successful.

Due to the unsuccessful coupling of fragments **114** and **137**, the first convergent strategy was abandoned. Instead, a more familiar linear sequence^{1,205} was employed to generate intermediate **148**. Boronic ester **135** was subjected to nine rounds of homologation (**Scheme 31**), alternating between the enantiomers of stannane **93**, to deliver intermediate **148** in 48% yield over nine steps. One more homologation step was necessary to access intermediate **150**. Using the same transition-metal-free cross-coupling methodology as described above,¹⁸ both targets **149** and **151** were synthesised in 66% and 57% yield, respectively. With both compounds in hand, their conformational behaviour in solution was studied by ¹H NMR.



Scheme 31. Preparation of target compounds **149** and **151**, using unidirectional iterative homologation of boronic ester methodology.

1.2.2. Preliminary NMR analysis and Molecular Mechanics

For both compounds, $^3J_{\text{H-H}}$ coupling constant values were studied by ^1H NMR analysis. In the case of **149**, most of the core CH signals were overlapped, and a constrained rotation, due to steric effects of the naphthyl group, broadened signals 22 and 24 (**Chart 6**). Nevertheless, $^3J_{\text{H6-H8}} = 9.9\text{ Hz}$ and $^3J_{\text{H8-H10}} = 2.8\text{ Hz}$ could be obtained.

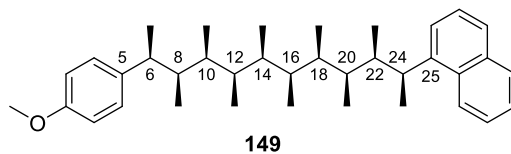


Chart 6. Atom numbering of target compound **149**.

According to Karplus equation,²⁰⁶ the first value (9.9 Hz) suggested that H6 and H8 were likely to be in an antiperiplanar relationship in the major conformer, and thus depicted C5–C6–C8–C10 as a *gauche* dihedral angle. The second coupling constant (2.8 Hz) showed that H8 and H10 stood in a *gauche* relationship, indicating that C6–C8–C10–C12 was an antiperiplanar dihedral angle in the major conformer. Despite the lack of information concerning the other dihedral angles,

these initial results indicated that compound **149** presented a certain conformational preference in solution.

The same analysis was applied to compound **151** (**Chart 7**): the first and the last coupling constant values, $^3J_{\text{H6-H8}} = 7.0$ Hz and $^3J_{\text{H24-H26}} = 6.9$ Hz, were extracted from the ^1H NMR spectrum. These values of 7.0 and 6.9 Hz were unexpected but can be interpreted in two different ways.

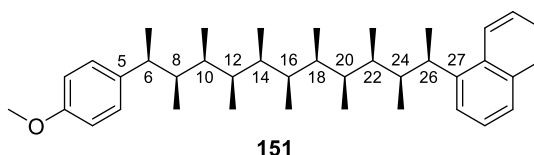


Chart 7. Atom numbering of target compound **151**.

The first explanation is that dihedral angle C5–C6–C8–C10 (respectively, C22–C24–C26–C27) can adopt two different conformations in solution: a *gauche* conformation with $^3J_{\text{H6-H8}} > 7$ Hz (respectively, $^3J_{\text{H24-H26}} > 7$ Hz) and an antiperiplanar conformation with $^3J_{\text{H6-H8}} < 7$ Hz (respectively, $^3J_{\text{H24-H26}} < 7$ Hz), with each conformation accounting for 50% of the overall dihedral angle population. The NMR spectrum would then represent the average of both conformations, with the resulting average coupling constant of 7 Hz. This interpretation could suggest that the molecule exists as a 50:50 mixture of the left-handed (*M*) helix and the right-handed (*P*) helix. A second explanation is that both dihedral angles do not have any conformational preference. This would also result in an average coupling constant of 7 Hz. Assuming that the other dihedral angles behave in the same way, this second interpretation could imply that the molecule does not adopt any controlled conformation in solution.

Molecular mechanics was employed to confirm the presumed conformational preference of **149** and better interpret the results obtained in the case of compound **151**. Pleasingly, a Monte Carlo molecular mechanics conformational search (using the MMFFs force field, 500,000 iterations and in the gas phase) corroborated the strong conformational preference expected for **149**. As shown in **Figure 8**, molecular mechanics predicted that the most populated conformers of **149** would exhibit backbones with an alternating *gauche*/antiperiplanar dihedral angle sequence. The three-dimensional structure of the molecule can be represented on a diamond lattice (**Figure 9a**), with dihedral angle values rounded to 60° for each *gauche* dihedral angle and 180° for each antiperiplanar dihedral angle. As a result, an *M* helix is obtained, as predicted by Huc's model⁸¹ for compounds bearing end-groups with a (*R*^S) configuration.

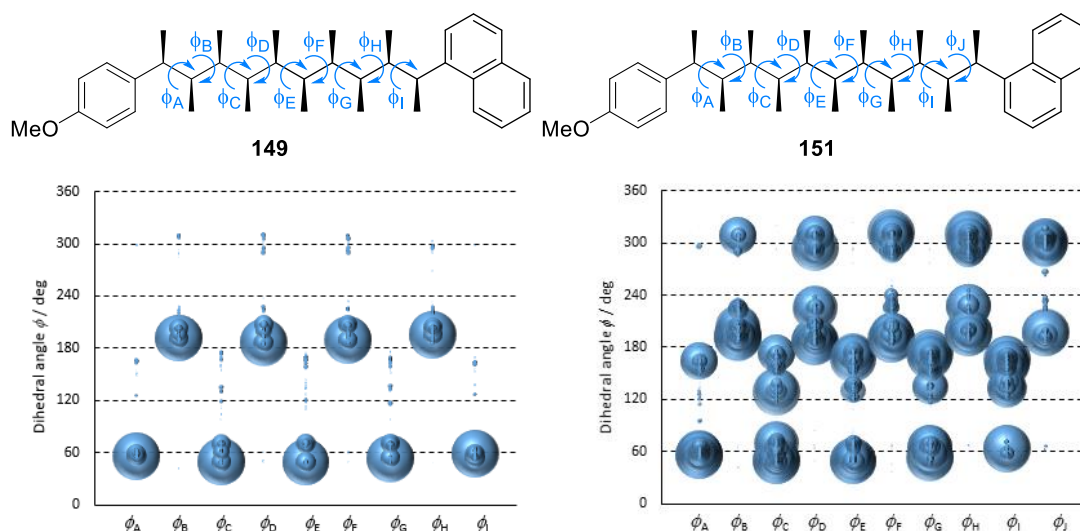


Figure 8. Bubble plots representing the different populations of dihedral angles in the backbone. The size of the bubble is proportional to the percentage of the corresponding calculated Boltzmann population. These data were extracted and processed by Dr. Siying Zhong.

However, in opposition to Huc's model, Newman projections along C6→C8 or C24→C22 axes (**Figure 9b**) show that the larger groups (*i.e.*, *para*-methoxyphenyl and naphthyl groups) are not pointing away from the helix but instead are set themselves as if they are part of the continued backbone. Therefore, the accordance between the prediction of Huc's model and the observed screw-sense is assumed to be a coincidence.

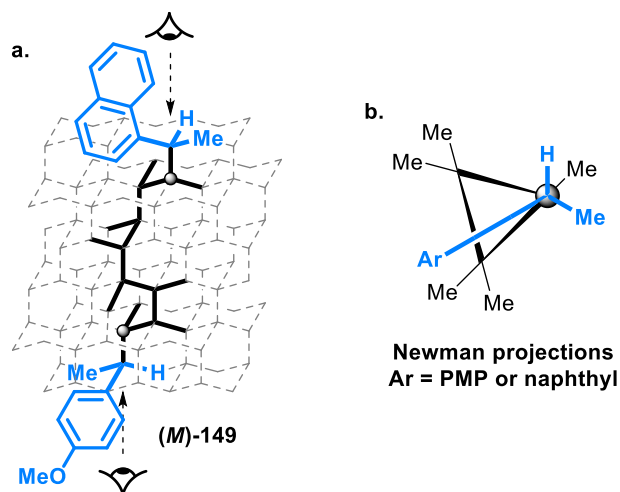


Figure 9. **a.** Compound **149** represented as a left-handed helix on a diamond lattice, according to its bubble plot showed above. **b.** The Newman projections at both chain-ends showed that the aromatic groups were not pointing away from the helix. PMP = *para*-methoxy-phenyl.

Moreover, in the case of compound **151**, Huc's model predicts that if the end-groups have different absolute configurations, the biggest end-group (here, the naphthyl group) would dominate and dictate the screw-sense. However, the same molecular mechanics conformational search of **151** predicted that 12% of the overall population would exist as a left-handed helix, 8% as a right-handed helix and 80% would adopt non-helical conformations (**Figure 8**). These results are in

line with the coupling constant values obtained by ^1H NMR. This indicates that the second interpretation is correct and discredits, once again, the applicability of Huc's model to such molecules. Therefore, the development of a new stereochemical model accounting for the experimental observations is essential to better understand the conformational preference of these all-*syn* methyl-substituted compounds.

1.2.3. Towards a new stereochemical model

A diamond lattice analysis reveals that, for a chain containing ten stereocentres such as **ent-111**, only two conformers bear no *syn*-pentane interaction (**Figure 10**). One of these conformers is a left-handed (*M*) helix and the other conformer a right-handed (*P*) helix.

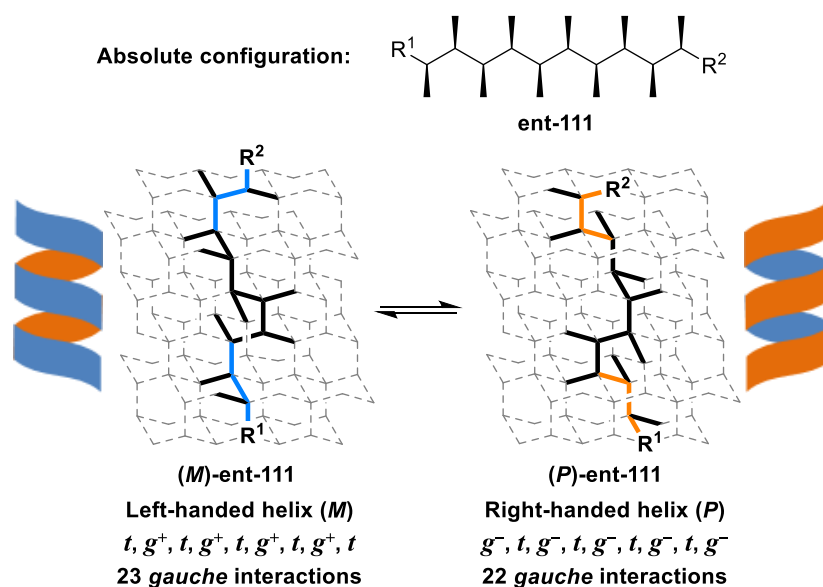


Figure 10. Equilibrium between left- and right-handed helices bearing an even number (10) of stereocentres in the backbone drawn on a diamond lattice.

From this initial three-dimensional analysis, it appears that any antiperiplanar dihedral angle ($t = 180^\circ$) in the *M* helix becomes a *gauche*[−] dihedral angle ($g^- = -60^\circ$) in the *P* helix after a conformational switch. Similarly, any *gauche*⁺ dihedral angle ($g^+ = +60^\circ$) in the *M* helix becomes an antiperiplanar dihedral angle ($t = 180^\circ$) in the *P* helix. The dihedral angle sequence in the *M* conformer could then be described as $t, g^+, t, g^+, t, g^+, t, g^+, t$, whereas the dihedral angle sequence in the *P* conformer could be described as $g^-, t, g^-, t, g^-, t, g^-, t, g^-, t$.

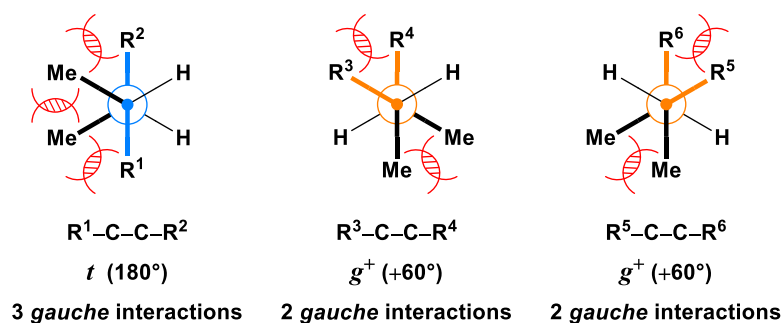


Figure 11. Newman projections of t , g^+ and g^- dihedral angles. The *gauche* interactions are represented by red steric clash signs.

Newman projections of t , g^+ and g^- dihedral angles (**Figure 11**) reveal that each t dihedral angle generates three *gauche* interactions, while each g (g^+ or g^-) dihedral angle generates only two *gauche* interactions. Based on this observation, the dihedral angle sequence in the M helix ($5 \times t + 4 \times g^+$) creates 23 *gauche* interactions, whereas the dihedral angle sequence in the P helix ($5 \times g^- + 4 \times t$) creates only 22 *gauche* interactions. Consequently, according to these numbers, the P conformer is expected to be dominant in this case (*i.e.*, for this specific absolute configuration). More generally, for any given absolute configuration and assuming that all the *gauche* interactions are equivalent in terms of energy penalty, an all-*syn* methyl-substituted chain with an even number of stereocentres should favour the conformer which bears no *syn*-pentane interactions and with the smallest number of t dihedral angles in the backbone.

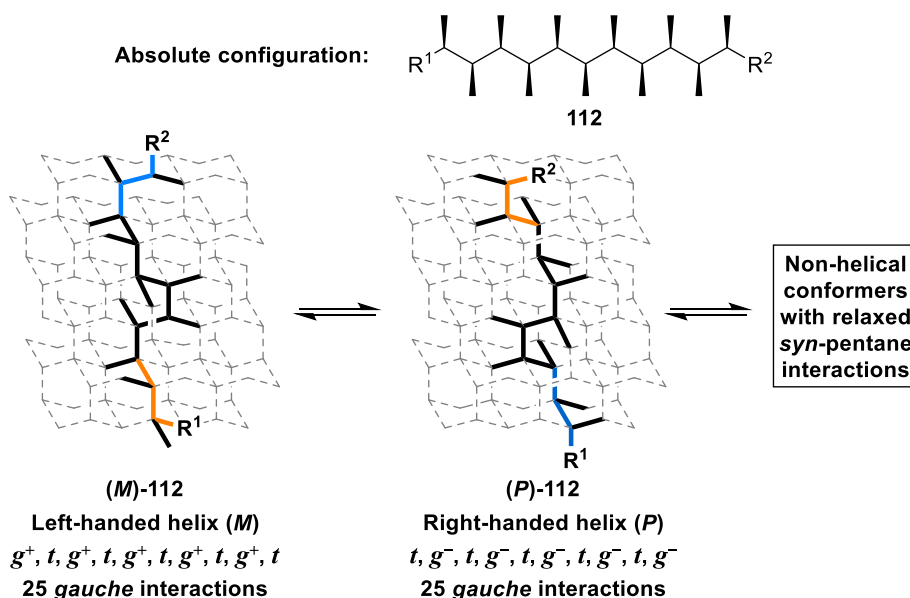


Figure 12. Equilibrium between left-handed helix, right-handed helix and non-helical conformers with an odd number (11) of stereocentres in the backbone drawn on a diamond lattice.

The same diamond lattice analysis on a chain composed of eleven stereocentres shows that only two conformers can exist with no *syn*-pentane interactions (**Figure 12**). As for a chain with an even number of stereocentres, one of these conformers is an M helix, while the other is a P helix.

The same dihedral angle interconversions from g^+ to t and from t to g^- is observed when the molecule switches from M to P . The dihedral angle sequence in the M form can be described as $g^+, t, g^+, t, g^+, t, g^+, t, g^+, t$, whereas the dihedral angle sequence in the P form can be described as $t, g^-, t, g^-, t, g^-, t, g^-, t, g^-$. However, in this case, the number of *gauche* interactions is identical for both helices ($5 \times t + 5 \times g = 25$). As a consequence, the ratio between the population of helical conformers adopting a M -helical conformation and the population of helical conformers adopting a P -helical conformation should be close to 50:50.

Interestingly, a molecular mechanics (MM) conformational search of **112** (eleven stereocentres) predicted that only 20% of the overall population would adopt a helical conformation (**Figure 8**), in a 60:40 $M:P$ ratio. This suggests that, with eleven stereocentres, the helical conformers (*i.e.*, conformers with no *syn*-pentane and 25 *gauche* interactions) are very close in energy to the non-helical structures which necessarily contain a *syn*-pentane interaction. Most likely, both C–C bonds involved in this *syn*-pentane interaction do not lie in the exact same plane to reduce the energetic cost of the steric clash (this type of interaction could be described as a pseudo- or relaxed *syn*-pentane interaction).

Assuming that any all-*syn* methyl-substituted hydrocarbon with an even number (respectively, odd number) of stereocentres possesses the same conformational behaviour as compound **149** (respectively, compound **151**), an initial model can be established (**Table 1**) to predict the screw-sense of such molecules.

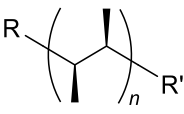
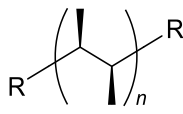
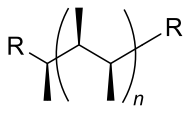
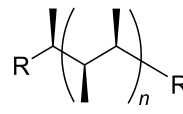
	Even number of stereocentres		Odd number of stereocentres	
Absolute configuration				
Predicted screw-sense	Right-handed helix (P)	Left-handed helix (M)	Mixture of M , P and non-helical conformers	

Table 1. Screw-sense prediction table.

However, this new model relies only on a combination of molecular mechanics results and highly congested ^1H NMR spectra of only two compounds with two different chain lengths (ten and eleven stereocentres). Therefore, to confirm the general applicability of the model, it was necessary to prove that the screw-sense can be successfully predicted for any chain lengths.

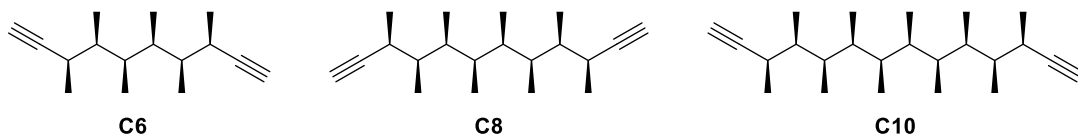
1.2.4. Design of new targets

The objective was to design and synthesise a series of compounds with different chain lengths to study their conformations using the QM/NMR approach.^{1,188} One of the limitations of this technique appears when NMR spectra are too congested, preventing the extraction of NMR parameters, such as chemical shifts or coupling constants. To avoid this issue, only C_2 -symmetric and *meso* compounds were selected. Indeed, introducing symmetry elements creates pairs of chemically equivalent atoms, reducing the number of NMR signals and, therefore, lowers the risk of spectrum congestion.

The nature of the end-groups would certainly play a role in the conformational behaviour of these molecules. To avoid any steric interactions with the backbone, terminal alkynyl groups were chosen as the end-groups. Their linear geometry and small size ($d_{C\equiv C} \approx 1.2 \text{ \AA}$) would prevent terminal alkynes from generating any steric hindrance and the electron density of the $C\equiv C$ triple bond would spread the NMR chemical shifts and thus reduce the number of overlapping NMR signals.

Finally, in terms of synthesis, the target molecules would ideally be accessible from the same synthetic intermediate, using the iterative homologation of boronic esters. According to all of the requirements listed above, a series of six molecules (three C_2 -symmetric and three *meso* compounds) were chosen (**Chart 8**) to validate the new stereochemical model.

C_2 -symmetric targets:



meso targets:

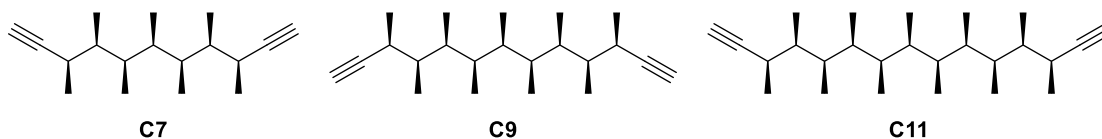


Chart 8. Two series of target molecules were designed to study the impact of the chain length on the conformation in solution.

According to the proposed model, one could represent the three C_2 -symmetric compounds **C6**, **C8** and **C10** on a diamond lattice (**Figure 13a**). The scalar coupling constant value $^3J_{H-H}$ for each pair of consecutive protons attached to the backbone could then be theoretically estimated, based on the Karplus equation.²⁰⁶ According to Karplus' graph, an antiperiplanar (*t*) $H-C-C-H$ dihedral angle would give a coupling constant value $> 8 \text{ Hz}$ (*large*), whereas a *gauche* (*g*) $H-C-C-H$ dihedral angle would give a coupling constant value $< 6 \text{ Hz}$ (*small*). For example, in compound **C10**, the predicted $H-C-C-H$ dihedral angle sequence being *t*, g^+ , *t*, g^+ , *t*, g^+ , *t*, g^+ , *t*, the $^3J_{H-H}$

sequence was expected to be *large, small, large, small, large, small, large, small, large*. If the experimental measurements showed the opposite $^3J_{\text{H-H}}$ sequence (i.e., *small, large, small, large, small, large, small, large, small*), it would suggest that the opposite helix was dominant in solution (**Figure 13b**). If the experimental values were all about 7 Hz, the conclusion would be that there was no dominant conformer in solution. Consequently, a simple ^1H NMR measurement would establish the accuracy of the model. After these theoretical considerations, the next task was to synthesise the target compounds.

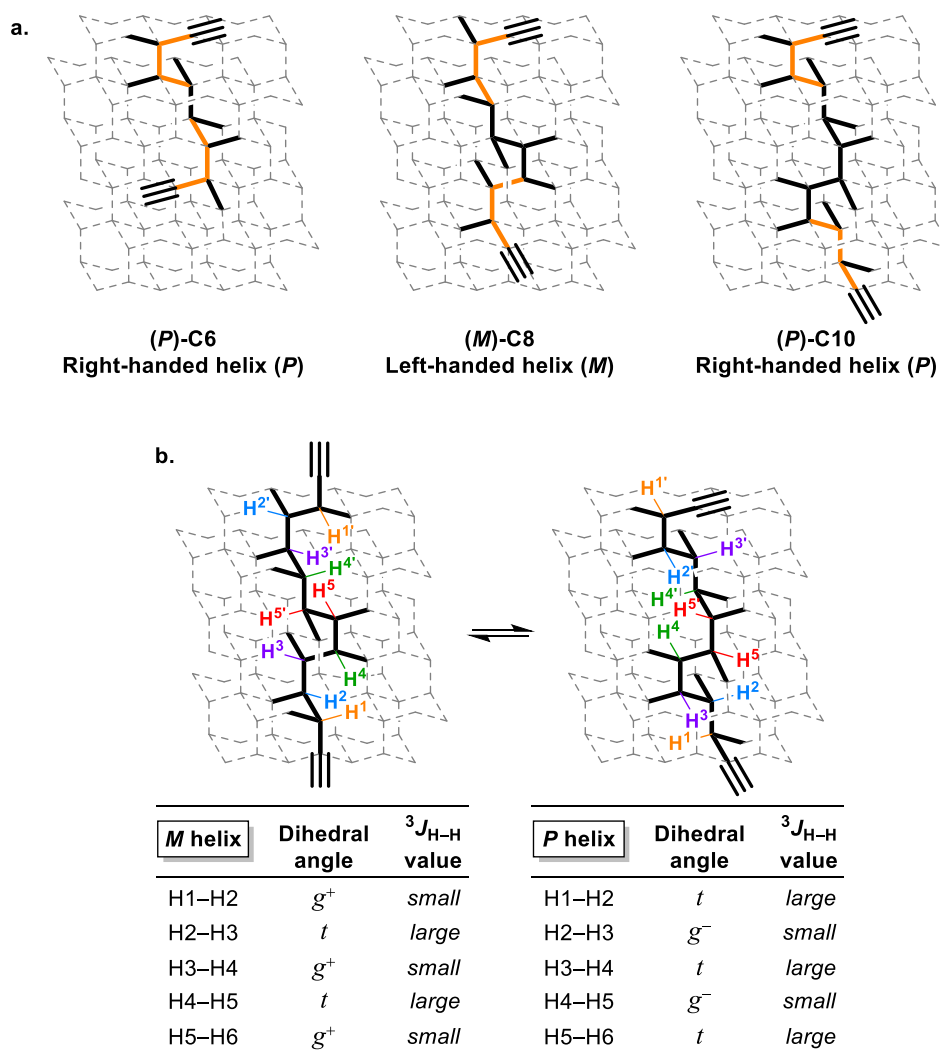
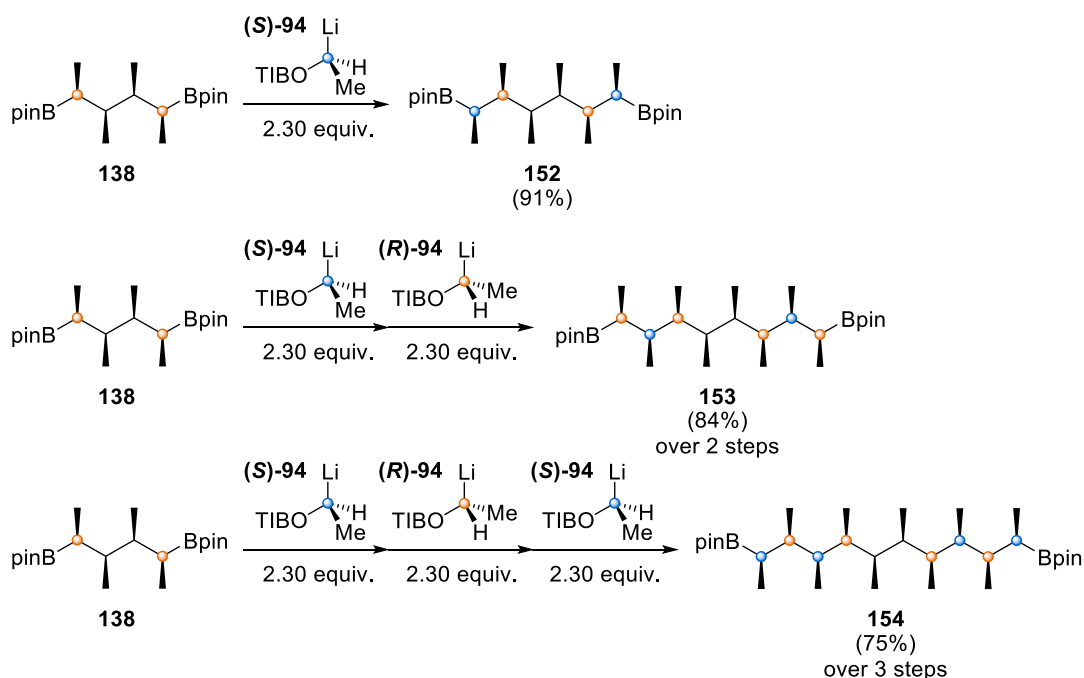


Figure 13. **a.** Predicted conformers for compounds **C6**, **C8** and **C10** drawn on a diamond lattice. **b.** Expected coupling constant values for both helical conformers of compound **C10**.

1.2.5. Synthesis and preliminary NMR results

Boronic ester **138** was bidirectionally homologated once to give intermediate **152** (containing six stereocentres), twice to obtain compound **153** (with eight stereocentres) and, finally, three times to access boronic ester **154** bearing ten stereocentres. Remarkably, compounds **153** and **154** were

generated in an iterative manner, with only one purification step at the end of the homologation sequence (**Scheme 32**). The extraction of the $^3J_{\text{H-H}}$ values by ^1H NMR analysis revealed that the conformational behaviour of the three compounds was in line with the prediction of the new model. Surprisingly however, an X-ray crystal structure of **154** (**Scheme 31**) showed that the molecule underwent a helical switch from *P* helix in solution to *M* helix in the solid state. It would seem that for efficient crystal packing, the pinacol boronic ester moieties adopt an extended conformation, forcing the chain to switch (as a consequence of the avoidance of *syn*-pentane interactions).



Scheme 32. Preparation of *C*₂-symmetric boronic esters **152**, **153** and **154** using bidirectional iterative homologation methodology.

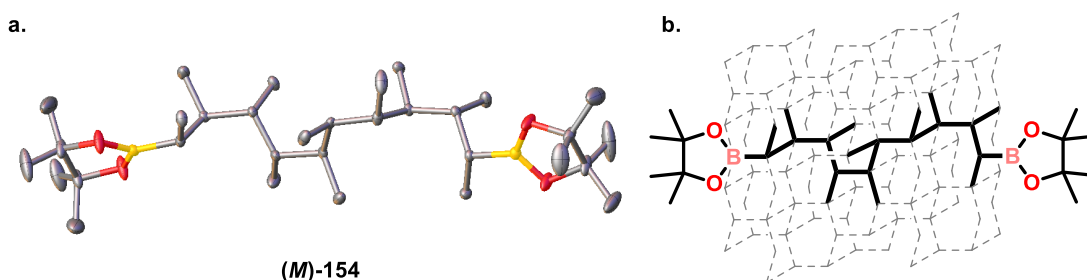
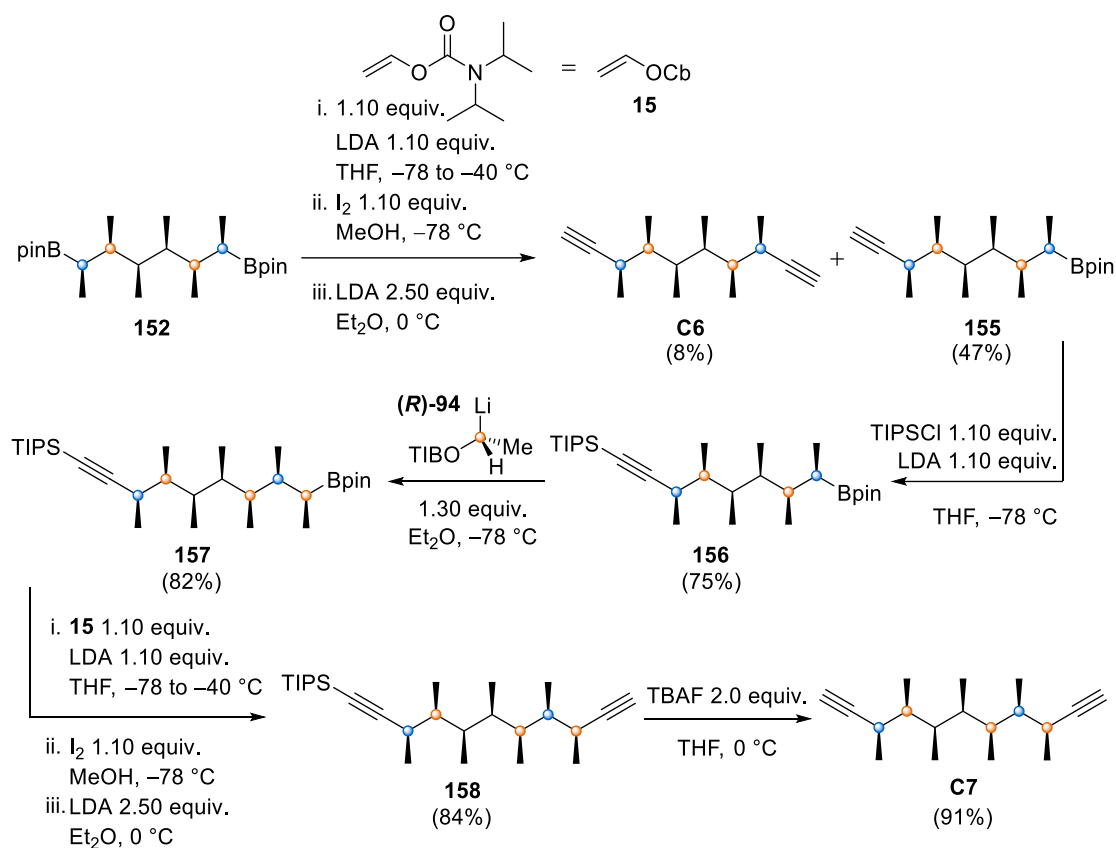


Figure 14. **a.** X-ray crystal structure of boronic ester **154** Ellipsoids shown at 50% probability. Hydrogen atoms and solvent molecules have been omitted for clarity. **b.** Conformation of compound **154** in the solid state drawn on a diamond lattice.



Scheme 33. Example of desymmetrisation of a C_2 -symmetric boronic ester (here **152**) to access two target compounds (here, **C6** and **C7**). Carbamate **15** was synthesised in one step from the corresponding carbamoyl chloride.²⁰⁷

The C_2 -symmetric intermediates were then desymmetrised using the alkynylation methodology developed in the Aggarwal group in 2016.¹⁷ Each desymmetrisation reaction resulted in a mixture of starting material, monoalkyne and dialkyne. After isolation of each of these three species, monoalkyne intermediates were protected, homologated, alkanylated and finally deprotected to access the last three target molecules (**Scheme 33**).

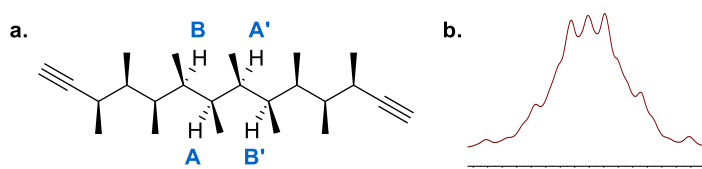


Figure 15. a. HA and HA' are chemically equivalent but magnetically inequivalent. b. 1H NMR signal of the proton pair HA/HA'.

Pleasingly, no signal overlap was observed when NMR spectra were recorded in deuterated toluene. In the case of C_2 -symmetric molecules, measurements of $^3J_{H-H}$ were relatively straightforward, except for the HA–HA' proton pair depicted in **Figure 15a**. HA couples to HB with $^3J_{HA-HB}$ and to HB' with $^4J_{HA-HB'}$ whereas HA' couples to HB with $^4J_{HA'-HB}$ and to HB' with $^3J_{HA'-HB'}$.

Therefore, HA and HA' are chemically equivalent but not magnetically equivalent to each other. As a consequence, the ^1H NMR signal of HA/HA' appears as a complex multiplet (**Figure 15b**) from which no $^3J_{\text{H-H}}$ could be extracted. This limitation was not observed for *meso* compounds where all the coupling constants could be obtained. Gratifyingly, these preliminary results (**Table 2**) are in accordance with the proposed model (**Table 1**). Unlike boronic ester **154**, dialkyne **C10** was found to adopt the same conformation in solution and in the solid state, as shown by its X-ray crystal structure (**Figure 16**).

	C6	C7	C8	C9	C10	C11
$^3J_{\text{H1-H2}}$	9.2 Hz	6.8 Hz	9.2 Hz	6.9 Hz	9.2 Hz	6.9 Hz
$^3J_{\text{H2-H3}}$	2.8 Hz	5.6 Hz	3.4 Hz	5.3 Hz	3.6 Hz	6.9 Hz
$^3J_{\text{H3-H4}}$	-	6.5 Hz	8.5 Hz	6.7 Hz	8.8 Hz	6.8 Hz
$^3J_{\text{H4-H5}}$			-	6.1 Hz	3.1 Hz	6.8 Hz
$^3J_{\text{H5-H6}}$					-	6.6 Hz
Major conformer	<i>P</i> helix	?	<i>M</i> helix	?	<i>P</i> helix	?

Table 2. Extraction of $^3J_{\text{H-H}}$ values from ^1H NMR spectra of compounds **C6**, **C7**, **C8**, **C9**, **C10** and **C11**. The atom numbering refers to **Figure 13a**.

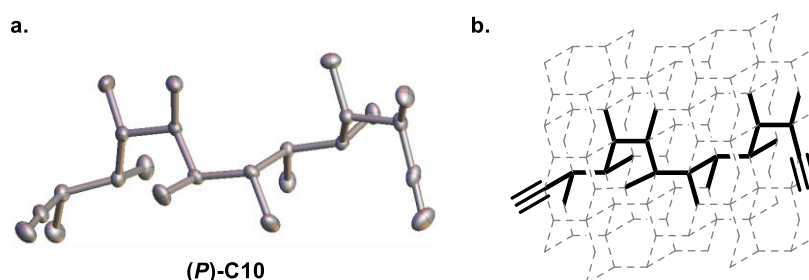


Figure 16. **a.** X-ray crystal structure of dialkyne **C10**. Ellipsoids shown at 50% probability. Hydrogen atoms and solvent molecules have been omitted for clarity. **b.** Conformation of compound **C10** in the solid state drawn on a diamond lattice.

As expected, the simultaneous addition of two stereocentres at both ends of **152** to give **153** led to an inversion of screw-sense from **C6** (*P* helix) to **C8** (*M* helix). The same interesting phenomenon was observed when **153** was bidirectionally homologated to deliver **154**, resulting in a second screw-sense inversion from **C8** (*M* helix) to **C10** (*P* helix). According to the model, this phenomenon can be rationalised by the tendency of the chain to reduce the number of *gauche* interactions (**Figure 17**). This iterative bidirectional homologation process can therefore be described as a remarkable example of helical switching by bidirectional chain extension.

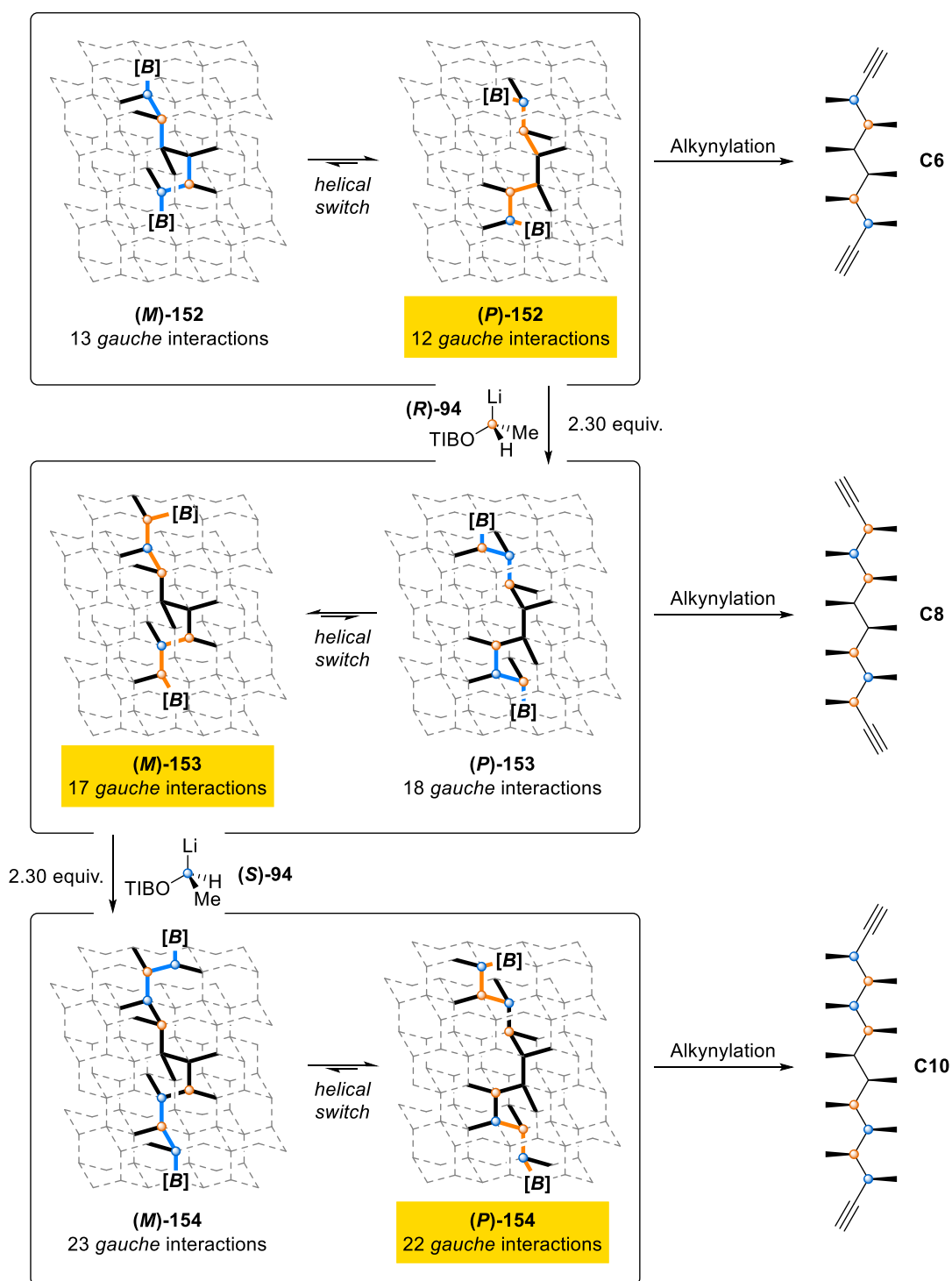


Figure 17. Helical switching by bidirectional chain extension. $[B] = \text{Bpin}$.

Pleasingly, the same analysis revealed that compounds with an odd number of carbon atoms in the backbone (**C7**, **C9** and **C11**) exhibited an average coupling constant value ($^3J_{\text{H-H}} \approx 7 \text{ Hz}$) for each proton pair. As discussed in Section 1.2.3., one interpretation could be that both helical conformers were dominant in solution and present in a 50:50 ratio, or a second explanation could be that the conformational ensemble did not have a preferred conformation.

At that time, all of these results only relied on preliminary ^1H NMR measurements. To support them, a more thorough quantitative conformational analysis was required. In the case of fully flexible molecules with controlled conformations, one of the most powerful techniques to confidently describe the populations of conformers in solution was the QM/NMR approach, as shown by Butts and Aggarwal^{1,188} over the last few years. This approach was employed to validate the conclusions depicted above and obtain the structures and ratios of the different populations of conformers of the target compounds.

1.2.6. Application of the QM/NMR approach

This part of the project was conducted by Dr. Siying Zhong who extracted all the required NMR parameters, including NOE-distances, and performed all the molecular mechanics (MM) and density functional theory (DFT) calculations. Her results²⁰⁸ were included in this thesis to provide a complete picture of the project.

First, the conformational landscape of compound **C10** was explored by molecular mechanics (MM). A Monte Carlo MM conformational search predicted that 90% of the overall population would adopt a helical conformation (**Figure 18**). The energy difference between both *P* and *M* conformers was found to be quite small ($\Delta E \approx 1.0 \text{ kJ mol}^{-1}$), resulting in a 50:50 ratio of right- and left-handed helices.

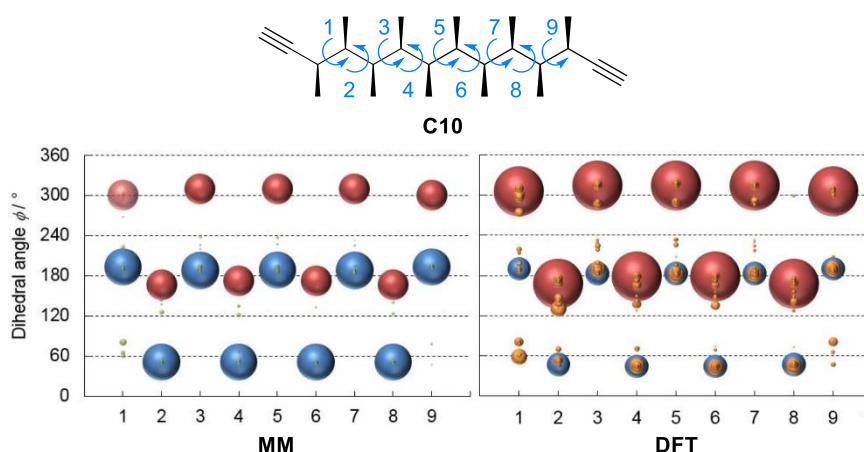


Figure 18. Dihedral angle populations of dialkyne **C10** predicted by MM (left) and DFT (right) and represented as bubble plots. Red dots belong to a *P* helix, blue dots belong to an *M* helix, orange dots belong to non-helical conformers.

By contrast, DFT geometry optimisation and frequency calculations using B3LYP-D2/6-311G(d) level of theory gave a different outcome. According to this method, 65% of the overall population would fold into a *P* helix, 14% would exist as an *M* helix and 21% would present non-helical conformations. The energy difference between both helical populations was predicted to be about

1 kcal mol⁻¹, a difference that is in line with the expected energy penalty for the one extra *gauche* interaction between methyl groups in the *M* conformers.⁷⁰

Prior to performing DFT calculations to predict the ensemble-average scalar coupling constants, it was necessary to find the optimal level of theory for calculating conformer geometries and energies. The predictions of eleven sets of DFT methods, involving four different functionals (mPW1PW91, B3LYP, B3LYP-D2 and M06-2X), in combination with five basis sets (6-31G(d), 6-311G(d), 6-311+G(d), 6-311G(d,p) and 6-311+G(d,p)), were compared to experimentally-derived NOE-distances. Pleasingly, B3LYP-D2/6-311G(d) level of theory in gas phase provided the best fit to the experimental values.

After optimisation of the DFT method to calculate conformer geometries and energies, the coupling constant values of the major conformers (making up 90% of the overall population) were subjected to DFT calculations using mPW1PW91/6-311G(d,p) level of theory, with implicit toluene (IEFPCM), to establish the ensemble-averaged scalar coupling constants. The ⁴J_{H-H} coupling constant between the terminal alkyne proton and the first CH of the chain was not included in this analysis because it did not give any information about the conformation of the backbone. Moreover, this computed ⁴J_{H-H} value (4.2 Hz) deviated significantly from the experimental value (2.4 Hz), probably because the sp orbitals of the alkyne bond were not described accurately by the level of theory employed here. Apart from this coupling constant, all the NMR parameters were in good agreement with the measured values (**Table 3** and **Figure 19**).

	MAD	StDev	χ ² (reduced)
¹ H– ¹ H scalar coupling	0.6 Hz	0.7 Hz	0.44
NOE distances	3.8%	4.9%	1.97

Table 3. Mean averaged deviation (MAD), standard deviation (StDev) and χ² (reduced) values for calculated NMR parameters of **C10**.

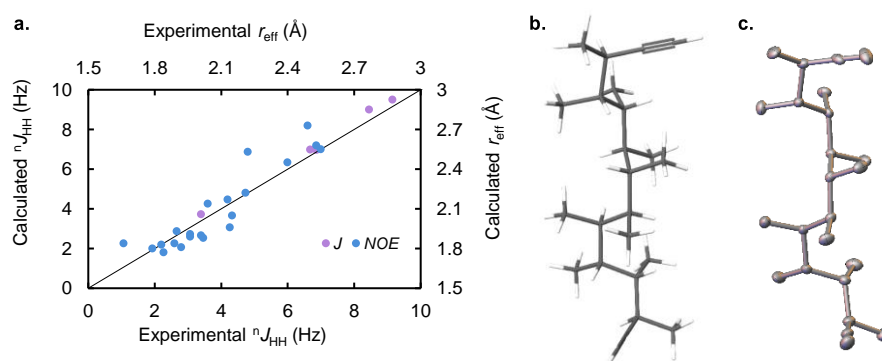


Figure 19. **a.** Comparison of DFT-computed ensemble- averaged ¹H–¹H scalar coupling constants and ¹H–¹H distances to the experimental values. **b.** DFT-predicted lowest energy conformer (*P* helix) of **C10**. **c.** X-ray crystal structure of **C10** Ellipsoids shown at 50% probability. Hydrogen atoms and solvent molecules have been omitted for clarity.

Encouraged by these results, the same Monte Carlo MM conformational search was applied to compounds **C6** and **C8**. The resulting conformations were then subjected to DFT geometry optimisation and energy calculations, using the appropriate level of theory B3LYP-D2/6-311G(d), with a correction derived from single point energy calculations with a bigger basis set 6-311G(d,p) and solvation (toluene, IEFPCM). About 86% of the overall conformer population of **C6** and 80% of the overall conformer population of **C8** were predicted to be helical. As anticipated by the diamond lattice-based model, compound **C6** mainly existed as a *P* helix, whereas compound **C8** preferred to fold into an *M* helix (**Figure 20**). The energy difference between *M* and *P* helices was, in both cases, around 1 kcal mol⁻¹. For both compounds, the calculated averaged NMR parameters were in good agreement with experimental data (**Table 4**).

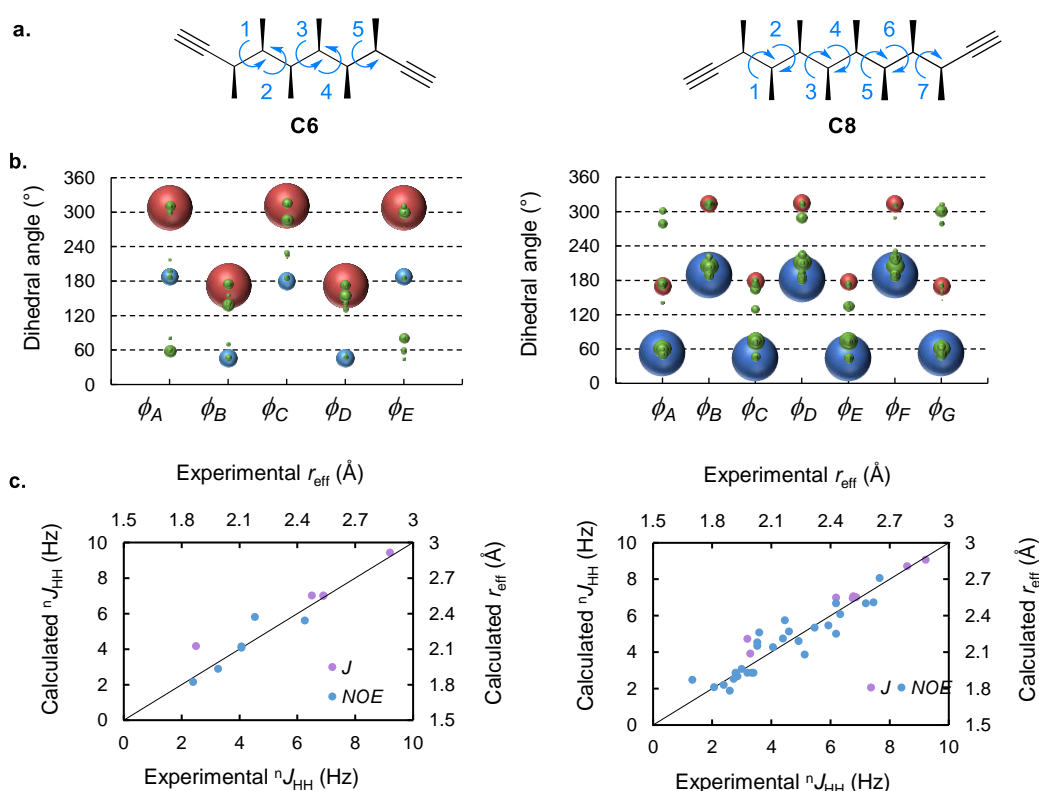


Figure 20. **a.** Dihedral angle numbering for compound **C6** (left) and **C8** (right). **b.** Dihedral angle populations of dialkynes **C6** (left) and **C8** (right) represented as bubble plots. Red dots belong to a *P* helix, blue dots belong to an *M* helix, green dots belong to non-helical conformers. **c.** Comparisons of DFT-computed ensemble-averaged ¹H-¹H scalar coupling constants and ¹H-¹H distances to the experimental values for **C6** (left) and **C8** (right).

Interestingly, the fraction of helical conformers in the overall population was inversely proportional to the chain length of the compound. Presumably, adding more rotatable bonds to the molecule increased the entropic cost associated with the conformational control.

	C6			C8		
	MAD	StDev	χ^2 (reduced)	MAD	StDev	χ^2 (reduced)
^1H–^1H scalar coupling	0.5 Hz	0.7 Hz	0.80	0.1 Hz	0.1 Hz	0.02
NOE distances	2.9%	1.8%	1.6	4.3%	5.4%	2.6

Table 4. Mean averaged deviation (MAD), standard deviation (StDev) and χ^2 (reduced) values of calculated NMR parameters for compounds **C6** (left) and **C8** (right).

The next step was the QM/NMR analysis of compounds with an odd number of stereocentres. **C7** was subjected to the same methodology as described above. Although helical conformers still remained the lowest-energy conformers, DFT calculations predicted that only 63% of the overall conformer population would adopt a helical shape, with a 50:50 ratio of *M* and *P* helices, as symmetry rules require (**Figure 21**). Helical conformations still represented the local minima but were really close in energy to non-helical structures (<1 kcal mol $^{-1}$). The computed ensemble-averaged ^1H – ^1H coupling constants were in agreement with the experimental values (*i.e.*, the mean averaged deviation (MAD) and the standard deviation (StDev) were both lower than 0.25 Hz with a χ^2 (reduced) value of 0.08). However, the same calculations applied to an artificial population containing only helical conformers (with the same 50:50 ratio of *M* and *P* helices) also gave an ensemble-averaged ^1H – ^1H coupling constants in good agreement with the measure $J_{\text{H-H}}$ values (both MAD and StDev <0.36 Hz and χ^2 (reduced) = 0.24). Hence, the analysis of coupling constants alone was not enough to determine whether non-helical conformers were present in the population or not.

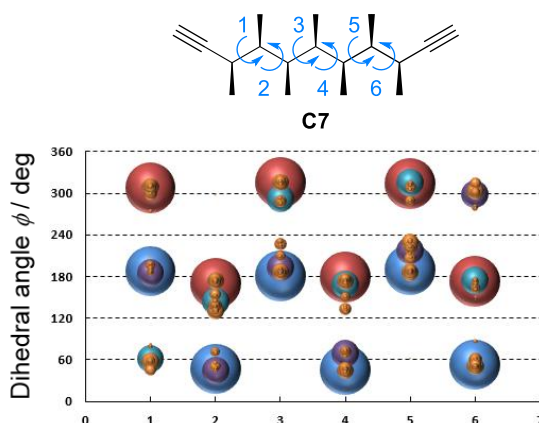


Figure 21. Dihedral angle populations of dialkyne **C7** predicted by DFT and represented as a bubble plot. Red dots belong to a *P* helix, blue dots belong to an *M* helix, orange, purple and turquoise dots belong to non-helical conformers.

To face this problem, two distinct sets of ensemble-averaged NMR parameters (δH , δC , J values and NOE-derived ^1H – ^1H distances) were calculated by DFT. The first set of parameters derived from the initial predicted population—consisting of 63% of helical conformers (50:50 $M:P$ ratio) and 37% of non-helical conformers—whereas the second set of parameters was based on a population containing only helical conformers (with the same 50:50 $M:P$ ratio). The comparison of both sets of data to the experimental values revealed that computed chemical shifts (δH and δC) and coupling constants (J) were insensitive to the change in conformer population, giving similar χ^2 (reduced) values in both cases. By contrast, the calculated NOE-derived ^1H – ^1H distances were found to be affected by the presence of non-helical conformers in the population. Indeed, the χ^2 (reduced) value for NOE distances generated from the population containing non-helical conformers was 3.76 while the other set of NOE distances derived from a population containing only helical conformers gave a χ^2 (reduced) value of 6.08. These values indicated that non-helical conformers were present in solution. DFT calculations showed that helical conformations still represented the local minima but were really close in energy to non-helical structures ($<1\text{ kcal mol}^{-1}$).

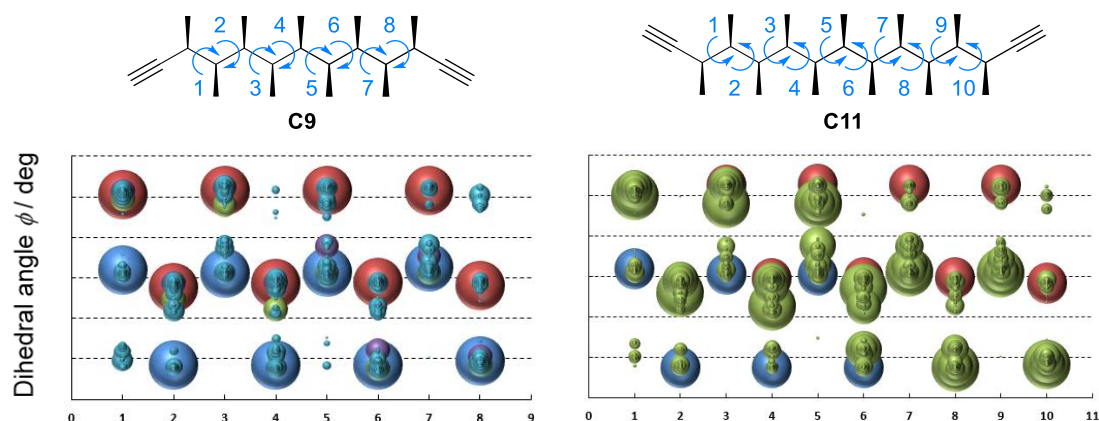


Figure 22. Dihedral angle populations of dialkynes **C9** and **C11** predicted by DFT and represented as bubble plots. Red dots belong to a P helix, blue dots belong to an M helix, green, purple and turquoise dots belong to non-helical conformers.

The same computational analysis was applied to compounds **C9** and **C11**. In both cases, DFT results showed a mixture of non-helical and helical conformers (**Figure 22**). As expected for *meso* compounds, the helical population was composed of a 50:50 ratio of M and P helices. Interestingly, the percentage of helical conformers (*i.e.*, combined M and P helices) dramatically decreased as the chain length increased (from 63% for **C7** to 27% for **C11**) (**Figure 23**). Once again, the entropic cost associated with the conformational control of a higher number of rotatable bonds could be invoked to rationalise this observation.

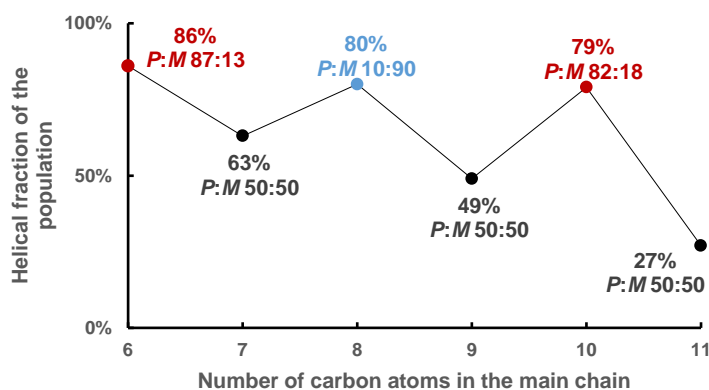


Figure 23. Combined helical conformer population of **C6**, **C7**, **C8**, **C9**, **C10** and **C11**.

In conclusion, a thorough QM/NMR approach confirmed the theoretical results predicted by the new diamond lattice-based model. It showed that C_2 -symmetric compounds such as **C6**, **C8** and **C10** had a strong conformational preference towards helical conformations, *P* helix for **C6** and **C10**, *M* helix for **C8**. These observations proved that the remarkable ‘helical switching by bidirectional chain extension’ described in Section 1.2.5. indeed occurred. *Meso* compounds such as **C7**, **C9** and **C11**, displayed a very different conformational behaviour. Interestingly, this series of molecules revealed a rare odd–even effect in alkanes that is not associated with bulk intermolecular interactions. To further confirm the QM/NMR results, vibrational circular dichroism was employed.

1.2.7. Vibrational Circular Dichroism analysis

*This part of the project was conducted by Márton Baglyas and György Tarczay who performed the calculations to access the vibrational circular dichroism (VCD) theoretical spectra and measured the experimental VCD response of compound **C10**. Their results were included in this thesis to provide a complete picture of the project.*

With the optimised geometries of both helical conformers of **C10** in hand, the vibrational circular dichroism (VCD) spectra of both helices could be simulated *in silico*. Surprisingly, although both conformers did not form a pair of enantiomeric structures, their calculated VCD spectra were almost mirror images of each other. They displayed maximal absorptions at the same wavenumbers (1420, 1065 and 980 cm^{-1}) but with opposite intensities (**Figure 24**). The measured experimental response showed the same pattern of absorption, slightly shifted towards the higher wavenumbers (1450, 1080 and 1010 cm^{-1}). The sign of these signals clearly indicated the presence of a *P* helix in solution. These results confirmed the previous QM/NMR studies performed by Dr. Siying Zhong.

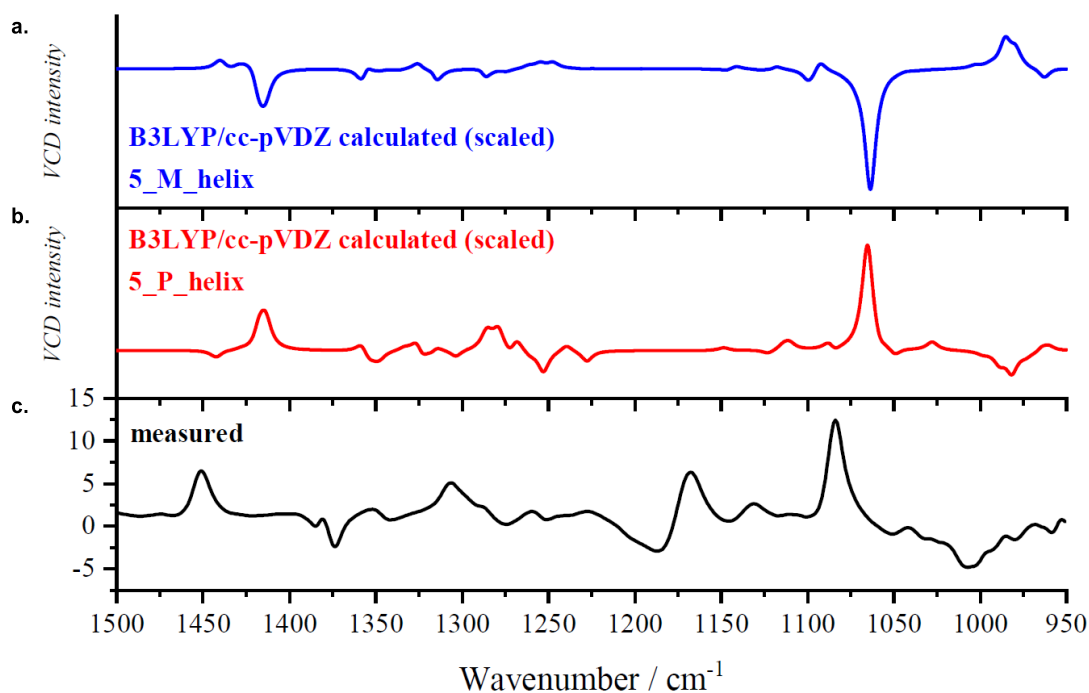


Figure 24. Comparison of calculated and experimental VCD spectra. **a.** Calculated VCD spectrum of the optimised lowest energy *M* conformer of **C10**. **b.** Calculated VCD spectrum of the optimised lowest energy *P* conformer of **C10**. **c.** Experimental VCD response of **C10** in chloroform-*d* (the signals between 1150 and 1200 cm^{-1} correspond to the solvent).

1.2.8. Influence of the end-groups on the conformation

Having established the rules that dictated the conformation preference of the backbone itself, the next task of the project was to study the influence of the end-groups on the conformation of the chain. In the previous part of the study, all the *gauche* interactions were considered to be equivalent in terms of energy penalty. In this section, it was necessary to distinguish the different types of *gauche* interactions encountered in such molecules. To do so, a more careful inventory was made based on the proposed model. To simplify the analysis, C_2 -symmetric molecule were chosen to begin with.

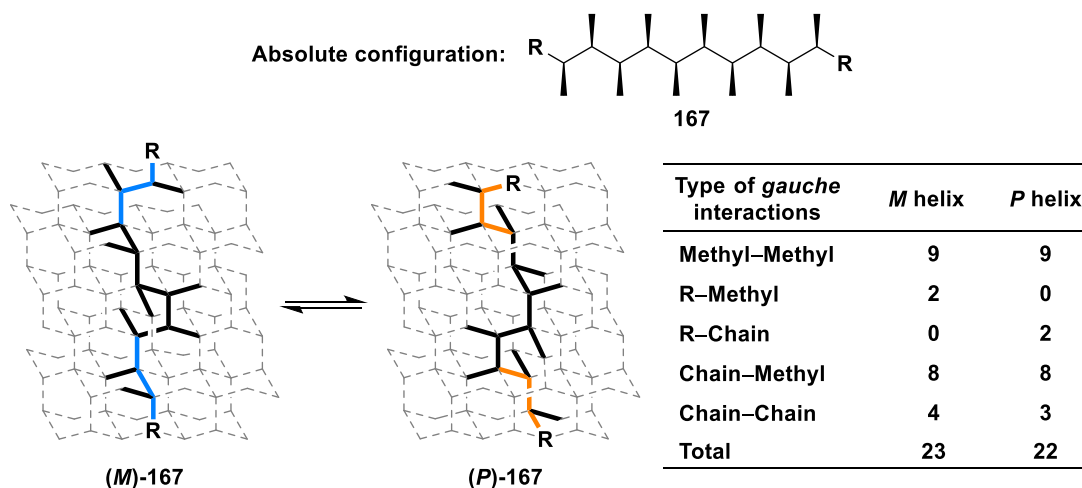


Figure 25. Detailed inventory of the different *gauche* interactions present in both helical conformers of a C_2 -symmetric compound bearing an even number (10) of stereocentres in the backbone.

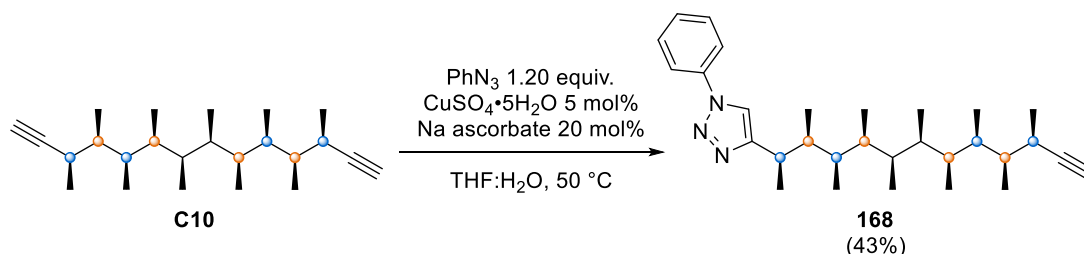
For example, in the case of a compound with ten stereocentres in the backbone and with the absolute configuration depicted in **Figure 25**, one could count nine Methyl–Methyl, two R–Methyl, eight Chain–Methyl and four Chain–Chain *gauche* interactions in the *M* conformer. On the other hand, in the *P* conformer, one could identify nine Methyl–Methyl, two R–Chain, eight Chain–Methyl and three Chain–Chain *gauche* interactions. By crossing out the interactions present in both helices, it was established that the *P* form would be favoured if the energy penalty (*E*) of two R–Chain *gauche* interactions was lower than the sum of the energy penalty of two R–Methyl *gauche* interactions and one Chain–Chain *gauche* interaction. Conversely, the *M* form would be favoured if the energy penalty of two R–Chain *gauche* interactions was higher than the sum of the energy penalty of two R–Methyl *gauche* interactions and one Chain–Chain *gauche* interaction, as summarised by these two equations:

$$(I) \quad P \text{ helix favoured} \Leftrightarrow 2 \times E(\text{R} - \text{Chain}) < 2 \times E(\text{R} - \text{Methyl}) + 1 \times E(\text{Chain} - \text{Chain})$$

$$(II) \quad M \text{ helix favoured} \Leftrightarrow 2 \times E(\text{R} - \text{Chain}) > 2 \times E(\text{R} - \text{Methyl}) + 1 \times E(\text{Chain} - \text{Chain})$$

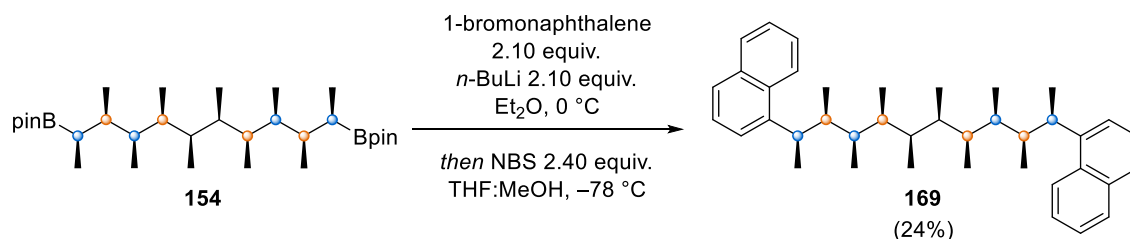
Intuitively, it seemed really difficult to find an end-group (R) able to satisfy equation (II). A first idea to reach this goal was to install large groups at the end of the chain to generate a steric clash with the backbone and make the helix switch. It was important to notice that compounds such as **158** did not show any helicity change, in spite of bulky TIPS groups attached to their alkyne moieties. However, in these examples, the sterically demanding silyl group was separated from the backbone by a 4.6 Å-long linear spacer composed of one C–C single bond (≈ 1.5 Å), one $\text{C}\equiv\text{C}$ triple bond (≈ 1.2 Å) and one C–Si bond (≈ 1.9 Å). The bulky group needed to be closer to the chain to interact in an efficient manner.

One of the easiest ways to increase the size of the alkyne terminal group was to make it react with an azide-containing molecule to generate a triazole ring. According to this strategy, compound **C10** was engaged in a 1,3-dipolar cycloaddition reaction with phenyl azide to obtain triazole **168** (Scheme 34). Unfortunately, ^1H NMR analysis revealed that both end-groups were in a predominantly *gauche* conformation, characteristic of a *P* helix for this absolute configuration.



Scheme 34. Synthesis of triazole **168** using a 1,3-dipolar cycloaddition methodology.

Having one large group at the end of the chain was not enough to make the screw-sense change. Therefore, the next molecule synthesised from boronic ester **154** via the transition metal-free cross-coupling reaction described above was compound **169** (Scheme 35). The bicyclic naphthyl ring was thought to be substantially bigger than a triazole ring and therefore have a better chance to interact significantly with the chain. Sadly, the first two CHs of the backbone gave very broad signals by ^1H NMR—probably because of constrained rotation of the aromatic rings—and their $^3J_{\text{H-H}}$ values could not be extracted from the spectrum.



Scheme 35. Preparation of compound **169** using a transition metal-free cross-coupling methodology.

Yet, an X-ray structure of compound **169** could be obtained (Figure 26) and showed that the aromatic rings presented their flat face to the chain, reducing their steric hindrance. In this conformation, the naphthyl group became a small group which did not interact with the backbone.

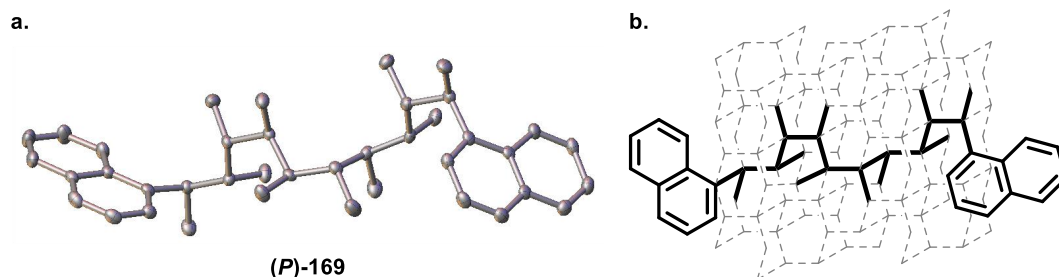
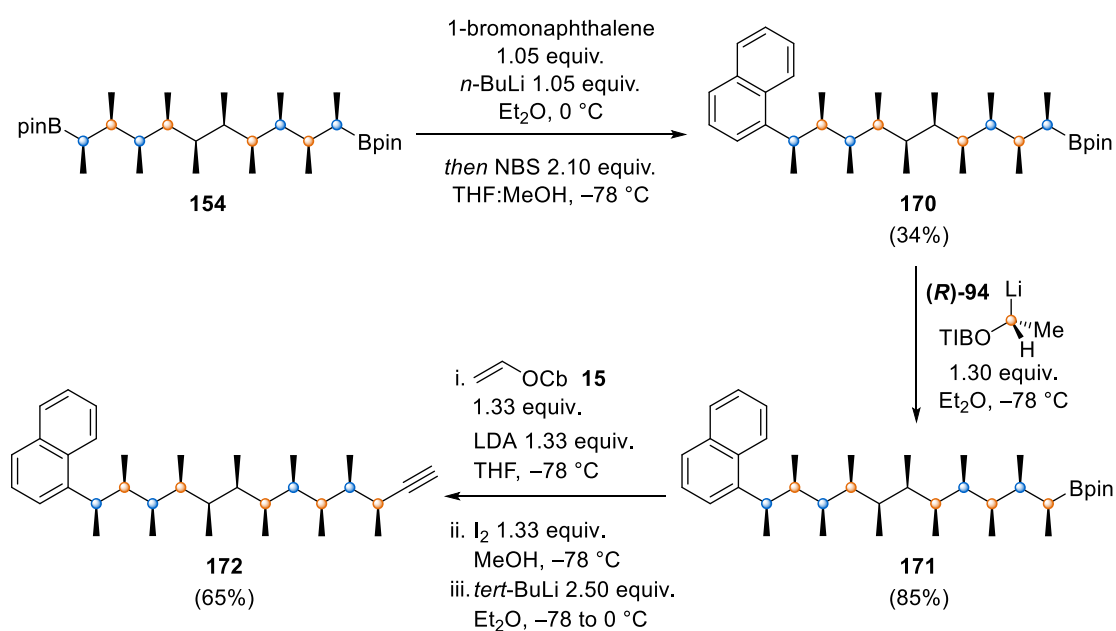


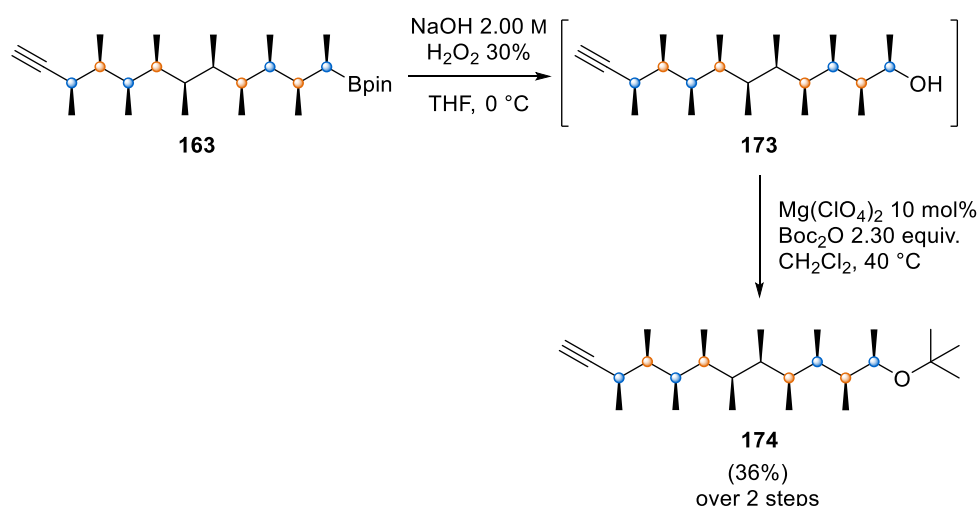
Figure 26. **a.** X-ray crystal structure of **169**. Ellipsoids shown at 50% probability. Hydrogen atoms and solvent molecules have been omitted for clarity. **b.** Conformation of compound **169** in the solid state drawn on a diamond lattice.

According to the model, for compounds with an odd number of stereocentres in the chain, the helical conformers would have one end-group in a *gauche* conformation and the other in an *anti* conformation. One could then design a molecule with a bulky end-group which would prefer to stand in an *anti* conformation and a small group which would adopt a *gauche* conformation. Based on this analysis, compound **172** was synthesised in three steps from boronic ester **154** (**Scheme 36**). ^1H NMR showed that the naphthyl group oriented the first dihedral angle towards the *gauche* conformation ($^3J_{\text{H-H}} = 7.9$ Hz) and the second angle towards the antiperiplanar conformation ($^3J_{\text{H-H}} = 4.6$ Hz). However, apart from these two bonds, the rest of the chain did not exhibit any conformational preference ($5.1 \text{ Hz} < ^3J_{\text{H-H}} < 7.0 \text{ Hz}$). As shown by QM/NMR results in Section 1.2.6., the effect of entropy might have been too strong in this case (eleven rotatable C–C bonds). The desired control might be achieved using the same end-group design but on a small chain (*i.e.*, containing seven or nine stereocentres).



Scheme 36. Preparation of alkyne **172** from C_2 -symmetric boronic ester **154**.

The previous results clearly showed that an aromatic group was not large enough to verify equation (II). Consequently, the next objective was to install a bulkier end-group, such as a *tert*-butyl group. Steric hindrance was not the only advantage of the *tert*-butyl moiety. A few years ago, Hoffmann pointed out that having a *tert*-butyl group at the end of a non-substituted aliphatic chain could control the conformation of the first three bonds by avoidance of *syn*-pentane interactions, forcing the first dihedral angle of the chain to adopt an antiperiplanar conformation.^{64,184,209,210} This conformation was in agreement with equation (II). From these considerations, attaching a *tert*-butyl group to the chain seemed to be the best option to observe the opposite helicity (*M*). However, from a more practical point of view, ¹H NMR signals of an aliphatic molecule with no heteroatom were likely to be overlapped and thus the extraction of NMR parameters might be difficult. Therefore, one oxygen atom was included in the target molecule *via* oxidation of desymmetrised boronic ester **163** (Scheme 37). Finally, the *tert*-butyl group was installed using the methodology developed by Bartoli and co-workers.²¹¹



Scheme 37. Synthesis of alkyne **174** *via* oxidation of boronic ester **163** and alkylation of intermediate **173**.

Preliminary ¹H NMR analysis revealed that the switch did not occur. Starting from the alkyne group, the first four coupling constant values were 7.9 Hz, 4.5 Hz, 7.6 Hz and 4.0 Hz. This *large, small, large, small* sequence accounted for a *P* helix. However, it was important to notice that these constants were significantly different from the values observed for dialkyne **C10**. By direct comparison of these numbers, one could infer that the conformational preference towards the *P* conformer was reduced due to the presence of a *tert*-butyl group.

To obtain more information about the effect of the *tert*-butyl group on the conformation of the chain, the QM/NMR approach described in Section 1.1.4.2. was applied to compound **174** in collaboration with Dr. Siying Zhong. Once again, a significant difference was observed between MM and DFT results (**Figure 27b**). Although MM predicted that 86% of the overall population would adopt a helical shape with an 81:19 *M*:*P* ratio, DFT geometry and energy calculations

showed that only 50% of the conformers would be helical with a strong conformational bias towards the opposite screw-sense (16:84 *M*:*P* ratio). The DFT-derived ensemble-averaged $J_{\text{H-H}}$ coupling constants were in good agreement with the measured values (MAD = 0.7 Hz; StDev = 0.9 Hz, χ^2 (reduced) = 0.9 Hz). Yet, the calculated ensemble-averaged ^1H - ^1H distances did not fit the experimental values, with a χ^2 (reduced) value of 4.60 (**Figure 27c**). At this stage, two explanations were plausible: either DFT inaccurately estimated the ratio between *M* and *P* helices, or inaccurately predicted the ratio between helical and non-helical populations.

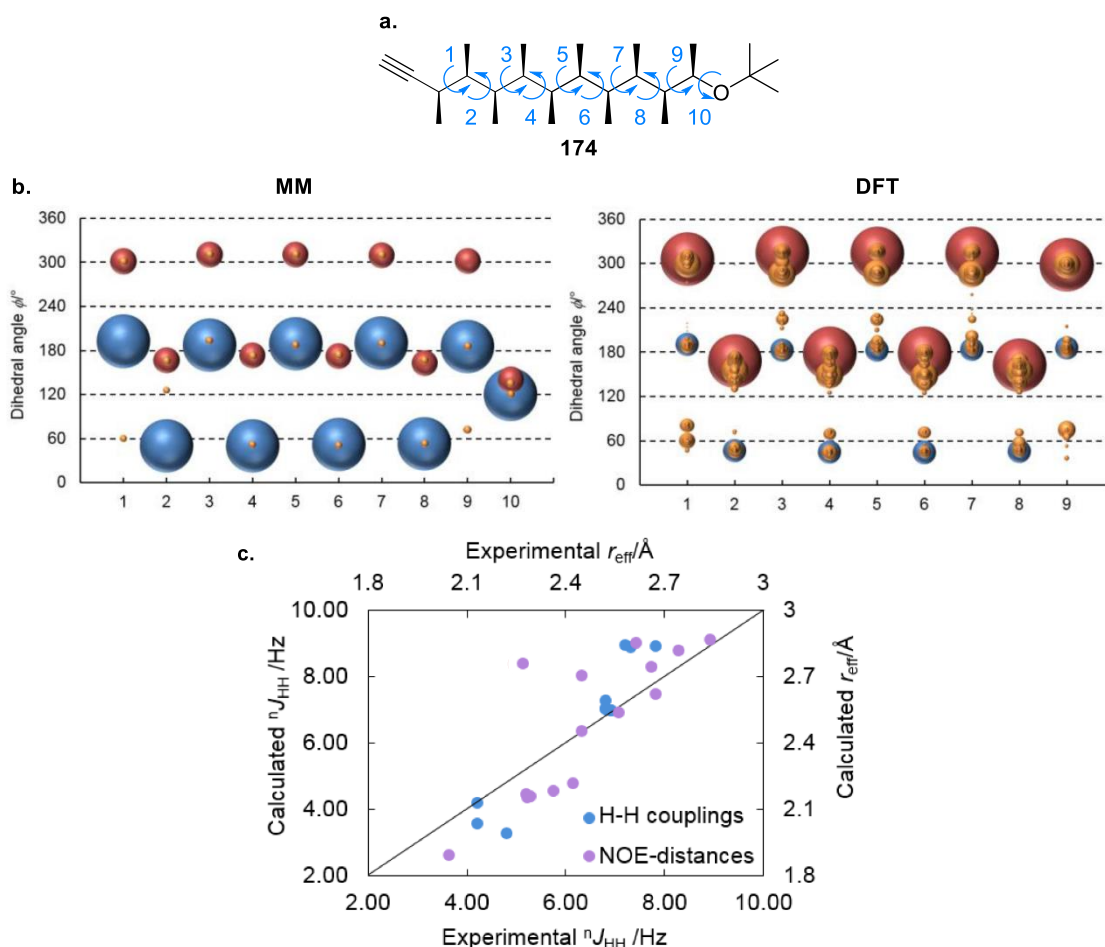
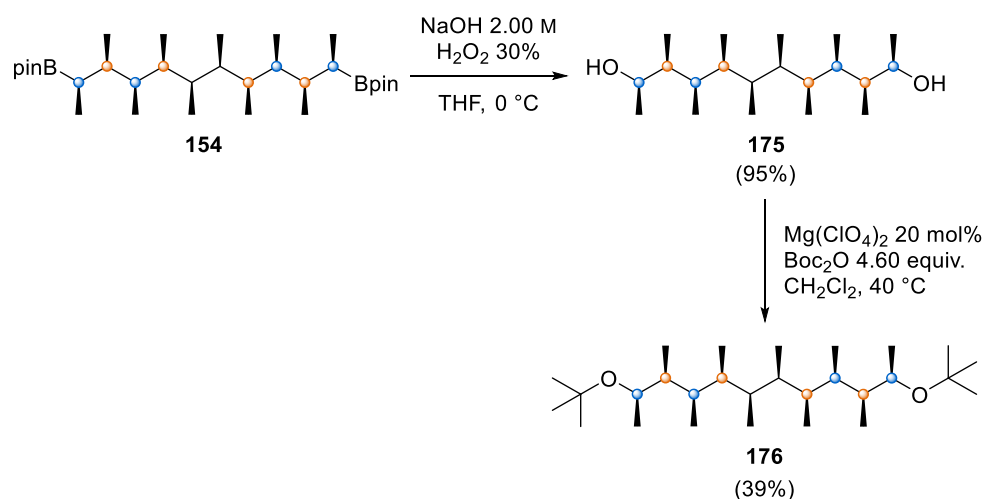


Figure 27. **a.** Dihedral angle numbering for compound 174. **b.** Dihedral angle populations of compound 174 predicted by MM (left) and DFT (right) and represented as a bubble plot. Red dots belong to a *P* helix, blue dots belong to an *M* helix, orange dots belong to non-helical conformers. **c.** Comparisons of DFT-computed ensemble-averaged ^1H - ^1H scalar coupling constants and ^1H - ^1H distances to the experimental values.

To better understand the effect of a *tert*-butyl group on the conformation of the chain, an analogue bearing two *tert*-butyl groups, compound 176, was synthesised in two steps from boronic ester 154 (**Scheme 38**). Intermediate diol 175 was isolated and analysed by NMR in a non-protic solvent to establish whether the propensity of the hydroxyl group to make intermolecular hydrogen bonds would encourage the molecule to aggregate and thus force the backbone to stand in an

extended conformation (*i.e.*, *M* helix). Unfortunately, once again, a *P* helix was observed in toluene-*d*₈, with the following coupling constant sequence: 8.1 Hz (*large*), 3.4 Hz (*small*) and 8.5 Hz (*large*). An X-ray structure (**Figure 28**) showed that hydrogen bonding was still allowed, despite the *P*-helical conformation of the chain.



Scheme 38. Oxidation of boronic ester **154** to obtain diol **175** and subsequent double alkylation to give ether **176**.

Concerning compound **176**, the extraction of chemical shifts, $J_{\text{H-H}}$ values and NOE distances was very difficult due to spectrum congestion. All the protons of the backbone were overlapped except the ones geminal to the oxygen atoms, which coupled to the next protons with a constant of 5.8 Hz. This rather small coupling constant might be indicative of a conformational change. At least, by comparison with compounds **C10** and **174**, one could infer that the *P* form was even more destabilised by the presence of a second *tert*-butyl group. Unfortunately, due to the lack of information about experimental NMR parameters (δH , δC , $J_{\text{H-H}}$, NOE distances), the QM/NMR approach was not applied to compound **176** and therefore the effect of the *tert*-butyl groups remains unclear.

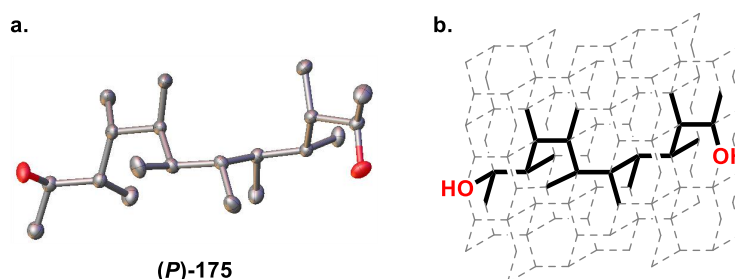


Figure 28. **a.** X-ray crystal structure of **175**. Ellipsoids shown at 50% probability. Hydrogen atoms and solvent molecules have been omitted for clarity. **b.** Conformation of compound **175** in the solid state drawn on a diamond lattice.

To summarise, the proposed theoretical model was refined based on the identification of different types of *gauche* interactions. These qualitative observations were translated into two equations which describe the relationship between the screw-sense of the molecule and the steric interactions involving end-groups and backbone. Six additional compounds with different combinations of end-groups were synthesised and analysed by ^1H NMR. This non-exhaustive “structure–conformation relationship” screening revealed that small substituents such as an alkyne group or a hydroxyl group verified equation (I). According to this study, aromatic groups could also be considered as small groups. The presence of one *tert*-butyl group seemed to decrease the helical preference described by equation (I). Interestingly, a molecule with two *tert*-butyl groups might verify equation (II) and therefore display the opposite screw-sense. Unfortunately, this hypothesis could not be validated nor refuted due to the lack of structural information about compound **176**. Nevertheless, the comparison of coupling constant values of compounds **C10**, **174** and **176** suggested that the combined effects of two *tert*-butyl groups could be used to design a switchable system.

1.2.9. Towards a new helical switch

The ultimate goal of this project was to design a helical molecule with the ability to switch from one screw-sense to another, in response to an external stimulus. In this section, the ability of such a compound to switch after chemical modification of its chain-ends was studied. In terms of potential applications, a reversible helical switch seemed to be more appealing than a non-reversible system. For this reason, only high-yielding reversible reactions were investigated.

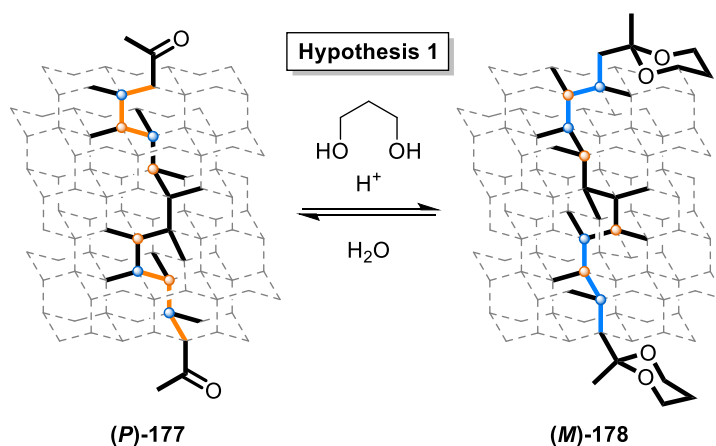
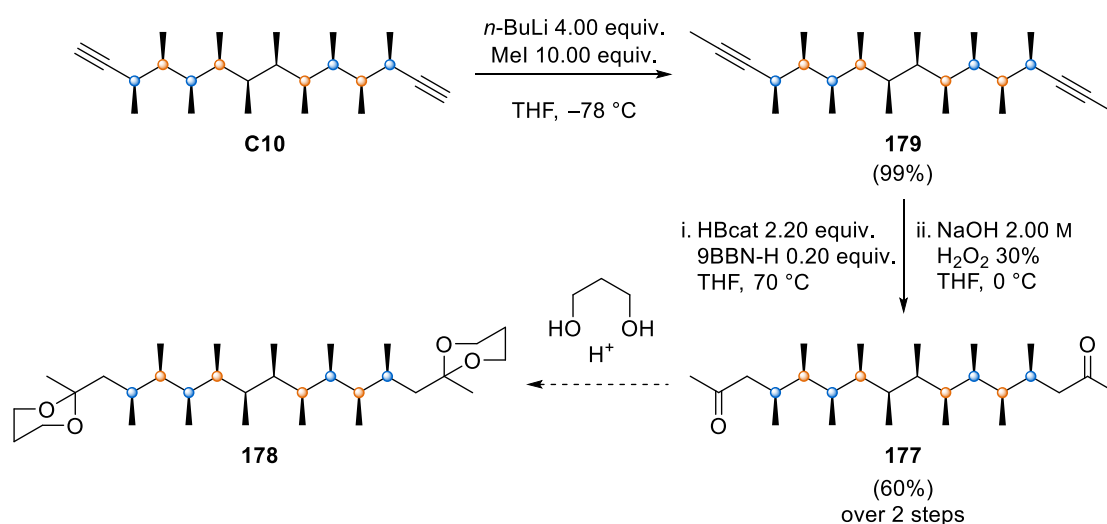


Figure 29. Hypothetical reversible helical switching from diketone **177** to diacetal **178**.

Based on previous results, the design of a switchable all-*syn* methyl-substituted chain might be achieved using the effect of *tert*-butyl groups. Ideally, a small end-group favouring one helical conformation would be transformed into a bulky *tert*-butyl group to induce a conformational

change. After that, the reverse conformational switch could be triggered by converting the *tert*-butyl group back to the initial small group. According to the previous section, end-groups with a sp^2 geometry could be considered as small groups and therefore should verify equation (I). They were generally easy to install by C–B bond derivatisation. However, the addition and removal of a *tert*-butyl group was more challenging in terms of synthesis. It appeared more practical to design a target molecule bearing an analogous end-group (*i.e.*, with the same geometry as the *tert*-butyl group), which could be efficiently installed and cleaved under mild conditions. Actually, the formation of an acetal from a ketone met all of the requirements. Indeed, in the course of this reversible reaction, the hybridisation of the carbon centre is modified from sp^2 in the ketone to sp^3 in the acetal, the latter acting as a *tert*-butyl mimic to force the first dihedral angle to adopt an antiperiplanar conformation (**Figure 29**). With this strategy in mind, diketone **177** was prepared in three steps, starting from dialkyne **C10**, in 58% overall yield (**Scheme 39**).



Scheme 39. Synthesis of diketone **177** via double alkylation of **C10**, followed by hydroboration and subsequent oxidation.

^1H NMR analysis of compound **177** was extremely surprising. Contrary to the predictions, the observed $^3J_{\text{H-H}}$ sequence was 4.1 Hz (*small*), 7.8 Hz (*large*), 4.0 Hz (*small*), 7.8 Hz (*large*). For the first time with this absolute configuration, a strong preference towards the *M* form was clearly identified. Counting the number of *gauche* interactions in both helical conformers of **177** did not fully rationalise this observation. In fact, these numbers depended on the position of the methyl-ketone group. To avoid *syn*-pentane interactions, the end-group could adopt two different orientations in each conformer (**Figure 30**). In the *P* helix, the end-group could generate either one or two *gauche* interactions; therefore, the overall number of *gauche* interactions in the molecule could be 24, 25 or 26. However, in the *M* helix, both orientations of the end-group created only one *gauche* interaction and therefore the overall number of *gauche* interactions was invariably

25. As a result, the molecule preferred adopting a *M*-helical conformation, which meant the end-group had a reduced steric impact.

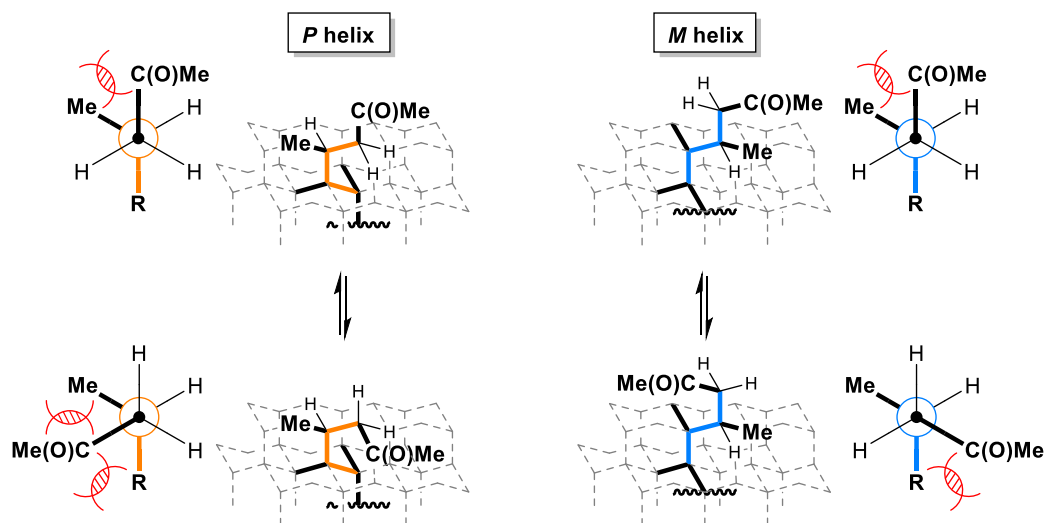
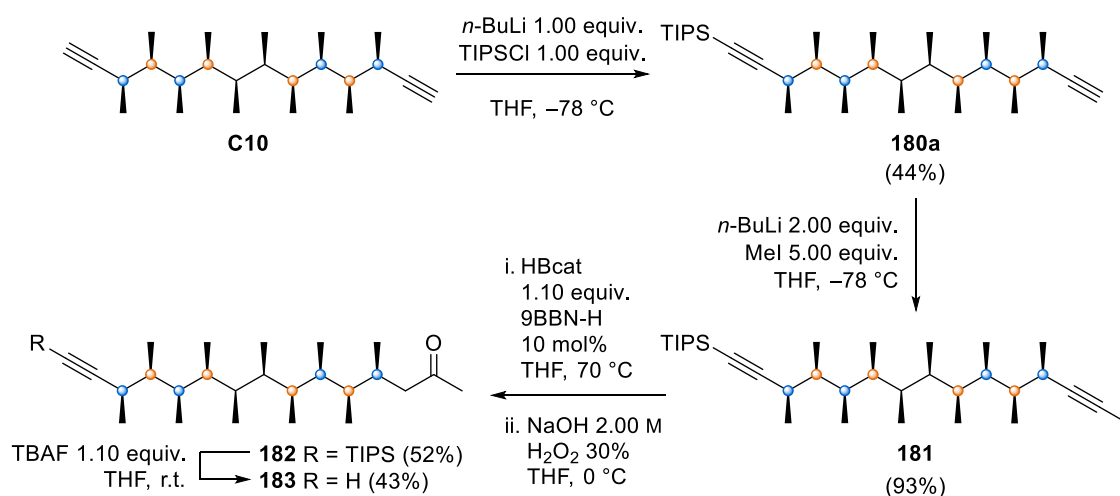


Figure 30. The end-group of compound **177** could adopt four different conformations to avoid *syn*-pentane interactions. The rotation of the end-group in the *P* helix was more constrained than in the *M* helix.

To test whether one directing group could dictate the screw-sense of the chain in the presence of another directing group with the opposite induction effect, an asymmetric compound (**183**) bearing one alkyne group, which favoured the *P* form, and one methylketone group, which was an *M*-helix inducer, was designed and synthesised (**Scheme 40**). ^1H NMR analysis revealed that, starting from the alkyne group, the first and the last coupling constants were close to 7 Hz ($5.9\text{ Hz} < {}^3J_{\text{H-H}} < 7.0\text{ Hz}$). Unfortunately, all the other CH signals were overlapped. Nevertheless, these average values indicated that compound **183** was likely to exist as a 50:50 mixture of *P* and *M* helices in solution.



Scheme 40. Preparation of ketone **183** by desymmetrisation of dialkyne **C10**.

With diketone **177** being an *M* helix, the initial strategy to form the acetal group and trigger a helical switch was abandoned. Alternatively, another approach was envisaged in which diol **175** (*P* helix) would be converted to diacetate **184** (**Figure 31**). This diester was structurally very similar to diketone **177** and, therefore, was expected to display the same conformational preference (*M* helix). To switch back to the *P*-helical conformation, a simple hydrolysis under basic conditions would then regenerate the starting diol. Pleasingly, a DMAP-catalysed esterification reaction with acetic anhydride delivered diacetate **184** in quantitative yield (**Scheme 41**).

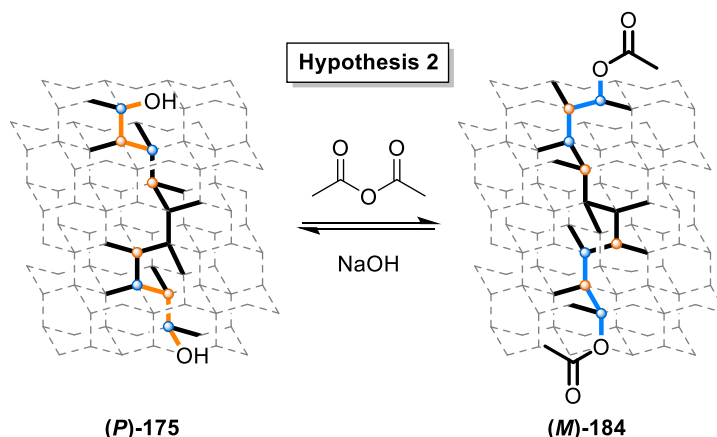
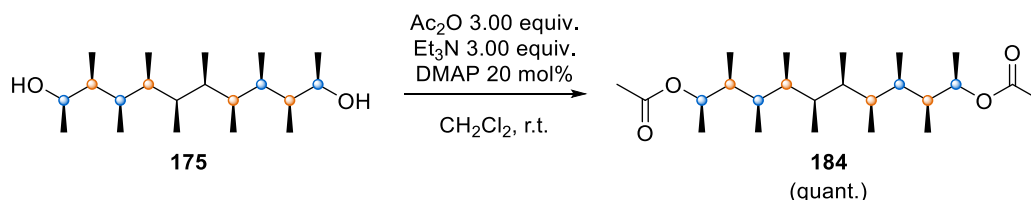


Figure 31. Hypothetical reversible helical switching from diol **175** to diacetate **184**.

Once again, ^1H NMR analysis was surprising. Instead of the expected *small, large, small, large* sequence, the first three coupling constant values were 7.8 Hz (*large*), 4.2 Hz (*small*) and 7.8 Hz (*large*), characteristic of a right-handed (*P*) screw-sense for this absolute configuration. This result might be rationalised by considering the A-value of an acetate group. According to the literature,^{212,213} this ester possesses an A-value between 0.60 and 0.79 kcal mol⁻¹. For comparison, the A-value of a methyl group is about 1.70 kcal mol⁻¹. These numbers showed that the acetate group was very small in terms of steric hindrance. For this reason, compound **184** verified equation (I) and thus folded into a *P* helix.



Scheme 41. Synthesis of diacetate **184** by esterification of diol **175**.

A different strategy was then envisaged based on the helical switching by chain extension described in Section 1.2.5. Indeed, the conformational preference of the backbone changed each time that two new stereocentres were added at both extremities. The chain switched from *P* to *M* to *P* as it grew from six to eight to ten stereocentres. One more bidirectional homologation would

then give an *M* helix with twelve stereocentres. From this observation, a new plan was designed involving diamine **185** (Figure 32). This primary amine bore ten stereocentres. According to its absolute configuration, it should behave like dialkyne **C10** and exist as a *P* helix in solution. Then, after alkylation, the molecule would be structurally analogous to a compound with twelve stereocentres and, therefore, should favour the *M* form to avoid *syn*-pentane interactions. In other words, the alkylation reaction would mimic a bidirectional chain extension.

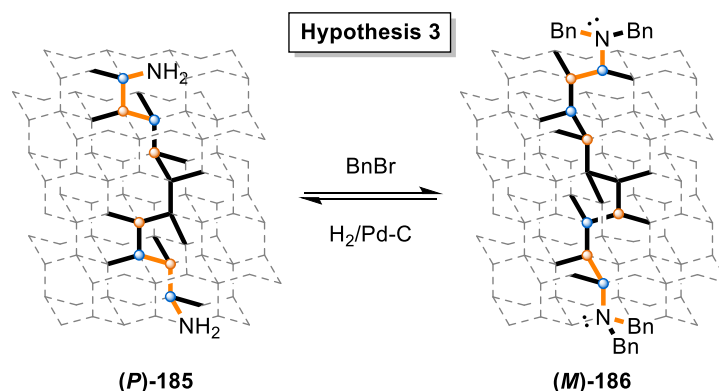
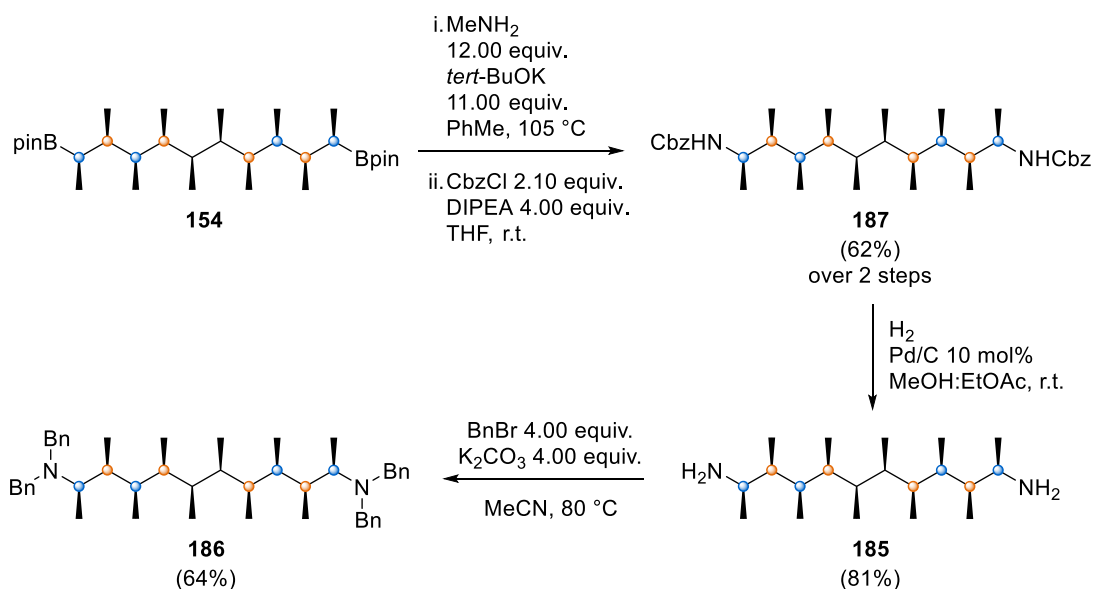


Figure 32. Hypothetical reversible helical switching from primary amine **185** to tertiary amine **186**.

Boronic ester **154** was subjected to Morken's amination conditions to obtain, after basic work-up, desired diamine **185** (Scheme 42). However, the crude compound was too polar to be purified and was converted to dicarbamate **187** to facilitate isolation. Finally, a palladium-catalysed hydrogenolysis gave the desired molecule in 50% yield over three steps.



Scheme 42. Synthesis of primary amine **185** using Morken's methodology. The crude primary amine was directly transformed into carbamate **187** to facilitate purification.

^1H NMR confirmed that the molecule adopted a right-handed helical conformation in solution, with the following coupling constant sequence: 7.9 Hz (*large*), 3.7 Hz (*small*), 8.3 Hz (*large*) and

3.3 Hz (*small*). Then, treatment with benzyl bromide afforded tertiary amine **186** in 64% yield. Unfortunately, ^1H NMR showed that the molecule still folded into a *P* helix, with an unusually high level of control. The first three $^3J_{\text{H-H}}$ values were 10.0 Hz (*large*), 2.4 Hz (*small*) and 9.9 Hz (*large*). Once again, the number of *gauche* interactions was key to understanding this result. The initial hypothesis relied on the fact that, for this absolute configuration, a chain containing twelve stereocentres bore 28 *gauche* interactions in the *P*-helical conformation and only 27 *gauche* interactions in the *M* form. Therefore, a left-handed helix was expected in solution. However, a closer look at the benzyl moieties revealed that the phenyl groups were involved in four additional *gauche* interactions in the *P* conformer and generated six additional *gauche* interactions in the *M* conformer (**Figure 33a**). As a consequence, the overall number of *gauche* interactions in the *M* helix (33) was higher than in the *P* helix (32), which became the lowest energy conformer, both in solution and in the solid state (**Figure 33b,c**).

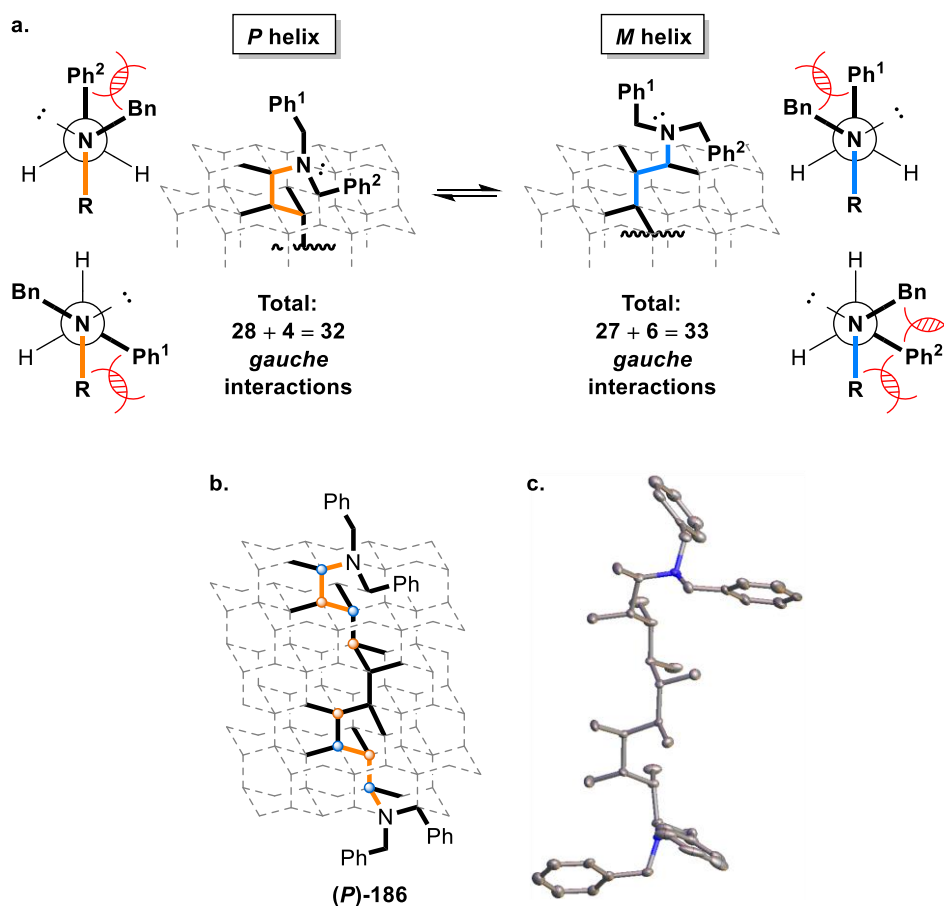


Figure 33. **a.** Phenyl groups were also involved in steric conflicts. They created four more *gauche* interactions in the *P* conformer and six more *gauche* interactions in the *M* helix. **b.** Major conformer (*P* helix) of amine **186** in solution, drawn on a diamond lattice. **c.** X-ray crystal structure of **186**. Ellipsoids shown at 50% probability. Hydrogen atoms and solvent molecules have been omitted for clarity.

In 1999, Hoffmann and co-workers showed that the conformation of 4-methylpentan-2-amine depended on the protonation state of the amino group.⁵⁹ They observed the conformational

switching of the C–C–C–N dihedral angle, from *gauche* to antiperiplanar, when acetic acid was added in the NMR tube. Based on this study, another strategy was proposed (**Figure 34**). According to Hoffmann's results, one could imagine that the *P* conformer of diamine **185** could undergo a helical switching in the presence of acid. Such a compound would therefore be described as a pH-responsive molecular switch and could eventually find practical applications.

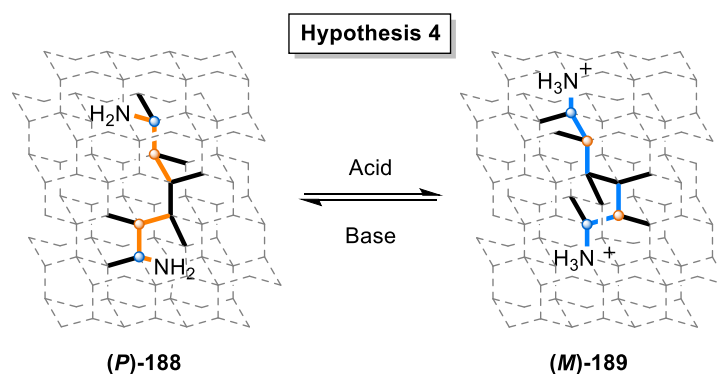
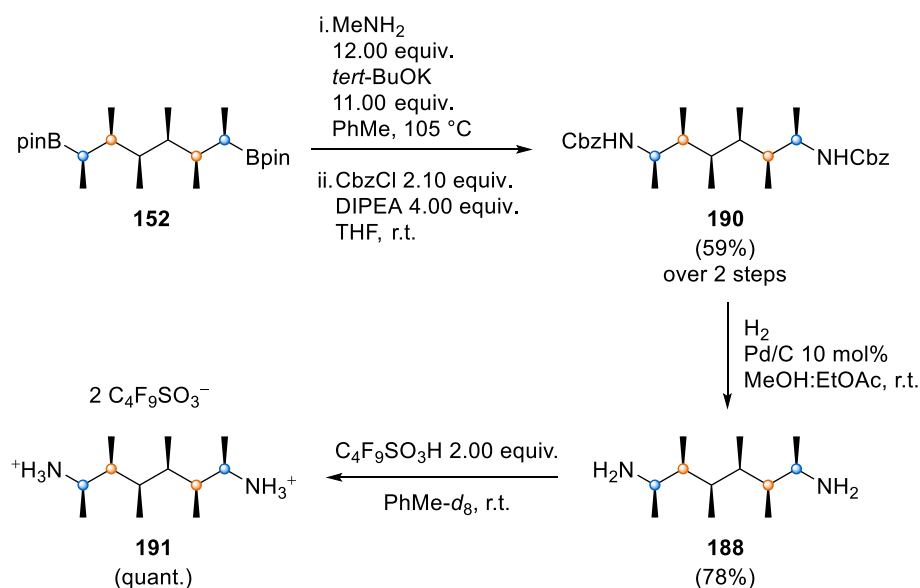


Figure 34. Hypothetical reversible helical switching from primary amine **188** to ammonium **189**.

To test this hypothesis, compound **185** was mixed with two equivalents of acetic acid in deuterated DMSO. Unfortunately, only the first coupling constant (5.0 Hz) could be extracted due to spectrum congestion. To face this problem, a shorter version of the molecule, diamine **188**, was synthesised (**Scheme 43**), using the same methodology as mentioned above. ^1H NMR confirmed that it adopted a right-handed conformation in solution. Addition of acetic acid in DMSO- d_6 led to the same overlap issues. Moreover, this time, the first coupling constant reached 5.9 Hz, which was less encouraging. In previous examples, the use of deuterated toluene improved the quality of the ^1H NMR spectrum. Therefore, diamine **188** was solubilised in toluene- d_8 and two equivalents of acetic acid were added. Immediately, a white precipitate formed, rendering the NMR analyses impossible. At that point, it seemed more sensible to replace acetic acid with a more organic proton source to improve the solubility of the resulting ammonium salt. Hence, two equivalents of nonafluorobutanesulfonic acid were added to a solution of diamine **188** in deuterated toluene. Pleasingly, no precipitation was observed and $^3J_{\text{H-H}}$ values could be obtained. The first two coupling constants were found to be 6.3 Hz and 5.0 Hz. Sadly, these values were not indicative of an *M* helix. They showed that either the molecule was present as a mixture of both conformers or it completely lost its conformational preference. Due to a lack of time, no further hypotheses were explored.



Scheme 43. Synthesis of primary amine **188** and protonation with nonafluorobutanesulfonic acid to access ammonium **191**.

1.3. Conclusion

This research project aimed to develop a new class of helical molecules which, upon activation from an external stimulus, would be able to reversibly switch from one screw-sense to the other. All-*syn* methyl-substituted hydrocarbons, as described by Aggarwal¹ in 2014, were shown to adopt helical conformations with very high levels of control. More importantly, one of these unique molecules could access either the *M* or the *P* screw-sense, depending on its physical state. Therefore, all-*syn* methyl-substituted hydrocarbons seemed to be promising candidates for the design of a new class of molecular switches.

To achieve this goal, it was necessary to understand what controlled the conformation of such molecules. A first assumption suggested that a link existed between the absolute configuration of the termini, the relative size of the end-groups and the screw-sense of the backbone. To test this hypothesis, two target molecules (with ten and eleven stereocentres in their backbones) were designed and synthesised. Unfortunately, the initial convergent synthetic route failed due to the unsuccessful lithiation–borylation coupling between two bulky advanced intermediates. Consequently, a more linear approach was employed, involving nine or ten iterative homologations of boronic ester *via* a methodology called ‘assembly-line synthesis’, to prepare both target compounds. Their analysis by ¹H NMR and MM was surprising. While the first molecule with an even number of stereocentres displayed the expected controlled helical conformation, the second

compound with an odd number of stereocentres showed a more disordered conformational landscape. This observation served as a starting point to establish a new stereochemical model able to predict the screw-sense of such helical hydrocarbons.

	Even number of stereocentres		Odd number of stereocentres	
Absolute configuration				
Predicted screw-sense	Right-handed helix (<i>P</i>)	Left-handed helix (<i>M</i>)	Mixture of <i>M</i> , <i>P</i> and non-helical conformers	

Table 5. Screw-sense prediction table.

A diamond lattice-based analysis revealed that the number of *gauche* interactions in the chain was one of the key parameters that dictated its conformational preference. The model established that, to completely avoid *syn*-pentane interactions, these compounds could adopt two conformations, an *M* helix or a *P* helix. However, in the case of a molecule with an even number of stereocentres, one of these two helical conformers possessed one more *gauche* interaction and therefore was higher in energy. In the case of a molecule with an odd number of stereocentres, both helical conformers showed the same number of *gauche* interactions. They could reduce this number by allowing their terminal dihedral angles to adopt a *gauche* conformation. However, by doing so, the helicity of the chain was broken, diminishing the percentage of helical conformers in the overall population. Therefore, by minimizing the number of *gauche* interactions, molecules with an even number of stereocentres increased their conformational preference towards one helical form, whereas molecules with an odd number of stereocentres tended to expand their non-helical conformer populations.

To validate this model, the relationship between conformational control and chain length was studied. A series of six compounds of different chain lengths (from six to eleven stereocenters) was designed and synthesised using an efficient bidirectional iterative homologation of C_2 -symmetric boronic esters. A QM/NMR approach was employed to quantitatively describe the conformational landscape of these molecules. This technique relies on the comparison of DFT-derived NMR parameters (δH , δC , J_{H-H} , NOE distances) to experimental values. Once all the predicted parameters are in good agreement with the measured values, the corresponding DFT-derived conformational population has a high probability to reflect the reality. Pleasingly, this approach confirmed the theoretical model with a good degree of confidence. Another analytical technique, VCD analysis, also corroborated these results.

In this study, the link between screw-sense and end-groups was investigated. Based on the different types of *gauche* interactions present in the backbone, two equations were established to model this relationship.

$$(I) \quad P \text{ helix favoured} \Leftrightarrow 2 \times E(R - \text{Chain}) < 2 \times E(R - \text{Methyl}) + 1 \times E(\text{Chain} - \text{Chain})$$

$$(II) \quad M \text{ helix favoured} \Leftrightarrow 2 \times E(R - \text{Chain}) > 2 \times E(R - \text{Methyl}) + 1 \times E(\text{Chain} - \text{Chain})$$

A screening of different substituents at the termini revealed that alkyne, hydroxyl, amino or aromatic groups could be considered as ‘small’ groups, favouring the helical conformer with both terminal dihedral angles in a *gauche* conformation. In line with Hoffmann’s work,^{64,184} *tert*-butyl groups were found to have a dramatic impact on the backbone conformation. According to QM/NMR analysis, one of these bulky end-group was not enough to induce the helical switching. However, the combined effects of two *tert*-butyl groups might force both terminal dihedral angles to adopt an antiperiplanar conformation, thus favouring the opposite screw-sense.

These findings set the experimental basis to design a new molecular switch. Several strategies were attempted, involving reversible chemical reactions (ketone to acetal, alcohol to acetate, amine to benzyl-protected amine, amine to ammonium). However, none of them were successful, due to a series of unexpected and surprising results. To avoid these issues in the future, more computation is required to refine the proposed stereochemical model. A more systematic screening of different end-groups *in silico* would save time and support the structural design of the required molecules.

CHAPTER 2 – DECARBOXYLATIVE BORYLATION

METHODOLOGY AND ITS APPLICATION TO α -AMINO BORONIC ESTERS

*The data presented in this chapter has been partially published in: Fawcett A., Pradeilles J., Wang Y., Mutsuga T., Myers E. L., Aggarwal V. K., Science **2017**, 357, 283.² Where indicated ([†]), the data presented was obtained by Dr. Alexander Fawcett,²¹⁴ Dr Yahui Wang or Dr Tatsuya Mustuga, and is included in this thesis to provide a complete picture of the work.*

2.1. Introduction

2.1.1. Applications and synthesis of α -amino boronates

In the early 1970s, boronic acids were found to inhibit enzymatic processes.^{215–222} More precisely, they showed promising activities against serine proteases, a class of enzymes involved in the cleavage of peptidic bonds. Since then, boron-containing molecules have become an important class of anticancer agents, as exemplified by two marketed drugs: bortezomib (**192**) and ixazomib (**193**). These protease inhibitors are prescribed to treat lymphoma and myeloma, respectively. Oncology is not the only field of medicinal chemistry in which boronic acid-derived approved drugs can be found (**Chart 9**). Vaborbactam (**194**) is used in combination with β -lactam-type antibiotics to treat bacterial infections due to its ability to inhibit bacterial β -lactamases. And tavaborole (**195**), an antifungal compound, has applications in the treatment of onychomycosis.

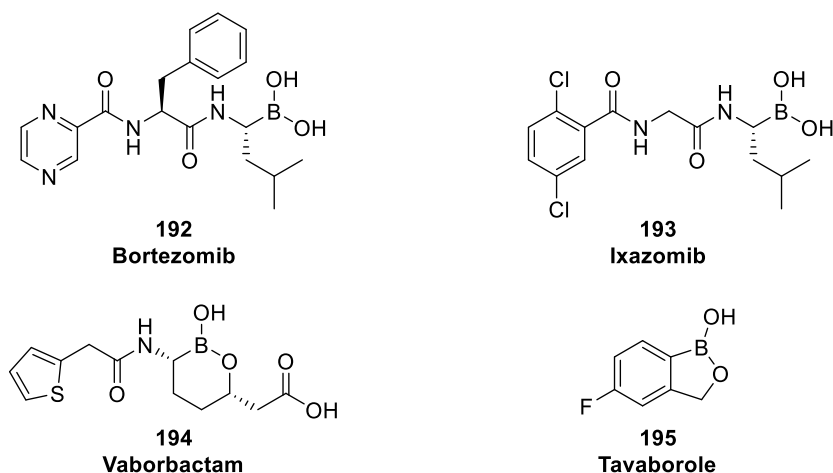
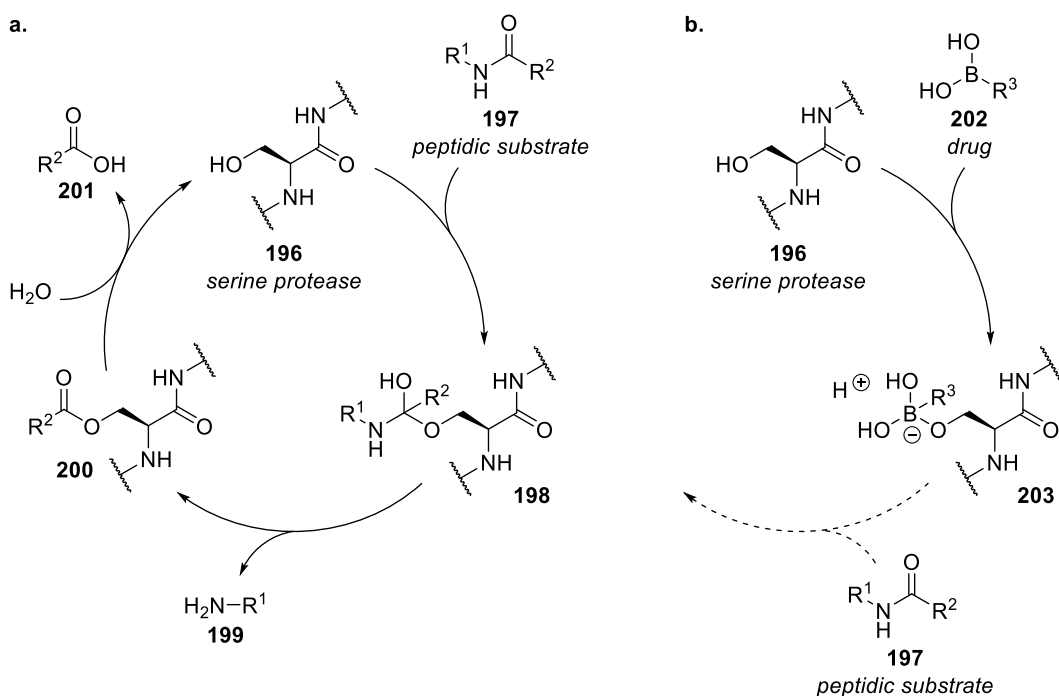


Chart 9. Four examples of boron-containing marketed drugs.

The typical mode of action by which boron-containing bioactive compounds inhibit enzymatic processes is *via* the formation of boronate complexes as described in Section 1.1.1. For example, in the case of serine proteases,^{223–225} the pendant hydroxyl group on the side chain of a serine

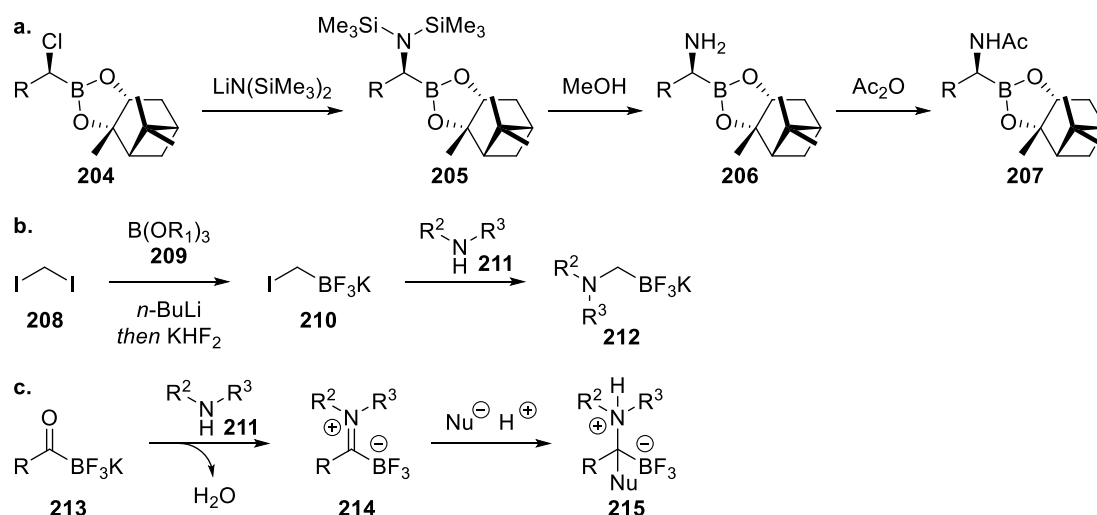
residue in the active site of the enzyme can interact with the sp^2 -hybridised boron centre of the drug to form a stable tetrahedral boronate complex which prevents the natural substrate of the protease entering the active site²²⁶ (**Scheme 44**).



Scheme 44. **a.** Cleavage of peptide bonds by serine proteases. **b.** Inhibition of serine proteases by boron-containing drug molecules.

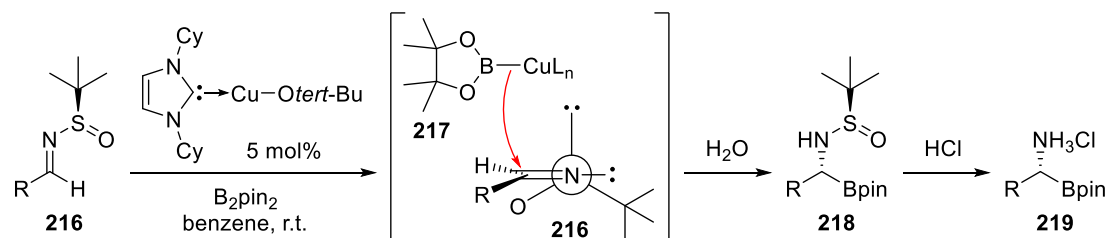
Interestingly, the improved specificity of bortezomib and ixazomib was achieved by thorough design of their peptide chains.^{227,228} Based on this observation, methodologies providing access to α -amino boronic acids (or esters) appear to be valuable synthetic tools to develop potent and selective anticancer molecules.

Matteson contributed to this field in the early 1980s, reporting that α -amido-boronic esters could be synthesised by nucleophilic substitution of the chlorine atom in α -chloro-boronic esters, such as **204**, with lithium hexamethyldisilazane, followed by cleavage of N–Si bonds and protection of the free amine with acetic anhydride²²⁹ (**Scheme 45a**). In a related application, Molander and co-workers described the alkylation of primary and secondary amines with potassium trifluoro(iodomethyl)borate (**210**)²³⁰ (**Scheme 45b**). More recently, Bode also reported the synthesis of α -amino trifluoroborate salts from potassium acyltrifluoroborates (**213**). This reaction proceeds *via* the initial formation of trifluoroborate-iminium zwitter ions (**214**) by condensation with secondary amines.²³¹ Then, a nucleophile attacks the electrophilic sp^2 -hybridised carbon centre to deliver the compounds of interest (**Scheme 45c**).



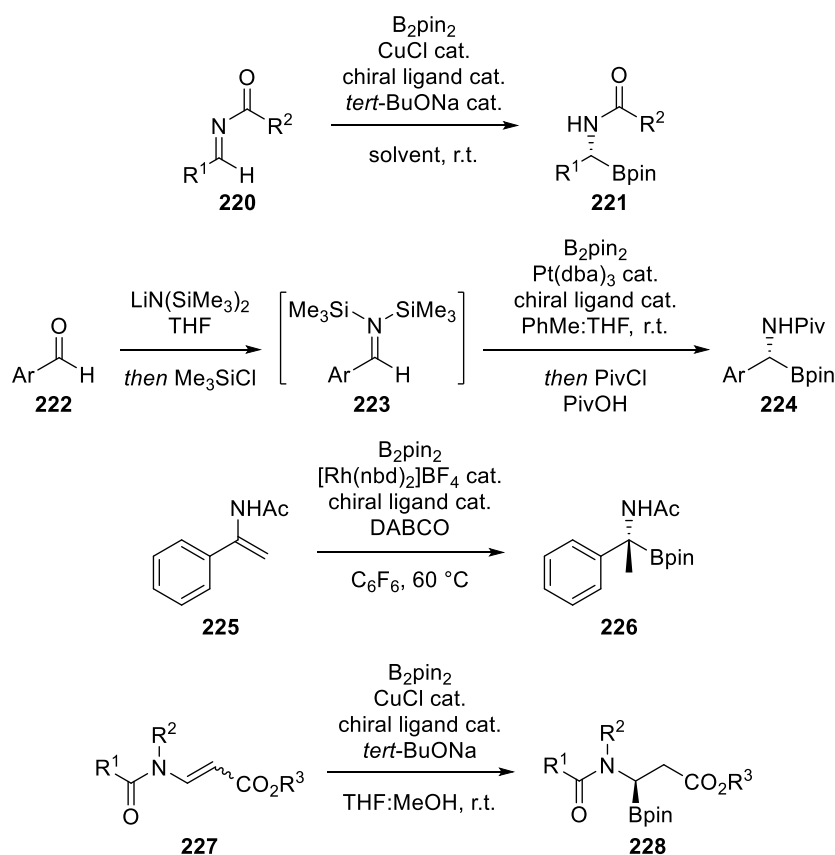
Scheme 45. **a.** Matteson's methodology to synthesise α -amido-boronic esters. **b.** Molander's methodology to synthesise α -amino trifluoroborates. **c.** Bode's methodology to synthesise α -amino trifluoroborates. Brackets have been omitted for clarity.

Another strategy, initially developed by Ellman^{232,233} and further explored by Zhihua,^{234–236} involved a copper-catalysed addition of a diboron reagent to chiral *N*-*tert*-butanesulfinyl imines **216** (**Scheme 46**). The resulting boronic ester **218**, generally obtained in almost perfect *d.r.* (>98:2), gives, after acid-mediated cleavage of the chiral auxiliary, the α -amino boronic ester in excellent *e.r.*



Scheme 46. Ellman's synthesis of chiral α -amino boronic esters.

Other methodologies to access chiral α -amino boronic esters from achiral starting materials have also been reported. For instance, the addition of B_2pin_2 to aldimines **220** or **223**,^{237–241} α -arylenamides **225**²⁴² or β -amidoacrylates **227**^{243,244} can be rendered highly enantioselective when a chiral ligand is used in combination with copper, platinum or rhodium catalysts (**Scheme 47**). Alternatively, a copper-catalysed enantioselective hydroamination of vinyl boronates reported by Hirano and Miura²⁴⁵ afforded a range of α -amino boronates in good to moderate yields and high *e.r.*



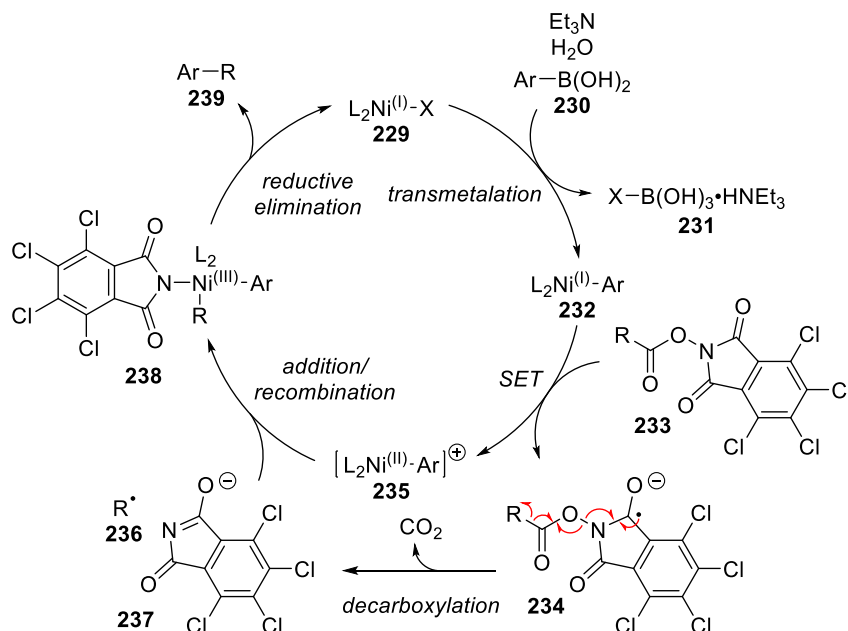
Scheme 47. Selection of reported methodologies for the synthesis of α -amino boronic esters from achiral starting materials.

Although all these procedures give access to α -amino boronates, they often require starting materials which are not easy to synthesise. Therefore, a more general synthetic method to convert inexpensive, widely available carboxylic acids into useful boronic ester building blocks (see Chapter 1) would be a valuable tool for medicinal chemists. One could imagine that a late stage sequence, including the transformation of a carboxylate into a boronic ester with subsequent C–B bond derivatisation to a broad range of functional groups,⁵ would be highly beneficial for any structure–activity relationship (SAR) study.

2.1.2. Development of a new decarboxylative borylation methodology

In 2016, Baran and co-workers reported that alkyl carboxylic acids—activated as their corresponding tetrachloro-*N*-hydroxyphthalimide redox-active esters^{246–250}—and aryl boronic acids could be engaged in a nickel-catalysed alkyl–aryl cross-coupling.²⁵¹ The substrate scope was found to be broad, including primary and secondary carboxylic acids, and substituted (hetero)aromatic boronic acids. In the proposed mechanism (**Scheme 48**), bipyridine–nickel(I) complex **229** undergoes transmetalation with aryl boronic acid **230** in the presence of triethylamine and water to generate complex **232**. This species reduces activated ester **233**, through single-electron

transfer (SET), which then undergoes a radical cascade leading to the decarboxylation event and, eventually, to the formation of alkyl radical **236**. This radical adds to positively-charged nickel(II) complex **235** to afford a nickel(III) centre which, upon a reductive elimination process, is reduced to nickel(I) and delivers the cross-coupled product **239**.

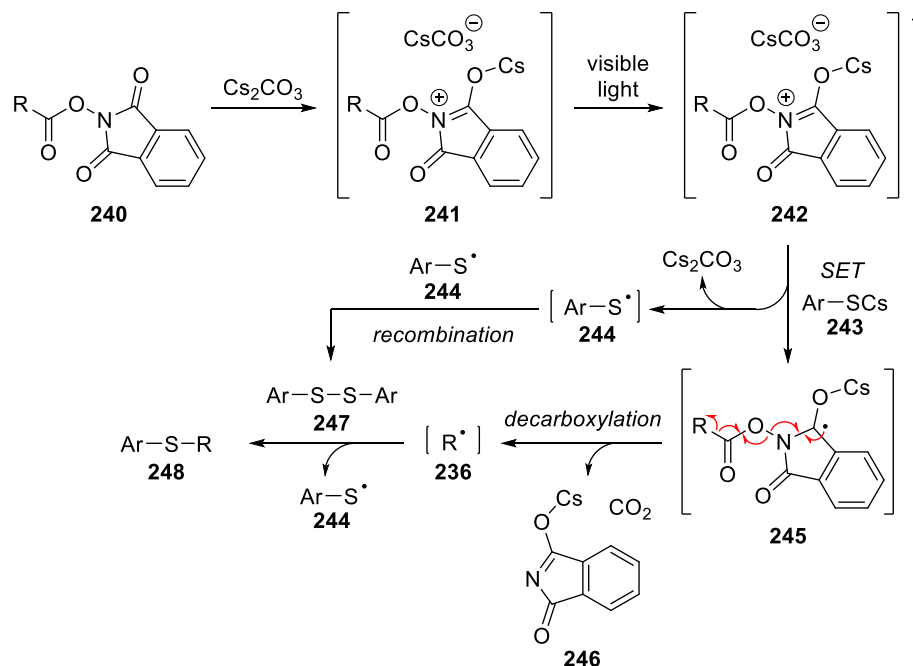


Scheme 48. Proposed mechanism of Baran's nickel-catalysed cross-coupling of redox-active esters with boronic acids. Brackets have been omitted for clarity.

Inspired by this interesting study, one could envisage an analogous mechanism in which the aryl boronic acid coupling partner could be replaced with a diboron reagent ($B_2(OR)_2$) to synthesise alkyl boronic esters. Such a two-step methodology (*i.e.*, activation of the carboxylic acid substrate, followed by borylation of the corresponding activated ester) would be described as a net decarboxylative borylation process. To test this hypothesis, an initial screening of reaction conditions involving model compound **249** and a variety of diboron sources, nickel catalysts, ligands, organic and inorganic bases, solvents and temperatures was conducted.[†] Unfortunately, no desired product was observed under these different sets of conditions.

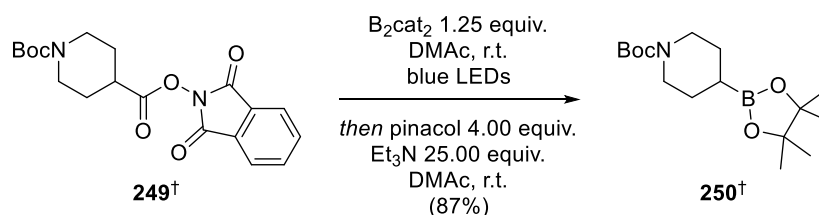
Another strategy was then explored in which a diboron reagent is activated by complexation to a nucleophile or a Lewis base to generate an electron-rich boronate complex prone to oxidation.^{252–254} This species would transfer an electron^{255–257} to a redox-active ester, thus enhancing the decarboxylation process. The resulting alkyl radical would then recombine with a stabilised boryl radical (or with another molecule of activated diboron reagent) to afford the desired alkyl boronic ester. The key redox step would be facilitated by light irradiation. Indeed, *N*-phthalimide esters are known to easily undergo single electron transfers in their photoexcited state, with a redox potential of +1.6 V vs SCE.^{258–260} For example, Fu and co-workers used these activated esters

(**240**) to oxidise thiolate anions (**243**) in the presence of cesium carbonate, under visible-light irradiation, in the absence of a photocatalyst²⁶¹ (**Scheme 49**).



Scheme 49. Proposed mechanism of Fu's decarboxylative arylthiation reaction.

A second screening of conditions was carried out by Dr. Alexander Fawcett according to this strategy. Model compound **249** was mixed with various boron sources (1.00 equiv.) and cesium carbonate (1.50 equiv.) in *N,N*-dimethylformamide (DMF) under blue light irradiation at room temperature. After 14 hours, pinacol and triethylamine were added to form a more stable pinacol boronic ester before GC–FID analysis. Pleasingly, desired boronic ester **250** was formed in 8% yield when bis(catecholato)diboron (B_2cat_2) was used as the boron source. Further optimisation screening[†] showed that cesium carbonate was inhibiting the transformation. In fact, when the reaction was conducted in the absence of this inorganic base, the desired product was formed in 69% yield. This observation quickly led to the discovery of optimised conditions (**Scheme 50**) which, after isolation by column chromatography, gave pinacol boronic ester **250** in 87% yield. Interestingly, the reaction only took place when amide- or urea-based solvents, such as *N,N*-dimethylformamide (DMF), *N,N*-dimethylacetamide (DMAc), *N,N'*-dimethylpropyleneurea (DMPU), tetramethylurea (TMU) or 1,3-dimethyl-2-imidazolidinone (DMI), were used. Degasing the solvent and purging the reaction vessel with nitrogen or argon was necessary to obtain high yields and reproducible results. Finally, light irradiation was found to be crucial for the reaction to reach acceptable levels of conversion.



Scheme 50. Optimised conditions for transition metal-free photoinduced decarboxylative borylation.[†]

In terms of substrate scope, this new methodology successfully converted a broad range of primary and secondary alkyl activated esters to the corresponding boronic esters in high yields. In addition, the reaction conditions showed excellent functional group tolerance, which allowed the transformation of carboxylic acid-containing natural products into their previously-unreported boronic ester analogues (**Chart 10**). Unfortunately, aryl, vinyl, allyl and flexible tertiary alkyl activated esters failed to deliver the decarboxylative borylation products. The reaction was also unsuccessful when the starting material bore a heteroatom in the α -position, making α -amino acids unsuitable substrates.

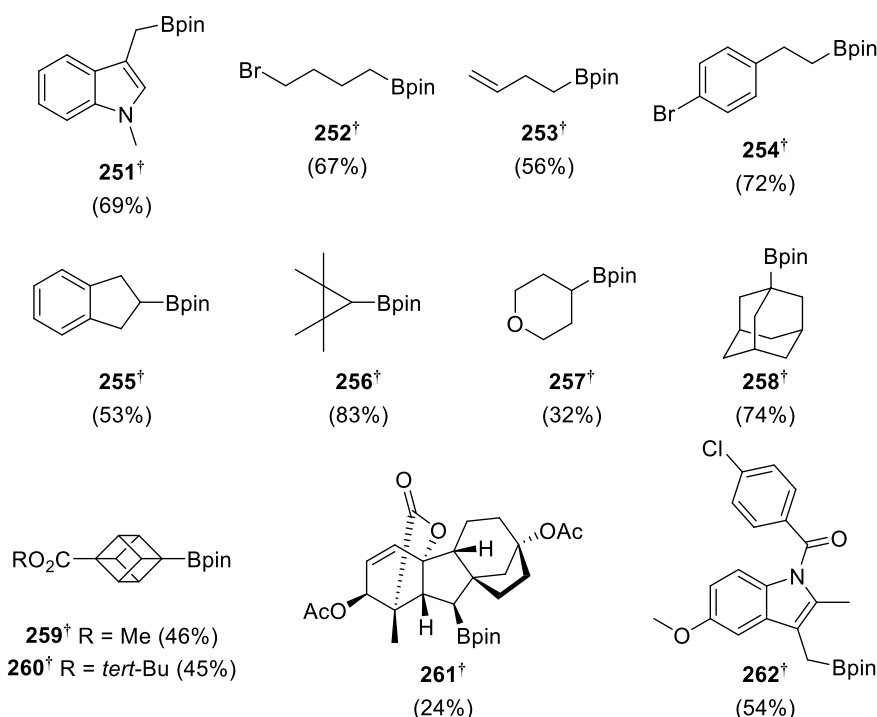


Chart 10. Selection of pinacol boronic esters synthesised according to Aggarwal's decarboxylative borylation methodology.[†]

The mechanistic investigation started with the identification of the light-absorbing species in solution. A UV–visible spectroscopy study[†] revealed that isolated reagents in solution (DMAC) only absorbed in the UV region (303 nm for B_2cat_2 and 314 nm for activated ester **249**). Knowing that blue LEDs used in the reaction emit between 452 and 475 nm, it seemed unlikely that any of the reagents absorbed light independently. However, when both reagents were mixed together in

DMAc according to the optimised reaction conditions (*i.e.*, 0.125 M for B₂cat₂ and 0.10 M for activated ester **249**), a bathochromic shift was observed in the absorption spectrum (**Figure 35a**), suggesting the presence of a new species in solution absorbing in the blue light domain. Interestingly, the intensity of this new absorption shoulder linearly increased with B₂cat₂ concentration (**Figure 35b**).

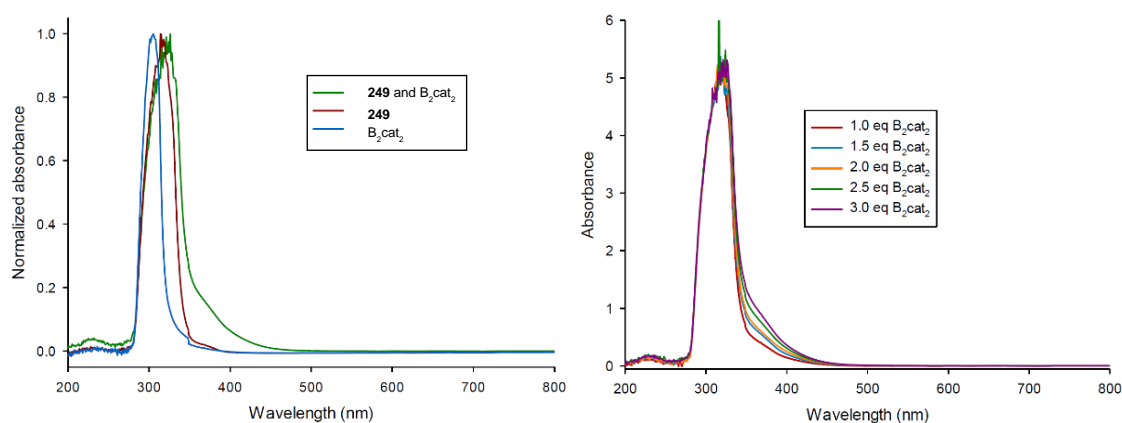


Figure 35. a. UV–visible absorbance spectra of activated ester **249**, B₂cat₂, and the two combined, in DMAc.[†] b. Effect of the concentration of B₂cat₂ on the absorbance spectrum.[†]

Further ¹¹B NMR studies showed that B₂cat₂ gave a single signal at 29.7 ppm in dichloromethane. Interestingly however, in DMAc, this diboron reagent gave two different signals, at 25.7 and 13.8 ppm (**Figure 36**). This observation indicated that, in amide-based solvents, B₂cat₂ existed in an equilibrium between a non-coordinated form (free B₂cat₂) and a solvent-complexed form (DMAc–B₂cat₂ adduct). When activated ester **249** was added to a solution of B₂cat₂ in DMAc, the ¹¹B NMR spectrum remained the same.

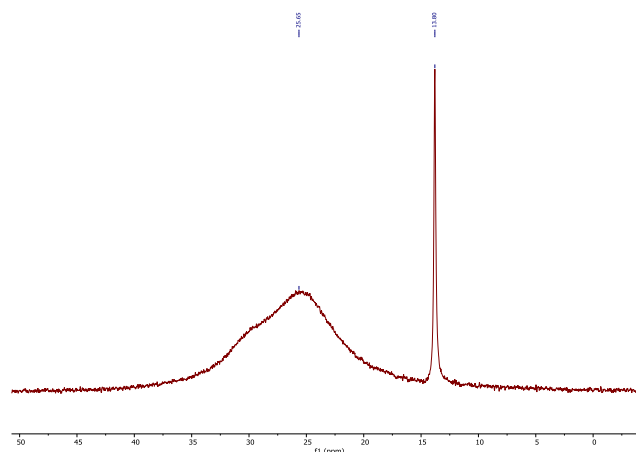
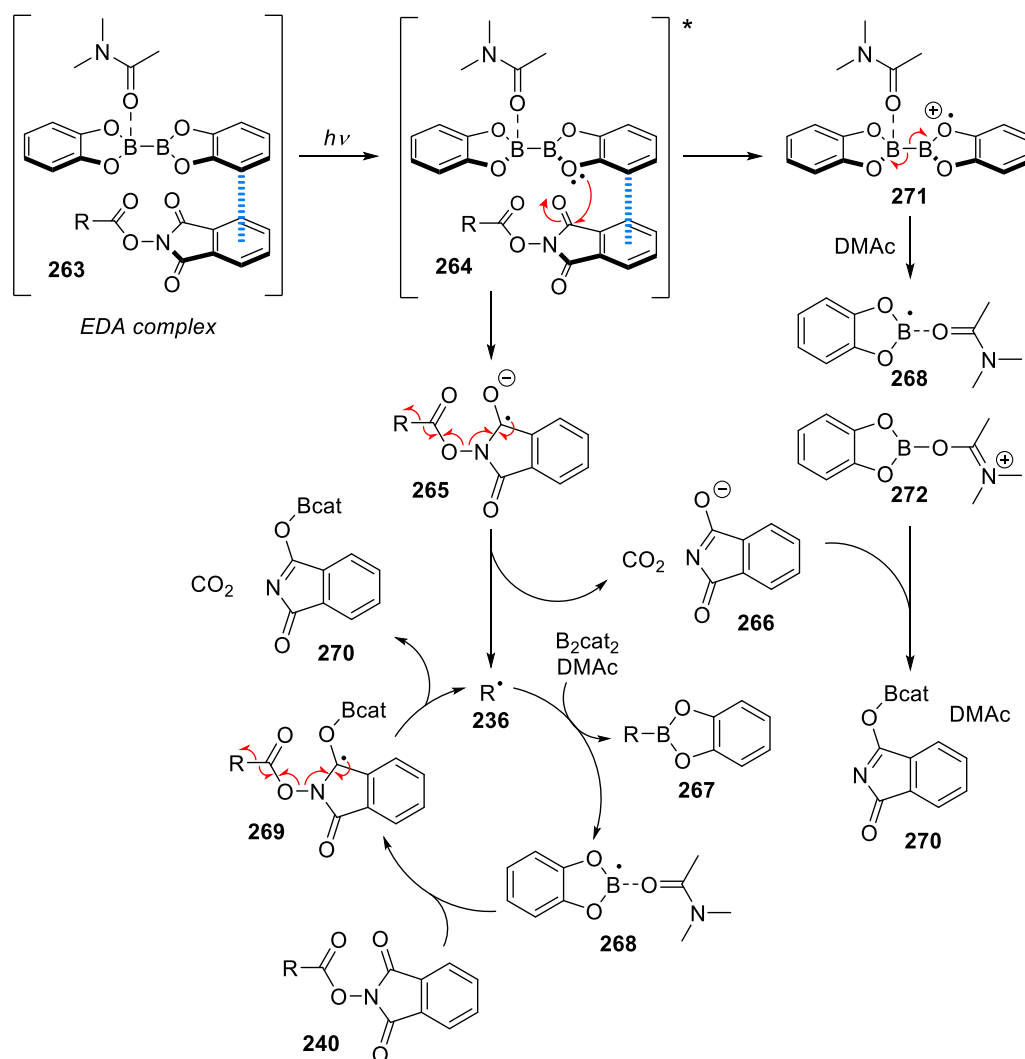


Figure 36. ¹¹B NMR spectrum of B₂cat₂ (0.125 M) in DMAc. $\delta_1 = 25.7$ ppm; $\delta_2 = 13.8$ ppm.

Based on these UV–visible and NMR spectroscopy experiments, it has been suggested that a blue light-absorbing π -stacking electron donor–acceptor (EDA) complex^{262–264} (**263**) was formed between the electron-deficient phthalimide aromatic ring²⁶⁵ of activated esters and electron-rich

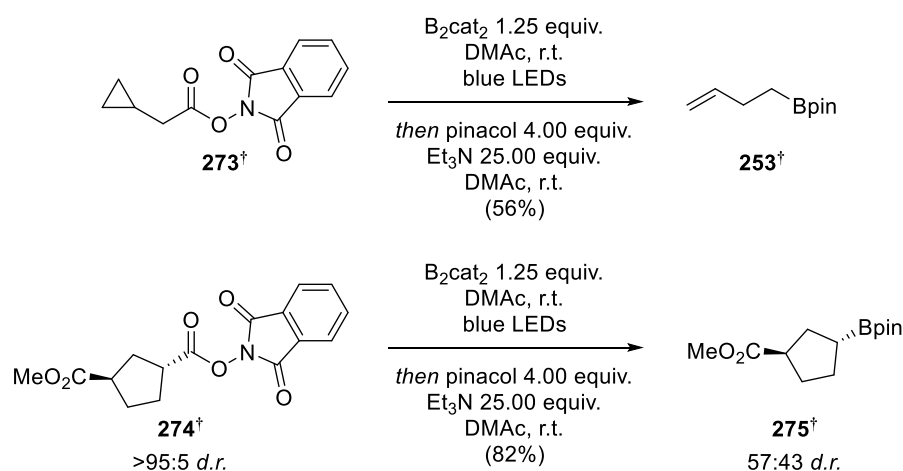
catechol aromatic ring of B_2cat_2 when both species are mixed in DMAc (**Scheme 51**). After absorbing a photon, excited EDA complex **264** undergoes intra-complex electron transfer from a catechol moiety to the phthalimide ring. After diffusive separation of both charged radical species, compound **265** fragments to afford phthalimide by-product **266**, carbon dioxide and alkyl radical **236**. In parallel, the B–B bond in radical **271** is cleaved to generate stabilised boryl radical **268** and positively-charged DMAc adduct **272**, which can eventually recombine with phthalimide by-product **266** to give compound **270**. Alkyl radical **236** then reacts with B_2cat_2 ²⁶⁶ to provide desired alkyl boronic ester **267** and another stabilised boryl radical **268**. This highly reactive species can reduce a molecule of activated ester **240**, thus initiating a chain reaction process.



Scheme 51. Proposed mechanism of Aggarwal's decarboxylative borylation. Brackets have been omitted for clarity.

Evidence for a radical pathway was identified when substrates **273** and **274** were subjected to the reaction conditions (**Scheme 52**). In the case of **273**, only linear boronic ester **253** could be observed and isolated after work-up, suggesting that the initially-generated radical intermediate underwent ring opening (rate constant = $1.3 \times 10^8 \text{ s}^{-1}$) before being trapped by the boron source. In

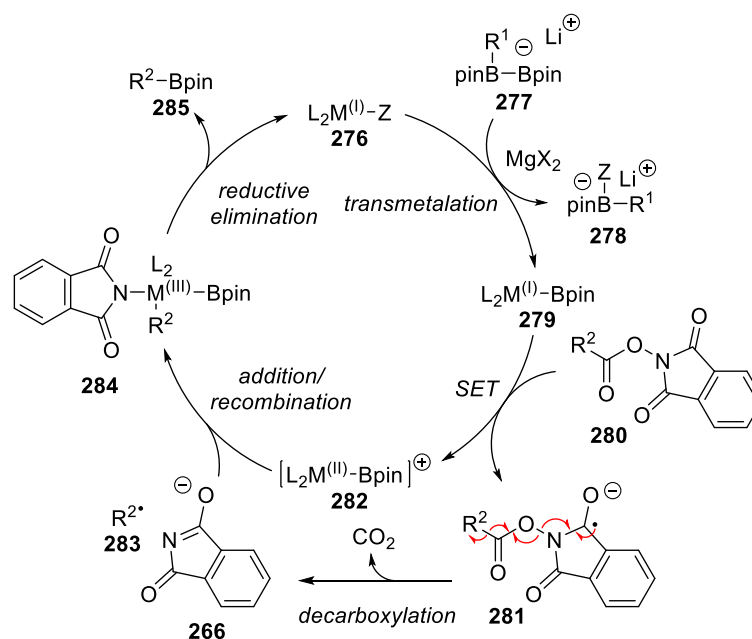
addition, activated ester **274**, engaged as a single diastereoisomer (>95:5 *d.r.*), gave corresponding boronic ester **275** in only 57:43 *d.r.* This erosion of diastereopurity also suggested that the reaction proceeds through a radical pathway.



Scheme 52. Experimental proofs of a radical reaction pathway.[†]

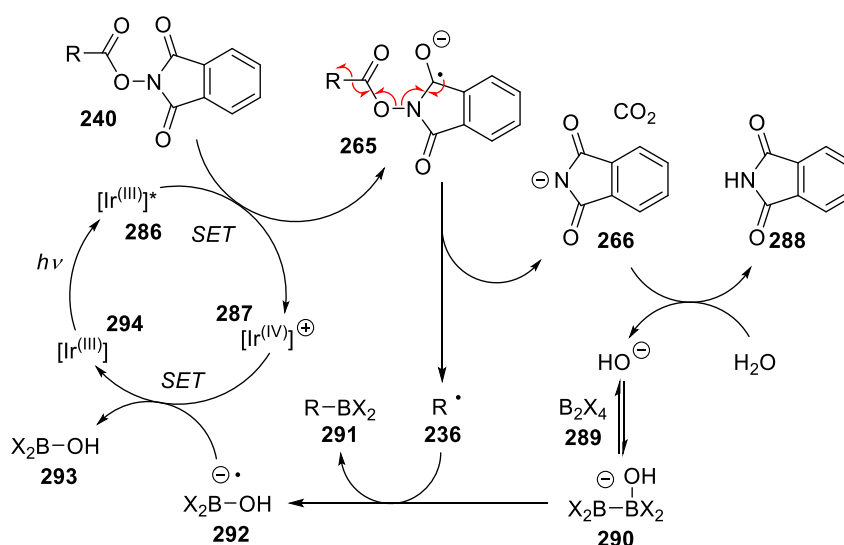
2.1.3. Other decarboxylative borylation methodologies

A few other examples of decarboxylative borylation were reported in the literature shortly after submission of the manuscript describing Aggarwal's methodology.²⁶⁷ Further investigations on nickel-catalysed cross-couplings led Baran and co-workers to discover a related procedure²⁶⁸ in which an *in situ*-activated carboxylic acid (**280**) is reduced by a nickel(I)–bipyridine complex in the presence of a pre-activated boron source and magnesium bromide to afford alkyl radical **283** which, after recombination with the nickel centre and subsequent reductive elimination gives the desired pinacol boronic ester **285** (**Scheme 53**). The substrate scope was found to be very broad, for example, valuable α -amino boronic esters could be accessed using this method. However, the borylation step involved the use of six different reagents (including sensitive methyl lithium), which must be mixed in different reaction vessels, sonication and transfer of suspensions from one flask to another. To improve the practicability of the method, Baran and co-workers reported a simpler copper-catalysed decarboxylative borylation reaction²⁶⁹ one year after their initial publication. This transformation follows the same reaction pathway as the nickel-catalysed method. However, α -amino acids could not be converted to the corresponding α -amino boronic esters using these conditions.



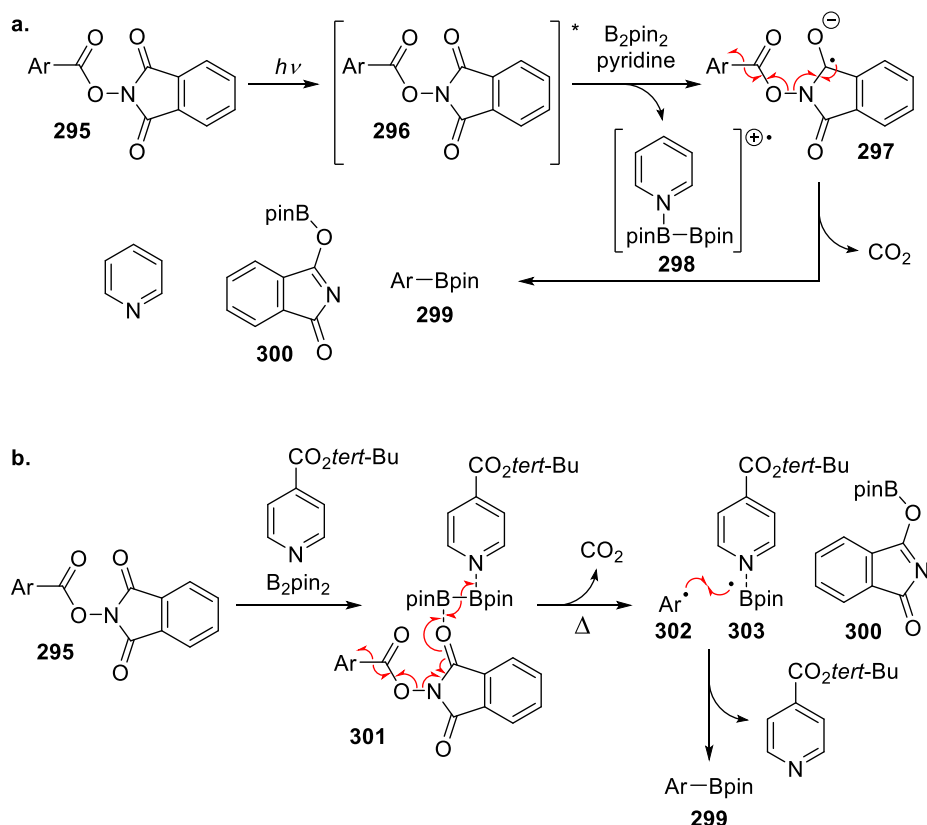
Scheme 53. Mechanism of nickel-catalysed ($M = \text{Ni}$, $R^2 = \text{Me}$, $X = \text{Br}$) and copper-catalysed ($M = \text{Cu}$, $R^2 = \text{OH}$, $X = \text{Cl}$) decarboxylative borylations. $Z = \text{Cl}$ or phthalimide anion **266**. Brackets have been omitted for clarity.

A different approach involving the use of an iridium photocatalyst was developed by Li and co-workers²⁷⁰ (**Scheme 54**). Upon light irradiation, the catalyst reaches an excited state and can then transfer an electron to activated ester **240**. After decarboxylation, alkyl radical **236** is trapped by the boron source to afford the desired product. The authors suggested that boryl radical **292** is able to reduce iridium(IV) to iridium(III), thus closing the catalytic cycle. Interestingly, no example of tertiary boronic ester or α -amino boronic ester was reported in this article and most of the final products were isolated as potassium trifluoroborate salts.



Scheme 54. Proposed mechanism of Li's decarboxylative borylation. Brackets have been omitted for clarity.

Additional complementary strategies for the decarboxylative borylation of aryl carboxylic acids were also disclosed. A first report by Glorius and co-workers²⁷¹ showed that aryl activated esters undergo decarboxylation under purple light irradiation in the presence of a boron source, pyridine and cesium carbonate in ethyl acetate (**Scheme 55a**). Fu and co-workers²⁷² also described an analogous thermal process involving aryl activated esters, a boron source and a catalytic amount of *tert*-butyl isonicotinate ester at 110 °C (**Scheme 55b**). These methodologies could not be used to convert alkyl carboxylic acids into alkyl boronic esters.



Scheme 55. **a.** Proposed mechanism of Glorius' decarboxylative borylation. **b.** Proposed mechanism of Fu's decarboxylative borylation. Brackets have been omitted for clarity.

2.1.4. Research proposal

The first objective of this project was to improve the substrate scope of the decarboxylative borylation methodology developed in the Aggarwal lab and this was achieved before its publication.² As the main idea of this research program was to provide a new synthetic tool to be used in medicinal chemistry, it was necessary to include substrates containing some structural motifs commonly encountered in drug-like molecules. In addition, a few more examples of natural products had to be tested under the reaction conditions, notably to test the functional group tolerance of the method and to prove that it could be used in a late-stage functionalisation.

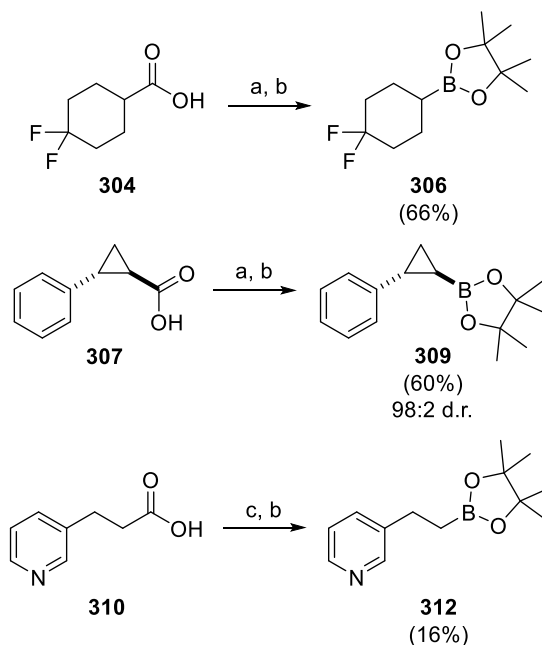
The second task, also completed before publication,² was to perform more experiments to confirm the postulated radical mechanism. Usual radical trap experiments or radical cyclisation experiments were investigated to obtain additional evidences in favour of a radical pathway.

Finally, the ultimate ambition of applying this new methodology to α -amino acids will be reconsidered. Two issues needed to be addressed here: first, the purification procedure had to be optimised to isolate amino boronic esters as pure compounds; then, new conditions allowing for the decarboxylative borylation of proteogenic amino acids had to be discovered through optimisation studies.

2.2. Results and discussion

2.2.1. Improvement of the substrate scope

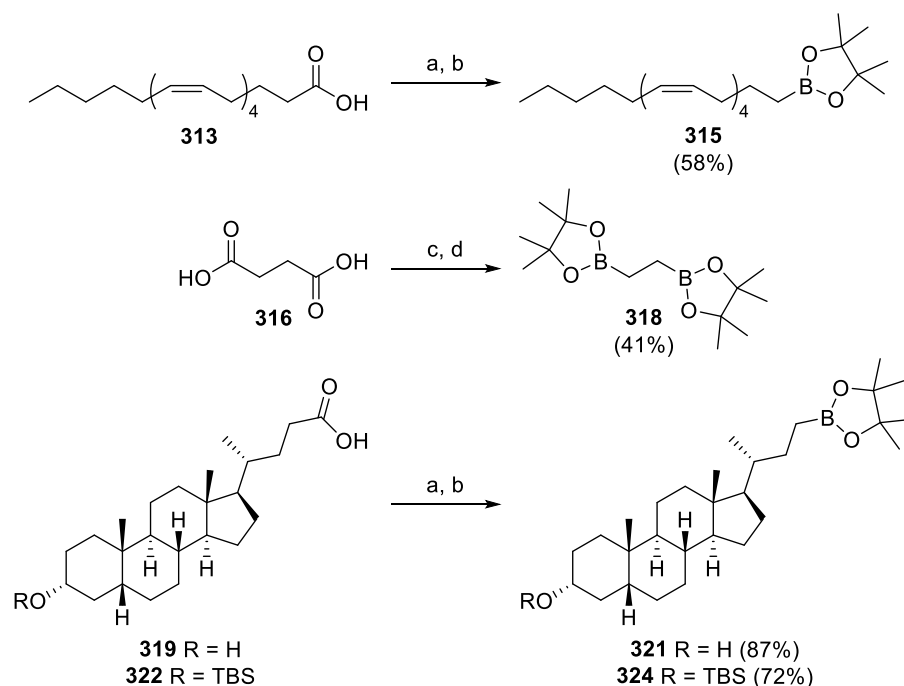
To prove the general applicability of this new methodology, a broader substrate scope was explored. More precisely, some medicinal chemistry-type building blocks such as fluorine-substituted cyclohexanes, phenylcyclopropanes and pyridine derivatives were tested under the reaction conditions (**Scheme 56**). Carboxylic acids **304** and **307** were successfully activated and converted to the corresponding boronic esters **306** and **309** in 66% and 60% yield, respectively.



Scheme 56. Photoinduced decarboxylative borylation applied to medicinal chemistry-type building blocks. (a) *N*-hydroxyphthalimide 1.00 equiv., DIC 1.00 equiv., DMAP 0.10 equiv., CH₂Cl₂, r.t.; (b) B₂cat₂ 1.25 equiv., DMAc, blue LEDs, *then* pinacol 4.00 equiv., Et₃N 25.00 equiv., r.t.; (c) *N*-hydroxyphthalimide 1.00 equiv., DCC 1.00 equiv., THF, r.t.

Interestingly, boronic ester **309** was obtained in a 98:2 *d.r.* This result suggested that the trapping of the cyclopropyl radical was very sensitive to steric hindrance. Pyridine derivative **310** was activated using slightly different activation conditions. DCC (dicyclohexylcarbodiimide) coupling reagent was employed instead of DIC to circumvent previously observed purification issues. Subsequent borylation step gave the desired boronic ester **312** in 42% NMR yield. Unfortunately, this molecule was highly unstable on silica gel and decomposed upon purification, resulting in a 16% isolated yield.

To expand the scope even more, natural products such as arachidonic acid, succinic acid, lithocholic acid or penicillin G were activated and subjected to the optimised conditions (**Scheme 57**). Pleasingly, boronic ester **315** was isolated in 58% yield. As predicted by Baldwin's rules, 4-*exo-trig* or 5-*endo-trig* intra-molecular cyclisations were not observed. Succinic acid gave bis(boronic ester) **318** in 41% yield, showing that the reaction could occur twice on the same substrate molecule.

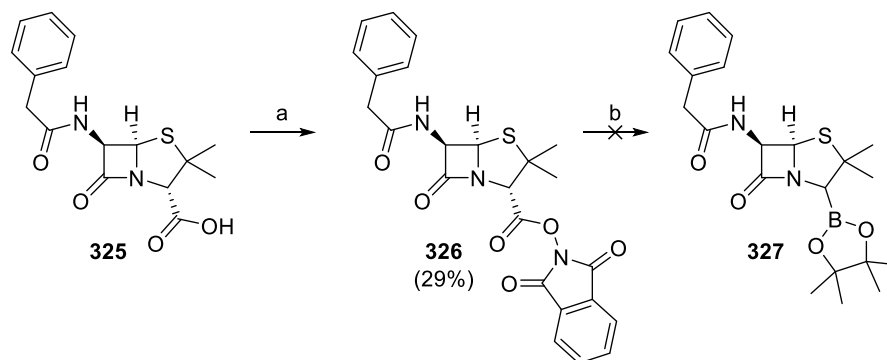


Scheme 57. Photoinduced decarboxylative borylation applied to natural products. (a) *N*-hydroxyphthalimide 1.00 equiv., DIC 1.00 equiv., DMAP 0.10 equiv., CH₂Cl₂, r.t.; (b) B₂cat₂ 1.25 equiv., DMAc, blue LEDs, *then* pinacol 4.00 equiv., Et₃N 25.00 equiv., r.t.; (c) *N*-hydroxyphthalimide 2.00 equiv., DIC 2.00 equiv., DMAP 0.20 equiv., CH₂Cl₂, r.t.; (d) B₂cat₂ 5.50 equiv., DMAc, blue LEDs, *then* pinacol 8.00 equiv., Et₃N 25.00 equiv., r.t.

2.2.2. Unsuccessful substrates

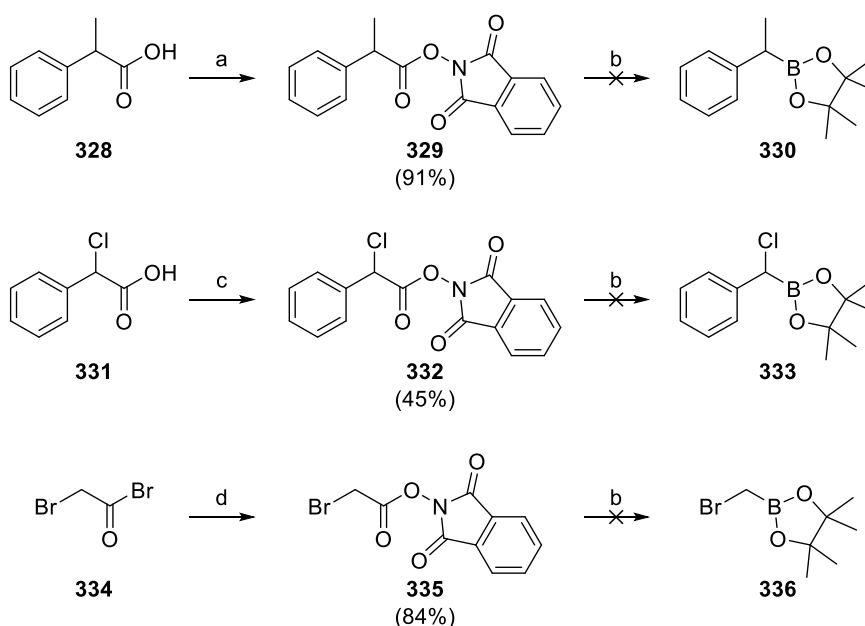
Unfortunately, activated penicillin G **326** decomposed under the reaction conditions (**Scheme 58**). Presumably, generating a radical next to a strained system (β-lactam) and in β-position with

respect to the sulphur atom led to an intramolecular side-reaction pathway which degraded the molecule before the boron trapping step.



Scheme 58. Unsuccessful decarboxylative borylation of penicillin G. (a) *N*-hydroxyphthalimide 1.00 equiv., DCC 1.00 equiv., THF, r.t.; (b) B_2cat_2 1.25 equiv., DMAc, blue LEDs, *then* pinacol 4.00 equiv., Et_3N 25.00 equiv., r.t.

Penicillin G was not the only substrate which could not be converted to the desired product. Although benzylic starting materials **329** and **332** were fully consumed, no corresponding boronic esters could be identified after 14 hours of reaction (**Scheme 59**).



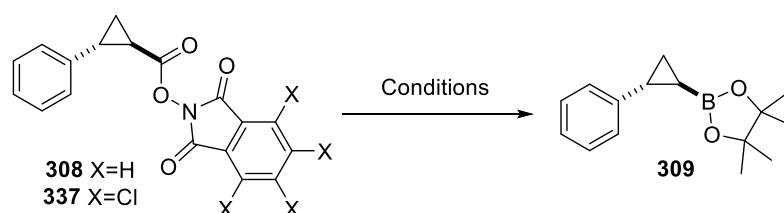
Scheme 59. Unsuccessful substrates. (a) *N*-hydroxyphthalimide 1.00 equiv., DIC 1.00 equiv., DMAP 0.10 equiv., CH_2Cl_2 , r.t.; (b) B_2cat_2 1.25 equiv., DMAc, blue LEDs, *then* pinacol 4.00 equiv., Et_3N 25.00 equiv., r.t.; (c) oxalyl chloride 1.10 equiv., DMF cat., CH_2Cl_2 , 0 °C *then* *N*-hydroxyphthalimide 1.00 equiv., DIPEA 1.50 equiv., CH_2Cl_2 , 0 °C to r.t.; (d) *N*-hydroxyphthalimide 1.00 equiv., DIPEA 1.00 equiv., CH_2Cl_2 , 0 °C to r.t.

An explanation might be that, in both cases, the intermediate benzylic radical species had been oxidised to the benzylic carbocation before being trapped by the boron source. The nature of the oxidant remains unknown. Similarly, the radical intermediate derived from the decarboxylation

of activated ester **335** could be too unstable to be trapped or maybe the desired product itself might decompose under the reaction conditions.

2.2.3. Optimisation study on cyclopropane derivatives

Considering all the unsuccessful examples, another optimisation study was conducted on phenylcyclopropane derivative **308**. Its average yield of 60% obtained under standard conditions seemed to be a good starting point to observe substantial changes in reaction outcome. Phthalimide substitution, boron sources, light sources, solvents, concentrations and transesterification conditions were investigated (**Table 6**).



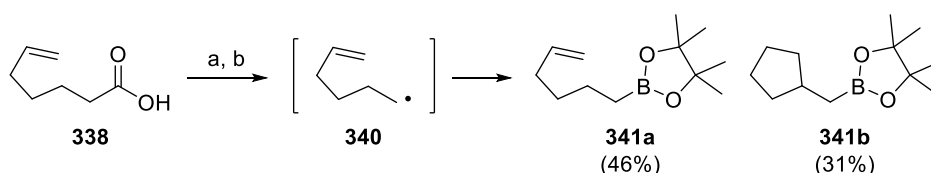
X	Boron source	Light source	Solv.	Conc.	Transesterification conditions	Isolated yield
H	B ₂ cat ₂ 1.25 equiv.	blue LEDs	DMAc	0.10 M	pinacol 4.00 equiv., Et ₃ N 25.00 equiv., 1.5 h, r.t.	60%
H	B ₂ cat ₂ 1.50 equiv.	blue LEDs	DMAc	0.10 M	pinacol 4.00 equiv., Et ₃ N 25.00 equiv., 1.5 h, r.t.	28%
H	B ₂ cat ₂ 1.00 equiv.	blue LEDs	DMAc	0.10 M	pinacol 4.00 equiv., Et ₃ N 25.00 equiv., 1.5 h, r.t.	38%
H	B ₂ cat ₂ 0.50 equiv., B₂(OH)₄ 1.00 equiv.	blue LEDs	DMAc	0.10 M	pinacol 4.00 equiv., Et ₃ N 25.00 equiv., 1.5 h, r.t.	41%
H	B ₂ cat ₂ 1.25 equiv.	blue LEDs	DMAc	0.20 M	pinacol 4.00 equiv., Et ₃ N 25.00 equiv., 1.5 h, r.t.	47%
H	B ₂ cat ₂ 1.25 equiv.	blue LEDs	DMAc	0.05 M	pinacol 4.00 equiv., Et ₃ N 25.00 equiv., 1.5 h, r.t.	50%
H	B ₂ cat ₂ 1.25 equiv.	blue LEDs	DMF	0.10 M	pinacol 4.00 equiv., Et ₃ N 25.00 equiv., 1.5 h, r.t.	44%
H	B ₂ cat ₂ 1.25 equiv.	40W blue lamp	DMAc	0.10 M	pinacol 4.00 equiv., Et ₃ N 25.00 equiv., 1.5 h, r.t.	50%
H	B ₂ cat ₂ 1.25 equiv.	white bulb	DMAc	0.10 M	pinacol 4.00 equiv., Et ₃ N 25.00 equiv., 1.5 h, r.t.	25%
Cl	B ₂ cat ₂ 1.25 equiv.	blue LEDs	DMAc	0.10 M	pinacol 4.00 equiv., Et ₃ N 25.00 equiv., 1.5 h, r.t.	25%
H	B ₂ cat ₂ 1.25 equiv.	blue LEDs	DMAc	0.10 M	pinacol 4.00 equiv., Et ₃ N 25.00 equiv., 3.0 h , r.t.	57%
H	B ₂ cat ₂ 1.25 equiv.	blue LEDs	DMAc	0.10 M	pinacol 4.00 equiv., AcOH 4.00 equiv., 4.0 h , r.t.	47%

Table 6. Second optimisation study using activated ester **308** as a model substrate.

Unfortunately, none of the attempted modifications afforded the desired boronic ester in better yield (*i.e.*, greater than 60%). Nevertheless, this second optimisation table confirmed that the conditions used to build up the substrate scope were the optimal conditions. At that point, the remaining task was to provide experimental evidences to validate the proposed reaction mechanism.

2.2.4. Further mechanistic investigations

In terms of mechanism elucidation, an additional experiment was carried out to prove the postulated radical pathway. Carboxylic acid **338**, bearing a terminal C=C double bond, was activated and subjected to the optimised borylation conditions. The presence of cyclized product **341b** in the resulting mixture confirmed the hypothesis of a radical pathway, with the *5-exo-trig* cyclisation (rate constant = $1.0 \times 10^5 \text{ s}^{-1}$) occurring rapidly after the formation of intermediate radical **340** before trapping with boron (**Scheme 60**).



Scheme 60. Radical cyclisation experiment. (a) *N*-hydroxyphthalimide 1.00 equiv., DIC 1.00 equiv., DMAP 0.10 equiv., CH₂Cl₂, r.t.; (b) B₂cat₂ 1.25 equiv., DMAc (0.10 M), blue LEDs, *then* pinacol 4.00 equiv., Et₃N 25.00 equiv., r.t.

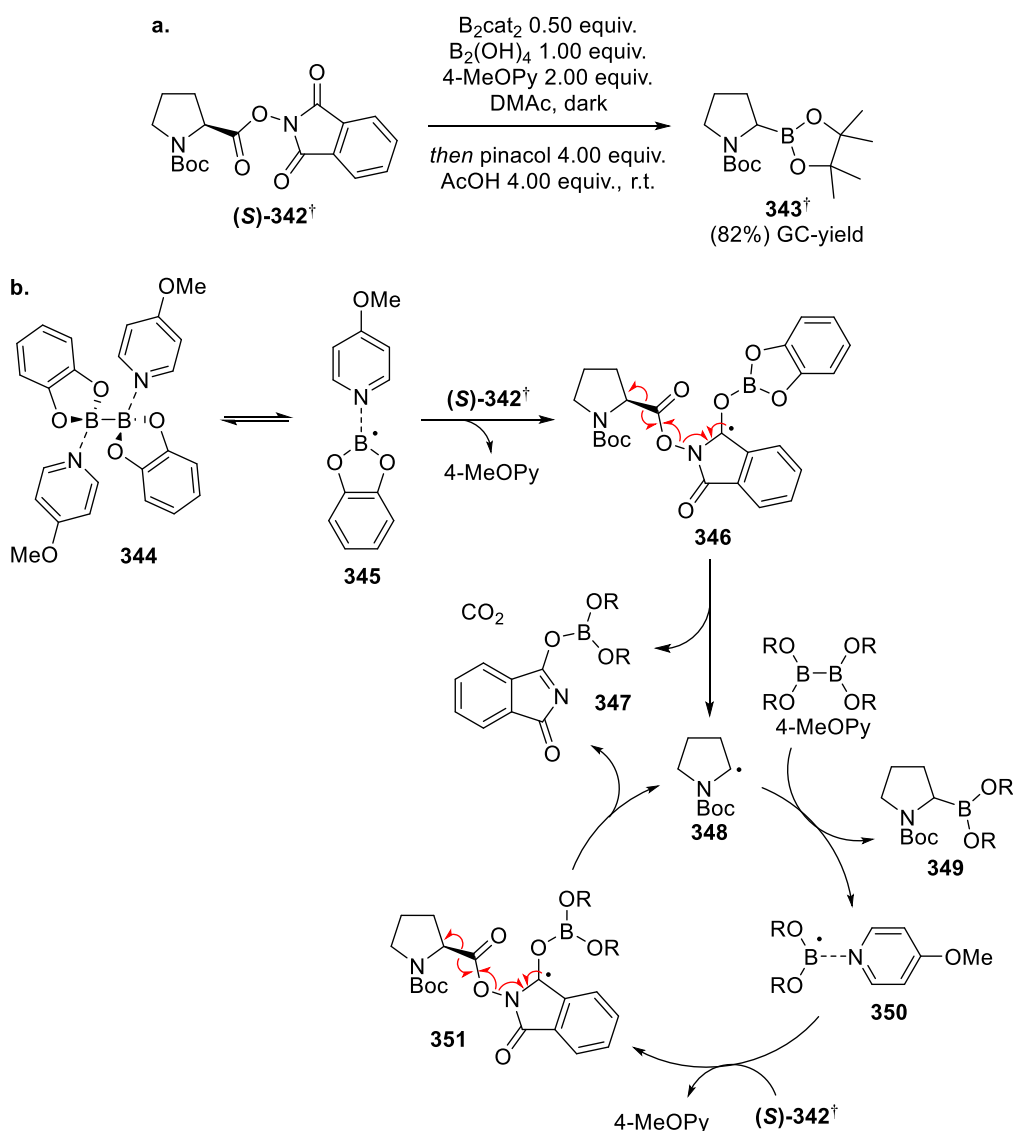
This experiment was repeated at different concentrations (from 0.01 M to 1.00 M). It clearly appeared that the cyclisation reaction was favoured at lower concentrations (**Table 7**). This result was in line with an outer-sphere trapping of the alkyl radical with the boron source. Presumably, the diboron molecule responsible for the reduction of the activated ester (with subsequent fragmentation and decarboxylation) was not the same as the diboron species which trapped radical intermediate **340**. This could be indicative of a radical chain reaction.

Concentration	341a	341b	Ratio 341a:341b
1.00 M	36.5%	6.3%	85:15
0.50 M	41.1%	9.1%	82:18
0.20 M	48.6%	20.3%	71:29
0.01 M	34.3%	48.8%	41:59

Table 7. Effect of the concentration on a radical cyclisation reaction.[†]

2.2.5. Decarboxylative borylation of proline

As mentioned above, the optimised reaction conditions developed in the Aggarwal lab² failed to afford α -amino boronic esters. Considering the value of these building blocks (for example, in medicinal chemistry^{223–225}), this limitation had to be addressed. To solve this issue, 22 sets of reaction conditions were screened,[†] using proline derivative (**(S)**-**342**[†] as a model substrate. Yields were determined by calibrated GC–FID with trimethoxybenzene as the internal standard.

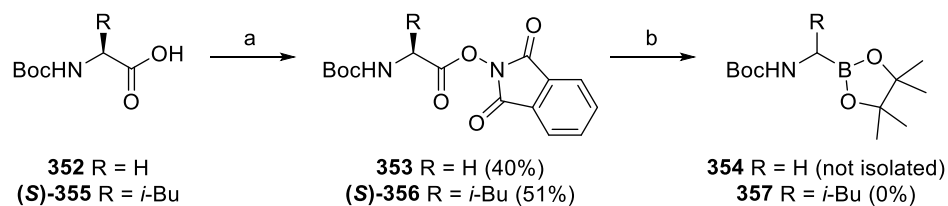


Scheme 61. **a.** Optimised conditions[†] for the decarboxylative borylation of proline-derived activated ester (**(S)**-**342**). **b.** Proposed reaction mechanism using 4-methoxypyridine. B(OR)₂ = B(OH)₂ or Bcat. Brackets have been omitted for clarity.

The best conditions (**Scheme 61a**) involved a mixture of two different boron sources (B₂cat₂, 0.50 equiv. and B₂(OH)₄, 1.00 equiv.) and a Lewis base, 4-methoxypyridine (4-MeOPy, 2.00 equiv.), which presumably formed a complex with either diboron species and enhanced the

reaction (**Scheme 61b**). These conditions did not require any light irradiation to deliver the desired boronic ester.

Despite a GC-yield of 82%,[†] boronic ester **343** could not be separated from other reaction by-products, such as B₂pin₂ or phthalimide. A screening of purification conditions was conducted to find the best method to isolate the compound. Two column chromatography steps on deactivated silica gel with two different eluent systems were necessary to obtain it pure. However, due to the instability of compound **343** on silica gel, the isolated yield dropped to 41%.



Scheme 62. Decarboxylative borylation of glycine and leucine derivatives **353** and **(S)-356** under new optimised conditions. (a) *N*-Hydroxyphthalimide 1.00 equiv., DCC 1.00 equiv., THF, r.t.; (b) B₂cat₂ 0.50 equiv., B₂(OH)₄ 1.00 equiv., 4-MeOPy 2.00 equiv., DMAc, dark, *then* pinacol 4.00 equiv., AcOH 4.00 equiv., r.t.

Other amino acids were then activated and tested under these new reaction and purification conditions (**Scheme 62**). Glycine derivative **353** gave a promising spot by TLC, but the product could not be separated from impurities. Unfortunately, when the same conditions were applied to other amino acids, no desired product was observed. For example, leucine derivative **(S)-356** did not afford corresponding boronic ester **357** and was mostly recovered after work-up.

2.2.6. Effect of N–H bonds

The main difference between compound **(S)-342** and other Boc-protected amino acids is the absence of free N–H bond in the proline derivative. One could test whether a free N–H bond was inhibiting the reaction pathway by spiking the reaction mixture with an additive bearing a free N–H bond. A selection of protected benzylamine derivatives were synthesised (**Chart 11**) and engaged into decarboxylative borylation reactions. By screening different protecting groups, this study also aimed to identify the best option to protect the amino acid substrates.

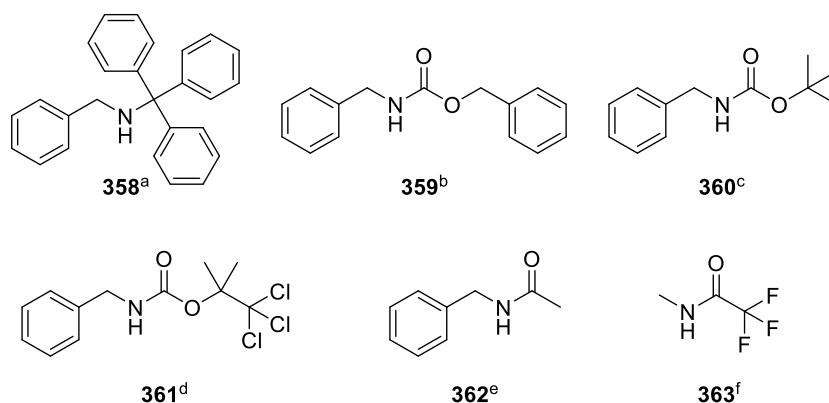
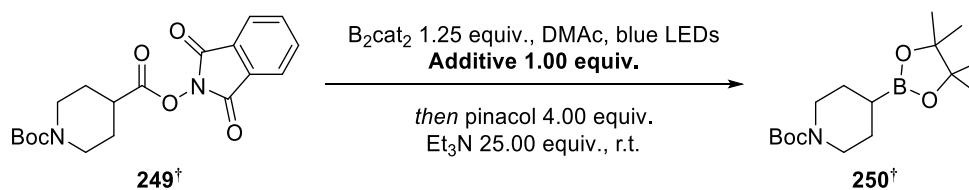


Chart 11. Additives **358–363**. Conditions: (a) BnNH₂ 1.00 equiv., TrCl 1.10 equiv., DMAP 0.10 equiv., CH₂Cl₂, r.t., (49%); (b) BnNH₂ 1.00 equiv., CbzCl 1.20 equiv., I₂ 0.02 equiv., MeOH, r.t., (48%); (c) BnNH₂ 1.00 equiv., Boc₂O 1.10 equiv., EtOH, 30 °C, (88%); (d) BnNH₂ 1.00 equiv., ClCO₂C(CH₃)₂CCl₃ 1.00 equiv., Et₃N 2.00 equiv., CH₂Cl₂, r.t., (30%); (e) BnNH₂ 1.00 equiv., Ac₂O 1.00 equiv., Et₃N 2.00 equiv., DMAP 0.10 equiv., CH₂Cl₂, r.t., (74%); (f) Commercially available.

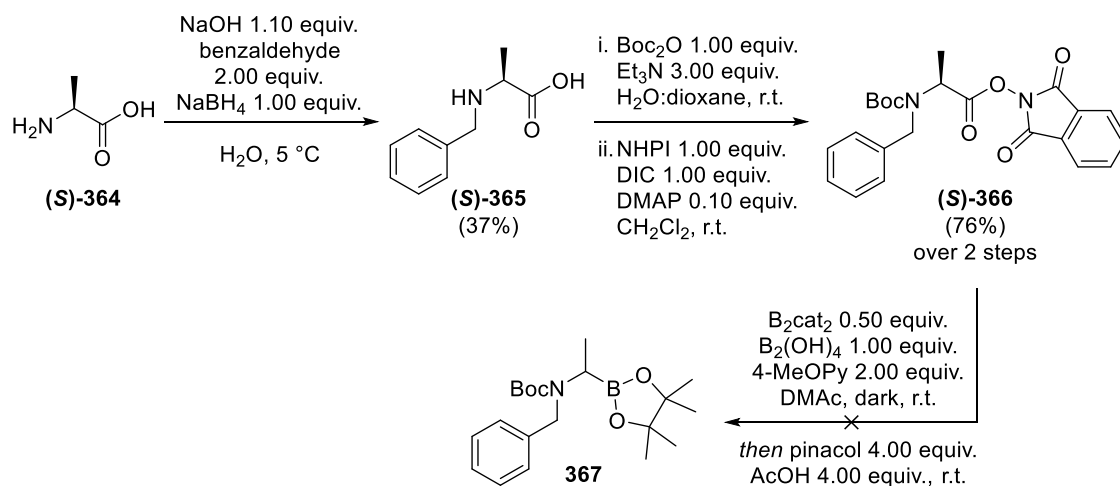
These spiking experiments (**Table 8**) indicated that the reaction was not affected by the presence of additives bearing a free N–H bond. More precisely, no intermolecular inhibition of the reaction was observed when mono-substituted carbamates, amides or di-substituted amines were added to the reaction medium.



Additive	none	358	359	360	361	362	363
GC Yield	73%	68%	75%	71%	76%	75%	59%

Table 8. Spiking experiments. The crude mixtures were analysed by GC directly after work-up. Activated ester **249** and boronic ester **250** were previously synthesised, isolated and characterised by Dr. Alexander Fawcett.

An additional experiment was carried out to determine whether there was an intramolecular inhibition of the reaction by subjecting fully substituted carbamate (*S*)-**366** to the second-generation conditions (**Scheme 63**). Unfortunately, no desired product was observed and most of the starting activated ester was recovered. These results showed that the free N–H bond in Boc-protected amino acids was not the inhibiting factor and suggested that another property of amino acids prevented the reaction from occurring.



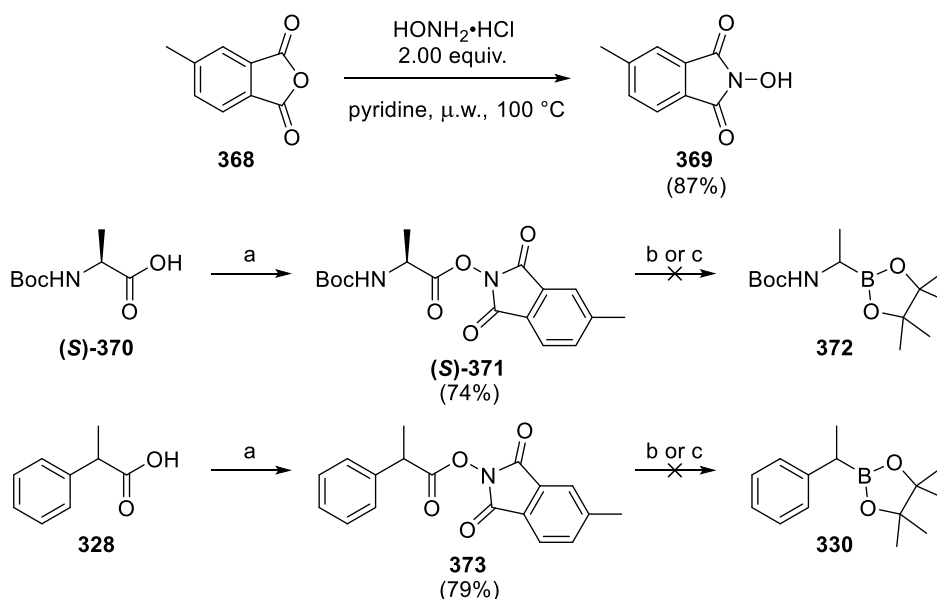
Scheme 63. Disubstituted carbamate **(S)-366** did not undergo decarboxylative borylation under second-generation reaction conditions. NHPI = *N*-hydroxyphthalimide.

2.2.7. Effect of redox potentials

Based on the proposed radical mechanism (**Scheme 51**), one would suggest that amino acids failed to provide the desired boronic esters because a reaction component (either starting material or by-product) could oxidise the intermediate radical species before it was trapped by the boron source. One way to face this issue would be to modify the redox potential of the starting material or postulated by-product **270**. Hence, Boc-protected alanine **(S)-370** was activated by a coupling reaction with methyl-substituted phthalimide **369**, easily synthesised in one step²⁷³ from methyl-substituted phthalic anhydride **368**, and subjected to the optimised conditions (**Scheme 64**). A control experiment was performed in parallel, using compound **373**.

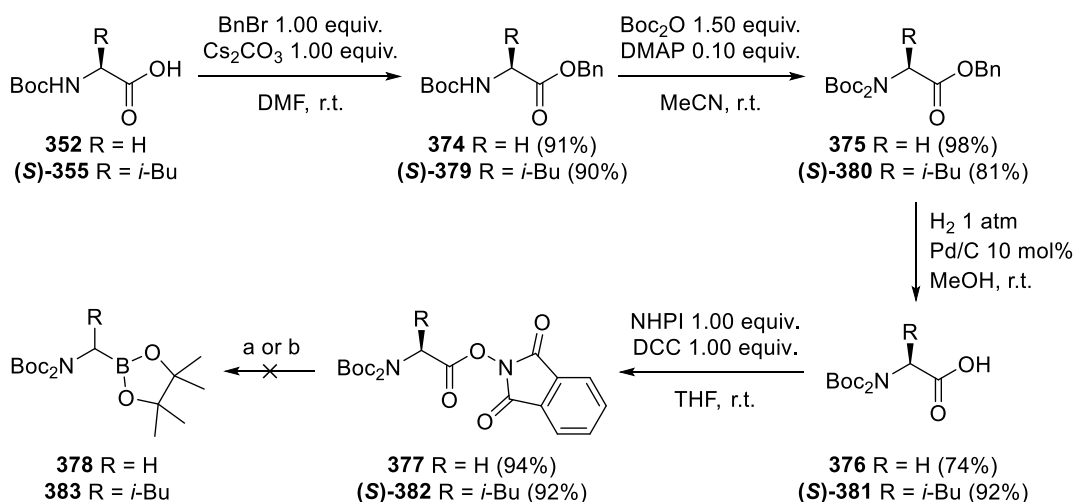
Unfortunately, in both cases, about 90% of the intermediate activated ester (**(S)-371** or **373**) was recovered by column chromatography. The control experiment showed that the α -nitrogen of alanine was not the cause of failure. Presumably, the presence of a methyl group on the phthalimide moiety could lead to an inefficient formation of the light-absorbing complex formation due to steric hindrance or could change the redox potential of the activated ester itself, thus preventing the decarboxylation step from taking place.

An alternative strategy was envisaged to change the redox potential of the radical intermediate. Indeed, having a second electron-withdrawing group (*i.e.*, Boc group) attached to the nitrogen atom would make the reactive radical less prone to oxidation. Therefore, compounds **377** and **(S)-382** were synthesised (**Scheme 65**) and tested under the reaction conditions.



Scheme 64. Attempt to change the redox potential of the phthalimide derivatives by using methyl-substituted *N*-hydroxyphthalimide **369** as an activating group. (a) **369** 1.00 equiv., DIC 1.00 equiv., DMAP 0.10 equiv., CH₂Cl₂, r.t.; (b) B₂cat₂ 1.25 equiv., DMAc, blue LEDs, *then* pinacol 4.00 equiv., Et₃N 25.00 equiv., r.t.; (c) B₂cat₂ 0.50 equiv., B₂(OH)₄ 1.00 equiv., 4-MeOPy 2.00 equiv., DMAc, dark, *then* pinacol 4.00 equiv., AcOH 4.00 equiv., r.t.

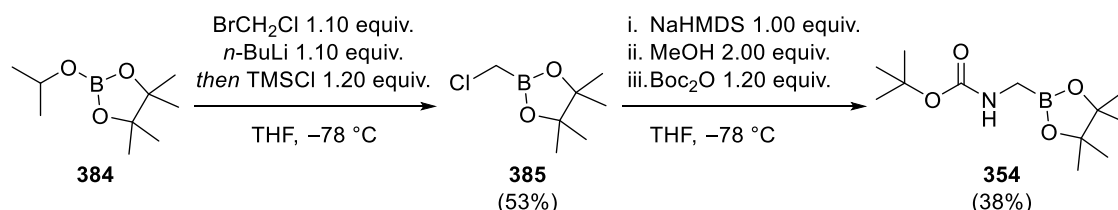
After work-up, TLC revealed that starting materials were still present. Unfortunately, no desired product could be isolated in both cases. At that point, it seemed sensible to use a different methodology to synthesise an α -amino boronate, which could then serve as a reference for optimisation studies.



Scheme 65. Preparation of doubly Boc-protected activated esters **377** and **(S)-382**. (a) B₂cat₂ 1.25 equiv., DMAc, blue LEDs, *then* pinacol 4.00 equiv., Et₃N 25.00 equiv., r.t.; (c) B₂cat₂ 0.50 equiv., B₂(OH)₄ 1.00 equiv., 4-MeOPy 2.00 equiv., DMAc, dark, *then* pinacol 4.00 equiv., AcOH 4.00 equiv., r.t. NHPI = *N*-hydroxyphthalimide.

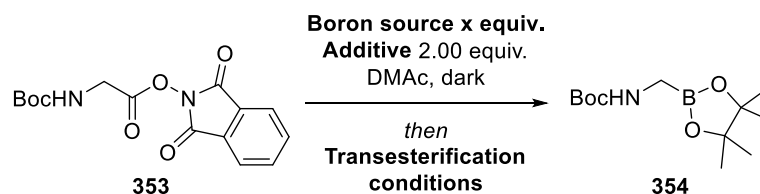
2.2.8. Optimisation study on activated glycine

Inspired by Matteson's seminal investigations (**Scheme 45a**), Ley described an easy methodology²⁷⁴ to access α -amino boronate **354** from boronic ester **385**. In this one-pot reaction (**Scheme 66**), NaHMDS acted as a nucleophile to displace the chloride. Then, addition of methanol cleaved both N–Si bonds to release a free α -amino boronate. Finally, treatment with Boc_2O yielded the desired product which could be isolated by column chromatography. Pleasingly, the desired compound could be synthesised according to this methodology and subjected to gas chromatography.



Scheme 66. Synthesis of α -amino boronic ester **354** according to Ley's methodology to serve as a GC reference in subsequent optimisation study.

With the reference compound in hand, the decarboxylative borylation of activated ester **353** was investigated. Three parameters were screened, including boron source, additive and transesterification conditions (**Table 9**).

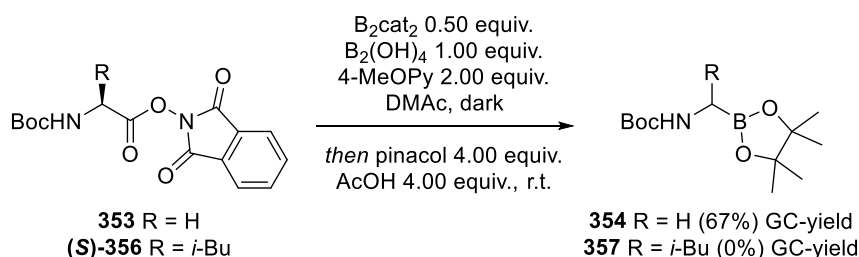


Boron source	Additive (2.00 equiv.)	Transesterification conditions	GC-yield
B₂cat₂ 0.50 equiv., B₂(OH)₄ 1.00 equiv.	4-MeOPy	pinacol 4.00 equiv., AcOH 4.00 equiv., 4 h, r.t.	67%
B ₂ cat ₂ 0.50 equiv., B ₂ (OH) ₄ 1.00 equiv.	4-MeOPy	pinacol 4.00 equiv., 4 h, r.t.	46%
B₂cat₂ 1.25 equiv.	4-MeOPy	pinacol 4.00 equiv., AcOH 4.00 equiv., 4 h, r.t.	20%
B₂pin₂ 1.25 equiv.	4-MeOPy	pinacol 4.00 equiv., AcOH 4.00 equiv., 4 h, r.t.	7%
B₂(OH)₄ 1.25 equiv.	4-MeOPy	pinacol 4.00 equiv., AcOH 4.00 equiv., 4 h, r.t.	25%
B₂(OH)₄ 1.50 equiv.	4-MeOPy	pinacol 4.00 equiv., AcOH 4.00 equiv., 4 h, r.t.	29%
B₂(OH)₄ 2.00 equiv.	4-MeOPy	pinacol 4.00 equiv., AcOH 4.00 equiv., 4 h, r.t.	24%
B ₂ cat ₂ 0.50 equiv., B ₂ (OH) ₄ 1.00 equiv.	4-AcPy	pinacol 4.00 equiv., AcOH 4.00 equiv., 4 h, r.t.	9%

B ₂ cat ₂ 0.50 equiv., B ₂ (OH) ₄ 1.00 equiv.	4,4'-bipyridine	pinacol 4.00 equiv., AcOH 4.00 equiv., 4 h, r.t.	8%
B ₂ cat ₂ 0.50 equiv., B ₂ (OH) ₄ 1.00 equiv.	4-<i>tert</i>-BuPy	pinacol 4.00 equiv., AcOH 4.00 equiv., 4 h, r.t.	38%
B ₂ cat ₂ 0.50 equiv., B ₂ (OH) ₄ 1.00 equiv.	4-NCPy	pinacol 4.00 equiv., AcOH 4.00 equiv., 4 h, r.t.	8%
B ₂ cat ₂ 0.50 equiv., B ₂ (OH) ₄ 1.00 equiv.	DMAP	pinacol 4.00 equiv., AcOH 4.00 equiv., 4 h, r.t.	6%
B ₂ cat ₂ 0.50 equiv., B ₂ (OH) ₄ 1.00 equiv.	4-PhPy	pinacol 4.00 equiv., AcOH 4.00 equiv., 4 h, r.t.	23%
B ₂ cat ₂ 0.50 equiv., B ₂ (OH) ₄ 1.00 equiv.	pyridine	pinacol 4.00 equiv., AcOH 4.00 equiv., 4 h, r.t.	15%
B ₂ cat ₂ 0.50 equiv., B ₂ (OH) ₄ 1.00 equiv.	4-MePy	pinacol 4.00 equiv., AcOH 4.00 equiv., 4 h, r.t.	11%
B ₂ cat ₂ 0.50 equiv., B ₂ (OH) ₄ 1.00 equiv.	Methyl isonicotinate	pinacol 4.00 equiv., AcOH 4.00 equiv., 4 h, r.t.	10%

Table 9. Optimisation study using Boc-protected glycine derivative **353** as a model substrate. 4-MeOPy = 4-methoxypyridine; 4-AcPy = 4-acetylpyridine; 4-*tert*-BuPy = 4-*tert*-butylpyridine; 4-NCPy = 4-cyanopyridine; 4-MePy = 4-methylpyridine.

The best conditions matched those discovered by Dr. Alexander Fawcett after his first optimisation study on proline derivative (*S*)-**342** and gave the desired boronic ester **354** in 67% GC-yield (**Scheme 67**). Unfortunately, as explained in Section 2.2.5., in the case of glycine, the desired product could not be separated from the reaction by-products, even when the optimised purification procedure was used. Sadly, no new spot was observed by TLC when leucine derivative (*S*)-**356** was subjected to the optimised reaction conditions.

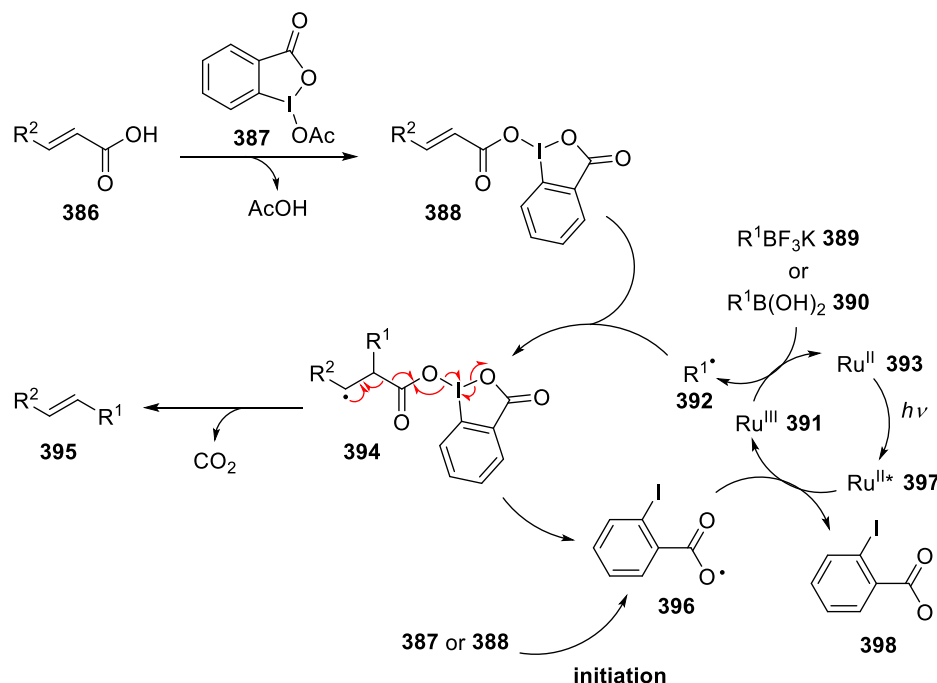


Scheme 67. Optimised conditions for the decarboxylative borylation of Boc-protected glycine **353** failed to convert Boc-protected valine (*S*)-**356**.

2.2.9. Hypervalent iodine derivatives

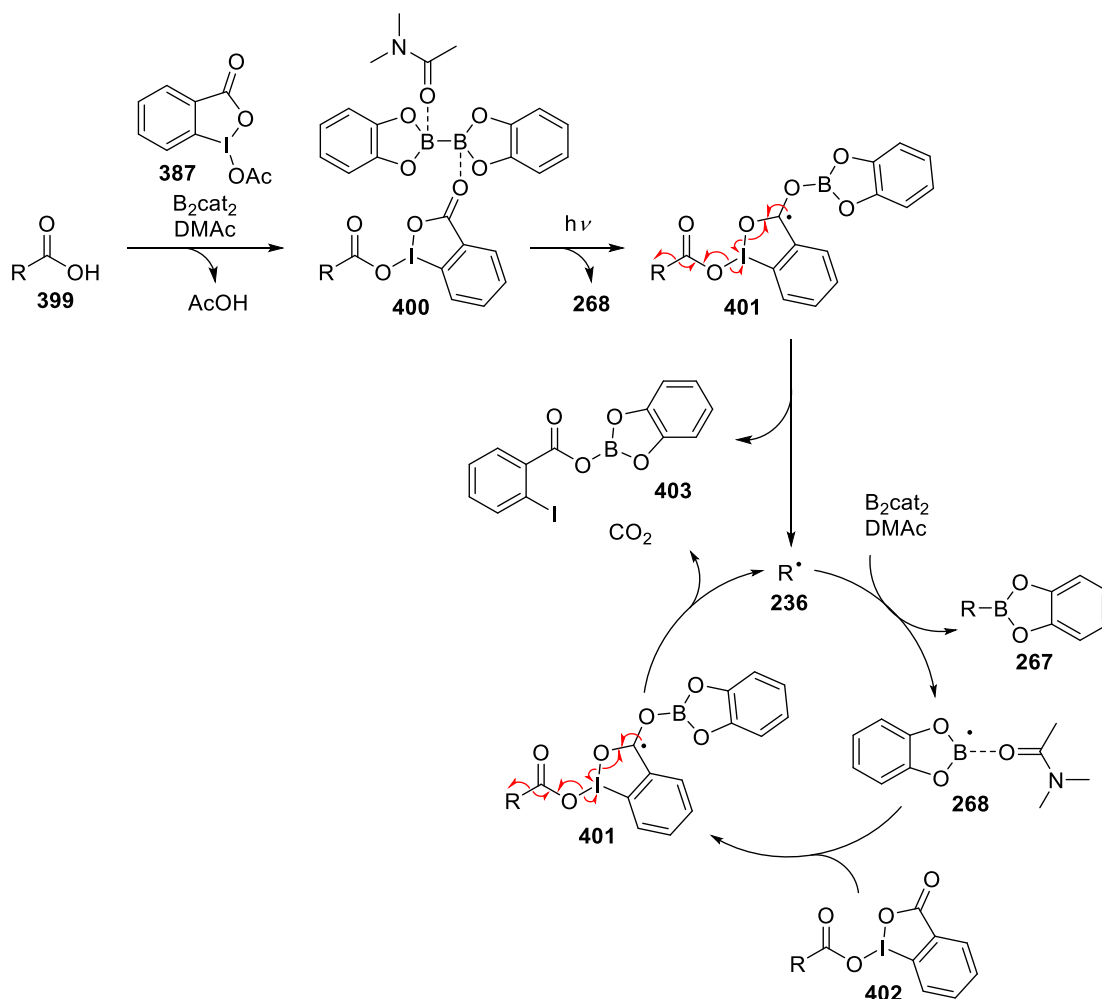
In 2015, Chen and co-workers published an interesting study²⁷⁵ about the ability of hypervalent iodine reagents to enable chemoselective decarboxylative alkenylation in the presence of a photocatalyst. They proposed a mechanism (**Scheme 68**) in which a ruthenium(II) photocatalyst was sequentially excited with light and oxidised to ruthenium(III) by an O-centred radical, derived from the radical decomposition of hypervalent iodine species **387** or **388**. The catalyst could then

be reduced with trifluoroborate salt **389** or boronic acid **390** to complete the catalytic cycle and generate alkyl radical **392**. This highly reactive species added to *in situ*-activated ester **388** to give benzylic radical **394** ($R' = \text{aryl}$). At this stage, a radical fragmentation occurred to deliver alkene **395** with concomitant release of carbon dioxide and O-centred radical **396**.



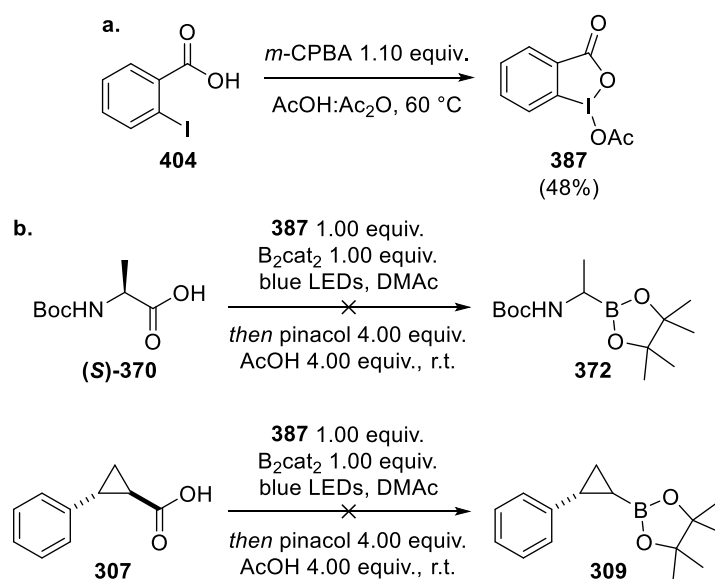
Scheme 68. Chen's mechanistic proposal for the hypervalent iodine-mediated alkenylation reaction. $R^1 = \text{alkyl}$; $R^2 = \text{aryl, heteroaryl, acyl}$. Brackets have been omitted for clarity.

Inspired by this methodology, a reaction mechanism for the hypervalent iodine-mediated decarboxylative borylation was proposed (**Scheme 69**). Carboxylic acid **399** would be activated *in situ* by ligand exchange at the hypervalent iodine centre. The corresponding activated ester would form a light-absorbing complex **400** in the presence of B_2cat_2 and DMAc. Under light irradiation, an electron could be transferred from the boron source to the activated ester to give putative radical intermediate **401**. This unstable species would then undergo a radical fragmentation resulting in the reduction of the iodine centre with concomitant release of boron carboxylate by-product **403**, carbon dioxide and alkyl radical **236**. After that, a chain reaction mechanism would take place, in which radical **236** would be trapped by B_2cat_2 in the presence of DMAc to deliver the desired borylated compound **267** and a stabilised boryl radical **268**. This radical could then add to another molecule of activated ester **402** to form unstable intermediate **401**, which would fragment to generate alkyl radical **236** and propagate the chain mechanism.



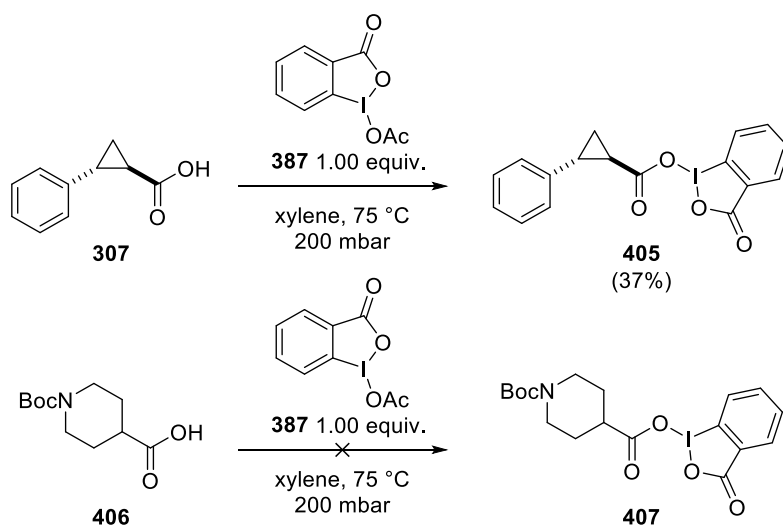
Scheme 69. Proposed mechanism of decarboxylative borylation using hypervalent iodine reagent **387** as activating agent. Brackets have been omitted for clarity.

To test this hypothesis, a stoichiometric amount of hypervalent iodine derivative **387**²⁷⁶ was added to a solution of B_2cat_2 and carboxylic acid (*S*)-**370** or **307** in DMAc to trigger the decarboxylation event (**Scheme 70**). Interestingly, the order of introduction of the reagents was important. In fact, when compound **387** was mixed with B_2cat_2 in DMAc in the absence of carboxylic acid, the colourless solution rapidly turned black and released heat. However, in the presence of a carboxylic acid, a yellow solution was formed and the resulting mixture could be irradiated with blue LEDs for 14 hours. Unfortunately, in both cases, TLC showed no desired product after work-up.

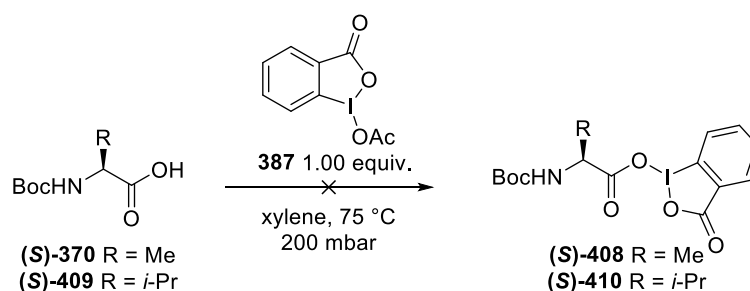


Scheme 70. a. Preparation of compound **387**. b. Unsuccessful decarboxylative borylation reactions using **398** as activating agent.

Interestingly, Chen and co-workers managed to synthesise activated ester intermediate **388** by refluxing a mixture of carboxylic acid **386** and hypervalent iodine derivative **387** in xylenes at 70°C under reduced pressure. Under these conditions, the equilibrium was shifted towards the formation of the product by constant removal of acetic acid from the reaction mixture. Similar conditions were applied to carboxylic acids **307** and **406** (**Scheme 71**). In the first case, pure compound **405** was obtained as a white solid after recrystallisation. However, the other substrates led to an inseparable mixture of starting materials and decomposition products. Intermediate **405** was then mixed with B_2cat_2 in DMAc and stirred overnight under blue light irradiation. TLC showed traces of product which, after chromatography, was obtained in only 2% yield.

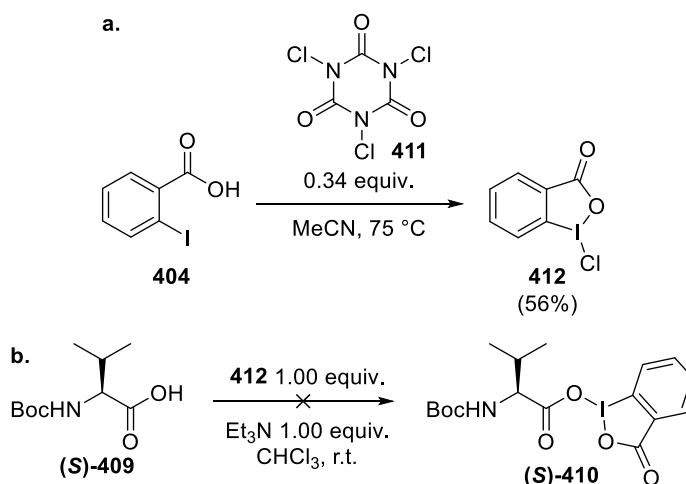


Scheme 71. Activation of carboxylic acids **307** and **406** using hypervalent iodine reagent **397**.



Scheme 72. Unsuccessful activation of Boc-protected alanine (**(S)**-370 and valine (**(S)**-409) using hypervalent iodine reagent **387**.

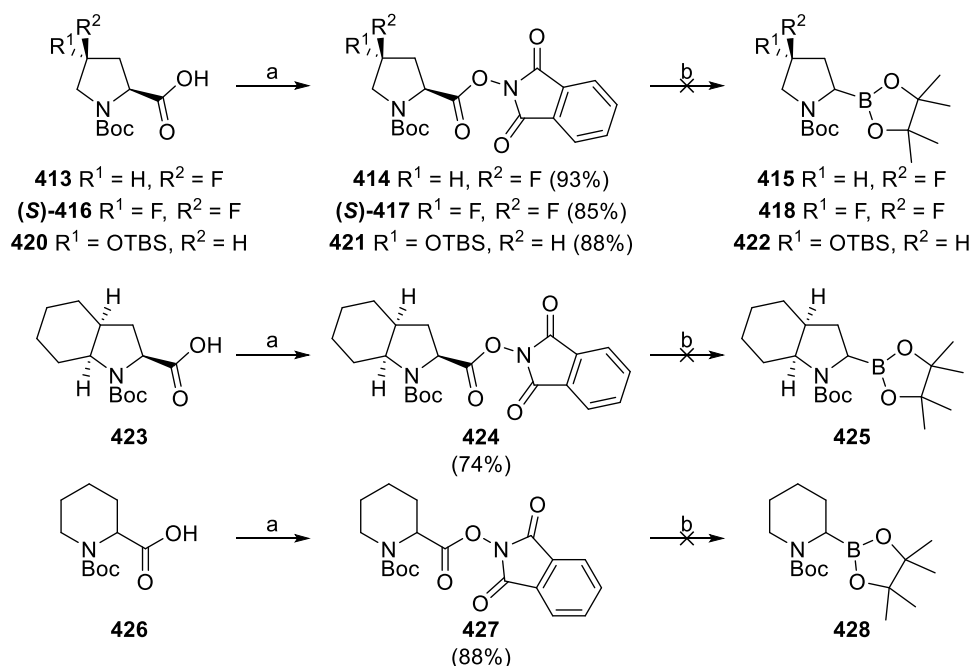
Boc-protected alanine and valine were subjected to the same activation conditions (**Scheme 72**) but the corresponding activated intermediates could not be isolated. An alternative route was attempted, which involved mixing the amino acid with hypervalent iodine derivative **412**—easily made in one step²⁷⁷ from 2-iodobenzoic acid **404**—in the presence of a base (**Scheme 73**). Unfortunately, the desired activated esters could not be formed under these conditions and this strategy was abandoned.



Scheme 73. **a.** Preparation of hypervalent iodine compound **412**. **b.** Unsuccessful activation of Boc-protected valine (**(S)**-409).

2.2.10. Limited substrate scope

Despite repeated efforts, only α -amino boronate (**(S)**-343) could be synthesised and isolated. An unidentified key feature of the pyrrolidine ring was crucial for the reaction to succeed. Based on this observation, some proline derivatives were synthesised and subjected to the second set of conditions developed by Dr. Alexander Fawcett to build a new substrate scope. Three substituted pyrrolidine rings (**413**, (**(S)**-416 and **420**), one bicyclic system (**423**) and one piperidine ring (**426**) were successfully activated (**Scheme 74**).



Scheme 74. Activation and decarboxylative borylation of proline derivatives. (a) *N*-hydroxyphthalimide 1.00 equiv., DIC 1.00 equiv., DMAP 0.10 equiv., CH_2Cl_2 , r.t.; (b) B_2cat_2 0.50 equiv., $B_2(OH)_4$ 1.00 equiv., 4-MeOPy 2.00 equiv., DMAc, dark, r.t.

Surprisingly, none of the five substrates gave the corresponding boronic ester. Instead, complex mixtures were obtained when fluorinated analogues **414** and **(S)-417** were used and starting activated esters were recovered in the case of compounds **421**, **424** and **427**. These results showed that the reaction was very sensitive to steric hindrance or the conformation of the 5-membered ring and, maybe, to electronic effects of the substituents.

2.3. Conclusion

The decarboxylative borylation of carboxylic acids has been investigated. The substrate scope of this new methodology was improved by including some medicinal chemistry-type examples, such as a fluorine-containing cyclohexane, a pyridine derivative and a substituted cyclopropane. Three additional natural products were successfully converted to the corresponding boronic esters. Key mechanistic experiments were conducted to prove the radical pathway and provide support for an outer sphere radical trapping process.

To improve the applicability of this methodology, a study on the decarboxylative borylation of amino acids was conducted. First, the reaction conditions were optimised on a proline derivative by Dr. Alexander Fawcett. Unfortunately, he could not separate the material from other by-products. A purification screening was performed to address this issue. With these new conditions in

hand, other activated amino acids were tested. However, most of them did not afford the desired product.

To face this problem, the effect of free N–H bonds on the reaction outcome was studied. Spiking experiments showed that the reaction was not affected by the presence of additives bearing free N–H bonds. Moreover, a fully protected alanine derivative could not be converted to the corresponding boronic ester. Therefore, the presence of a N–H bond was removed from the list of potential inhibiting factors. An investigation on redox potentials was carried out to determine whether changing the substitution pattern of the activated ester (either at the nitrogen atom or at the phthalimide moiety) could lead to an improvement. Unfortunately, doubly protected amino acids or methyl-substituted activated esters failed to deliver the desired boronic esters.

At this stage, another optimisation study on glycine revealed that this amino acid could also be converted to the desired product under the conditions developed earlier for proline. Yet, the corresponding boronic ester could not be separated from the reaction by-product. To overcome this problem, a different mode of activation was envisaged.

Inspired by the work of Chen and co-workers on hypervalent iodine-mediated decarboxylative alkenylation,²⁷⁵ different sets of conditions involving the use of hypervalent iodine derivatives were tested. Attempts to activate carboxylic acids *in* and *ex situ* showed that these species were very unstable and difficult to make. This strategy was abandoned after several unsuccessful results.

Finally, as proline seemed to be the only amino acid to be transformed into a boronic ester which could be successfully purified, a limited substrate scope composed of proline derivatives was subjected to the reaction conditions. Sadly, none of these examples gave the desired product. After these discouraging results, the project was abandoned.

EXPERIMENTAL SECTION

3.1. General experimental

3.1.1. Computation

Molecular mechanics calculations were performed using the MacroModel software package²⁷⁸ (version 9.9) accessed through the Maestro²⁷⁹ (version 9.2) program. All geometry optimisations, frequency calculations and NMR calculations were performed using the Gaussian 09 Software package.²⁸⁰ All molecular mechanics calculations were performed using the Unix computational resource of the School of Chemistry, University of Bristol. All DFT calculations were performed using either the Unix computational resource or the computational facilities of the advanced computing research centre at the University of Bristol (<http://www.bris.ac.uk/acrc>).

3.1.2. Solvents and reagents

All air- and water-sensitive reactions were carried out in flame-dried glassware under a nitrogen or argon atmosphere using standard Schlenk manifold technique. Anhydrous solvents were commercially supplied or provided and dried using a purification column composed of activated alumina and stored over thoroughly dried 3 Å molecular sieves by the communal stills of the School of Chemistry, University of Bristol.²⁸¹

n-Butyl lithium [CAS: 109-72-8] was purchased from Acros (181271000) as a 1.60 M solution in *n*-hexane. *s*-Butyl lithium [CAS: 598-30-1] was purchased from Acros (187541000) as a 1.30 M solution in cyclohexane:*n*-hexane 98:2. *tert*-Butyl lithium [CAS: 594-19-4] was purchased from Sigma-Aldrich (186198) as a 1.70 M solution in *n*-pentane. (+)-Sparteine and (–)-sparteine were obtained from the commercially available sulphate pentahydrate salt (99%, Acros) and isolated according to literature procedure.²⁸² The sparteine free base readily absorbs atmospheric carbon dioxide (CO₂) and so should be stored under argon/nitrogen at –20 °C in a sealed Schlenk-tube. The molarity of organolithium solutions was regularly determined by titration using *N*-benzyl benzamide as an indicator.²⁸³ B₂cat₂ [CAS: 13826-27-2] was purchased either from Sigma-Aldrich (473286) or Fluorochem (211650), and both yielded the same results (despite their appearances differing). We have noticed that different batches contain differing amounts of catechol, however this does not appear to affect the yield. Anhydrous *N,N*-dimethylacetamide [CAS: 127-19-5] was purchased from Sigma-Aldrich (271012).

All other reagents were purchased from various commercial sources and used as received or synthesised according to the procedures given.

3.1.3. Chromatography and data analysis

Analytical TLC was performed on aluminium backed silica plates (Merck, Silica Gel 60 F254, 0.25 mm). Compounds were visualised by fluorescence quenching or by staining the plates with either 5% solution of phosphomolybdic acid ($\text{H}_3\text{PMo}_{12}\text{O}_{40}$) in EtOH, KMnO_4 , ninhydrin, or anisaldehyde followed by heating.

Flash column chromatography was performed on either silica gel (Merk, Silica Gel 60, 40–63 μm). All mixed solvent eluents are reported as v/v solutions.

^1H , ^{13}C , ^{11}B and ^{19}F NMR spectra were recorded using JEOL ECS 300 MHz, JEOL ECS 400 MHz, Varian 400 MR or Varian VNMRs 500 MHz NMR spectrometers equipped with direct observe two-channel probes, or Bruker AVANCE III HD 500 MHz NMR spectrometer with 5 mm DCH $^{13}\text{C}/^1\text{H}/\text{D}$ Cryo Probe. Chemical shifts (δ) are given in parts per million (ppm) and referenced to the residual protio-solvent resonances (Chloroform = [^1H] 7.26 ppm, [^{13}C] 77.0 ppm; Dimethyl sulfoxide = [^1H] 2.50 ppm, [^{13}C] 39.5 ppm; Toluene = [^1H] 2.09 ppm, [^{13}C] 20.4 ppm). Coupling constants (J) are given in Hertz (Hz), rounded to the nearest 0.1 Hz. ^1H NMR spectra are reported as follows: δ (number of protons, multiplicity, coupling constants, assignment) ppm. Multiplicity is reported as follows: s = singlet, br. s = broad singlet, d = doublet, t = triplet, q = quartet, pent = pentet, sext = sextet, hept = heptet, m = multiplet, dd = doublet of doublet, etc. The abbreviation *app.* is added when apparent multiplicities and corresponding apparent coupling constants are reported. NMR assignments are made according to spin systems, using two-dimensional NMR spectroscopy (COSY, HSQC, HMBC), where appropriate, to assist the assignment. ^{11}B NMR spectra were measured using Norell S-200-QTZ quartz NMR tubes at 96 or 128 MHz with complete proton decoupling. ^{13}C signals adjacent to boron are generally not observed due to quadrupolar relaxation.

High resolution mass spectra (HRMS) were recorded by the University of Bristol, School of Chemistry departmental mass spectrometry service using a Bruker Daltonics MicrOTOF II by Electrospray Ionisation (ESI) or on a VG Micromass Autospec (Triple-sector) by Electronic Impact (EI) or on a Bruker Daltonics UltrafleXtreme (MALDI).

IR spectra were recorded on a Perkin Elmer Spectrum One FT–IR as a thin film, if a liquid, or in the solid state, if solid. Only selected absorption maxima (ν_{max}) are reported.

Melting points were recorded in degrees Celsius ($^{\circ}\text{C}$) using a Kofler hot-stage microscope apparatus or a Stuart SMP30 melting point apparatus and are uncorrected.

Optical rotation ($[\alpha]_D^T$) was measured on a Bellingham and Stanley Ltd. ADP220 polarimeter at 589 nm (Na D-line) in a cell with a path length of 1 dm. Specific rotation values are given in $^{\circ}\text{cm}^3\text{g}^{-1}\text{dm}^{-1}$.

Gas Chromatography (GC) was performed on an Agilent 7890A using an Agilent HP-5 column (15 m \times 0.25 mm \times 0.25 μ m).

GC–MS was performed using an Agilent HP-5MS column (15 m \times 0.250 mm), an Agilent 6890 GC, and Agilent 5973 MS system. Compounds were identified through extract ion chromatogram and molecular ion analysis. Method 70-1X: Inlet temperature 250 °C; Flow rate: 1.00 mL min⁻¹; hold at 70 °C for 0 min; ramp 20 °C min⁻¹ to 200 °C; ramp 45.0 °C min⁻¹ to 300 °C; hold at 300 °C for 2 min.

Chiral high-performance liquid chromatography (HPLC) separations were performed on an Agilent 1100 Series HPLC unit equipped with UV-vis diode-array detector monitored at 210.8 nm, using Daicel Chiralpak IA, IB or IC columns (4.6 \times 250 mm², 5 μ m) fitted with respective guards (4 \times 10 mm²).

Supercritical fluid chromatography (SFC) was performed on a Thar SFC investigator using a Daicel Chiralpak IA, IB, IC columns or a Whelk-O1 column (4.6 \times 250 mm², 5 μ m).

UV-visible spectroscopy was performed using a Lambda 35 spectrometer with standard glass cells with a 1 cm path length at wavelengths 200–800 nm.

Single crystal X-ray diffraction experiments on **C10**, **154**, **169**, **175** and **186** were carried out at 100(2) K on a Bruker APEX II CCD diffractometer using Mo-K α radiation (λ = 0.71073 Å). Single crystal X-ray diffraction experiments on **138** were carried out at 100(2) K on a Bruker Microstar rotating anode CCD diffractometer using Cu-K α radiation (λ = 1.54184 Å). Intensities were integrated in SAINT²⁸⁴ and absorption corrections were based on equivalent reflections using SADABS.²⁸⁵ The structure was solved using either Superflip^{286,287} or SHELXT^{288,289} and refined by full matrix least squares against F² in SHELXL^{288,289} using Olex2.²⁹⁰ All of the non-hydrogen atoms were refined anisotropically, while all of the hydrogen atoms were located geometrically and refined using a riding model.

3.1.4. Naming of compounds

Compound names are those generated by ChemDraw Professional 16.0 software (PerkinElmer Informatics, Inc.), following the IUPAC nomenclature.

3.1.5. Photoreactor

Photoreactors comprised of a 5.0 m strip of Fluxia blue SMD3528 LEDs coiled around a glass crystallising dish. The average power output per LED was recorded at 3.05 mW on a Coherent

LabMax-TOP laser power meter equipped with a Coherent Power/Max PS10 sensor with a 10 mm diameter aperture, 10 mm from aperture. The emission spectra of the blue LEDs were recorded on an Ocean Optics HR4000CG-UV-NIR spectrometer. The spectrum was normalised to 1.0 at the maximum (450 nm).

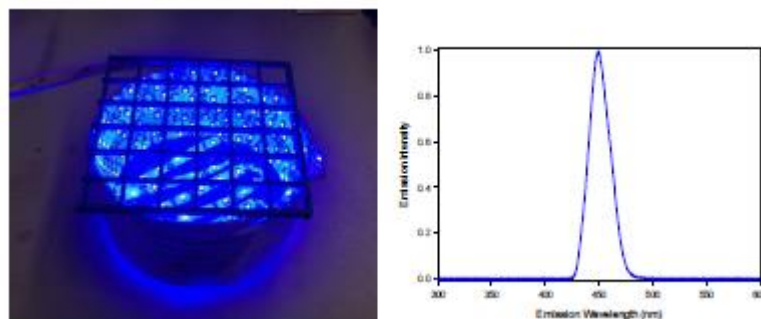


Figure 37. Photoreactor setup and emission spectrum of LEDs.

3.2. Supplementary materials – Chapter 1

3.2.1. General procedures

General procedure 1 (GP1): A premixed aqueous solution of NaOH (2 M) and H₂O₂ (30%) (2:1, 6.00 mL) was added dropwise to a solution of the boronic ester (1.00 equiv.) in THF (4.00 mL) at 0 °C. The reaction mixture was vigorously stirred at room temperature for 4–16 h. The reaction mixture was diluted with water (10.00 mL) and Et₂O (10.00 mL). The layers were separated and the aqueous phase extracted with Et₂O (3 × 10.00 mL). The combined organic layers were washed with brine, dried over MgSO₄ and concentrated under reduced pressure. Residual pinacol was sublimed under high vacuum for 18 h to give the desired product.

General procedure 2 (GP2): In a flame-dried Schlenk tube, stannane **93** (1.30 or 2.30 equiv.) was dissolved in anhydrous Et₂O (0.20 M) under an atmosphere of nitrogen. The reaction mixture was cooled to –78 °C (a white precipitate of stannane appeared) and a solution of *n*-BuLi (1.50–1.60 M in *n*-hexane, 1.30 or 2.30 equiv.) was added dropwise *via* syringe. After the addition, the reaction mixture was stirred at –78 °C for 1.5 h. A solution of the boronic ester (1.00 equiv.) in anhydrous Et₂O (0.20 M) was then added dropwise *via* syringe. The reaction mixture was stirred at –78 °C for 30 min. The acetone/dry ice bath was removed, and the reaction mixture was allowed to stir at room temperature for 1 h. The white suspension was filtered through silica (2 cm depth of wetted (Et₂O) silica, using a filter frit connected directly to a flame-dried receiving vessel). The filter was washed with Et₂O and the filtrate was concentrated under reduced pressure.

The crude boronic ester was analysed by GC chromatography and could be re-dissolved in anhydrous Et₂O (to make a 0.20 M solution) and used in further homologations or isolated and purified by flash column chromatography.

General procedure 3 (GP3): Part A: In a flame-dried Schlenk tube, the boronic ester (1.00 equiv.) and vinyl carbamate **15** (1.10 equiv.) were dissolved in anhydrous THF (0.15 M) at $-78\text{ }^{\circ}\text{C}$ under an atmosphere of nitrogen. A freshly prepared solution of LDA (0.86 M in THF, 1.10 equiv.) was added and the reaction mixture was stirred at the same temperature for 1 h. The acetone/dry ice bath was replaced with an acetonitrile/dry ice bath and the reaction mixture was stirred at $-40\text{ }^{\circ}\text{C}$ for 1 h. After cooling the reaction mixture back to $-78\text{ }^{\circ}\text{C}$, a freshly prepared solution of iodine (1.10 equiv.) in MeOH (0.20 M) was added dropwise *via* syringe. After the addition, the reaction mixture was allowed to stir at room temperature for 1 h. A saturated aqueous solution of NH₄Cl was added and the biphasic mixture was extracted 3 times with Et₂O. The organic layers were combined, washed with brine, dried over MgSO₄, filtered through silica (2 cm depth of dry silica, using a filter frit connected directly to a flame-dried receiving vessel), concentrated under reduced pressure and dried under high vacuum for (at least) 1 h. **Part B:** The dried crude residue was dissolved in anhydrous Et₂O (0.10 M) at $-78\text{ }^{\circ}\text{C}$ under an atmosphere of nitrogen. A freshly prepared solution of LDA (0.86 M in THF, 2.50 equiv.) was added and the reaction mixture was allowed to stir at room temperature for 1 h. A saturated aqueous solution of NH₄Cl was added *via* syringe and the biphasic mixture was extracted 3 times with Et₂O. The organic layers were combined, washed with brine, dried over MgSO₄, filtered and concentrated under reduced pressure. The residue was purified by flash column chromatography to give the desired product(s).

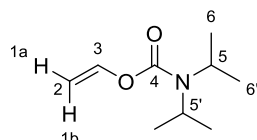
General procedure 4 (GP4): In a flame-dried Schlenk tube, the alkyne (1.00 equiv.) and TIPSCl (1.10 equiv.) were dissolved in anhydrous THF (0.20 M) at $-78\text{ }^{\circ}\text{C}$ under an atmosphere of nitrogen. A freshly prepared solution of LDA (0.86 M in THF, 1.10 equiv.) was added and the mixture was stirred at the same temperature for 1 h. The white suspension was allowed to warm to room temperature and gently heated with a heat-gun ($50\text{ }^{\circ}\text{C}$) until the white solid dissolved. The clear solution was stirred at room temperature for 16 h, quenched with a saturated aqueous solution of NH₄Cl and extracted 3 times with Et₂O. The organic layers were combined, washed with brine, dried over MgSO₄, filtered and concentrated under reduced pressure. The residue was purified by flash column chromatography to give the desired product.

General procedure 5 (GP5): In a Schlenk tube, the protected alkyne (1.00 equiv.) was dissolved in THF (0.20 M) at $0\text{ }^{\circ}\text{C}$ under an atmosphere of nitrogen. A solution of TBAF (1.00 M in THF,

2.00 equiv.) was added *via* syringe and the mixture was stirred at room temperature for 2 h. A saturated aqueous solution of NH₄Cl was added and the biphasic mixture was extracted 3 times with Et₂O. The organic layers were combined, washed with brine, dried over MgSO₄, filtered and concentrated under reduced pressure. The residue was purified by flash column chromatography to give the desired product.

3.2.2. Experimental procedures and characterisation data

Vinyl diisopropylcarbamate (**15**)



In a flame-dried Schlenk tube, THF (12.00 mL) was cooled to -78°C under an atmosphere of nitrogen. A solution of *n*-BuLi (1.60 M in *n*-hexane, 11.46 mL, 18.33 mmol, 1.50 equiv.) was added *via* syringe. After the addition, the acetone/dry ice bath was removed, and the reaction mixture was stirred at room temperature for 16 h. A solution of *N,N*-diisopropylcarbamoyl chloride (2.00 g, 12.22 mmol, 1.00 equiv.) in anhydrous DMPU (7.00 mL) was added *via* syringe and the reaction mixture was stirred at room temperature for 4 h. A saturated aqueous solution of NH₄Cl (20.00 mL) was added, followed by water (5.00 mL) and Et₂O (20.00 mL). The phases were separated, and the aqueous layer was extracted with Et₂O (3×20.00 mL). The organic layers were combined, washed with brine, dried over MgSO₄, filtered and concentrated under reduced pressure. The orange residue was purified by flash column chromatography (*n*-pentane:Et₂O 95:5) to give carbamate **15** (1.34 g, 64%) as a colourless liquid.

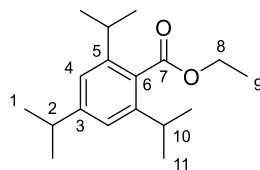
TLC: $R_f = 0.47$ (*n*-pentane:Et₂O 90:10)

¹H NMR: (400 MHz, Chloroform-*d*) δ 7.24 (1H, dd, $J = 14.1, 6.3$ Hz, H3), 4.75 (1H, dd, $J = 14.1, 1.4$ Hz, H1b), 4.41 (1H, dd, $J = 6.3, 1.4$ Hz, H1a), 4.04 (1H, br. s, H5), 3.84 (1H, br. s, H5'), 1.24 (12H, d, $J = 6.9$ Hz, H6 & H6') ppm

¹³C NMR: (101 MHz, Chloroform-*d*) δ 152.9 (C4), 142.5 (C3), 94.7 (C2), 46.8 (C5), 45.9 (C5'), 21.7 (C6), 20.5 (C6') ppm

Spectral data were in accordance with that reported in the literature.²⁰⁷

Ethyl 2,4,6-triisopropylbenzoate (**91**)



In a 2-L round-bottomed flask, 2,4,6-triisopropylbenzoic acid (40.00 g, 161.10 mmol, 1.00 equiv.) and 1-bromoethane (60.10 mL, 805.30 mmol, 5.00 equiv.) were dissolved in CHCl_3 (800.00 mL) at room temperature. A solution of NaOH (20.00 g, 499.30 mmol, 3.10 equiv.) and $n\text{-Bu}_4\text{N}(\text{HSO}_4)$ (4.40 g, 12.90 mmol, 0.08 equiv.) in water (640.00 mL) was added and the biphasic mixture was vigorously stirred at room temperature for 18 h. The phases were separated, and the aqueous layer was extracted with CH_2Cl_2 (3×200.00 mL). The organic phases were combined, washed with brine, dried over MgSO_4 and concentrated under reduced pressure. The crude product was suspended in n -pentane (120.00 mL) and the insoluble salts were filtered off. The filtrate was concentrated under reduced pressure to give benzoate **91** (44.50 g, 99%) as a colourless liquid.

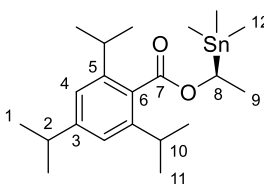
TLC: $R_f = 0.32$ (n -pentane:EtOAc 97:3)

^1H NMR (400 MHz, Chloroform- d): δ 7.00 (2H, s, H4), 4.37 (2H, q, $J = 7.1$ Hz, H8), 3.01 – 2.71 (3H, m, H2 & H10), 1.37 (3H, t, $J = 7.1$ Hz, H9), 1.31 – 1.15 (18H, m, H1 & H11) ppm

^{13}C NMR (101 MHz, Chloroform- d): δ 14.4 (C9), 24.1 (C1), 24.2 (C11), 31.6 (C10), 34.6 (C2), 60.9 (C8), 121.0 (C4), 130.8 (C6), 144.95 (C5), 150.2 (C3), 170.9 (C7) ppm

Spectral data were in accordance with that reported in the literature.⁴⁷

(*S*)-1-(Trimethylstannyl)ethyl 2,4,6-triisopropylbenzoate ((*S*)-**93**)



In a flame-dried 1-L round-bottomed flask, ethyl 2,4,6-triisopropylbenzoate **91** (10.00 g, 36.20 mmol, 1.00 equiv.) and (–)-sparteine (10.80 mL, 47.00 mmol, 1.30 equiv.) were dissolved in anhydrous Et_2O (200.00 mL). The solution was cooled to -78°C and allowed to equilibrate for 10 min. A solution of $s\text{-BuLi}$ (1.30 M in hexanes, 36.20 mL, 47.00 mmol, 1.30 equiv.) was

added dropwise *via* syringe to the reaction mixture at $-78\text{ }^{\circ}\text{C}$ over 20 min (colour change: colourless \rightarrow dark brown). The reaction mixture was stirred at $-78\text{ }^{\circ}\text{C}$ for 4 h. A solution of trimethyltin chloride (1.00 M in *n*-hexane, 47.00 mL, 47.00 mmol, 1.30 equiv.) was added dropwise to the reaction mixture *via* syringe over 10 min (colour change: dark brown \rightarrow pale yellow). The reaction mixture was stirred at $-78\text{ }^{\circ}\text{C}$ for 20 min before being warmed to room temperature and stirred for 1 h. The reaction mixture was quenched with an aqueous solution of HCl (2.00 M, 100.00 mL) and stirred for a further 20 min. The phases were separated, and the organic layer was washed with an aqueous solution of HCl (2.00 M, $3 \times 100.00\text{ mL}$). The combined aqueous layers were extracted with Et_2O ($3 \times 100.00\text{ mL}$). The combined organic layers were dried over MgSO_4 and concentrated under reduced pressure to give crude stannane (**(S)-93**) (16.25 g). The opposite enantiomer (**(R)-93**) was synthesised in identical yields by substituting (–)-sparteine for (+)-sparteine.

Sparteine recovery²⁸²

The combined aqueous layers were basified ($\sim \text{pH } 12$) by addition of an aqueous solution of NaOH (20% w/w). The aqueous phase was extracted with Et_2O ($3 \times 100.00\text{ mL}$). The combined organic layers were washed with brine, dried over MgSO_4 , filtered and concentrated under reduced pressure to give crude sparteine. Distillation* of the residual oil over CaH_2 gave (–)-sparteine (9.90 g, 92%) as a colourless liquid.

*Distillation conditions: bulb-to-bulb; 10 cm Vigreux column; pressure: 2 mbar; oil bath: $150\text{ }^{\circ}\text{C}$; CaH_2 (100 mg mL^{-1}); b.p.: $137 - 138\text{ }^{\circ}\text{C}$ (1.33 mbar).

Recrystallisation of enantioenriched stannane

MeOH (3.00 mL g^{-1}) was added to the crude stannane in a one neck round-bottomed flask. A condenser was fitted to the round-bottom flask and the solution was brought to reflux (heat gun) until all the solids had dissolved. The solution was then allowed to cool to room temperature. Crystals appeared after 10 min to 5 h depending on the purity of crude stannane. The crystals were then filtered and dried under reduced pressure to give a white solid (10.31 g, 99.2:0.8 *e.r.*). The product was then recrystallised once more from MeOH (3.00 mL g^{-1}) to give, after two crops, **(S)-93** (8.41 g, 53%, 99.9:0.1 *e.r.*) as a white solid.

TLC: $R_f = 0.42$ (*n*-pentane: Et_2O 97:3)

^1H NMR (400 MHz, Chloroform-*d*): δ 7.00 (2H, s, H4), 5.04 (1H, q, $J = 7.6\text{ Hz}$, H8), 2.94 – 2.76 (3H, m, H2 & H10), 1.59 (3H, d, $J = 7.6\text{ Hz}$, H9), 1.25 – 1.23 (18H, m, H1 & H11), 0.18 (9H, d, $J_{^{119}\text{Sn}-^1\text{H}} = 54.2\text{ Hz}$, d, $J_{^{117}\text{Sn}-^1\text{H}} = 51.7\text{ Hz}$ and s, H12) ppm

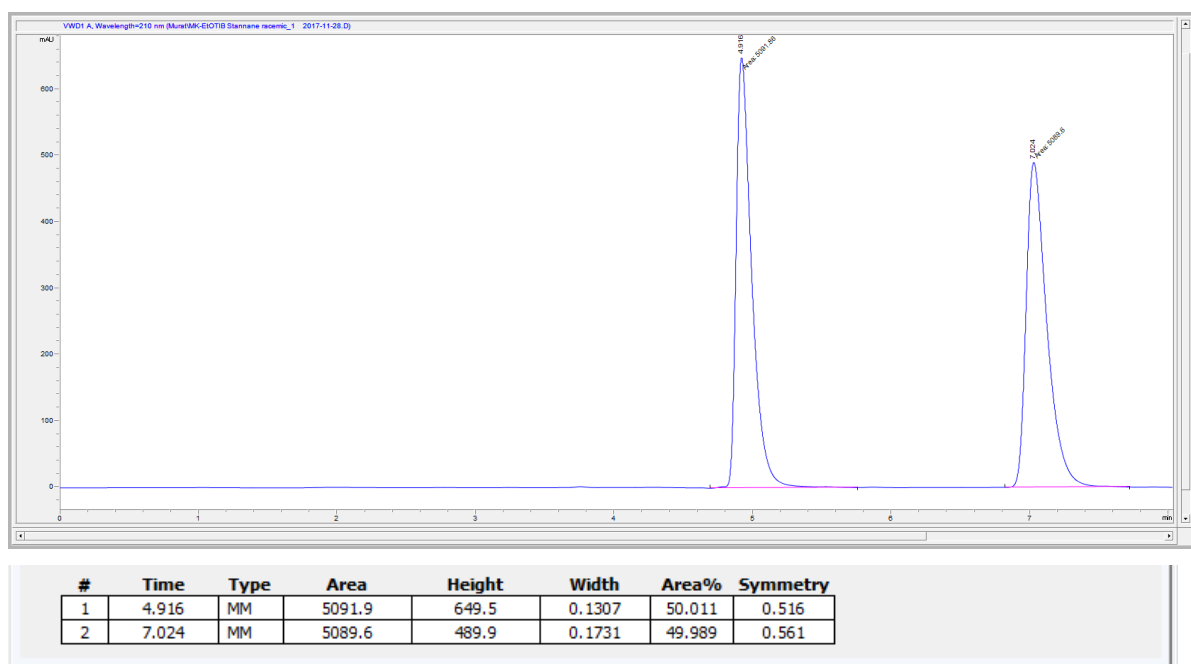
^{13}C NMR (101 MHz, Chloroform-*d*): δ 171.4 (C7), 150.1 (C3), 145.0 (C5), 130.9 (C6), 120.9 (C4), 67.2 (C8), 34.6 (C2), 31.5 (C10), 24.5 (C1 or C11 or C11'), 24.2 (C1 or C11 or C11'), 24.1

(C1 or C11 or C11'), 19.4 (C9), -9.8 (d, $J_{119\text{Sn}-13\text{C}} = 333.5$ Hz, d, $J_{117\text{Sn}-13\text{C}} = 319.3$ Hz and s, C12) ppm

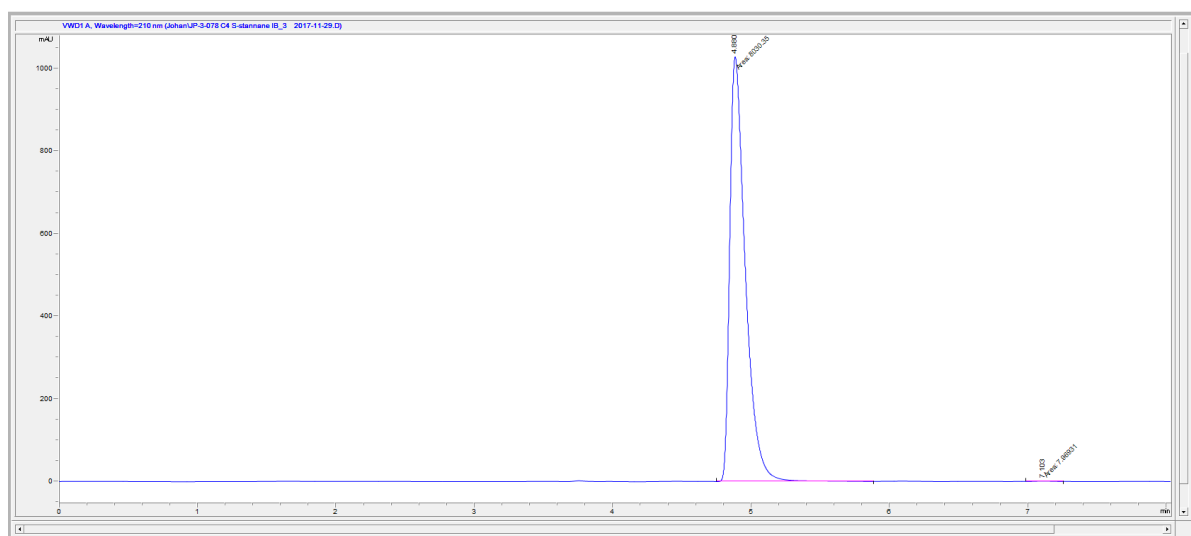
Spectral data were in accordance with that reported in the literature.¹

Chiral HPLC: Daicel Chiralpak IB column (25 cm) with guard, 100% *n*-hexane, 0.90 mL min⁻¹, room temperature, 210 nm: $t_R = 4.9$ min (major), 7.1 min (minor), 99.9:0.1 *e.r.*

(+/-)-1-(Trimethylstannyl)ethyl 2,4,6-triisopropylbenzoate (rac-93)

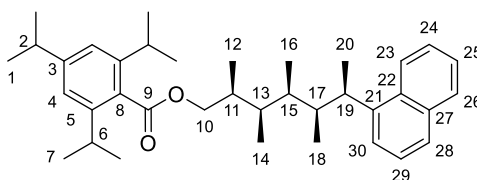


(S)-1-(Trimethylstannyl)ethyl 2,4,6-triisopropylbenzoate ((S)-93)



#	Time	Type	Area	Height	Width	Area%	Symmetry
1	4.88	MM	8030.4	1028.8	0.1301	99.901	0.507
2	7.103	MM	8	9.3E-1	0.1422	0.099	0.849

(2*S*,3*R*,4*S*,5*S*,6*R*)-2,3,4,5-Tetramethyl-6-(naphthalen-1-yl)heptyl 2,4,6-triisopropylbenzoate (114**)**



In a flame-dried Schlenk tube, 1-bromonaphthalene (0.01 mL, 0.08 mmol, 1.20 equiv.) was dissolved in anhydrous Et₂O (0.50 mL) at 0 °C under an atmosphere of nitrogen. A solution of *n*-BuLi (1.55 M in *n*-hexane, 0.05 mL, 0.08 mmol, 1.20 equiv.) was added dropwise and the resulting white suspension was stirred at 0 °C for 1 h. A solution of boronic ester **126** (36 mg, 0.07 mmol, 1.00 equiv.) in anhydrous Et₂O (0.25 mL) was added dropwise and the resulting pale yellow solution was stirred at 0 °C for 2 h. Solvents were removed under vacuum and the white residue was re-dissolved in anhydrous MeOH (1.00 mL) at –78 °C. A solution of NBS (29 mg, 0.16 mmol, 2.40 equiv.) in anhydrous MeOH (1.50 mL) was added dropwise over 20 min. After the addition, the acetone/dry ice bath was removed and the reaction mixture was allowed to stir at room temperature for 1 h. A saturated aqueous solution of Na₂S₂O₃ (1.00 mL) was added. The cloudy mixture was vigorously stirred for 5 min, diluted with water (10.00 mL) and extracted with Et₂O (3 × 5.00 mL). The organic layers were combined, washed with brine, dried over MgSO₄, filtered and concentrated to afford a yellow residue. The crude material was purified by flash column chromatography (*n*-pentane:Et₂O 98:2) to give benzoate **114** (17 mg, 47%) as a colourless liquid.

TLC: *R*_f = 0.51 (*n*-pentane:Et₂O 90:10)

¹H NMR (400 MHz, Chloroform-*d*): δ 8.17 (1H, d, *J* = 9.4 Hz, H23), 7.86 (1H, m, H26), 7.69 (1H, d, *J* = 8.0 Hz, H28), 7.40 – 7.52 (3H, m, H24, H25 & H29), 7.36 (1H, d, *J* = 7.2 Hz, H30), 7.03 (2H, s, H4), 4.10 – 4.14 (2H, m, H10), 3.53 (1H, m, H19), 2.84 – 2.94 (3H, m, H2 & H6), 2.09 – 2.13 (2H, m, H11 & H17), 1.56 (1H, m, H13), 1.31 (3H, d, *J* = 6.9 Hz, H20), 1.27 (18H, m, H1 & H7), 1.10 (1H, m, H15), 0.93 (3H, d, *J* = 6.7 Hz, H18), 0.70 (3H, d, *J* = 6.8 Hz, H16), 0.62 (3H, d, *J* = 6.9 Hz, H14), 0.53 (3H, d, *J* = 6.8 Hz, H12) ppm

¹³C NMR (101 MHz, Chloroform-*d*): δ 171.4 (C9), 150.1 (C3), 144.9 (C5), 144.1 (C21), 134.1 (C27), 131.9 (C22), 130.9 (C8), 129.2 (C26), 126.3 (C28), 125.7 (C25 or C29), 125.6 (C25 or C29), 125.3 (C24), 124.0 (C30), 123.3 (C23), 121.0 (C4), 69.7 (C10), 39.8 (C17), 36.9* (C19),

36.2 (C13 or C15), 36.1 (C15 or C13), 34.6 (C2), 32.9 (C11), 31.7 (C6), 24.4 (C7'), 24.3 (C7), 24.1 (C1), 20.7 (C20), 12.1 (C16), 11.9 (C18), 11.6 (C14), 11.1 (C12) ppm

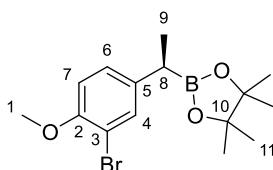
**shift value determined by HSQC correlation.*

HRMS (*m/z*): (ESI⁺) calc'd. for C₃₇H₅₂NaO₂ [M+Na]⁺: 551.3860; found 551.3867

IR (ν_{\max}): 2962, 2873, 1722, 1606, 1460, 1383, 1250, 1136, 1069, 778, 732 cm⁻¹

[α]_D²⁰: +21 (CHCl₃, *c* = 1.0)

(*R*)-2-(1-(3-Bromo-4-methoxyphenyl)ethyl)-4,4,5,5-tetramethyl-1,3,2-dioxaborolane
((*R*)-120)



In a flame-dried Schlenk vessel, freshly purified CuCl (29 mg, 0.30 mmol, 0.03 equiv.), *tert*-BuOK (44 mg, 0.39 mmol, 0.04 equiv.) and (*S*)-DTBM-SEGPHOS (348 mg, 0.30 mmol, 0.03 equiv.) were mixed in degassed (*i.e.*, sparged with nitrogen for 1 h) anhydrous toluene (5.00 mL) at room temperature under an atmosphere of nitrogen. Freshly distilled pinacolborane (1.71 mL, 11.80 mmol, 1.20 equiv.) was added and the yellow solution turned brown. After 10 min, a solution of 2-bromo-1-methoxy-4-vinylbenzene (2.10 g, 9.84 mmol, 1.00 equiv.) in degassed anhydrous toluene (4.00 mL) was added and the reaction mixture was stirred under an atmosphere of nitrogen for 16 h. The dark suspension was filtered through Celite[®], washed with *n*-pentane (50.00 mL) and the filtrate was concentrated under reduced pressure. The residue was purified by flash column chromatography (*n*-pentane:Et₂O 90:10) to give boronic ester (**(*R*)-120**) (2.94 g, 88%, 98.9:1.1 *e.r.*) as a pale yellow liquid.

TLC: *R*_f = 0.20 (*n*-pentane:Et₂O 90:10)

¹H NMR (400 MHz, Chloroform-*d*): δ 7.39 (1H, d, *J* = 2.2 Hz, H4), 7.11 (1H, dd, *J* = 8.4, 2.2 Hz, H6), 6.81 (1H, d, *J* = 8.4 Hz, H7), 3.85 (3H, s, H1), 2.34 (1H, q, *J* = 7.5 Hz, H8), 1.28 (3H, d, *J* = 7.5 Hz, H9), 1.21 (6H, s, H11), 1.20 (6H, s, H11') ppm

¹³C NMR (101 MHz, Chloroform-*d*): δ 153.6 (C2), 138.8 (C5), 132.6 (C4), 127.8 (C6), 112.1 (C7), 111.5 (C3), 83.5 (C10), 56.4 (C1), 24.8 (C11), 24.7 (C11'), 17.3 (C9) ppm

The signal corresponding to C8 was not observed due to quadrupolar relaxation.

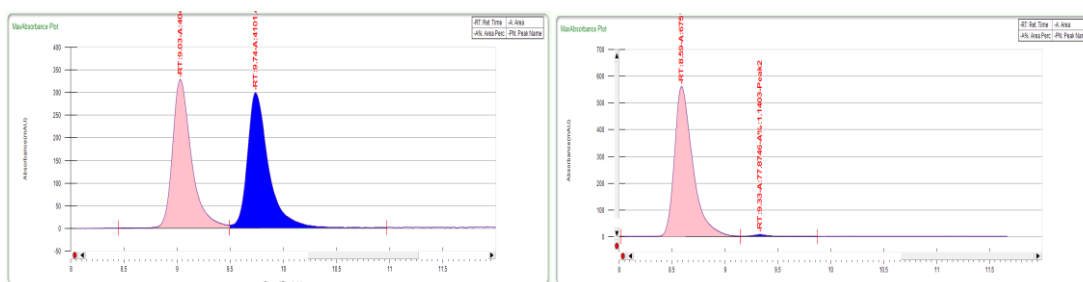
HRMS (*m/z*): (ESI⁺) calc'd. for C₁₅H₂₂B⁷⁹BrNaO₃ [M+Na]⁺: 363.0740; found 363.0746

IR (ν_{\max}): 2975, 2873, 1495, 1321, 1251, 1140, 1054, 849 cm⁻¹

$[\alpha]_D^{23}$: -8 (CHCl₃, *c* = 1.0)

Boronic ester (**R**)-**120** (about 20 mg) was oxidised to the corresponding alcohol according to **GP1** for chiral SFC analysis.

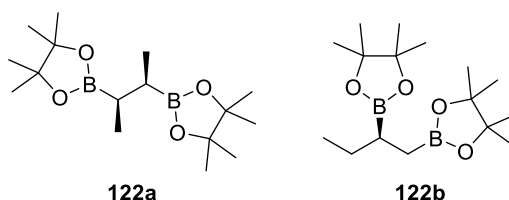
Chiral SFC: Daicel Chiralpak IA column (25 cm), 20.0% co-solvent (*n*-hexane:IPA 90:10), 4.00 mL min⁻¹, 39.6 °C, 124 bar, 210.0 nm): *t*_R = 9.03 min (major), 9.74 min (minor), 98.9:1.1 *e.r.*



Peak Information

Peak No	% Area	Area	Ret. Time	Height	Cap. Factor
1	49.6431	4043.3105	9.03 min	327.9011	9028.6333
2	50.3569	4101.4426	9.74 min	298.5023	9735.25

2,2'-((2*R*,3*R*)-Butane-2,3-diyl)bis(4,4,5,5-tetramethyl-1,3,2-dioxaborolane) (122a) and **(*S*)-2,2'-((Butane-1,2-diyl)bis(4,4,5,5-tetramethyl-1,3,2-dioxaborolane) (122b)**



In a flame-dried Schlenk tube, Rh(nbd)(acac) (124 mg, 0.42 mmol, 0.05 equiv.) and (*S*)-QUINAP (185 mg, 0.42 mmol, 0.05 equiv.) were dissolved in anhydrous THF (10.00 mL) at room temperature under an atmosphere of nitrogen. A solution of B₂cat₂ (2.00 g, 8.41 mmol, 1.00 equiv.) in anhydrous THF (30.00 mL) was added and the yellow solution turned brown. The reaction mixture was then cooled to -10 °C. In a separated flame-dried Schlenk tube, a solution of *trans*-but-2-ene in THF was made by slow addition of anhydrous THF (3.00 mL) to condensed *trans*-but-2-ene (3.00 mL, 32.08 mmol, 3.80 equiv.) at -78 °C under an atmosphere of nitrogen. This colourless solution was then quickly transferred to the reaction mixture *via* syringe and the dark solution was stirred at -10 °C for 10 min. The NaCl/ice bath was removed, and the reaction mixture was stirred at room temperature for 18 h under an atmosphere of nitrogen. Pinacol (1.99 g, 16.82 mmol, 2.00 equiv.) was then added and the reaction was stirred at room temperature for 16 h. The dark suspension was concentrated under reduced pressure to afford a brown

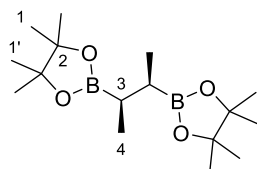
oil. The crude residue was purified by flash column chromatography (*n*-hexane:EtOAc 95:5) to give 1.80 g of a 74:26 mixture* of boronic ester **122a** (1.33 g, 51%, >99.5:0.5 *e.r.*, >95:5 *d.r.*) and boronic ester **122b** (0.47 g, 18%, 77.8:22.2 *e.r.*) as a colourless liquid.

*The corresponding regioisomeric ratio (74:26 *r.r.*) was determined by ¹H NMR analysis.

Note 1: Both products are unstable under air and on silica.

Note 2: For full characterisation and *e.r.* determination of both products, a few fractions containing pure materials could be obtained by multiple slow chromatography steps (*n*-pentane:Et₂O 98:2). However, this iterative purification process led to a massive loss of products. For this reason, the 74:26 mixture of products was directly engaged in the next homologation step after the first quick column chromatography (*n*-hexane:EtOAc 95:5) as described above.

2,2'-((2*R*,3*R*)-Butane-2,3-diyl)bis(4,4,5,5-tetramethyl-1,3,2-dioxaborolane) (**122a**)



TLC: *R*_f = 0.62 (*n*-pentane:Et₂O 80:20)

¹H NMR (400 MHz, Chloroform-*d*): δ 1.22 (12H, s, H1), 1.21 (12H, s, H1'), 1.12 (2H, m, H3), 0.95 (6H, d, *J* = 7.1 Hz, H4) ppm

¹³C NMR (101 MHz, Chloroform-*d*): δ 82.9 (C2), 24.8 (C1), 25.0 (C1'), 14.0 (C4) ppm

The signal corresponding to C3 was not observed due to quadrupolar relaxation.

HRMS (*m/z*): (ESI⁺) calc'd. for C₁₆H₃₂B₂NaO₄ [M+Na]⁺: 333.2385; found: 333.2385

IR (*ν*_{max}): 2977, 2927, 2873, 1457, 1370, 1307, 1214, 1140, 969 cm⁻¹

[α]_D²⁴: +9 (CHCl₃, *c* = 1.0; 99.7:0.3 *e.r.*)

Enantiomeric ratio (*e.r.*) determination:

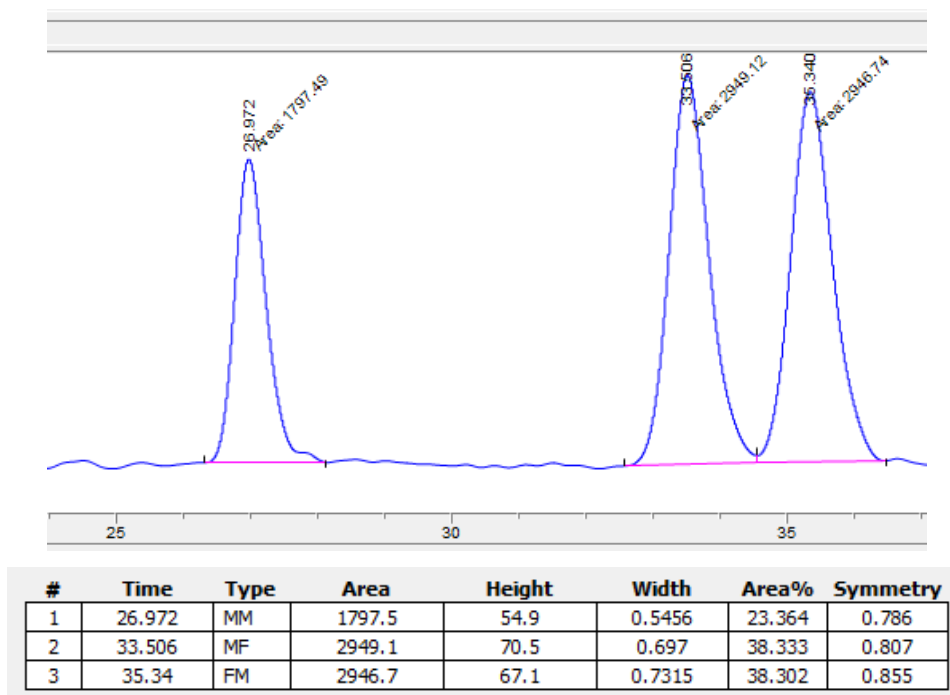
Part A: A solution of pure boronic ester **122a** (35 mg, 0.11 mmol, 1.00 equiv.) in THF (2.00 mL) was slowly added into a mixture NaOH (2.00 M in water, 2.00 mL) and H₂O₂ (30% in water, 1.00 mL) at 0 °C. The reaction mixture was stirred at 0 °C for 4 h. Na₂SO₄ (614 mg) was added and the biphasic mixture was stirred at room temperature for 16 h. The layers were separated, and the aqueous phase was extracted with EtOAc 5 times. The organic phases were combined, dried over MgSO₄, filtered and the volume of solvent was reduced to 0.20 mL by rotary evaporation. *n*-Pentane (0.20 mL) was added and the colourless solution was loaded on column chromatography. The desired diol was separated from pinacol using *n*-hexane:EtOAc 50:50 as eluent.

Pure fractions were combined and concentrated at 45 °C under atmospheric pressure (volatile material) to a volume of solvent of about 0.20 mL. **Part B:** Tosyl chloride (42 mg, 0.22 mmol, 2.00 equiv.) and triethylamine (0.03 mL, 0.22 mmol, 2.00 equiv.) were added and the reaction mixture was stirred at room temperature for 16 h. The brown solution was diluted with CH₂Cl₂ (1.00 mL) and water (1.00 mL). The layers were separated, and the aqueous phase was extracted with CH₂Cl₂ (3 × 1.00 mL). The organic phases were combined, dried over MgSO₄, filtered and concentrated. The crude residue was purified by flash column chromatography (*n*-hexane:EtOAc 85:15) to give the desired bis(tosylate), which was analysed by chiral HPLC.

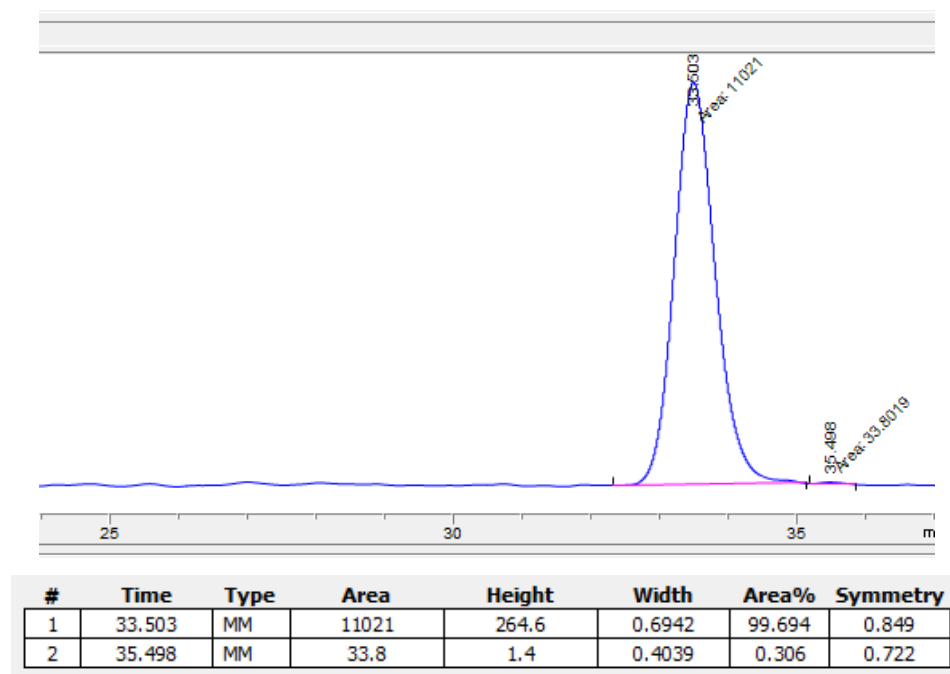
Note: A commercially available mixture of (2*R*,3*S*)-, (2*R*,3*R*)- and (2*S*,3*S*)-butane-2,3-diol was tosylated according to the same procedure (**Part B**) to give the analytical reference for *e.r.* determination by chiral HPLC.

Chiral HPLC: Daicel Chiralpak IA column (25 cm) with guard, *n*-hexane:IPA 90:10, 0.70 mL min⁻¹, room temperature, 210 nm: *t*_R = 27.0 min (*meso*), 33.5 min (major), 35.3 min (minor), >99.5:0.5 *e.r.*

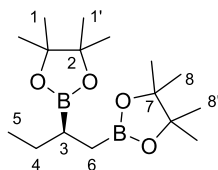
(2*R*,3*S*)-Butane-2,3-diyl bis(4-methylbenzenesulfonate), (2*R*,3*R*)-Butane-2,3-diyl bis(4-methylbenzenesulfonate) and (2*S*,3*S*)-Butane-2,3-diyl bis(4-methylbenzenesulfonate)



(2*R*,3*R*)-butane-2,3-diyl bis(4-methylbenzenesulfonate)



(S)-2,2'-(Butane-1,2-diyl)bis(4,4,5,5-tetramethyl-1,3,2-dioxaborolane) (122b)



TLC: R_f = 0.58 (*n*-pentane:Et₂O 80:20)

¹H NMR (500 MHz, Chloroform-*d*): δ 1.47 (1H, ddq, J = 13.5, 8.4, 7.4 Hz, H₄), 1.37 (1H, dqd, J = 13.5, 7.4, 5.7 Hz, H₄'), 1.23 (24H, m, H₁, H₁', H₈ & H₈'), 1.06 (1H, m, H₃), 0.92 – 0.83 (4H, m, H₅ & H₆), 0.78 (1H, dd, J = 15.7, 5.8 Hz, H₆') ppm

¹³C NMR (126 MHz, Chloroform-*d*): δ 82.9 (C₂), 82.9 (C₇), 26.9 (C₄), 25.1 (C₁), 25.0 (C₈), 24.9 (C₁'), 24.9 (C₈'), 20.5 (C₃), 13.5 (C₅), 12.5 (C₆) ppm

HRMS (m/z): (ESI⁺) calc'd. for C₁₆H₃₃B₂O₄ [M+H]⁺: 311.2565; found: 311.2577

IR (ν_{\max}): 2977, 2929, 2874, 1370, 1311, 1141, 968 cm⁻¹

$[\alpha]_D^{24}$: +1 (CHCl₃, c = 1.0; 77.8:22.2 *e.r.*)

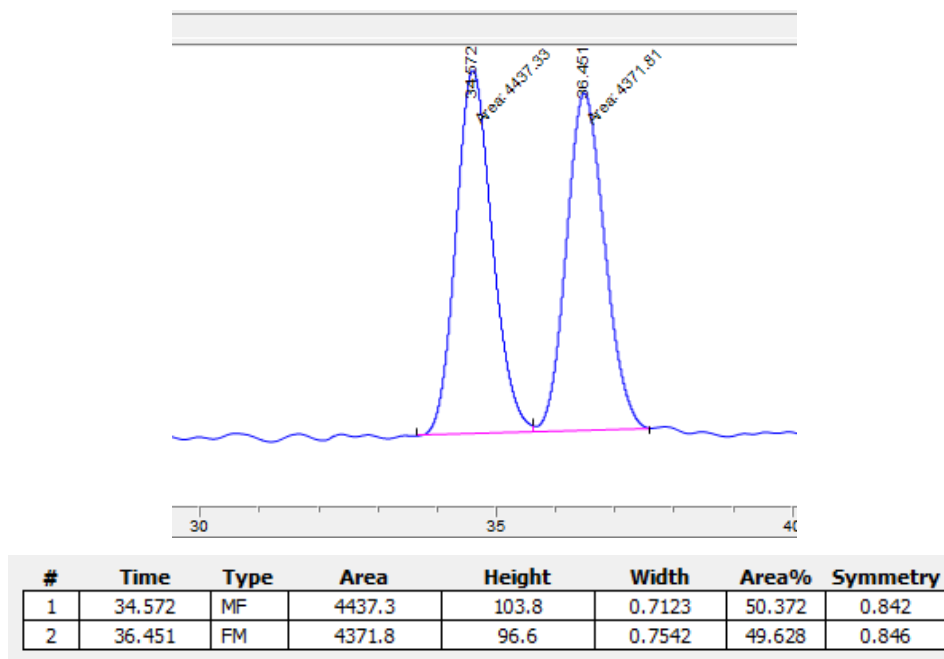
Enantiomeric ratio (*e.r.*) determination:

Part A: A solution of pure boronic ester **122b** (53 mg, 0.17 mmol, 1.00 equiv.) in THF (2.00 mL) was slowly added into a mixture of NaOH (2.00 M in water, 2.00 mL) and H₂O₂ (30% in water, 1.00 mL) at 0 °C. The reaction mixture was stirred at 0 °C for 4 h. Na₂SO₄ (614 mg) was added and the biphasic mixture was stirred at room temperature for 16 h. The layers were separated, and the aqueous phase was extracted with EtOAc 5 times. The organic phases were combined, dried over MgSO₄, filtered and the volume of solvent was reduced to 0.20 mL by rotary evaporation. *n*-Pentane (0.20 mL) was added and the colourless solution was loaded on column chromatography. The desired diol was separated from pinacol using *n*-hexane:EtOAc 50:50 as eluent. Pure fractions were combined and concentrated at 45 °C under atmospheric pressure (volatile material) to a volume of solvent of about 0.20 mL. **Part B:** Tosyl chloride (65 mg, 0.34 mmol, 2.00 equiv.) and triethylamine (0.05 mL, 0.34 mmol, 2.00 equiv.) were added and the reaction mixture was stirred at room temperature for 16 h. The brown solution was diluted with CH₂Cl₂ (1.00 mL) and water (1.00 mL). The layers were separated, and the aqueous phase was extracted with CH₂Cl₂ (3 × 1.00 mL). The organic phases were combined, dried over MgSO₄, filtered and concentrated. The crude residue was purified by flash column chromatography (*n*-hexane:EtOAc 85:15) to give the desired bis(tosylate), which was analysed by chiral HPLC.

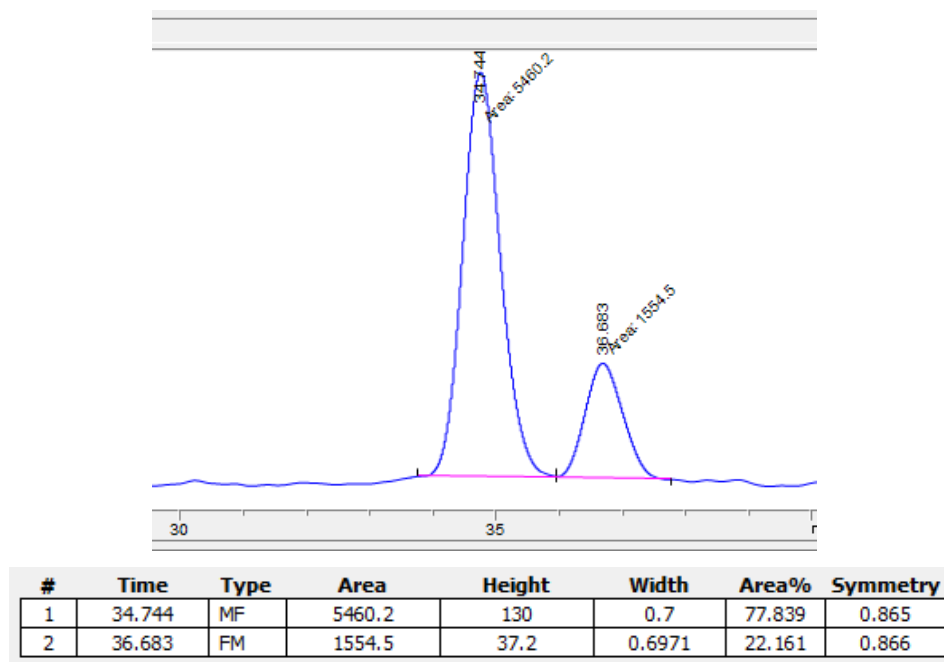
Note: Commercially available (+/–)-Butane-1,2-diol was tosylated according to the same procedure (**Part B**) to give the analytical reference for *e.r.* determination by chiral HPLC.

Chiral HPLC: Daicel Chiralpak IA column (25 cm) with guard, *n*-hexane:IPA 90:10, 0.70 mL min⁻¹, room temperature, 210 nm: *t*_R = 34.6 min (major), 36.6 min (minor), 77.8:22.2 *e.r.*

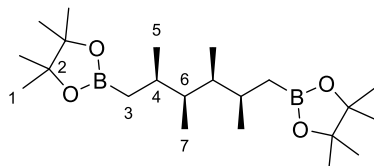
(+/-)-Butane-1,2-diyl bis(4-methylbenzenesulfonate)



(*R*)-Butane-1,2-diyl bis(4-methylbenzenesulfonate)



2,2'-((2*R*,3*S*,4*S*,5*R*)-2,3,4,5-Tetramethylhexane-1,6-diyl)bis(4,4,5,5-tetramethyl-1,3,2-dioxaborolane) (123)



In a flame-dried Schlenk vessel, boronic ester **138** (75 mg, 0.20 mmol, 1.00 equiv.) and bromochloromethane (0.08 mL, 1.23 mmol, 6.00 equiv.) were dissolved in anhydrous Et₂O (0.80 mL) at –78 °C under an atmosphere of nitrogen. A solution of *n*-BuLi (1.50 M in *n*-hexane, 0.68 mL, 1.02 mmol, 5.00 equiv.) was added dropwise and the reaction mixture was stirred at –78 °C for 30 min. The acetone/dry ice bath was removed and the reaction mixture was stirred at room temperature for 1 h. The white suspension was filtered through silica (~10 mm depth of wetted (Et₂O) silica, using a filter frit connected directly to a receiving vessel) to give a yellow translucent solution. The silica was washed with Et₂O (reagent grade) and the filtrate was concentrated under reduced pressure to give boronic ester **123** (80 mg, quantitative yield, >95:5 *d.r.*) as a colourless liquid.

TLC: *R*_f = 0.29 (*n*-pentane:Et₂O 90:10)

¹H NMR (400 MHz, Chloroform-*d*): δ 1.88 (2H, dqdd, *J*=8.6, 6.8, 4.1 Hz, H4), 1.31 – 1.17 (26H, m, H1 & H6), 0.81 (2H, dd, *J* = 15.4, 6.4 Hz, H3), 0.80 (6H, d, *J* = 6.8 Hz, H5), 0.70 (6H, d, *J* = 6.6 Hz, H7), 0.67 (2H, dd, *J*=15.4, 8.6 Hz, H3') ppm

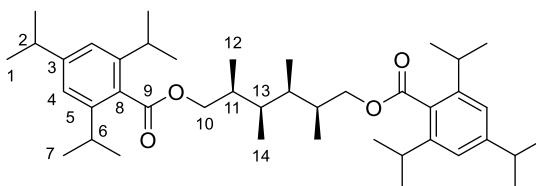
¹³C NMR (101 MHz, Chloroform-*d*): δ 82.9 (C2), 41.1 (C6), 30.8 (C4), 25.1 (C1), 24.9 (C1'), 18.5 (C3), 17.6 (C5), 11.5 (C7) ppm

HRMS (*m/z*): (ESI⁺) calc'd. for C₂₂H₄₄B₂NaO₄ [M+Na]⁺: 417.3326; found 417.3316

IR (*ν*_{max}): 2975, 2877, 1369, 1310, 1145, 969, 846 cm⁻¹

[α]_D²⁴: +9 (CHCl₃, *c* = 1.0)

(2*S*,3*R*,4*R*,5*S*)-3,4-Dimethylhexane-2,5-diyl bis(2,4,6-triisopropylbenzoate) (124)



In a flame-dried Schlenk vessel, 2,4,6-triisopropylbenzoic acid (383 mg, 1.54 mmol, 2.10 equiv.), triphenylphosphine (405 mg, 1.54 mmol, 2.10 equiv.) and diol **139** (128 mg,

0.73 mmol, 1.00 equiv.) were dissolved in anhydrous THF (4.00 mL) at 0 °C under an atmosphere of nitrogen. DIAD (0.30 mL, 1.54 mmol, 2.10 equiv.) was added dropwise and the colourless solution turned yellow. After the addition, the reaction mixture was stirred at room temperature for 18 h. The reaction mixture was diluted with water (10.00 mL) and extracted with Et₂O (3 × 10.00 mL). The organic layers were combined, washed with brine, dried over MgSO₄, filtered and concentrated to afford a yellow oil. The crude residue was purified by flash column chromatography (*n*-pentane:Et₂O 99:1) to give benzoate **124** (397 mg, 85%, >95:5 *d.r.*) as a white solid.

TLC: *R*_f = 0.31 (*n*-pentane:Et₂O 90:10)

m.p.: 76 – 81 °C (methanol)

¹H NMR (400 MHz, Chloroform-*d*): δ 7.01 (4H, s, H4), 4.24 (2H, dd, *J* = 10.9, 6.8 Hz, H10'), 4.13 (2H, dd, *J* = 10.9, 7.3 Hz, H10), 2.79 – 2.85 (6H, m, H2 & H6), 2.09 (2H, m, H11), 1.62 (2H, m, H13), 1.24 – 1.26 (36H, m, H1 & H7), 0.87 (6H, d, *J* = 6.8 Hz, H12), 0.85 (6H, d, *J* = 5.9 Hz, H14) ppm

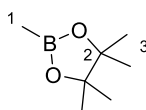
¹³C NMR (101 MHz, Chloroform-*d*): δ 171.3 (C9), 150.1 (C3), 144.8 (C5), 130.8 (C8), 121.0 (C4), 69.2 (C10), 35.8 (C11), 34.5 (C13), 33.3 (C2), 31.7 (C6), 24.4 (C7), 24.3 (C7'), 24.1 (C1), 11.6 (C12), 11.4 (C14) ppm

HRMS (*m/z*): (ESI⁺) calc'd. for C₄₂H₆₆NaO₄ [M+Na]⁺: 657.4853; found 657.4833

IR (*ν*_{max}): 2960, 2870, 1723, 1460, 1282, 1248, 1136, 1068, 876 cm⁻¹

[α]_D²²: +11 (CHCl₃, *c* = 1.0)

2,4,4,5,5-Pentamethyl-1,3,2-dioxaborolane (**125**)



MgSO₄ (3.02 g, 25.10 mmol, 1.00 equiv.) was dried in a flame-dried Schlenk vessel at 500 °C (heat gun) under high vacuum until gas evolution ceased. After cooling at room temperature, the flask was refilled with nitrogen and charged with a solution of methylboronic acid (1.50 g, 25.10 mmol, 1.00 equiv.) and pinacol (3.11 g, 26.30 mmol, 1.05 equiv.) in anhydrous Et₂O (70.00 mL). The flask was sealed and the white suspension was vigorously stirred at room temperature for 20 h. The reaction was filtered and the solid was washed several times with Et₂O. The filtrate was concentrated at 35 °C under atmospheric pressure to afford a colourless liquid. The ¹H NMR spectrum revealed that pinacol was still present. The product was filtered through

~10 mm depth of wetted silica (*n*-pentane:Et₂O 90:10), using a filter frit connected directly to a flame-dried receiving vessel). The silica was washed with a mixture *n*-pentane:Et₂O 90:10 and the filtrate was concentrated at 35 °C under atmospheric pressure to give boronic ester **125** (1.97 g, 55%) as a colourless liquid.

TLC: *R*_f = 0.39 (*n*-pentane:Et₂O 90:10)

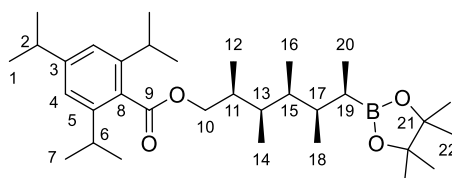
¹H NMR (400 MHz, Chloroform-*d*): δ 1.22 (12H, s, H3), 0.21 (3H, s, H1) ppm

¹³C NMR (101 MHz, Chloroform-*d*): δ 83.1 (C2), 25.0 (C3) ppm

The signal corresponding to C3 was not observed due to quadrupolar relaxation.

Spectral data were in accordance with that reported in the literature.²⁰²

(2*S*,3*R*,4*S*,5*R*,6*R*)-2,3,4,5-Tetramethyl-6-(4,4,5,5-tetramethyl-1,3,2-dioxaborolan-2-yl)heptyl 2,4,6-triisopropylbenzoate (126**)**



In a flame-dried Schlenk vessel, compound **124** (505 mg, 0.80 mmol, 1.00 equiv.) and (+)-sparteine (0.20 mL, 0.87 mmol, 1.10 equiv.) were dissolved in anhydrous Et₂O (5.00 mL) at –78 °C under an atmosphere of nitrogen. A solution of *s*-BuLi (1.30 M in hexanes, 0.67 mL, 0.87 mmol, 1.10 equiv.) was added dropwise and the reaction was stirred at –78 °C for 4.5 h. A solution of methyl pinacol boronic ester **125** (158 mg, 1.11 mmol, 1.40 equiv.) in anhydrous THF (1.60 mL) was added dropwise over 25 min and the reaction mixture was stirred at –78 °C for 3.5 h. The acetone/dry ice bath was removed and the reaction mixture was stirred at room temperature. Solvents were removed *in situ* under reduced pressure and the residue was re-dissolved in CHCl₃ (10.00 mL). The yellow solution was stirred at 40 °C for 18 h under an atmosphere of nitrogen. The white suspension was diluted an aqueous solution of HCl (1.00 M, 3 × 10.00 mL). The aqueous layers were combined and extracted with CH₂Cl₂ (3 × 30.00 mL). The organic layers were combined and washed with brine, dried over MgSO₄, filtered and concentrated to afford a colourless oil. The residue was purified by flash column chromatography (*n*-pentane:CH₂Cl₂ 80:20→60:40) to give boronic ester **126** (287 mg, 68%) as a colourless liquid.

TLC: *R*_f = 0.40 (*n*-pentane:CH₂Cl₂ 50:50)

¹H NMR (400 MHz, Chloroform-*d*): δ 7.00 (2H, s, H4), 4.24 (1H, dd, *J* = 10.8, 6.7 Hz, H10'), 4.11 (1H, dd, *J* = 10.8, 7.4 Hz, H10), 2.82 – 2.92 (3H, m, H2 & H6), 1.67 (1H, m, H13), 2.10

(1H, m, H11), 1.53 (1H, m, H15), 1.38 (1H, m, H17), 1.19 – 1.27 (30H, m, H1, H7, H22 & H22'), 1.02 (1H, m, H19), 0.88 – 0.92 (6H, m, 2 × CH₃), 0.68 – 0.82 (9H, m, 3 × CH₃) ppm

¹³C NMR (101 MHz, Chloroform-*d*): δ 171.4 (C9), 150.0 (C3), 144.9 (C5), 130.9 (C8), 120.9 (C4), 82.9 (C21), 69.5 (C10), 39.1 (CH), 36.2 (CH), 36.0 (CH), 34.5 (CH), 33.3 (C2), 31.7 (C6), 25.0 (C22), 24.8 (C22'), 24.4 (C7), 24.3 (C7'), 24.1 (C1), 12.8 (CH₃), 12.6 (CH₃), 11.9 (CH₃), 11.7 (CH₃), 11.6 (CH₃) ppm

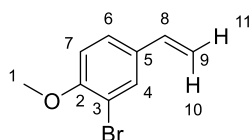
The signal corresponding to C19 was not observed due to quadrupolar relaxation.

HRMS (*m/z*): (ESI⁺) calc'd. for C₃₃H₅₇BNaO₄ [M+Na]⁺: 551.4248; found 551.4267

IR (*ν*_{max}): 2961, 2874, 1725, 1460, 1382, 1313, 1250, 1143, 1069, 876 cm⁻¹

[α]_D²⁶: +11 (CHCl₃, *c* = 1.0)

2-Bromo-1-methoxy-4-vinylbenzene (**133**)



In a flame-dried Schlenk vessel, methyltriphenylphosphonium bromide (1.83 g, 5.10 mmol, 1.10 equiv.) was suspended in anhydrous THF (10.00 mL) at 0 °C under an atmosphere of nitrogen. A solution of *n*-BuLi (1.53 M in *n*-hexane, 3.41 mL, 5.10 mmol, 1.10 equiv.) was added dropwise and the reaction was stirred at 0 °C for 30 min (white suspension → orange solution). A solution of 3-bromo-4-methoxybenzaldehyde (1.00 g, 4.70 mmol, 1.00 equiv.) in anhydrous THF (10.00 mL) was added dropwise at 0 °C (orange solution → yellow suspension). After the addition, the suspension was stirred at room temperature for 2 h. The reaction was slowly quenched with water (100.00 mL), extracted with CH₂Cl₂ (3 × 100.00 mL), dried over MgSO₄, filtered and concentrated under reduced pressure. The resulting yellow oil was triturated in cold Et₂O. The resulting white solid was removed by filtration, washed with cold Et₂O and the filtrate was concentrated under reduced pressure. The yellow residue was purified by flash column chromatography (*n*-hexane:EtOAc 95:5) to give 2-bromo-1-methoxy-4-vinylbenzene **133** (0.94 g, 95%) as a pale yellow liquid.

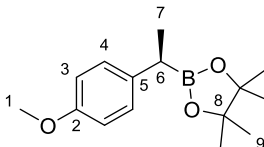
TLC: *R*_f = 0.43 (*n*-pentane:Et₂O 90:10)

¹H NMR (400 MHz, Chloroform-*d*): δ 7.62 (1H, d, *J* = 2.2 Hz, H4), 7.29 (1H, dd, *J* = 8.5, 2.2 Hz, H6), 6.85 (1H, d, *J* = 8.5 Hz, H7), 6.60 (1H, dd, *J* = 17.6, 10.9 Hz, H8), 5.62 (1H, dd, *J* = 17.6, 0.7 Hz, H10), 5.18 (1H, dd, *J* = 10.9, 0.7 Hz, H11), 3.90 (3H, s, H1) ppm

¹³C NMR (101 MHz, Chloroform-*d*): δ 155.6 (C2), 135.1 (C8), 131.9 (C5), 131.0 (C4), 126.6 (C6), 113.1 (C9), 112.0 (C3), 111.8 (C7), 56.4 (C1) ppm

Spectral data were in accordance with that reported in the literature.²⁹¹

(*R*)-2-(1-(4-Methoxyphenyl)ethyl)-4,4,5,5-tetramethyl-1,3,2-dioxaborolane ((*R*)-135)



In a flame-dried Schlenk vessel, freshly purified CuCl (33 mg, 0.34 mmol, 0.03 equiv.), *tert*-BuOK (51 mg, 0.45 mmol, 0.04 equiv.) and (*S*)-DTBM-SEGPHOS (398 mg, 0.34 mmol, 0.03 equiv.) were mixed in degassed (*i.e.*, sparged with nitrogen for 1 h) anhydrous toluene (5.00 mL) at room temperature under an atmosphere of nitrogen. Freshly distilled pinacolborane (1.96 mL, 13.50 mmol, 1.20 equiv.) was added and the yellow solution turned brown. After 10 min, a solution of 1-methoxy-4-vinylbenzene (1.51 g, 11.25 mmol, 1.00 equiv.) in degassed anhydrous toluene (4.00 mL) was added and the reaction was stirred under an atmosphere of nitrogen for 16 h. The dark suspension was filtered through Celite®, washed with *n*-pentane (50.00 mL) and the filtrate was concentrated under reduced pressure. The residue was purified by flash column chromatography (*n*-pentane:Et₂O 90:10) to give boronic ester (**(*R*)-135**) (2.07 g, 77%, 99.4:0.6 *e.r.*) as a pale yellow liquid.

TLC: R_f = 0.20 (*n*-pentane:Et₂O 90:10)

¹H NMR (400 MHz, Chloroform-*d*): δ 7.13 (2H, dd, J = 8.4, 2.2 Hz, H4), 6.81 (2H, d, J = 8.4 Hz, H3), 3.78 (3H, s, H1), 2.37 (1H, q, J = 7.5 Hz, H6), 1.30 (3H, d, J = 7.5 Hz, H7), 1.21 (6H, s, H9), 1.20 (6H, s, H9') ppm

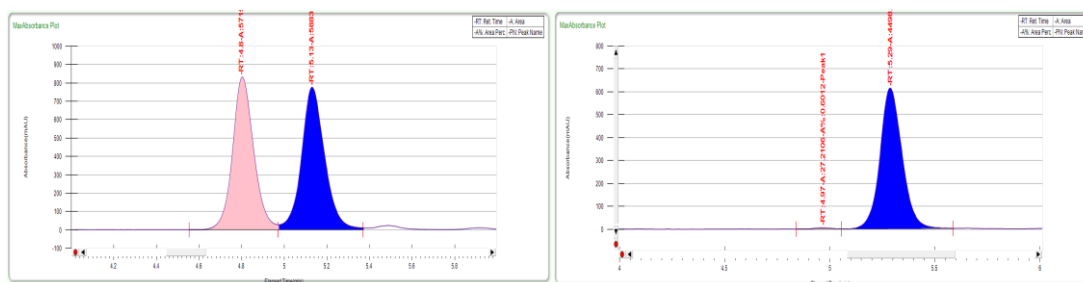
¹³C NMR (101 MHz, Chloroform-*d*): δ 157.4 (C2), 137.2 (C5), 128.8 (C4), 113.9 (C3), 83.4 (C8), 55.3 (C1), 25.0 (C9), 24.8 (C9'), 17.5 (C7) ppm

The signal corresponding to C6 was not observed due to quadrupolar relaxation.

Spectral data were in accordance with that reported in the literature.²⁹²

Boronic ester (**(*R*)-135**) (about 20 mg) was oxidised to the corresponding alcohol according to **GP1** for chiral SFC analysis.

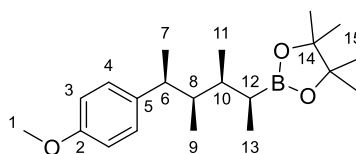
Chiral SFC: Whelk-01 column (25 cm), 20.0% co-solvent (*n*-hexane:IPA 90:10), 4.00 mL min⁻¹, 41.6 °C, 130 mbar, 210.0 nm): t_R = 4.80 min (minor), 5.13 min (major), 99.4:0.6 *e.r.*



Peak Information

Peak No	% Area	Area	Ret. Time	Height	Cap. Factor
1	49.2757	5715.365	4.8 min	832.2126	4802.2667
2	50.7243	5883.3822	5.13 min	776.6333	5128.9167

2-((2*S*,3*S*,4*R*,5*S*)-5-(4-Methoxyphenyl)-3,4-dimethylhexan-2-yl)-4,4,5,5-tetramethyl-1,3,2-dioxaborolane (**136**)



Boronic ester (**R**)-**135** (156 mg, 0.49 mmol, 1.00 equiv.) was homologated with stannane (**R**)-**93**, (**S**)-**93** and (**R**)-**93** (281 mg, 0.64 mmol, 1.30 equiv.) and *n*-BuLi (1.55 M in *n*-hexane, 0.42 mL, 0.64 mmol, 1.30 equiv.) according to **GP2**. The crude residue was purified by flash column chromatography (*n*-pentane:Et₂O 100:0→95:5) to give boronic ester **136** (104 mg, 61% over 3 steps, >95:5 *d.r.*) as a colourless liquid.

TLC: *R*_f = 0.47 (*n*-pentane:Et₂O 90:10)

¹H NMR (400 MHz, Chloroform-*d*): δ 7.09 (2H, d, *J* = 8.6 Hz, H4), 6.82 (2H, d, *J* = 8.7 Hz, H3), 3.79 (3H, s, H1), 2.65 (1H, *app.* pent, *J*^{*app.*} = 7.1 Hz, H6), 1.64 (1H, m, H8), 1.46 (1H, m, H10), 1.27 (6H, s, H15), 1.25 (6H, s, H15'), 1.15 (3H, d, *J* = 7.1 Hz, H7), 1.07 (1H, *app.* pent, *J*^{*app.*} = 7.0 Hz, H12), 0.85 (3H, d, *J* = 7.3 Hz, CH₃), 0.81 (3H, d, *J* = 6.8 Hz, CH₃), 0.73 (3H, d, *J* = 7.0 Hz, CH₃) ppm

¹³C NMR (101 MHz, Chloroform-*d*): δ 157.6 (C2), 139.8 (C5), 128.5 (C4), 113.6 (C3), 82.8 (C14), 55.3 (C1), 43.0 (C8), 42.1 (C6), 36.3 (C10), 25.0 (C15), 24.9 (C15'), 19.0 (C11), 12.8 (C7), 12.4 (C9), 11.6 (C13) ppm

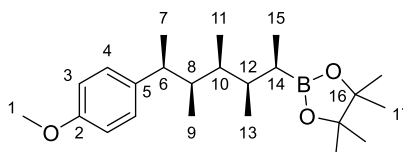
The signal corresponding to C12 was not observed due to quadrupolar relaxation.

HRMS (*m/z*): (ESI⁺) calc'd. for C₂₁H₃₅BNaO₃ [M+Na]⁺: 369.2575; found 369.2575

IR (*ν*_{max}): 2967, 2933, 2834, 1612, 1512, 1456, 1369, 1312, 1245, 1144, 1035, 830 cm⁻¹

[α]_D²⁵: −10 (CHCl₃, *c* = 1.0)

2-((2*R*,3*R*,4*S*,5*R*,6*S*)-6-(4-Methoxyphenyl)-3,4,5-trimethylheptan-2-yl)-4,4,5,5-tetramethyl-1,3,2-dioxaborolane (137)



Boronic ester **136** (46 mg, 0.13 mmol, 1.00 equiv.) was homologated with stannane (*S*)-**93** (79 mg, 0.18 mmol, 1.35 equiv.) and *n*-BuLi (1.55 M in *n*-hexane, 0.13 mL, 0.17 mmol, 1.30 equiv.) according to **GP2**. The crude residue was purified by flash column chromatography (*n*-pentane:CH₂Cl₂ 100:0→70:30) to give boronic ester **137** (41 mg, 84%, >95:5 *d.r.*) as a white solid.

TLC: *R*_f = 0.23 (*n*-pentane:CH₂Cl₂ 70:30)

m.p.: 59 – 63 °C (amorphous)

¹H NMR (400 MHz, Chloroform-*d*): δ 7.08 (2H, d, *J* = 8.6 Hz, H4), 6.82 (2H, d, *J* = 8.6 Hz, H3), 3.79 (3H, s, H1), 2.69 (1H, *app.* pent., *J*^{*app.*} = 7.2 Hz, H6), 1.69 (2H, *app.* sext., *J*^{*app.*} = 6.9 Hz, H8 & H10), 1.24 (6H, s, H17), 1.23 (6H, s, H17'), 1.12 – 1.18 (5H, m, H7, H12 & H14), 0.74 – 0.79 (6H, m, 2 × CH₃), 0.62 – 0.72 (6H, m, 2 × CH₃) ppm

¹³C NMR (101 MHz, Chloroform-*d*): δ 157.6 (C2), 139.9 (C5), 128.4 (C4), 113.6 (C3), 82.9 (C16), 55.3 (C1), 41.3 (C6), 40.8 (C8 or C10), 37.1 (C12), 36.0 (C8 or C10), 25.1 (C17'), 24.7 (C17), 18.2 (C7), 14.46 (CH₃), 11.7 (CH₃), 11.4 (CH₃), 10.0 (CH₃) ppm

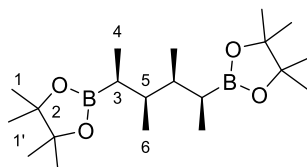
The signal corresponding to C14 was not observed due to quadrupolar relaxation.

HRMS (*m/z*): (ESI⁺) calc'd. for C₂₃H₃₉BNaO₃ [M+Na]⁺: 397.2889; found 397.2884

IR (*ν*_{max}): 2962, 2904, 1512, 1459, 1371, 1310, 1238, 1150, 1036, 828, 703, 554 cm⁻¹

[α]_D²³: +8 (CHCl₃, *c* = 1.0)

2,2'-((2*S*,3*S*,4*S*,5*S*)-3,4-Dimethylhexane-2,5-diyl)bis(4,4,5,5-tetramethyl-1,3,2-dioxaborolane) (138)



A mixture of boronic ester **122a** (1.30 g, 4.20 mmol, 0.74 equiv.) and boronic ester **122b** (0.46 g, 1.48 mmol, 0.26 equiv.) was homologated with stannane (*R*)-**93** (5.74 g, 13.06 mmol,

2.30 equiv.) and *n*-BuLi (1.52 M in *n*-hexane, 8.59 mL, 13.06 mmol, 2.30 equiv.) according to **GP2**. The crude residue was purified by flash column chromatography (*n*-pentane:Et₂O 97:3) and recrystallisation from *n*-hexane to give boronic ester **138** (0.94 g, 61%, >95:5 *d.r.*) as a white crystalline solid.

TLC: *R*_f = 0.39 (*n*-pentane:Et₂O 90:10)

m.p.: 131 – 137 °C (*n*-hexane)

¹H NMR (400 MHz, Chloroform-*d*): δ 1.60 (2H, m, H5), 1.22 (12H, s, H1), 1.22 (12H, s, H1'), 1.12 (2H, m, H3), 0.86 (6H, d, *J* = 7.4 Hz, H4), 0.80 (6H, d, *J* = 6.5 Hz, H6) ppm

¹³C NMR (101 MHz, Chloroform-*d*): δ 82.8 (C2), 37.8 (C5), 25.0 (C1), 24.9 (C1'), 14.2 (C6), 10.9 (C4) ppm

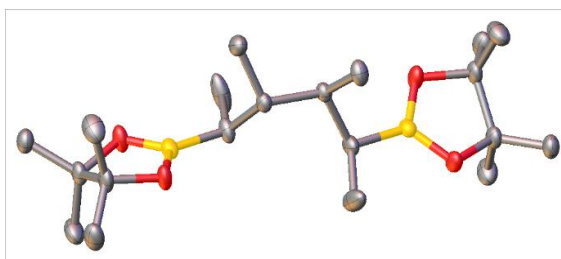
The signal corresponding to C3 was not observed due to quadrupolar relaxation.

HRMS: (ESI⁺) calc'd for C₂₀H₄₀B₂NaO₄ [M+Na]⁺: 389.3012; found: 389.3012

IR (ν_{max}): 2958, 2877, 1456, 1360, 1310, 1151, 1081, 850, 693 cm⁻¹

[α]_D²¹: −5 (CHCl₃, *c* = 1.0)

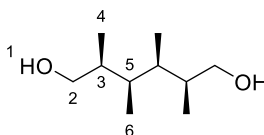
X-ray: Absolute configuration not determined.



Identification code	138
Empirical formula	C ₁₀ H ₂₀ BO ₂
Formula weight	183.07
Temperature/K	100(2)
Crystal system	orthorhombic
Space group	P2 ₁ 2 ₁ 2
<i>a</i> /Å	9.5751(16)
<i>b</i> /Å	16.626(3)
<i>c</i> /Å	7.2273(12)
α/°	90
β/°	90
γ/°	90
Volume/Å ³	1150.5(3)
<i>Z</i>	4
ρ _{calc} /g cm ⁻³	1.057
μ/mm ⁻¹	0.543

F(000)	404.0
Crystal size/mm ³	0.457 × 0.451 × 0.3
Radiation	CuKα (λ = 1.54178)
2θ range for data collection/°	10.642 to 134.042
Index ranges	-11 ≤ h ≤ 11, -19 ≤ k ≤ 18, -8 ≤ l ≤ 8
Reflections collected	14852
Independent reflections	2063 [R _{int} = 0.0455, R _{sigma} = 0.0264]
Data/restraints/parameters	2063/0/124
Goodness-of-fit on F ²	1.088
Final R indexes [I ≥ 2σ (I)]	R ₁ = 0.0446, wR ₂ = 0.1185
Final R indexes [all data]	R ₁ = 0.0448, wR ₂ = 0.1188
Largest diff. peak/hole / e Å ⁻³	0.31/-0.20
Flack parameter	0.08(12)

(2S,3R,4R,5S)-2,3,4,5-Tetramethylhexane-1,6-diol (139)



Boronic ester **123** (156 mg, 0.39 mmol, 1.00 equiv.) was oxidised according to **GP1** to give diol **139** (66 mg, 96%, >95:5 *d.r.*) as a colourless wax.

TLC: *R*_f = 0.37 (CH₂Cl₂:MeOH 90:10)

¹H NMR (400 MHz, Chloroform-*d*): δ 3.61 (2H, dd, *J* = 10.8, 5.2 Hz, H2), 3.45 (2H, dd, *J* = 10.8, 4.6 Hz, H2'), 2.59 (2H, br. s, H1), 1.46 – 1.72 (4H, m, H3 & H5), 0.86 (6H, d, *J* = 6.6 Hz, H6), 0.74 (6H, d, *J* = 6.5 Hz, H4) ppm

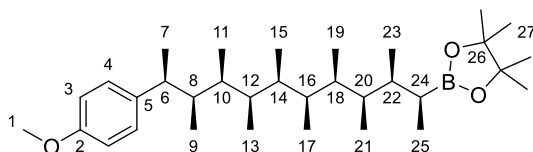
¹³C NMR (101 MHz, Chloroform-*d*): δ 66.7 (C2), 36.9 (C3), 34.5 (C5), 13.2 (C6), 11.5 (C4) ppm

HRMS (*m/z*): (ESI⁺) calc'd. for C₁₀H₂₂NaO₂ [M+Na]⁺: 197.1512; found 197.1513

IR (ν_{max}): 3284, 2953, 2933, 2878, 1459, 1381, 1035, 1005, 713 cm⁻¹

[α]_D²³: -7 (CHCl₃, *c* = 1.0)

2-((2*S*,3*S*,4*R*,5*S*,6*R*,7*S*,8*R*,9*S*,10*R*,11*S*)-11-(4-Methoxyphenyl)-3,4,5,6,7,8,9,10-octamethyl-dodecan-2-yl)-4,4,5,5-tetramethyl-1,3,2-dioxaborolane (148)



Boronic ester (**R**)-**135** (142 mg, 0.54 mmol, 1.00 equiv.) was homologated nine times with stan-
nane (**R**)- or (**S**)-**93** (309 mg, 0.70 mmol, 1.30 equiv.) and *n*-BuLi (1.55 M in *n*-hexane, 0.45 mL,
0.70 mmol, 1.30 equiv.) according to **GP2**. The crude residue was purified by flash column chro-
matography (*n*-pentane:Et₂O 100:0→99.5:0.5) to give boronic ester **148** (132 mg, 48% over 9
steps) as a colourless liquid.

TLC: *R*_f = 0.54 (*n*-pentane:Et₂O 90:10)

¹H NMR (400 MHz, Chloroform-*d*): δ 7.06 (2H, d, *J* = 8.6 Hz, H4), 6.81 (2H, d, *J* = 8.6 Hz, H3),
3.79 (3H, s, H1), 2.55 (1H, dq, *J* = 9.7, 6.9 Hz, H6), 1.74 (1H, dqd, *J* = 9.7, 7.0, 3.2 Hz, H8), 1.69
(1H, dqd, *J* = 9.5, 6.8, 3.9 Hz, CH), 1.51 – 1.38 (4H, m, 4 × CH), 1.31 (1H, dqd, *J* = 10.9, 6.8,
3.4 Hz, CH), 1.23 (6H, s, H27), 1.23 (6H, s, H27'), 1.18 (3H, d, *J* = 6.9 Hz, CH₃), 1.10 (1H, m,
CH), 1.01 (1H, m, CH), 0.92 (3H, d, *J* = 7.1 Hz, CH₃), 0.82 (3H, d, *J* = 6.7 Hz, CH₃), 0.77 – 0.64
(15H, m, 5 × CH₃), 0.59 (3H, d, *J* = 6.5 Hz, CH₃), 0.43 (3H, d, *J* = 6.1 Hz, CH₃) ppm

¹³C NMR (101 MHz, Chloroform-*d*): δ 157.7 (C2), 140.0 (C5), 128.3 (C4), 113.7 (C3), 82.8
(C26), 55.3 (C1), 42.6 (C6), 40.0 (CH), 39.9 (CH), 36.0 (CH), 35.7 (CH), 35.7 (CH), 35.6 (CH),
35.5 (CH), 35.2 (CH), 25.1 (C27), 24.7 (C27'), 20.3 (C7), 13.2 (CH₃), 12.6 (CH₃), 12.1 (CH₃),
12.0 (CH₃), 12.0 (CH₃), 11.8(9) (CH₃), 11.9(1) (CH₃), 11.7 (CH₃), 11.5 (CH₃) ppm

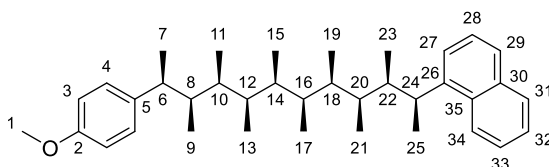
The signal corresponding to C24 was not observed due to quadrupolar relaxation.

HRMS (*m/z*): (ESI⁺) calc'd. for C₃₃H₅₉BNaO₃ [M+Na]⁺: 537.4455; found 537.4464

IR (*ν*_{max}): 2967, 2877, 1612, 1512, 1454, 1381, 1312, 1245, 1115, 829 cm⁻¹

[α]_D²⁰: −3 (CHCl₃, *c* = 1.0)

1-((2*S*,3*R*,4*S*,5*R*,6*S*,7*S*,8*R*,9*S*,10*R*,11*S*)-11-(4-Methoxyphenyl)-3,4,5,6,7,8,9,10-octamethyl-dodecan-2-yl)naphthalene (149)



In a flame-dried Schlenk tube, 1-bromonaphthalene (0.02 mL, 0.15 mmol, 1.20 equiv.) was dissolved in anhydrous Et₂O at 0 °C under an atmosphere of nitrogen. A solution of *n*-BuLi (1.60 M in *n*-hexane, 0.09 mL, 0.15 mmol, 1.20 equiv.) was added and the resulting suspension was stirred at the same temperature for 1 h. A solution of boronic ester **148** (64 mg, 0.12 mmol, 1.00 equiv.) in anhydrous Et₂O (0.60 mL) was added dropwise at 0 °C over 10 min. After the addition, the mixture was stirred at the same temperature for 2 h. Solvents were removed *in situ* and the residue was dissolved in dry MeOH (1.00 mL) at –78 °C under an atmosphere of nitrogen. A solution of NBS (53 mg, 0.30 mmol, 2.40 equiv.) in dry MeOH (1.50 mL) was added dropwise at the same temperature. After the addition, the acetone/dry ice bath was removed and the reaction mixture was stirred at room temperature for 1 h. A saturated aqueous solution of Na₂S₂O₃ (4.00 mL) was added. After 5 min, the suspension was extracted with Et₂O (3 × 10.00 mL). The organic layers were combined, washed with brine, dried over MgSO₄, filtered and concentrated under reduced pressure. The yellow residue was purified by flash column chromatography (*n*-pentane:Et₂O 100:0→99.5:0.5) to give compound **149** (42 mg, 66%) as a white solid.

TLC: *R*_f = 0.66 (*n*-pentane:Et₂O 90:10)

m.p.: 105 – 109 °C (acetonitrile)

¹H NMR (500 MHz, Chloroform-*d*): δ 8.19 (1H, d, *J* = 8.3 Hz, H34), 7.87 (1H, dd, *J* = 7.6, 2.0 Hz, H31), 7.70 (1H, d, *J* = 8.0 Hz, H29), 7.54 – 7.42 (3H, m, H28, H32 & H33), 7.38 (1H, d, *J* = 7.1 Hz, H27), 7.06 (2H, d, *J* = 8.7 Hz, H4), 6.83 (2H, d, *J* = 8.6 Hz, H3), 3.81 (3H, s, H1), 3.51 (1H, m, H24), 2.53 (1H, dq, *J* = 9.9, 6.9 Hz, H6), 2.14 (1H, m, H22), 1.74 (1H, dqd, *J* = 9.9, 6.8, 2.8 Hz, H8), 1.52 – 1.38 (3H, m, 3 × CH), 1.37 – 1.29 (4H, m, H25 & CH), 1.19 (3H, d, *J* = 6.9 Hz, H7), 1.12 – 1.04 (2H, m, H10 & H20), 0.96 (3H, d, *J* = 6.7 Hz, H23), 0.82 (3H, d, *J* = 6.8 Hz, H9), 0.72 – 0.67 (6H, m, H11 & H21), 0.63 (3H, d, *J* = 6.8 Hz, CH₃), 0.54 (3H, d, *J* = 6.8 Hz, CH₃), 0.41 (3H, d, *J* = 6.6 Hz, CH₃), 0.35 (3H, d, *J* = 6.4 Hz, CH₃) ppm

¹³C NMR (126 MHz, Chloroform-*d*): δ 157.7 (C2), 144.3 (C26), 140.0 (C5), 134.1 (C30), 132.0 (C35), 129.1 (C31), 128.3 (C4), 126.1 (C29), 125.7 (C28 or C32), 125.6 (C32 or C28), 125.2 (C33), 124.1 (C27), 123.4 (C34), 113.7 (C3), 55.3 (C1), 42.8 (C6), 39.6 (C8), 39.4 (C22), 37.1* (C24), 36.3 (C20), 36.0 (C10), 35.5 (CH), 35.5 (CH), 35.5 (CH), 35.3 (CH), 20.9 (C25), 20.7 (C7), 12.3 (CH₃), 12.2 (CH₃), 11.9 (CH₃), 11.9 (CH₃), 11.9 (CH₃), 11.8 (CH₃), 11.7 (CH₃), 11.6 (CH₃) ppm

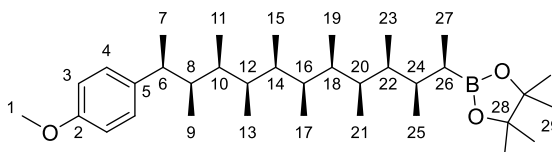
*shift value determined by HSQC correlation.

HRMS (*m/z*): (MALDI⁺) calc'd. for C₃₇H₅₄NaO [M+Na]⁺: 537.4067; found 537.4077

IR (*ν*_{max}): 2967, 2926, 1512, 1452, 1382, 1244, 1040, 778 cm^{–1}

[α]_D²⁵: –24 (CHCl₃, *c* = 1.0)

2-((2*R*,3*R*,4*S*,5*R*,6*S*,7*R*,8*S*,9*R*,10*S*,11*R*,12*S*)-12-(4-Methoxyphenyl)-3,4,5,6,7,8,9,10,11-nonamethyltridecan-2-yl)-4,4,5,5-tetramethyl-1,3,2-dioxaborolane (150)



Boronic ester **148** (66 mg, 0.13 mmol, 1.00 equiv.) was homologated with stannane (**S**)-**93** (73 mg, 0.17 mmol, 1.30 equiv.) and *n*-BuLi (1.60 M in *n*-hexane, 0.10 mL, 0.17 mmol, 1.30 equiv.) according to **GP2**. The crude residue was purified by flash column chromatography (*n*-pentane:Et₂O 100:0→99.5:0.5) to give boronic ester **150** (61 mg, 88%) as a colourless liquid.

TLC: *R*_f = 0.55 (*n*-pentane:Et₂O 90:10)

¹H NMR (500 MHz, Chloroform-*d*): δ 7.07 (2H, d, *J* = 8.6 Hz, H₄), 6.82 (2H, d, *J* = 8.6 Hz, H₃), 3.79 (3H, s, H₁), 2.63 (1H, dq, *J* = 8.5, 7.0 Hz, H₆), 1.77 – 1.63 (2H, m, 2 × CH), 1.56 – 1.35 (6H, m, 6 × CH), 1.24 (6H, s, H₂₉), 1.23 – 1.20 (7H, m, H₂₉' & CH), 1.20 – 1.13 (4H, m, CH & CH₃), 0.87 (3H, d, *J* = 7.3 Hz, CH₃), 0.84 – 0.77 (6H, m, 2 × CH₃), 0.74 – 0.66 (15H, m, 5 × CH₃), 0.65 (3H, d, *J* = 6.4 Hz, CH₃), 0.48 (3H, d, *J* = 6.0 Hz, CH₃) ppm

¹³C NMR (126 MHz, Chloroform-*d*): δ 157.7 (C₂), 140.0 (C₅), 128.4 (C₄), 113.7 (C₃), 82.9 (C₂₈), 55.3 (C₁), 41.9 (C₆), 40.7 (CH), 37.2 (CH), 36.1 (CH), 36.1 (CH), 36.1 (CH), 35.8 (CH), 35.8 (CH), 35.4 (CH), 35.4 (CH), 25.1 (C₂₉), 24.8 (C₂₉'), 19.0 (C₇), 14.5 (CH₃), 12.3 (CH₃), 12.2 (CH₃), 12.1 (CH₃), 11.9 (2 × CH₃), 11.8 (CH₃), 11.6 (CH₃), 11.4 (CH₃), 10.6 (CH₃) ppm

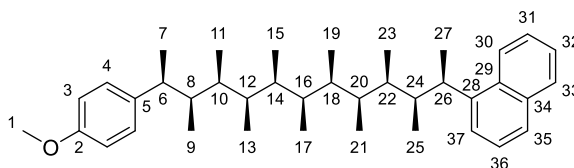
The signal corresponding to C₂₆ was not observed due to quadrupolar relaxation.

HRMS (*m/z*): (ESI⁺) calc'd. for C₃₅H₆₃BNaO₃ [M+Na]⁺: 565.4769; found 565.4748

IR (*ν*_{max}): 2965, 2870, 1599, 1511, 1454, 1306, 1249, 1113, 828 cm⁻¹

[α]_D²⁰: +5 (CHCl₃, *c* = 1.0)

2-((2*R*,3*R*,4*S*,5*R*,6*S*,7*R*,8*S*,9*R*,10*S*,11*R*,12*S*)-12-(4-Methoxyphenyl)-3,4,5,6,7,8,9,10,11-nonamethyltridecan-2-yl)-4,4,5,5-tetramethyl-1,3,2-dioxaborolane (151)



In a flame-dried Schlenk tube, 1-bromonaphthalene (0.02 mL, 0.13 mmol, 1.20 equiv.) was dissolved in anhydrous Et₂O at 0 °C under an atmosphere of nitrogen. A solution of *n*-BuLi (1.60 M in *n*-hexane, 0.08 mL, 0.13 mmol, 1.20 equiv.) was added and the resulting suspension was

stirred at the same temperature for 1 h. A solution of boronic ester **150** (61 mg, 0.11 mmol, 1.00 equiv.) in anhydrous Et₂O (0.60 mL) was added dropwise at 0 °C over 10 min. After the addition, the mixture was stirred at the same temperature for 2 h. Solvents were removed *in situ* and the residue was dissolved in dry MeOH (1.00 mL) at –78 °C under an atmosphere of nitrogen. A solution of NBS (48 mg, 0.27 mmol, 2.40 equiv.) in dry MeOH (1.50 mL) was added dropwise at the same temperature. After the addition, the acetone/dry ice bath was removed and the reaction mixture was stirred at room temperature for 1 h. A saturated aqueous solution of Na₂S₂O₃ (4.00 mL) was added. After 5 min, the suspension was extracted with Et₂O (3 × 10.00 mL). The organic layers were combined, washed with brine, dried over MgSO₄, filtered and concentrated under reduced pressure. The yellow residue was purified by flash column chromatography (*n*-pentane:Et₂O 100:0→99.5:0.5) to give compound **151** (35 mg, 57%) as a white solid.

TLC: *R*_f = 0.67 (*n*-pentane:Et₂O 90:10)

m.p.: 75 – 79 °C (acetonitrile)

¹H NMR (500 MHz, Chloroform-*d*): δ 8.17 (1H, d, *J* = 8.4 Hz, H30), 7.86 (1H, d, *J* = 7.7 Hz, H33), 7.69 (1H, d, *J* = 8.0 Hz, H35), 7.52 – 7.42 (3H, m, H31, H32 & H36), 7.39 (1H, d, *J* = 7.1 Hz, H37), 7.08 (2H, d, *J* = 8.6 Hz, H4), 6.83 (2H, d, *J* = 8.6 Hz, H3), 3.80 (3H, s, H1), 3.66 (1H, *app.* pent, *J*^{*app.*} = 6.9 Hz, H26), 2.68 (1H, dq, *J* = 7.0, 6.9 Hz, H6), 2.01 (1H, dqd, *J* = 6.9, 6.7, 4.6 Hz, H24), 1.68 (1H, dqd, *J* = 7.0, 6.3, 4.4 Hz, H8), 1.59 (1H, *app.* sext, *J*^{*app.*} = 6.3 Hz, H20), 1.55 – 1.39 (3H, m, 3 × CH), 1.37 (1H, m, H22), 1.32 (3H, d, *J* = 6.9 Hz, H27), 1.28 (1H, m, CH), 1.22 (1H, m, H10), 1.17 (3H, d, *J* = 6.9 Hz, H7), 0.89 (3H, d, *J* = 6.7 Hz, H25), 0.80 (3H, d, *J* = 6.7 Hz, H9), 0.72 – 0.64 (12H, m, 4 × CH₃), 0.62 (3H, d, *J* = 6.2 Hz, CH₃), 0.54 – 0.48 (6H, m, 2 × CH₃) ppm

¹³C NMR (126 MHz, Chloroform-*d*): δ 157.6 (C2), 143.9 (C28), 139.9 (C5), 134.1 (C34), 132.0 (C29), 129.1 (C33), 128.4 (C4), 126.2 (C35), 125.6 (C32 or C36), 125.5 (C36 or C32), 125.2 (C31), 124.3 (C37), 123.4 (C30), 113.6 (C3), 55.4 (C1), 41.5 (C6), 41.0 (C8), 40.2 (C24), 36.7 (C20), 36.6* (C26), 36.3 (CH), 36.2 (CH), 36.0 (C22), 35.7 (C10), 35.5 (CH), 35.3 (CH), 18.3 (C7 & C27), 12.5 (C25), 12.5 (CH₃), 12.4 (CH₃), 12.1 (CH₃), 11.9 (C9), 11.8 (CH₃), 11.8 (CH₃), 11.7 (CH₃), 11.6 (CH₃), 11.4 (CH₃) ppm

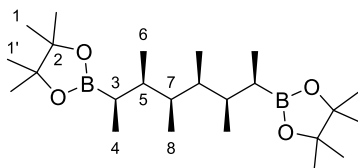
*shift value determined by HSQC correlation.

HRMS (*m/z*): (MALDI⁺) calc'd. for C₃₉H₅₈NaO [M+Na]⁺: 565.4380; found 565.4387

IR (*ν*_{max}): 2967, 2926, 2877, 1511, 1452, 1382, 1246, 1178, 1038, 830, 778 cm^{–1}

[α]_D²⁵: +19 (CHCl₃, *c* = 1.0)

2,2'-((2R,3R,4S,5S,6R,7R)-3,4,5,6-Tetramethyloctane-2,7-diyl)bis(4,4,5,5-tetramethyl-1,3,2-dioxaborolane) (152)



Boronic ester **138** (158 mg, 0.43 mmol, 1.00 equiv.) was homologated with stannane (**S**)-**93** (436 mg, 0.99 mmol, 2.30 equiv.) and *n*-BuLi (1.58 M in *n*-hexane, 0.63 mL, 0.99 mmol, 2.30 equiv.) according to **GP2**. The crude residue was purified by flash column chromatography (*n*-pentane:Et₂O 99:1) to give **152** (165 mg, 91%) as a white crystalline solid.

TLC: *R*_f = 0.50 (*n*-pentane:Et₂O 90:10)

m.p.: 115 – 118 °C (*n*-hexane)

¹H NMR: (400 MHz, Chloroform-*d*) δ 1.70 (2H, dqd, *J* = 8.6, 6.7, 4.1 Hz, H5), 1.33 (2H, m, H7), 1.22 (12H, s, H1), 1.22 (12H, s, H1'), 1.03 (2H, dq, *J* = 8.6, 7.1 Hz, H3), 0.91 (6H, d, *J* = 7.1 Hz, H4), 0.78 (6H, d, *J* = 6.7 Hz, H6), 0.72 (6H, d, *J* = 6.5 Hz, H8) ppm

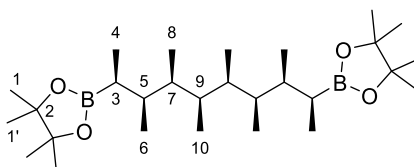
¹³C NMR: (101 MHz, Chloroform-*d*) δ 82.8 (C2), 39.5 (C7), 35.8 (C5), 25.0 (C1), 24.7 (C1'), 21.6 (C3), 12.8 (C4), 12.6 (C6), 11.9 (C8) ppm

HRMS (*m/z*): (MALDI⁺) calc'd for C₂₄H₄₈B₂NaO₄ [M+Na]⁺: 445.3639; found: 445.3630

IR (*ν*_{max}): 2974, 2932, 2865, 2877, 1456, 1370, 1311, 1146, 1078, 861 cm⁻¹

[α]_D²³: +14 (CHCl₃, *c* = 1.0)

2,2'-((2S,3S,4R,5S,6S,7R,8S,9S)-3,4,5,6,7,8-Hexamethyldecane-2,9-diyl)bis(4,4,5,5-tetramethyl-1,3,2-dioxaborolane) (153)



Boronic ester **138** (75 mg, 0.20 mmol, 1.00 equiv.) was homologated with stannane (**S**)-**93** and (**R**)-**93** (207 mg, 0.47 mmol, 2.30 equiv.), and *n*-BuLi (1.54 M in *n*-hexane, 0.31 mL, 0.47 mmol, 2.30 equiv.) according to **GP2**. The crude residue was purified by flash column chromatography (*n*-pentane:Et₂O 99:1) to give **153** (80 mg, 84% over 2 steps) as a white solid.

TLC: *R*_f = 0.50 (*n*-pentane:Et₂O 90:10)

m.p.: 82 – 85 °C (acetonitrile)

¹H NMR: (400 MHz, Chloroform-*d*) δ 1.69 (2H, dqd, J = 8.7, 6.8, 4.3 Hz, H5), 1.51 (2H, m, H9), 1.31 (2H, dqd, J = 7.4, 6.8, 4.3 Hz, H7), 1.23 (12H, s, H1), 1.22 (12H, s, H1'), 1.05 (2H, dq, J = 8.7, 7.2 Hz, H3), 0.91 (6H, d, J = 7.2 Hz, H4), 0.76 (6H, d, J = 6.8 Hz, H6), 0.75 (6H, d, J = 6.8 Hz, H8), 0.74 (6H, d, J = 6.5 Hz, H10) ppm

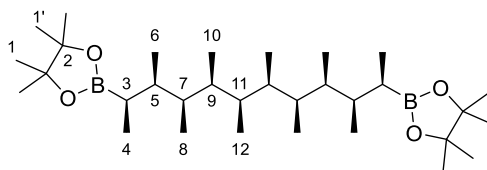
¹³C NMR: (101 MHz, Chloroform-*d*) δ 82.8 (C2), 39.5 (C7), 35.8 (C5), 35.8 (C9), 25.1 (C1), 24.7 (C1'), 21.8 (C3), 12.9 (C6), 12.8 (C4), 12.0 (C8), 11.9 (C10) ppm

HRMS (m/z): (MALDI⁺) calc'd for C₂₈H₅₆B₂NaO₄ [M+Na]⁺: 501.4267; found: 501.4276

IR (ν_{\max}): 2973, 2930, 2877, 1456, 1380, 1312, 1145, 967, 687 cm⁻¹

$[\alpha]_D^{20}$: -11 (CHCl₃, c = 1.0)

2,2'-((2*R*,3*R*,4*S*,5*R*,6*S*,7*S*,8*R*,9*S*,10*R*,11*R*)-3,4,5,6,7,8,9,10-Octamethyldodecane-2,11-diyl)bis(4,4,5,5-tetramethyl-1,3,2-dioxaborolane) (154)



Boronic ester **138** (75 mg, 0.20 mmol, 1.00 equiv.) was homologated with stannane (*S*)-**93**, (*R*)-**93** and (*S*)-**93** (207 mg, 0.47 mmol, 2.30 equiv.), and *n*-BuLi (1.54 M in *n*-hexane, 0.31 mL, 0.47 mmol, 2.30 equiv.) according to **GP2**. The crude residue was purified by flash column chromatography (*n*-pentane:Et₂O 99:1) to give **154** (82 mg, 75% over 3 steps) as a crystalline white solid.

TLC: R_f = 0.32 (*n*-pentane:Et₂O 95:5)

m.p.: 179 – 181 °C (*n*-hexane)

¹H NMR: (500 MHz, Chloroform-*d*) δ 1.70 (2H, dqd, J = 8.6, 6.8, 4.5 Hz, H5), 1.54 (2H, m, H11), 1.47 (2H, dqd, J = 7.7, 6.7, 3.7 Hz, H9), 1.32 (2H, dqd, J = 7.7, 6.8, 4.5 Hz, H7), 1.23 (12H, s, H1), 1.23 (12H, s, H1'), 1.05 (2H, dq, J = 8.6, 7.3 Hz, H3), 0.91 (6H, d, J = 7.3 Hz, H4), 0.75 (6H, d, J = 6.8 Hz, H6), 0.73 (12H, d, J = 6.8 Hz, H8 & H12), 0.69 (6H, d, J = 6.7 Hz, H10) ppm

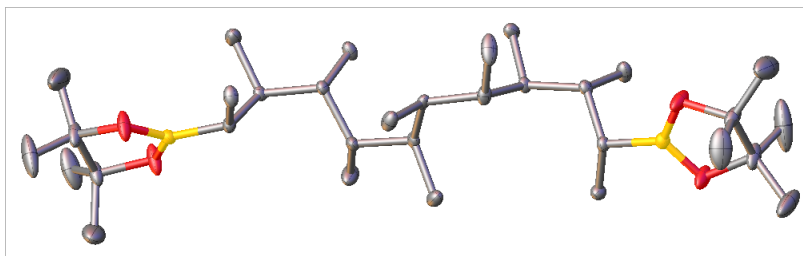
¹³C NMR: (126 MHz, Chloroform-*d*) δ 82.8 (C2), 39.5 (C7), 35.8 (C5 or C9), 35.8 (C9 or C5), 35.3 (C11), 25.1 (C1), 24.7 (C1'), 21.7 (C3), 13.0 (C6), 12.7 (C4), 12.1 (CH₃), 12.0 (CH₃), 11.9 (CH₃) ppm

HRMS (m/z): (ESI⁺) calc'd for C₃₂H₆₄B₂NaO₄ [M+Na]⁺: 557.4894; found: 557.4886

IR (ν_{max}): 2970, 1452, 1362, 1307, 1204, 1146, 1076, 967, 855, 702 cm⁻¹

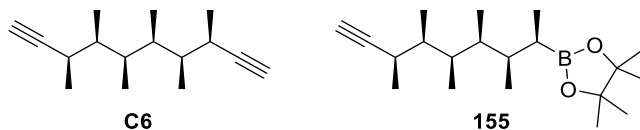
$[\alpha]_D^{22}$: +12 (CHCl₃, c = 1.0)

X-ray: Absolute configuration not determined.



Identification code	154
Empirical formula	C ₃₂ H ₆₄ B ₂ O ₄
Formula weight	534.45
Temperature/K	100(2)
Crystal system	monoclinic
Space group	C2
$a/\text{\AA}$	17.4769(9)
$b/\text{\AA}$	6.6261(3)
$c/\text{\AA}$	14.4394(8)
$\alpha/^\circ$	90
$\beta/^\circ$	91.494(3)
$\gamma/^\circ$	90
Volume/ \AA^3	1671.57(15)
Z	2
$\rho_{\text{calc}}/\text{g cm}^{-3}$	1.062
μ/mm^{-1}	0.066
$F(000)$	596.0
Crystal size/ mm^3	$0.527 \times 0.337 \times 0.248$
Radiation	MoK α (λ = 0.71073)
2θ range for data collection/ $^\circ$	4.662 to 56.014
Index ranges	$-22 \leq h \leq 14$, $-8 \leq k \leq 7$, $-18 \leq l \leq 19$
Reflections collected	7533
Independent reflections	3755 [R_{int} = 0.0236, R_{sigma} = 0.0344]
Data/restraints/parameters	3755/1/181
Goodness-of-fit on F^2	1.025
Final R indexes [$I \geq 2\sigma(I)$]	R_1 = 0.0499, wR_2 = 0.1271
Final R indexes [all data]	R_1 = 0.0548, wR_2 = 0.1314
Largest diff. peak/hole / $e \text{\AA}^{-3}$	0.41/-0.23
Flack parameter	-0.3(5)

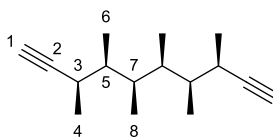
(3*R*,4*S*,5*R*,6*R*,7*S*,8*R*)-3,4,5,6,7,8-Hexamethyldeca-1,9-diyne (C6) and **4,4,5,5-Tetramethyl-2-((2*R*,3*R*,4*S*,5*R*,6*S*,7*R*)-3,4,5,6,7-pentamethylnon-8-yn-2-yl)-1,3,2-dioxaborolane (155)**



Boronic ester **152** (166 mg, 0.39 mmol, 1.00 equiv.) was alkynylated with vinyl carbamate **15** (74 mg, 0.43 mmol, 1.10 equiv.), LDA (0.86 M in THF, 0.50 mL, 0.43 mmol, 1.10 equiv.), iodine (110 mg, 0.43 mmol, 1.10 equiv.) and LDA (0.86 M in THF, 1.14 mL, 0.98 mmol, 2.50 equiv.) according to **GP3**. The crude residue was purified by flash column chromatography (pure *n*-pentane) to give **C6** (7 mg, 8%) as a colourless volatile liquid, followed by (*n*-pentane:CH₂Cl₂ 80:20) to give **155** as a colourless liquid (59 mg, 47%).

Note: Due to the volatility of compound **C6**, all solvents and volatiles were removed on rotary evaporator at 40 °C under atmospheric pressure.

(3*R*,4*S*,5*R*,6*R*,7*S*,8*R*)-3,4,5,6,7,8-Hexamethyldeca-1,9-diyne (C6)



TLC: R_f = 0.31 (*n*-pentane)

¹H NMR: (500 MHz, Toluene-*d*₈) δ 2.21 (2H, dqd, J = 9.3, 6.9, 2.4 Hz, H3), 1.94 (2H, m, H7), 1.83 (2H, d, J = 2.4 Hz, H1), 1.63 (2H, dqd, J = 9.3, 6.9, 2.5 Hz, H5), 1.09 (6H, d, J = 6.9 Hz, H4), 0.76 (6H, d, J = 6.9 Hz, H6), 0.76 (6H, d, J = 6.5 Hz, H8) ppm

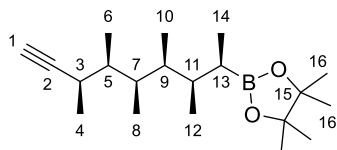
¹³C NMR: (126 MHz, Toluene-*d*₈) δ 88.7 (C2), 69.5 (C1), 38.9 (C5), 37.1 (C7), 30.0 (C3), 18.9 (C4), 11.7 (C8), 11.2 (C6) ppm

HRMS (m/z): (MALDI⁺) calc'd for C₁₆H₂₆ [M+H]⁺: 219.2107; found: 219.2100

IR (ν_{\max}): 3309, 2972, 2924, 2879, 1455, 1383, 1087, 627 cm⁻¹

$[\alpha]_D^{25}$: +5 (CHCl₃, c = 0.8)

4,4,5,5-Tetramethyl-2-((2*R*,3*R*,4*S*,5*R*,6*S*,7*R*)-3,4,5,6,7-pentamethylnon-8-yn-2-yl)-1,3,2-dioxaborolane (155)



TLC: R_f = 0.44 (*n*-pentane:Et₂O 95:5)

¹H NMR: (400 MHz, Chloroform-*d*) δ 2.35 (1H, dqd, J = 9.2, 6.9, 2.4 Hz, H3), 2.03 (1H, d, J = 2.4 Hz, H1), 1.83 (1H, dqd, J = 8.4, 6.9, 4.1 Hz, H7), 1.68 (1H, dqd, J = 9.3, 6.8, 4.3 Hz, H11), 1.65 (1H, dqd, J = 9.2, 6.8, 4.1 Hz, H5), 1.29 (1H, dqd, J = 8.4, 6.9, 4.3 Hz, H9), 1.23 (6H, s, H16), 1.22 (6H, s, H16'), 1.17 (3H, d, J = 6.9 Hz, H4), 1.03 (1H, m, H13) 0.92 (3H, d, J = 7.1 Hz, H14), 0.81 (3H, d, J = 6.8 Hz, H6), 0.77 (3H, d, J = 6.8 Hz, H12), 0.76 (3H, d, J = 6.9 Hz, H10), 0.73 (3H, d, J = 6.9 Hz, H8) ppm

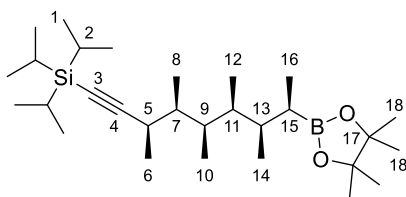
¹³C NMR: (101 MHz, Chloroform-*d*) δ 89.4 (C2), 82.9 (C15), 68.8 (C1), 39.7 (C9), 38.7 (C5), 36.9 (C7), 35.8 (C11), 29.6 (C3), 25.0 (C16), 24.7 (C16'), 21.8 (C13), 18.5 (C4), 13.1 (C14), 12.3 (C12), 11.8 (C8), 11.7 (C10), 11.5 (C6) ppm

HRMS (m/z): (MALDI⁺) calc'd for C₂₀H₃₇BNaO₂ [M+Na]⁺: 343.2782; found: 343.2788

IR (ν_{\max}): 3311, 2972, 2931, 2878, 1455, 1381, 1311, 1144, 1095, 854, 625 cm⁻¹

$[\alpha]_D^{22}$: +10 (CHCl₃, c = 1.0)

Triisopropyl((3*R*,4*S*,5*R*,6*S*,7*R*,8*R*)-3,4,5,6,7-pentamethyl-8-(4,4,5,5-tetramethyl-1,3,2-dioxaborolan-2-yl)non-1-yn-1-yl)silane (156)



Alkyne **155** (70 mg, 0.22 mmol, 1.00 equiv.) was protected with LDA (0.86 M in THF, 0.28 mL, 0.24 mmol, 1.10 equiv.) and TIPSCl (0.05 mL, 0.24 mmol, 1.10 equiv.) according to **GP4**. The crude residue was purified by flash column chromatography (*n*-pentane:CH₂Cl₂ 90:10) to give **156** (79 mg, 75%) as a colourless liquid.

TLC: R_f = 0.34 (*n*-pentane:CH₂Cl₂ 80:20)

¹H NMR: (400 MHz, Chloroform-*d*) δ 2.36 (1H, dq, J = 8.9, 6.8 Hz, H5), 1.92 (1H, dqd, J = 8.7, 6.8, 3.8 Hz, H9), 1.66 (1H, dqd, J = 9.4, 6.8, 3.9 Hz, H13), 1.60 (1H, dqd, J = 8.9, 6.8, 3.8 Hz,

H7), 1.27 (1H, dqd, $J = 8.7, 6.9, 3.9$ Hz, H11), 1.22 (12H, s, H18 & H18'), 1.17 (3H, d, $J = 6.8$ Hz, H6), 1.10 – 0.95 (22H, m, H1, H2 & H15), 0.92 (3H, d, $J = 6.9$ Hz, H16), 0.80 (3H, d, $J = 6.8$ Hz, H8), 0.76 (3H, d, $J = 6.8$ Hz, H14), 0.75 (3H, d, $J = 6.9$ Hz, H12), 0.74 (3H, d, $J = 6.8$ Hz, H10) ppm

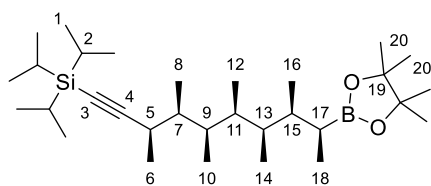
^{13}C NMR: (101 MHz, Chloroform- d) δ 113.7 (C4), 82.8 (C17), 80.5 (C3), 40.0 (C11), 38.7 (C7), 37.4 (C9), 35.7 (C13), 31.2 (C5), 25.0 (C18), 24.7 (C18'), 22.0 (C15), 19.2 (C6), 18.8 (C1), 13.4 (C16), 12.1 (C14), 11.8 (C10 or C12), 11.8 (C12 or C10), 11.5 (C2), 11.3 (C8) ppm

HRMS (m/z): (MALDI $^+$) calc'd for $\text{C}_{29}\text{H}_{57}\text{BNaO}_2\text{Si}$ $[\text{M}+\text{Na}]^+$: 499.4119; found: 499.4111

IR (ν_{max}): 2963, 2942, 2865, 2162, 1459, 1381, 1312, 1145, 1096, 882, 859, 663 cm^{-1}

$[\alpha]_D^{22}$: +13 (CHCl_3 , $c = 1.0$)

((3*R*,4*S*,5*R*,6*S*,7*R*,8*S*,9*S*)-3,4,5,6,7,8-Hexamethyl-9-(4,4,5,5-tetramethyl-1,3,2-dioxaborolan-2-yl)dec-1-yn-1-yl)triisopropylsilane (157**)**



Boronic ester **156** (79 mg, 0.17 mmol, 1.00 equiv.) was homologated with stannane (**R**)-**93** (95 mg, 0.22 mmol, 1.30 equiv.) and $n\text{-BuLi}$ (1.52 M in $n\text{-hexane}$, 0.14 mL, 0.22 mmol, 1.30 equiv.) according to **GP2**. The crude residue was purified by flash column chromatography ($n\text{-pentane}:\text{CH}_2\text{Cl}_2$ 95:5) to give **157** (70 mg, 82%) as a colourless liquid.

TLC: $R_f = 0.34$ ($n\text{-pentane}:\text{CH}_2\text{Cl}_2$ 80:20)

^1H NMR: (400 MHz, Chloroform- d) δ 2.46 (1H, dq, $J = 7.3, 6.9$ Hz, H5), 1.85 (1H, dqd, $J = 7.1, 6.8, 4.9$ Hz, H9), 1.67 (1H, *app.* pentd, $J^{\text{app.}} = 6.8, 5.7$ Hz, H15), 1.59 (1H, dqd, $J = 7.3, 6.8, 4.9$ Hz, H7), 1.43 (1H, dqd, $J = 7.1, 6.6, 5.1$ Hz, H11), 1.40 (1H, dqd, $J = 6.8, 5.1, 6.6$ Hz, H13), 1.23 (6H, s, H20), 1.22 (6H, s, H20'), 1.18 (1H, m, H17), 1.14 (3H, d, $J = 6.9$ Hz, H6), 1.09 – 0.96 (21H, m, H1 & H2), 0.86 (3H, d, $J = 7.4$ Hz, H18), 0.83 (3H, d, $J = 6.8$ Hz, H8), 0.80 (3H, d, $J = 6.8$ Hz, H16), 0.77 (3H, d, $J = 6.7$ Hz, H10), 0.75 – 0.72 (6H, m, H12 & H14) ppm

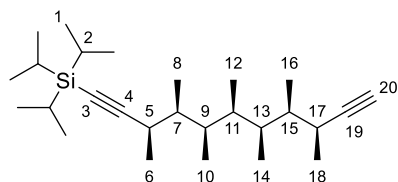
^{13}C NMR: (101 MHz, Chloroform- d) δ 114.0 (C4), 82.9 (C19), 80.3 (C3), 39.0 (C7), 36.9 (C13), 36.6 (C9), 36.2 (C11), 35.9 (C15), 30.6 (C5), 25.1 (C20), 24.8 (C20'), 20.0 (C17), 18.8 (C1), 18.1 (C6), 14.7 (C16), 12.2 (C8), 11.9 (C12 or C14), 11.7 (C10), 11.6 (C14 or C12), 11.5 (C2), 10.4 (C18) ppm

HRMS (m/z): (ESI $^+$) calc'd for $\text{C}_{31}\text{H}_{61}\text{BNaO}_2\text{Si}$ $[\text{M}+\text{Na}]^+$: 527.4432; found: 527.4426

IR (ν_{max}): 2965, 2941, 2865, 2163, 1461, 1381, 1311, 1146, 883, 676 cm^{-1}

$[\alpha]_D^{24}$: -4 (CHCl_3 , $c = 1.0$)

((3*R*,4*S*,5*R*,6*S*,7*S*,8*R*,9*S*)-3,4,5,6,7,8,9-Heptamethylundeca-1,10-diyn-1-yl)triisopropylsilane (158**)**



Boronic ester **157** (69 mg, 0.14 mmol, 1.00 equiv.) was alkynylated with vinyl carbamate **15** (26 mg, 0.15 mmol, 1.10 equiv.), LDA (0.86 M in THF, 0.17 mL, 0.15 mmol, 1.10 equiv.), iodine (38 mg, 0.15 mmol, 1.10 equiv.) and LDA (0.86 M in THF, 0.40 mL, 0.34 mmol, 2.50 equiv.) according to **GP3**. The crude residue was purified by flash column chromatography (pure *n*-pentane) to give **158** (46 mg, 84%) as a colourless liquid.

TLC: $R_f = 0.35$ (*n*-pentane)

^1H NMR: (400 MHz, Chloroform-*d*) δ 2.52 (1H, qdd, $J = 6.9, 6.8, 2.4$ Hz, H17), 2.48 (1H, qd, $J = 7.2, 6.9$ Hz, H5), 2.03 (1H, d, $J = 2.4$ Hz, H20), 1.83 (1H, dqd, $J = 7.0, 6.8, 5.1$ Hz, H9), 1.70 (1H, dqd, $J = 6.7, 6.5, 6.3$ Hz, H13), 1.61 (1H, *app.* pentd, $J^{\text{app.}} = 6.8, 6.3$ Hz, H15), 1.58 (1H, dqd, $J = 7.2, 6.8, 5.1$ Hz, H7), 1.35 (1H, ddq, $J = 7.0, 6.7, 6.5$ Hz, H11), 1.13 (3H, d, $J = 6.9$ Hz, H6), 1.10 (3H, d, $J = 6.9$ Hz, H18), 1.10 – 0.95 (21H, m, H1 & H2), 0.88 (3H, d, $J = 6.8$ Hz, H16), 0.84 (3H, d, $J = 6.8$ Hz, H8), 0.78 (3H, d, $J = 6.5$ Hz, H12), 0.77 (3H, d, $J = 6.8$ Hz, H10), 0.76 (3H, d, $J = 6.5$ Hz, H14) ppm

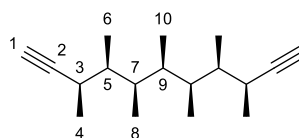
^{13}C NMR: (101 MHz, Chloroform-*d*) δ 113.8 (C4), 89.6 (C19), 80.4 (C3), 68.5 (C20), 39.4 (C15), 39.0 (C7), 36.6 (C11), 36.4 (C9), 35.7 (C13), 30.4 (C5), 28.5 (C17), 18.8 (C1), 17.9 (C6), 16.5 (C18), 12.7 (C16), 12.3 (C8), 11.9 (C12), 11.5 (C10), 11.5 (C2), 11.5 (C14) ppm

HRMS (m/z): (MALDI $^+$) calc'd for $\text{C}_{27}\text{H}_{50}\text{NaSi}$ $[\text{M}+\text{Na}]^+$: 425.3579; found: 425.2768

IR (ν_{max}): 3312, 2967, 2941, 2865, 2162, 1462, 1382, 1089, 996, 883, 664, 627 cm^{-1}

$[\alpha]_D^{25}$: +5 (CHCl_3 , $c = 1.0$)

(3R,4S,5R,6s,7S,8R,9S)-3,4,5,6,7,8,9-Heptamethylundeca-1,10-diyne (C7)



Protected alkyne **158** (45 mg, 0.11 mmol, 1.00 equiv.) was deprotected with TBAF (1.00 M in THF, 0.22 mL, 0.22 mmol, 2.00 equiv.) according to **GP5**. The crude residue was purified by flash column chromatography (pure *n*-pentane) to give **C7** (25 mg, 91%) as a colourless liquid.

TLC: R_f = 0.28 (*n*-pentane)

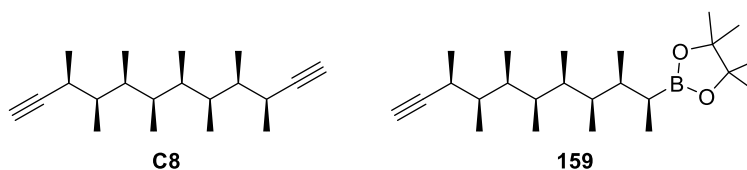
¹H NMR: (500 MHz, Toluene-*d*₈) δ 2.37 (2H, dqd, J = 7.1, 6.9, 2.4 Hz, H3), 1.83 (2H, d, J = 2.4 Hz, H1), 1.81 (2H, qdd, J = 6.8, 6.7, 5.6 Hz, H7), 1.62 (2H, dqd, J = 7.1, 6.9, 5.6 Hz, H5), 1.24 (1H, qt, J = 6.8, 6.5 Hz, H9), 1.04 (6H, d, J = 6.9 Hz, H4), 0.79 (6H, d, J = 6.9 Hz, H6), 0.76 (6H, d, J = 6.8 Hz, H8), 0.70 (3H, d, J = 6.8 Hz, H10) ppm

¹³C NMR: (126 MHz, Toluene-*d*₈) δ 88.9 (C2), 69.3 (C1), 39.4 (C5), 36.8 (C9), 36.1 (C7), 29.1 (C3), 17.0 (C4), 12.4 (C6), 11.7 (C10), 11.4 (C8) ppm

HRMS (m/z): *Despite repeated attempts, a HRMS could not be obtained.*

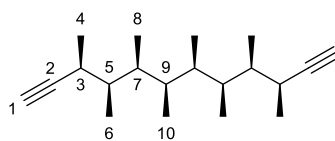
IR (ν_{\max}): 3309, 2972, 2937, 2880, 1454, 1383, 1088, 627 cm⁻¹

(3S,4R,5S,6R,7R,8S,9R,10S)-3,4,5,6,7,8,9,10-Octamethyldodeca-1,11-diyne (C8) and 2-((2S,3S,4R,5S,6R,7S,8R,9S)-3,4,5,6,7,8,9-Heptamethylundec-10-yn-2-yl)-4,4,5,5-tetramethyl-1,3,2-dioxaborolane (159)



Boronic ester **153** (152 mg, 0.32 mmol, 1.00 equiv.) was alkynylated with vinyl carbamate **15** (60 mg, 0.35 mmol, 1.10 equiv.), LDA (0.86 M in THF, 0.41 mL, 0.35 mmol, 1.10 equiv.), iodine (89 mg, 0.35 mmol, 1.10 equiv.) and LDA (0.86 M in THF, 0.92 mL, 0.79 mmol, 2.50 equiv.) according to **GP3**. The crude residue was purified by flash column chromatography (pure *n*-pentane) to give **C8** (8 mg, 9%) as a colourless liquid; followed by (*n*-pentane:CH₂Cl₂ 80:20) to give **159** (58 mg, 48%) as a colourless liquid.

(3S,4R,5S,6R,7R,8S,9R,10S)-3,4,5,6,7,8,9,10-Octamethyldodeca-1,11-diyne (C8)



TLC: R_f = 0.34 (*n*-pentane)

^1H NMR: (500 MHz, Toluene- d_8) δ 2.22 (2H, dqd, J = 9.2, 6.9, 2.4 Hz, H3), 2.05 (2H, dqd, J = 8.5, 6.8, 3.4 Hz, H7), 1.84 (2H, d, J = 2.4 Hz, H1), 1.67 (2H, dqd, J = 9.2, 6.8, 3.4 Hz, H5), 1.49 (2H, m, H9), 1.10 (6H, d, J = 6.9 Hz, H4), 0.88 (6H, d, J = 6.7 Hz, H10), 0.75 (6H, d, J = 6.8 Hz, H8), 0.70 (6H, d, J = 6.9 Hz, H6) ppm

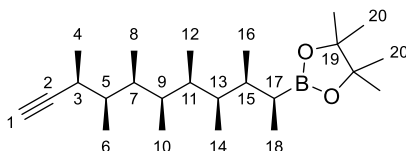
^{13}C NMR: (126 MHz, Toluene- d_8) δ 88.6 (C2), 69.6 (C1), 38.8 (C5), 37.1 (C7), 35.8 (C9), 30.1 (C3), 18.9 (C4), 11.9 (C8), 11.6 (C10), 11.4 (C6) ppm

HRMS (m/z): *Despite repeated attempts, a HRMS could not be obtained.*

IR (ν_{max}): 3310, 2970, 2921, 2879, 1453, 1383, 1086, 623 cm^{-1}

$[\alpha]_D^{24}$: +4 (CHCl_3 , c = 0.25)

2-((2S,3S,4R,5S,6R,7S,8R,9S)-3,4,5,6,7,8,9-Heptamethylundec-10-yn-2-yl)-4,4,5,5-tetramethyl-1,3,2-dioxaborolane (159)



TLC: R_f = 0.49 (*n*-pentane:Et₂O 95:5)

^1H NMR: (400 MHz, Chloroform- d) δ 2.36 (1H, dqd, J = 8.8, 6.9, 2.4 Hz, H3), 2.04 (1H, d, J = 2.4 Hz, H1), 1.84 (1H, dqd, J = 8.2, 6.8, 3.8 Hz, H7), 1.69 (1H, dqd, J = 9.0, 6.8, 4.1 Hz, H15), 1.62 (1H, dqd, J = 8.8, 6.8, 3.8 Hz, H5), 1.49 (1H, dqd, J = 8.2, 6.8, 4.2 Hz, H9), 1.47 (1H, dqd, J = 8.0, 6.6, 4.2 Hz, H11), 1.32 (1H, dqd, J = 8.0, 6.8, 4.1 Hz, H13), 1.23 (6H, s, H20), 1.23 (6H, s, H20'), 1.17 (3H, d, J = 6.9 Hz, H4), 1.04 (1H, m, H17), 0.92 (3H, d, J = 7.2 Hz, H18), 0.78 (3H, d, J = 6.8 Hz, H6), 0.77 (3H, d, J = 6.8 Hz, H10), 0.75 (3H, d, J = 6.8 Hz, H8), 0.75 (3H, d, J = 6.8 Hz, H14), 0.74 (3H, d, J = 6.8 Hz, H16), 0.73 (3H, d, J = 6.6 Hz, H12) ppm

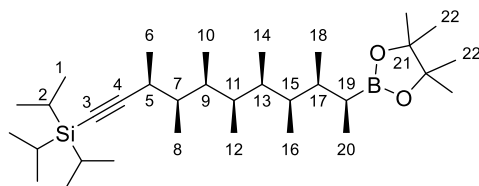
^{13}C NMR: (101 MHz, Chloroform- d) δ 89.4 (C2), 82.9 (C19), 68.8 (C1), 39.7 (C13), 38.7 (C5), 36.8 (C7), 35.8 (C11), 35.7 (C15), 35.5 (C9), 29.7 (C3), 25.1 (C20), 24.7 (C20'), 21.9 (C17), 18.5 (C4), 13.1 (C18), 12.6 (CH₃), 12.0 (CH₃), 11.9 (CH₃), 11.7 (CH₃), 11.7 (CH₃), 11.7 (CH₃) ppm

HRMS (*m/z*): (MALDI⁺) calc'd for C₂₄H₄₅BNaO₂ [M+Na]⁺: 399.3441; found: 399.3434

IR (ν_{\max}): 3311, 2970, 2931, 2878, 1455, 1381, 1312, 1145, 1086, 851, 626 cm⁻¹

[α]_D²³: -16 (CHCl₃, *c* = 1.0)

((3*S*,4*R*,5*S*,6*R*,7*S*,8*R*,9*S*,10*S*)-3,4,5,6,7,8,9-Heptamethyl-10-(4,4,5,5-tetramethyl-1,3,2-dioxaborolan-2-yl)undec-1-yn-1-yl)triisopropylsilane (160**)**



Alkyne **159** (50 mg, 0.13 mmol, 1.00 equiv.) was protected with LDA (0.86 M in THF, 0.17 mL, 0.28 mmol, 1.10 equiv.) and TIPSCl (0.03 mL, 0.28 mmol, 1.10 equiv.) according to **GP4**. The crude residue was purified by flash column chromatography (*n*-pentane:CH₂Cl₂ 95:5) to give **160** (50 mg, 71%) as a colourless liquid.

TLC: *R*_f = 0.32 (*n*-pentane:CH₂Cl₂ 80:20)

¹H NMR: (400 MHz, Chloroform-*d*) δ 2.37 (1H, dq, *J* = 9.0, 6.8 Hz, H5), 1.93 (1H, dqd, *J* = 8.4, 6.8, 3.7 Hz, H9), 1.70 (1H, dqd, *J* = 9.2, 6.8, 3.7 Hz, H17), 1.57 (1H, dqd, *J* = 9.0, 6.8, 3.7 Hz, H7), 1.49 (1H, dqd, *J* = 8.4, 6.6, 3.7 Hz, H11), 1.45 (1H, dqd, *J* = 8.5, 6.7, 3.7 Hz, H13), 1.30 (1H, dqd, *J* = 8.5, 6.8, 4.0 Hz, H15), 1.24 (6H, s, H22), 1.23 (6H, s, H22'), 1.18 (3H, d, *J* = 6.8 Hz, H6), 1.10 – 0.96 (22H, m, H1, H2 & H19), 0.93 (3H, d, *J* = 7.0 Hz, H20), 0.77 (3H, d, *J* = 6.8 Hz, H8), 0.77 (3H, d, *J* = 6.7 Hz, H12), 0.76 (3H, d, *J* = 6.8 Hz, H10), 0.75 (3H, d, *J* = 6.8 Hz, H16), 0.74 (3H, d, *J* = 6.8 Hz, H18), 0.72 (3H, d, *J* = 6.7 Hz, H14) ppm

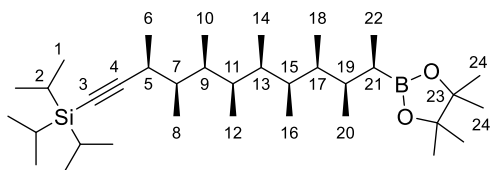
¹³C NMR: (101 MHz, Chloroform-*d*) δ 113.7 (C4), 82.9 (C21), 80.5 (C3), 40.0 (C15), 38.6 (C7), 37.2 (C9), 35.8 (C13), 35.6 (C11), 35.6 (C17), 31.3 (C5), 25.1 (C22), 24.7 (C22'), 22.2 (C19), 19.3 (C6), 18.8 (C1), 13.4 (C20), 12.4 (CH₃), 12.0 (CH₃), 11.8 (CH₃), 11.8 (CH₃), 11.7 (CH₃), 11.6 (CH₃), 11.5 (C2) ppm

HRMS (*m/z*): (ESI⁺) calc'd for C₃₃H₆₅BNaO₂Si [M+Na]⁺: 555.4745; found: 555.4736

IR (ν_{\max}): 2966, 2942, 2865, 2163, 1461, 1381, 1311, 1146, 1078, 883, 676 cm⁻¹

[α]_D²⁴: -4 (CHCl₃, *c* = 1.0)

Triisopropyl((3*S*,4*R*,5*S*,6*R*,7*S*,8*R*,9*S*,10*R*,11*R*)-3,4,5,6,7,8,9,10-octamethyl-11-(4,4,5,5-tetramethyl-1,3,2-dioxaborolan-2-yl)dodec-1-yn-1-yl)silane (161)



Boronic ester **160** (45 mg, 0.08 mmol, 1.00 equiv.) was homologated with stannane (**S**)-**93** (56 mg, 0.13 mmol, 1.30 equiv.) and *n*-BuLi (1.58 M in *n*-hexane, 0.08 mL, 0.13 mmol, 1.30 equiv.) according to **GP2**. The crude residue was purified by flash column chromatography (*n*-pentane:CH₂Cl₂ 95:5) to give **161** (41 mg, 87%) as a colourless liquid.

TLC: *R*_f = 0.33 (*n*-pentane:CH₂Cl₂ 80:20)

¹H NMR: (400 MHz, Chloroform-*d*) δ 2.46 (1H, dq, *J* = 7.6, 6.9 Hz, H5), 1.84 (1H, dqd, *J* = 7.1, 6.8, 4.7 Hz, H9), 1.68 (1H, dqd, *J* = 6.9, 6.8, 5.8 Hz, H19), 1.60 (1H, dqd, *J* = 7.6, 6.8, 4.7 Hz, H7), 1.52 (1H, dqd, *J* = 7.0, 6.5, 4.6 Hz, H15), 1.46 (1H, dqd, *J* = 7.0, 6.4, 6.8 Hz, H13), 1.42 (1H, dqd, *J* = 7.1, 6.7, 6.8 Hz, H11), 1.41 (1H, dqd, *J* = 6.9, 6.7, 4.6 Hz, H17), 1.23 (6H, s, H24), 1.23 (6H, s, H24'), 1.18 (1H, m, H21), 1.14 (3H, d, *J* = 6.9 Hz, H6), 1.07 – 0.98 (21H, m, H1 & H2), 0.87 (3H, d, *J* = 7.3 Hz, H22), 0.82 (3H, d, *J* = 6.8 Hz, H8), 0.80 (3H, d, *J* = 6.8 Hz, H20), 0.75 (3H, d, *J* = 6.8 Hz, H10), 0.74 (3H, d, *J* = 6.7 Hz, H12), 0.74 (3H, d, *J* = 6.5 Hz, H16), 0.72 (3H, d, *J* = 6.7 Hz, H18), 0.71 (3H, d, *J* = 6.4 Hz, H14) ppm

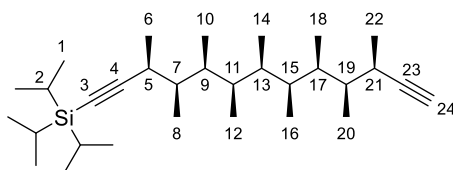
¹³C NMR: (101 MHz, Chloroform-*d*) δ 114.0 (C4), 82.9 (C23), 80.4 (C3), 39.1 (C7), 37.3 (C17), 36.7 (C9), 36.1 (C11 & C19), 36.0 (C13), 35.3 (C15), 30.7 (C5), 25.1 (C24), 24.8 (C24'), 20.2 (C21), 18.8 (C1), 18.2 (C6), 14.6 (C20), 12.2 (C8), 12.1 (2 × CH₃), 11.8 (CH₃), 11.8 (CH₃), 11.7 (CH₃), 11.5 (C2), 10.6 (C22) ppm

HRMS (*m/z*): (ESI⁺) calc'd for C₃₅H₆₉BNaO₂Si [M+Na]⁺: 583.5059; found: 583.5052

IR (ν_{max}): 2966, 2941, 2865, 2162, 1461, 1381, 1311, 1146, 1078, 883, 676 cm⁻¹

[α]_D²²: −1 (CHCl₃, *c* = 1.0)

Triisopropyl((3*S*,4*R*,5*S*,6*R*,7*S*,8*S*,9*R*,10*S*,11*R*)-3,4,5,6,7,8,9,10,11-nonamethyltrideca-1,12-diyn-1-yl)silane (162)



Boronic ester **161** (34 mg, 0.06 mmol, 1.00 equiv.) was alkynylated with vinyl carbamate **15** (12 mg, 0.07 mmol, 1.10 equiv.), LDA (0.86 M in THF, 0.08 mL, 0.07 mmol, 1.10 equiv.), iodine (17 mg, 0.07 mmol, 1.10 equiv.) and LDA (0.86 M in THF, 0.17 mL, 0.15 mmol, 2.50 equiv.) according to **GP3**. The crude residue was purified by flash column chromatography (pure *n*-pentane) to give **162** (21 mg, 75%) as a colourless liquid.

TLC: R_f = 0.32 (*n*-pentane)

¹H NMR: (400 MHz, Chloroform-*d*) δ 2.51 (1H, *app.* pentd, J^{app} = 6.9, 2.4 Hz, H21), 2.49 (1H, *app.* pent, J^{app} = 6.9 Hz, H5), 2.03 (1H, d, J = 2.4 Hz, H24), 1.82 (1H, *app.* pentd, J^{app} = 7.0, 5.0 Hz, H9), 1.73 (1H, *app.* pentd, J^{app} = 6.6, 6.0 Hz, H17), 1.61 (1H, *app.* sext, J^{app} = 6.7 Hz, H19), 1.59 (1H, dqd, J = 7.0, 6.8, 5.0 Hz, H7), 1.50 (1H, dqd, J = 6.5, 6.8, 5.5 Hz, H13), 1.47 – 1.34 (2H, m, H11 & H15), 1.14 (3H, d, J = 6.9 Hz, H6), 1.11 (3H, d, J = 6.9 Hz, H22), 1.08 – 0.98 (21H, m, H1 & H2), 0.87 (3H, d, J = 6.8 Hz, H20), 0.84 (3H, d, J = 6.8 Hz, H8), 0.77 – 0.72 (15H, m, 5 \times CH₃) ppm

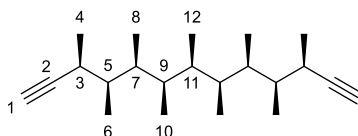
¹³C NMR: (101 MHz, Chloroform-*d*) δ 113.9 (C4), 89.7 (C23), 80.4 (C3), 68.5 (C24), 39.6 (C19), 39.2 (C7), 36.5 (C9), 36.3 (C11 or C15), 36.2 (C15 or C11), 35.9 (C17), 35.4 (C13), 30.5 (C5), 28.6 (C21), 18.8 (C1), 18.0 (C6), 16.7 (C22), 12.6 (C20), 12.3 (C8), 12.2 (CH₃), 12.1 (CH₃), 11.7 (CH₃), 11.6 (CH₃), 11.6 (CH₃), 11.5 (C2) ppm

HRMS (m/z): (MALDI⁺) calc'd for C₃₁H₅₈NaSi [M+Na]⁺: 481.4200; found: 481.4205

IR (ν_{max}): 3312, 2968, 2941, 2965, 2162, 1463, 1383, 1085, 883, 676, 628 cm⁻¹

$[\alpha]_D^{25}$: –2 (CHCl₃, c = 0.8)

(3*R*,4*S*,5*R*,6*S*,7*S*,8*R*,9*S*,10*R*,11*S*)-3,4,5,6,7,8,9,10,11-Nonamethyltrideca-1,12-diyne (C9)



Protected alkyne **162** (21 mg, 0.05 mmol, 1.00 equiv.) was deprotected with TBAF (1.00 M in THF, 0.09 mL, 0.09 mmol, 2.00 equiv.) according to **GP5**. The crude residue was purified by flash column chromatography (pure *n*-pentane) to give **C9** (12 mg, 87%) as a colourless liquid.

TLC: R_f = 0.26 (*n*-pentane)

¹H NMR: (500 MHz, Toluene-*d*₈) δ 2.39 (2H, qdd, J = 7.0, 6.9, 2.4 Hz, H3), 1.86 (2H, qdd, J = 6.9, 6.7, 5.3 Hz, H7), 1.84 (2H, d, J = 2.8 Hz, H1), 1.65 (2H, qdd, J = 7.0, 6.9, 5.3 Hz, H5), 1.57 (1H, qt, J = 7.0, 6.1 Hz, H11), 1.41 (2H, *app.* pentd, J^{app} = 6.7, 6.1 Hz, H9), 1.07 (6H, d,

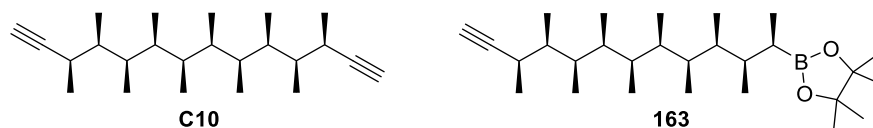
$J = 7.0$ Hz, H4), 0.84 (3H, d, $J = 7.0$ Hz, H12), 0.82 (6H, d, $J = 7.0$ Hz, H6), 0.73 (6H, d, $J = 6.9$ Hz, H8), 0.72 (6H, d, $J = 6.7$ Hz, H10) ppm

^{13}C NMR: (126 MHz, Toluene- d_8) δ 89.0 (C2), 69.3 (C1), 39.6 (C5), 36.4 (C9), 36.2 (C7), 35.6 (C11), 29.2 (C3), 17.2 (C4), 12.4 (C6), 12.1 (C10), 11.6 (C8), 11.5 (C12) ppm

HRMS (m/z): *Despite repeated attempts, a HRMS could not be obtained.*

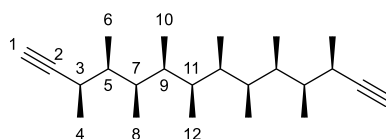
IR (ν_{max}): 3310, 2971, 2921, 2880, 1453, 1383, 1084, 627 cm^{-1}

(3*R*,4*S*,5*R*,6*S*,7*R*,8*R*,9*S*,10*R*,11*S*,12*R*)-3,4,5,6,7,8,9,10,11,12-Decamethyltetradeca-1,13-diyne (C10) and 4,4,5,5-Tetramethyl-2-((2*R*,3*R*,4*S*,5*R*,6*S*,7*R*,8*S*,9*R*,10*S*,11*R*)-3,4,5,6,7,8,9,10,11-nonamethyltridec-12-yn-2-yl)-1,3,2-dioxaborolane (163)



Boronic ester **154** (208 mg, 0.39 mmol, 1.00 equiv.) was alkynylated with vinyl carbamate **15** (73 mg, 0.43 mmol, 1.10 equiv.), LDA (0.86 M in THF, 0.50 mL, 0.43 mmol, 1.10 equiv.), iodine (109 mg, 0.43 mmol, 1.10 equiv.) and LDA (0.86 M in THF, 1.13 mL, 0.97 mmol, 2.50 equiv.) according to **GP3**. The crude residue was purified by flash column chromatography (pure *n*-pentane) to give **C10** (31 mg, 24%) as a white solid, followed by (*n*-pentane:CH₂Cl₂ 80:20) to give **163** (74 mg, 44%) as a colourless liquid.

(3*R*,4*S*,5*R*,6*S*,7*R*,8*R*,9*S*,10*R*,11*S*,12*R*)-3,4,5,6,7,8,9,10,11,12-Decamethyltetradeca-1,13-diyne (C10)



TLC: $R_f = 0.38$ (*n*-pentane:CH₂Cl₂ 90:10)

m.p.: 88 – 92 °C (acetonitrile)

^1H NMR: (500 MHz, Toluene- d_8) δ 2.24 (2H, dqd, $J = 9.2, 6.9, 2.4$ Hz, H3), 2.05 (2H, dqd, $J = 8.6, 6.8, 3.3$ Hz, H7), 1.85 (2H, d, $J = 2.4$ Hz, H1), 1.71 (2H, dqd, $J = 9.2, 6.8, 3.3$ Hz, H5), 1.62 (2H, m, H11), 1.52 (2H, dqd, $J = 8.6, 6.8, 3.2$ Hz, H9), 1.11 (6H, d, $J = 6.9$ Hz, H4), 0.87 (6H, d, $J = 6.2$ Hz, H12), 0.81 (6H, d, $J = 6.8$ Hz, H10), 0.77 (6H, d, $J = 6.8$ Hz, H8), 0.74 (6H, d, $J = 6.8$ Hz, H6) ppm

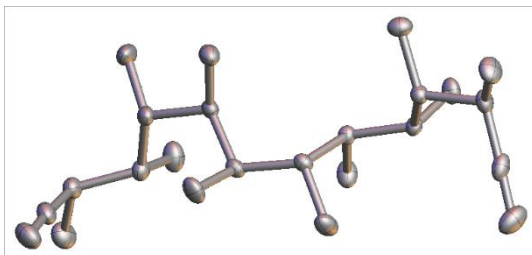
^{13}C NMR: (126 MHz, Toluene- d_8) δ 88.7 (C2), 69.9 (C1), 38.8 (C5), 37.2 (C7), 35.7 (C9), 35.7 (C11), 30.1 (C3), 18.8 (C4), 12.0 (C10), 11.9 (C8), 11.8 (C12), 11.6 (C6) ppm

HRMS (m/z): (MALDI $^-$) calc'd for $\text{C}_{24}\text{H}_{41}$ [$\text{M}-\text{H}$] $^-$: 329.3214; found: 329.3210

IR (ν_{max}): 3310, 2971, 2922, 2879, 1452, 1383, 1083 cm^{-1}

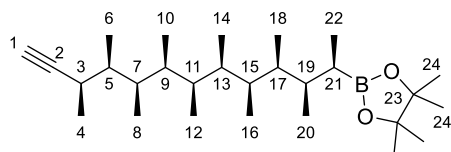
$[\alpha]_D^{23}$: +7 (CHCl_3 , $c = 1.0$)

X-ray: Absolute configuration not determined.



Identification code	C10
Empirical formula	$\text{C}_{24}\text{H}_{42}$
Formula weight	330.57
Temperature/K	100(2)
Crystal system	monoclinic
Space group	P2_1
$a/\text{\AA}$	9.6821(3)
$b/\text{\AA}$	8.6852(3)
$c/\text{\AA}$	13.3264(4)
$\alpha/^\circ$	90
$\beta/^\circ$	94.759(2)
$\gamma/^\circ$	90
Volume/ \AA^3	1116.77(6)
Z	2
$\rho_{\text{calc}}/\text{g cm}^{-3}$	0.983
μ/mm^{-1}	0.054
$F(000)$	372.0
Crystal size/ mm^3	$0.453 \times 0.398 \times 0.299$
Radiation	$\text{MoK}\alpha$ ($\lambda = 0.71073$)
2θ range for data collection/ $^\circ$	3.066 to 55.91
Index ranges	$-12 \leq h \leq 12$, $-11 \leq k \leq 11$, $-17 \leq l \leq 17$
Reflections collected	20700
Independent reflections	5341 [$R_{\text{int}} = 0.0352$, $R_{\text{sigma}} = 0.0337$]
Data/restraints/parameters	5341/1/227
Goodness-of-fit on F^2	1.043
Final R indexes [$I \geq 2\sigma(I)$]	$R_1 = 0.0384$, $wR_2 = 0.0935$
Final R indexes [all data]	$R_1 = 0.0442$, $wR_2 = 0.0973$
Largest diff. peak/hole / e \AA^{-3}	0.26/-0.13
Flack parameter	1.9(10)

4,4,5,5-Tetramethyl-2-((2*R*,3*R*,4*S*,5*R*,6*S*,7*R*,8*S*,9*R*,10*S*,11*R*)-3,4,5,6,7,8,9,10,11-nonamethyltridec-12-yn-2-yl)-1,3,2-dioxaborolane (163)



TLC: R_f = 0.41 (*n*-pentane:Et₂O 95:5)

¹H NMR: (500 MHz, Chloroform-*d*) δ 2.36 (1H, dqd, J = 8.8, 6.9, 2.5 Hz, H3), 2.04 (1H, d, J = 2.5 Hz, H1), 1.85 (1H, dqd, J = 8.2, 6.8, 3.9 Hz, H7), 1.70 (1H, dqd, J = 8.7, 6.7, 4.1 Hz, H19), 1.63 (1H, dqd, J = 8.8, 6.9, 3.9 Hz, H5), 1.55 (1H, dqd, J = 7.5, 6.8, 4.1 Hz, H11), 1.51 – 1.43 (2H, m, H13 & H15), 1.44 (1H, dqd, J = 8.2, 6.8, 4.1 Hz, H9), 1.32 (1H, dqd, J = 7.5, 6.8, 4.1 Hz, H17), 1.23 (6H, s, H24), 1.23 (6H, s, H24'), 1.17 (3H, d, J = 6.9 Hz, H4), 1.03 (1H, m, H21), 0.92 (3H, d, J = 7.2 Hz, H22), 0.78 (3H, d, J = 6.9 Hz, H6), 0.77 – 0.72 (18H, m, 6 \times CH₃), 0.69 (3H, d, J = 6.7 Hz, H14 or H16) ppm

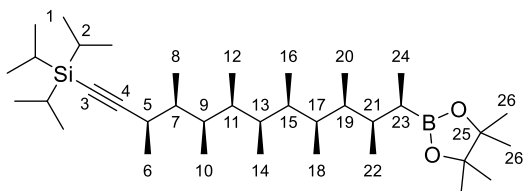
¹³C NMR: (126 MHz, Chloroform-*d*) δ 89.4 (C2), 82.9 (C23), 68.9 (C1), 39.7 (C17), 38.7 (C5), 36.9 (C7), 35.8 (CH), 35.7(3) (C19), 35.6(5) (CH), 35.4(4) (C11), 35.4(2) (CH), 29.6 (C3), 25.1 (C24), 24.7 (C24'), 21.9 (C21), 18.5 (C4), 12.9(4) (C22), 12.8(6) (CH₃), 12.0(4) (CH₃), 12.0(3) (2 \times CH₃), 12.0 (CH₃), 11.9 (C14 or C16), 11.7(4) (C6), 11.7(3) (CH₃) ppm

HRMS (m/z): (MALDI⁺) calc'd for C₂₈H₅₃BNaO₂ [M+Na]⁺: 455.4036; found: 455.4032

IR (ν_{\max}): 3311, 2970, 2932, 2879, 1454, 1382, 1313, 1146, 1081, 967 cm⁻¹

$[\alpha]_D^{24}$: +13 (CHCl₃, c = 1.0)

Triisopropyl((3*R*,4*S*,5*R*,6*S*,7*R*,8*S*,9*R*,10*S*,11*R*,12*R*)-3,4,5,6,7,8,9,10,11-nonamethyl-12-(4,4,5,5-tetramethyl-1,3,2-dioxaborolan-2-yl)tridec-1-yn-1-yl)silane (164)



Alkyne **163** (74 mg, 0.17 mmol, 1.00 equiv.) was protected with LDA (0.86 M in THF, 0.22 mL, 0.19 mmol, 1.10 equiv.) and TIPSCl (0.04 mL, 0.19 mmol, 1.10 equiv.) according to **GP4**. The crude residue was purified by flash column chromatography (*n*-pentane:CH₂Cl₂ 95:5) to give **164** (77 mg, 76%) as a colourless liquid.

TLC: R_f = 0.31 (*n*-pentane:CH₂Cl₂ 80:20)

¹H NMR: (400 MHz, Chloroform-*d*) δ 2.38 (1H, dq, J = 8.8, 6.8 Hz, H5), 1.93 (1H, dqd, J = 8.5, 6.9, 3.8 Hz, H9), 1.70 (1H, dqd, J = 8.9, 6.8, 3.8 Hz, H21), 1.58 (1H, dqd, J = 8.8, 6.8, 3.8 Hz, H7), 1.55 (1H, m, CH), 1.52 – 1.36 (3H, m, 3 \times CH), 1.31 (1H, dqd, J = 8.1, 6.8, 3.8 Hz, H19), 1.24 (6H, s, H26), 1.23 (6H, s, H26'), 1.17 (3H, d, J = 6.8 Hz, H6), 1.10 – 0.96 (22H, m, H1, H2 & H23), 0.92 (3H, d, J = 7.1 Hz, H24), 0.79 – 0.71 (21H, m, 7 \times CH₃), 0.69 (3H, d, J = 6.7 Hz, CH₃) ppm

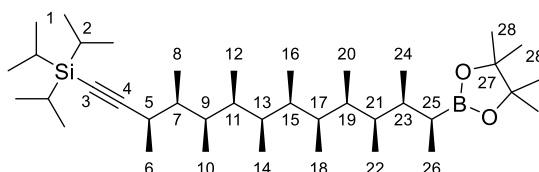
¹³C NMR: (101 MHz, Chloroform-*d*) δ 113.7 (C4), 82.8 (C25), 80.6 (C3), 40.0 (C19), 38.7 (C7), 37.3 (C9), 35.8 (CH), 35.7 (C21), 35.7 (CH), 35.4 (CH), 35.4 (CH), 31.2 (C5), 25.1 (C26), 24.7 (C26'), 22.1 (C23), 19.2 (C6), 18.8 (C1), 13.2 (C24), 12.7 (CH₃), 12.1 (CH₃), 12.1 (CH₃), 12.0 (CH₃), 11.9 (CH₃), 11.8 (CH₃), 11.8 (CH₃), 11.7 (CH₃), 11.5 (C2) ppm

HRMS (m/z): (ESI⁺) calc'd for C₃₇H₇₃BNaO₂Si [M+Na]⁺: 611.5372; found: 611.5373

IR (ν_{\max}): 2967, 2942, 2866, 2163, 1459, 1382, 1313, 1146, 1081, 883 cm⁻¹

$[\alpha]_D^{24}$: +16 (CHCl₃, c = 1.0)

((3*R*,4*S*,5*R*,6*S*,7*R*,8*S*,9*R*,10*S*,11*R*,12*S*,13*S*)-3,4,5,6,7,8,9,10,11,12-Decamethyl-13-(4,4,5,5-tetramethyl-1,3,2-dioxaborolan-2-yl)tetradec-1-yn-1-yl)triisopropylsilane (165)



Boronic ester **164** (70 mg, 0.12 mmol, 1.00 equiv.) was homologated with stannane (**R**)-**93** (68 mg, 0.15 mmol, 1.30 equiv.) and *n*-BuLi (1.54 M in *n*-hexane, 0.10 mL, 0.15 mmol, 1.30 equiv.) according to **GP2**. The crude residue was purified by flash column chromatography (*n*-pentane:CH₂Cl₂ 95:5) to give **165** (66 mg, 90%) as a colourless wax.

TLC: R_f = 0.31 (*n*-pentane:CH₂Cl₂ 80:20)

¹H NMR: (400 MHz, Chloroform-*d*) δ 2.46 (1H, dq, J = 7.5, 6.9 Hz, H5), 1.85 (1H, dqd, J = 7.5, 6.9, 4.7 Hz, H7), 1.68 (1H, m, H21), 1.59 (1H, dqd, J = 7.5, 6.9, 4.7 Hz, H23), 1.54 – 1.44 (4H, m, H11, H13, H15 & H17), 1.44 – 1.38 (2H, m, H9 & H19), 1.24 (6H, s, H28), 1.23 (6H, s, H28'), 1.19 (1H, m, H25), 1.14 (3H, d, J = 6.9 Hz, H4), 1.09 – 0.96 (21H, m, H1 & H2), 0.87 (3H, d, J = 7.4 Hz, H26), 0.82 (3H, d, J = 6.9 Hz, H6), 0.80 (3H, d, J = 6.8 Hz, H22), 0.75 (3H, d, J = 6.7 Hz, H8), 0.74 – 0.69 (18H, m, 6 \times CH₃) ppm

¹³C NMR: (101 MHz, Chloroform-*d*) δ 113.9 (C4), 82.9 (C27), 80.4 (C3), 39.0 (C7), 37.3 (C21), 36.7 (C9), 36.1 (C11), 36.1 (C23), 36.1 (CH), 35.7 (CH), 35.5 (CH), 35.4 (CH), 30.7 (C5), 25.1

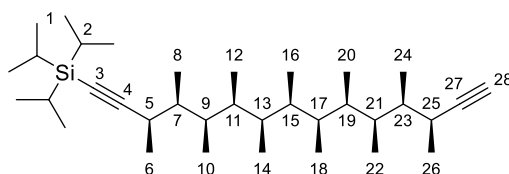
(C28), 24.8 (C28'), 20.3 (C25), 18.8 (C1), 18.2 (C6), 14.5 (C24), 12.3 (CH₃), 12.2 (CH₃), 12.1(2) (CH₃), 12.1(1) (CH₃), 11.9(3) (CH₃), 11.9(1) (CH₃), 11.8 (C10), 11.8 (CH₃), 11.5 (C2), 10.7 (C26) ppm

HRMS (*m/z*): (MALDI⁺) calc'd for C₃₉H₇₇BNaO₂Si [M+Na]⁺: 639.5685; found: 639.5689

IR (*v*_{max}): 2966, 2941, 2866, 2163, 1461, 1381, 1311, 1145, 1077, 883, 675 cm⁻¹

[*α*]_D²³: +10 (CHCl₃, *c* = 1.0)

Triisopropyl((3*R*,4*S*,5*R*,6*S*,7*R*,8*S*,9*S*,10*R*,11*S*,12*R*,13*S*)-3,4,5,6,7,8,9,10,11,12,13-undecamethylpentadeca-1,14-diyn-1-yl)silane (166**)**



Boronic ester **165** (66 mg, 0.11 mmol, 1.00 equiv.) was alkynylated with vinyl carbamate **15** (20 mg, 0.12 mmol, 1.10 equiv.), LDA (0.86 M in THF, 0.14 mL, 0.12 mmol, 1.10 equiv.), iodine (30 mg, 0.12 mmol, 1.10 equiv.) and LDA (0.86 M in THF, 0.31 mL, 0.27 mmol, 2.50 equiv.) according to **GP3**. The crude residue was purified by flash column chromatography (pure *n*-pentane) to give **166** (38 mg, 69%) as a colourless liquid.

TLC: *R*_f = 0.29 (*n*-pentane)

¹H NMR: (400 MHz, Chloroform-*d*) δ 2.50 (1H, qdd, *J* = 6.9, 6.6, 2.4 Hz, H25), 2.48 (1H, dq, *J* = 7.6, 6.9 Hz, H5), 2.03 (1H, d, *J* = 2.4 Hz, H28), 1.83 (1H, dqd, *J* = 7.0, 6.8, 4.9 Hz, H9), 1.74 (1H, qdd, *J* = 6.7, 6.3, 5.9 Hz, H21), 1.61 (1H, qdd, *J* = 6.8, 6.6, 6.3 Hz, H23), 1.59 (1H, dqd, *J* = 7.6, 6.8, 4.9 Hz, H7), 1.55 – 1.44 (3H, m, H13, H15 & H17), 1.48 – 1.37 (2H, m, H11 & H19), 1.14 (3H, d, *J* = 6.9 Hz, H6), 1.11 (3H, d, *J* = 6.9 Hz, H26), 1.10 – 0.94 (21H, m, H1 & H2), 0.87 (3H, d, *J* = 6.8 Hz, H24), 0.83 (3H, d, *J* = 6.8 Hz, H8), 0.77 – 0.70 (21H, m, 7 × CH₃) ppm

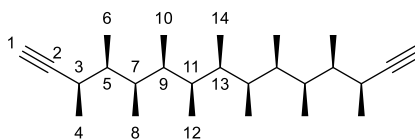
¹³C NMR: (101 MHz, Chloroform-*d*) δ 113.9 (C4), 89.6 (C27), 80.4 (C3), 68.6 (C28), 39.5 (C23), 39.2 (C7), 36.6 (C9), 36.4 (CH), 36.2 (CH), 36.0 (C21), 35.8 (CH), 35.5 (CH), 35.4 (CH), 30.5 (C5), 28.7 (C25), 18.8 (C1), 18.0 (C6), 16.8 (C26), 12.5 (C24), 12.4 (CH₃), 12.2 (C8), 12.2 (CH₃), 12.1 (CH₃), 11.8 (CH₃), 11.8 (CH₃), 11.7 (CH₃), 11.7 (CH₃), 11.5 (C2) ppm

HRMS (*m/z*): (MALDI⁺) calc'd for C₃₅H₆₆NaSi [M+Na]⁺: 537.4826; found: 537.4818

IR (*v*_{max}): 3312, 2967, 2941, 2865, 2162, 1462, 1383, 1082, 883, 664, 628 cm⁻¹

[*α*]_D²²: +3 (CHCl₃, *c* = 1.0)

(3*R*,4*S*,5*R*,6*S*,7*R*,8*S*,9*S*,10*R*,11*S*,12*R*,13*S*)-3,4,5,6,7,8,9,10,11,12,13-Undecamethylpenta-deca-1,14-diyne (C11)



Protected alkyne **166** (22 mg, 0.04 mmol, 1.00 equiv.) was deprotected with TBAF (1.00 M in THF, 0.09 mL, 0.09 mmol, 2.00 equiv.) according to **GP5**. The crude residue was purified by flash column chromatography (pure *n*-pentane) to give **C11** (12 mg, 78%) as a colourless liquid.

TLC: R_f = 0.24 (*n*-pentane)

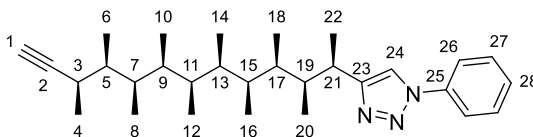
^1H NMR: (400 MHz, Toluene- d_8) δ 2.39 (2H, dqd, J = 7.0, 6.9, 2.4 Hz, H3), 1.89 (2H, dqd, J = 7.1, 6.8, 5.3 Hz, H7), 1.85 (2H, d, J = 2.4 Hz, H1), 1.67 (2H, dqd, J = 7.0, 6.9, 5.3 Hz, H5), 1.60 (2H, qdd, J = 6.6, 6.2, 5.3 Hz, H11), 1.56 (1H, qt, J = 6.4, 6.2 Hz, H13), 1.44 (2H, dqd, J = 7.1, 6.8, 5.3 Hz, H9), 1.08 (6H, d, J = 6.9 Hz, H4), 0.83 (6H, d, J = 6.9 Hz, H6), 0.81 (6H, d, J = 6.6 Hz, H12), 0.76 (6H, d, J = 6.8 Hz, H10), 0.75 (6H, d, J = 6.6 Hz, H8), 0.74 (3H, d, J = 6.4 Hz, H14) ppm

^{13}C NMR: (101 MHz, Toluene- d_8) δ 89.0 (C2), 69.3 (C1), 39.6 (C5), 36.5 (C9), 36.4 (C7), 36.1 (C13), 35.8 (C11), 29.3 (C3), 17.3 (C4), 12.4 (C14), 12.3 (C6), 12.2 (C10), 11.7 (C8), 11.7 (C12) ppm

HRMS (m/z): (MALDI $^+$) calc'd for $\text{C}_{26}\text{H}_{46}\text{Na}$ [$\text{M}+\text{Na}$] $^+$: 381.3492; found: 381.3503

IR (ν_{max}): 3310, 2970, 2920, 2879, 1452, 1383, 1081, 627 cm^{-1}

4-((2*R*,3*S*,4*R*,5*S*,6*R*,7*R*,8*S*,9*R*,10*S*,11*R*)-3,4,5,6,7,8,9,10,11-Nonamethyltridec-12-yn-2-yl)-1-phenyl-1*H*-1,2,3-triazole (168)



In a vial, alkyne **C10** (12 mg, 0.04 mmol, 1.00 equiv.) was dissolved in THF (0.20 mL) at room temperature. A solution of copper sulphate pentahydrate (0.18 M in water, 0.01 mL, 2 μmol , 0.05 equiv.) was added, followed by a solution of sodium ascorbate (0.04 M in water, 0.20 mL, 8 μmol , 0.20 equiv.). The colour of the solution evolved from blue to green to orange. A solution of phenyl azide (0.88 M in THF, 0.05 mL, 0.04 mmol, 1.20 equiv.) was added. The vial was capped and the reaction mixture was stirred at 50 $^{\circ}\text{C}$ for 16 h. The suspension was concentrated

under reduced pressure and the residue was purified by flash column chromatography (*n*-pentane:Et₂O 100:0→85:15) to give triazole **168** (7 mg, 43%) as a colourless liquid.

TLC: *R*_f = 0.33 (*n*-pentane:Et₂O 80:20)

¹H NMR (500 MHz, Chloroform-*d*): δ 7.73 (2H, m, H26), 7.67 (1H, s, H24), 7.51 (2H, m, H27), 7.42 (1H, m, H28), 3.03 (1H, dq, *J* = 8.6, 7.0 Hz, H21), 2.37 (1H, dqd, *J* = 8.5, 6.9, 2.4 Hz, H3), 2.04 (1H, d, *J* = 2.4 Hz, H1), 1.98 (1H, dqd, *J* = 8.6, 6.8, 4.0 Hz, H19), 1.84 (1H, dqd, *J* = 7.9, 6.9, 4.1 Hz, H7), 1.60 (1H, dqd, *J* = 8.5, 6.8, 4.1 Hz, H5), 1.55 – 1.43 (4H, m, 4 × CH), 1.30 (3H, d, *J* = 7.0 Hz, H22), 1.28 (1H, m, H17), 1.15 (3H, d, *J* = 6.9 Hz, H4), 0.87 (3H, d, *J* = 6.8 Hz, H20), 0.80 – 0.72 (15H, m, 5 × CH₃), 0.67 (3H, d, *J* = 6.6 Hz, H16), 0.54 (3H, d, *J* = 6.1 Hz, H12 or H14) ppm

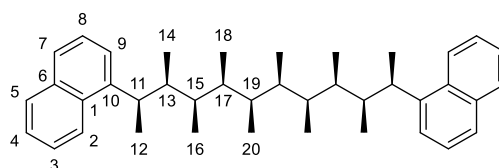
¹³C NMR (126 MHz, Chloroform-*d*): δ 154.3 (C23), 137.5 (C25), 129.8 (C27), 128.5 (C28), 120.5 (C26), 118.2 (C24), 89.3 (C2), 68.9 (C1), 39.3 (C19), 38.8 (C5), 36.7 (C7), 36.3 (C17), 35.6 (CH), 35.5 (CH), 35.4 (2 × CH), 34.3 (C21), 29.5 (C3), 18.3 (C4), 18.0 (C22), 12.0 (CH₃), 12.0(1) (CH₃), 12.0(0) (CH₃), 11.9(4) (CH₃), 11.8(8) (CH₃), 11.8(5) (CH₃), 11.8(4) (CH₃), 11.8(0) (CH₃), 11.7 (CH₃) ppm

HRMS (*m/z*): (ESI⁺) calc'd. for C₃₀H₄₇N₃Na [M+Na]⁺: 472.3662; found 472.3655

IR (*ν*_{max}): 3310, 3136, 3065, 2969, 2925, 2878, 1603, 1504, 1453, 1383, 1038, 758 cm⁻¹

[α]_D²⁴: +5 (CHCl₃, *c* = 1.0)

1,1'-((2*R*,3*S*,4*R*,5*S*,6*R*,7*R*,8*S*,9*R*,10*S*,11*R*)-3,4,5,6,7,8,9,10-Octamethyldodecane-2,11-diyl)dinaphthalene (169**)**



In a flame-dried Schlenk tube, 1-bromonaphthalene (0.03 mL, 0.20 mmol, 2.10 equiv.) was dissolved in anhydrous Et₂O (1.00 mL) at 0 °C under an atmosphere of nitrogen. A solution of *n*-BuLi (1.60 M in *n*-hexane, 0.12 mL, 0.20 mmol, 2.10 equiv.) was added and the resulting suspension was stirred at the same temperature for 1 h. A solution of boronic ester **154** (50 mg, 0.09 mmol, 1.00 equiv.) in anhydrous Et₂O (1.00 mL) was added dropwise at 0 °C over 10 min. After the addition, the mixture was stirred at the same temperature for 2 h. Solvents were removed *in situ* and the residue was dissolved in a mixture of dry MeOH and anhydrous THF (2:1) at –78 °C under an atmosphere of nitrogen. A solution of NBS (80 mg, 0.45 mmol, 4.80 equiv.) in

dry MeOH (2.50 mL) was added dropwise at the same temperature. After the addition, the acetone/dry ice bath was removed and the reaction mixture was stirred at room temperature for 1 h. A saturated aqueous solution of Na₂S₂O₃ (5.00 mL) was added. After 5 min, the suspension was extracted with Et₂O (3 × 5.00 mL). The organic layers were combined, washed with brine, dried over MgSO₄, filtered and concentrated under reduced pressure. The yellow residue was purified by flash column chromatography (*n*-pentane:Et₂O 100:0→99.5:0.5) to give compound **169** (12 mg, 24%) as a white solid.

TLC: *R*_f = 0.69 (*n*-pentane:Et₂O 95:5)

m.p.: 157 – 159 °C (acetonitrile)

¹H NMR (500 MHz, Chloroform-*d*): δ 8.17 (2H, dd, *J* = 8.2, 1.6 Hz, H2), 7.85 (2H, dd, *J* = 7.6, 2.0 Hz, H5), 7.68 (2H, dd, *J* = 8.0, 1.2 Hz, H7), 7.48 (2H, ddd, *J* = 8.2, 6.6, 2.0 Hz, H3), 7.45 (2H, ddd, *J* = 7.6, 6.7, 1.6 Hz, H4), 7.43 (2H, dd, *J* = 8.0, 7.3 Hz, H8), 7.36 (2H, dd, *J* = 7.2, 1.2 Hz, H9), 3.50 (2H, m, H11), 2.10 (2H, m, H13), 1.46 (2H, dqd, *J* = 8.8, 6.8, 2.5 Hz, H17), 1.37 (2H, m, H19), 1.30 (6H, d, *J* = 6.9 Hz, H12), 1.07 (2H, dqd, *J* = 8.8, 6.8, 2.9 Hz, H15), 0.92 (6H, d, *J* = 6.7 Hz, H14), 0.67 (6H, d, *J* = 6.8 Hz, H16), 0.55 (6H, d, *J* = 6.8 Hz, H18), 0.33 (6H, m, H20) ppm

¹³C NMR (126 MHz, Chloroform-*d*): δ 144.3 (C10), 134.1 (C6), 132.0 (C1), 129.1 (C5), 126.1 (C7), 125.7 (C4 or C8), 125.6 (C8 or C4), 125.2 (C3), 124.1 (C9), 123.4 (C2), 39.4 (C13), 37.2* (C11), 36.3 (C15), 35.6 (C17), 35.5 (C19), 20.8 (C12), 12.3 (C16), 12.1 (C14), 11.9 (C18 or C20), 11.9 (C20 or C18) ppm

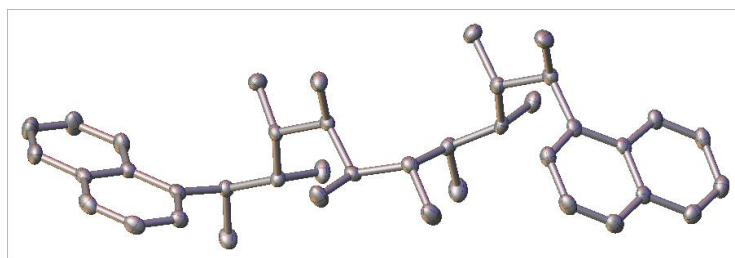
*shift value determined by HSQC correlation.

HRMS (*m/z*): (MALDI⁺) calc'd. for C₄₀H₅₄Na [M+Na]⁺: 557.4118; found 557.4110

IR (*ν*_{max}): 3049, 2966, 2925, 1453, 1382, 1260, 1083, 778 cm⁻¹

[α]_D²⁵: +45 (CHCl₃, *c* = 1.0)

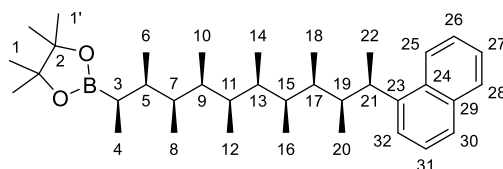
X-ray: Absolute configuration not determined. The compound undergoes a phase transition between 180 and 160 K. The cell above the transition is monoclinic, P2₁ with half the volume, Z'=2.



Identification code	169
Empirical formula	C ₄₀ H ₅₄
Formula weight	534.83

Temperature/K	100(2)
Crystal system	monoclinic
Space group	P2 ₁
a/Å	13.1097(3)
b/Å	36.9860(9)
c/Å	14.5028(4)
$\alpha/^\circ$	90
$\beta/^\circ$	112.8517(14)
$\gamma/^\circ$	90
Volume/Å ³	6480.1(3)
Z	8
$\rho_{\text{calc}}/\text{g cm}^{-3}$	1.096
μ/mm^{-1}	0.061
F(000)	2352.0
Crystal size/mm ³	0.458 × 0.304 × 0.287
Radiation	MoK α (λ = 0.71073)
2 θ range for data collection/ $^\circ$	3.048 to 52.742
Index ranges	-16 ≤ h ≤ 16, -40 ≤ k ≤ 46, -17 ≤ l ≤ 18
Reflections collected	80431
Independent reflections	25125 [R_{int} = 0.0539, R_{sigma} = 0.0639]
Data/restraints/parameters	25125/1/1481
Goodness-of-fit on F ²	1.013
Final R indexes [$I \geq 2\sigma(I)$]	R_1 = 0.0498, wR_2 = 0.0963
Final R indexes [all data]	R_1 = 0.0818, wR_2 = 0.1102
Largest diff. peak/hole / e Å ⁻³	0.16/-0.20
Flack parameter	-4.2(10)

4,4,5,5-Tetramethyl-2-((2*R*,3*R*,4*S*,5*R*,6*S*,7*R*,8*S*,9*R*,10*S*,11*R*)-3,4,5,6,7,8,9,10-octamethyl-11-(naphthalen-1-yl)dodecan-2-yl)-1,3,2-dioxaborolane (170)



In a flame-dried Schlenk tube, 1-bromonaphthalene (30 μL , 0.20 mmol, 1.05 equiv.) was dissolved in anhydrous *n*-hexane (1.00 mL) with one drop of anhydrous THF at 0 $^\circ\text{C}$ under an atmosphere of nitrogen. A solution of *n*-BuLi (1.60 M in *n*-hexane, 0.12 mL, 0.20 mmol, 1.05 equiv.) was added and the reaction mixture was stirred at 0 $^\circ\text{C}$ for 40 min. Anhydrous Et₂O (0.30 mL) was slowly added to dissolve the white precipitate. In a second flame-dried Schlenk tube, boronic ester **154** (100 mg, 0.19 mmol, 1.00 equiv.) was dissolved in anhydrous Et₂O

(2.00 mL) at 0 °C under an atmosphere of nitrogen. The previously prepared solution of naphthyllithium was added *via* syringe and the suspension was stirred at 0 °C for 1 h. Solvents were removed under reduced pressure *in situ* and the residue was re-dissolved in a mixture of anhydrous MeOH (2.00 mL) and anhydrous THF (2.20 mL) at –78 °C under an atmosphere of nitrogen. A solution of NBS (70 mg, 0.39 mmol, 2.10 equiv.) in anhydrous MeOH (2.50 mL) was added dropwise, the acetone/dry ice bath was removed and the reaction mixture was allowed to warm to room temperature for 1 h. A saturated aqueous solution of Na₂S₂O₃ (1.00 mL) was added and the biphasic mixture was extracted with Et₂O (3 × 10.00 mL). The organic layers were combined, washed with brine, dried over MgSO₄, filtered and concentrated. The crude residue was purified by flash column chromatography (*n*-pentane:Et₂O 100:0→99.5:0.5) to give boronic ester **170** (34 mg, 34%) as a colourless liquid.

TLC: *R*_f = 0.21 (*n*-pentane:CH₂Cl₂ 80:20)

¹H NMR: (500 MHz, Chloroform-*d*) δ 8.18 (1H, dd, *J* = 8.2, 1.6 Hz, H25), 7.85 (1H, dd, *J* = 7.6, 1.7 Hz, H28), 7.68 (1H, dd, *J* = 8.2, 1.3 Hz, H30), 7.48 (1H, ddd, *J* = 8.2, 6.6, 1.7 Hz, H26), 7.45 (1H, ddd, *J* = 7.6, 6.6, 1.6 Hz, H27), 7.44 (1H, dd, *J* = 8.0, 7.3 Hz, H31), 7.38 (1H, dd, *J* = 7.3, 1.3 Hz, H32), 3.54 (1H, dq, *J* = 9.4, 6.9 Hz, H21), 2.12 (1H, dqd, *J* = 9.4, 6.8, 3.3 Hz, H19), 1.67 (1H, dqd, *J* = 9.0, 6.7, 4.0 Hz, H5), 1.54 – 1.41 (4H, m, 4 × CH), 1.32 (3H, d, *J* = 6.9 Hz, H22), 1.30 (1H, m, H7), 1.24 (6H, s, H1), 1.23 (6H, s, H1'), 1.13 (1H, dqd, *J* = 9.1, 6.8, 3.3 Hz, H17), 1.03 (1H, dq, *J* = 9.0, 7.2 Hz, H3), 0.94 (3H, d, *J* = 6.8 Hz, H20), 0.91 (3H, d, *J* = 7.2 Hz, H4), 0.75 – 0.70 (12H, m, 4 × CH₃), 0.68 (3H, d, *J* = 6.8 Hz, H18), 0.55 (3H, d, *J* = 6.7 Hz, CH₃), 0.38 (3H, d, *J* = 6.0 Hz, CH₃) ppm

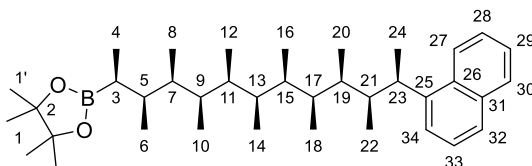
¹³C NMR: (126 MHz, Chloroform-*d*) δ 144.3 (C23), 134.1 (C29), 132.0 (C24), 129.1 (C28), 126.1 (C30), 125.6(3) (CH_{Ar}), 125.5(8) (CH_{Ar}), 125.2 (CH_{Ar}), 124.1 (C32), 123.4 (25), 82.8 (C2), 39.8 (C7), 39.6 (C19), 37.2 (C21), 36.3 (C17), 35.8 (2 × CH), 35.7 (C5), 35.6 (CH), 35.4 (CH), 25.1 (C1), 24.7 (C1'), 21.9 (C3), 20.4 (C22), 13.1 (C4), 12.7 (CH₃), 12.3 (C20), 12.2 (CH₃), 12.1 (C18), 12.0(2) (CH₃), 11.9(8) (CH₃), 11.9(6) (CH₃), 11.8 (CH₃) ppm

HRMS (*m/z*): (MALDI⁺) calc'd for C₃₆H₅₉BNaO₂ [M+Na]⁺: 557.4507; found: 557.4500

IR (*ν*_{max}): 2968, 2876, 1451, 1378, 1362, 1358, 1307, 1205, 1146, 1077 cm⁻¹

[α]_D²⁴: +16 (CHCl₃, *c* = 1.0)

4,4,5,5-Tetramethyl-2-((2*S*,3*S*,4*R*,5*S*,6*R*,7*S*,8*R*,9*S*,10*R*,11*S*,12*R*)-3,4,5,6,7,8,9,10,11-nonamethyl-12-(naphthalen-1-yl)tridecan-2-yl)-1,3,2-dioxaborolane (171)



Boronic ester **170** (55 mg, 0.10 mmol, 1.00 equiv.) was homologated with stannane (**R**)-**93** (59 mg, 0.13 mmol, 1.30 equiv.) and *n*-BuLi (1.60 M in *n*-hexane, 0.08 mL, 0.13 mmol, 1.30 equiv.) according to **GP2**. The crude residue was purified by flash column chromatography (*n*-pentane:CH₂Cl₂ 100:0→20:80) to give **171** (49 mg, 85%) as a white solid.

TLC: *R*_f = 0.22 (*n*-pentane:CH₂Cl₂ 80:20)

m.p.: 181 – 185 °C (*n*-hexane)

¹H NMR: 500 MHz, Chloroform-*d*) δ 8.17 (1H, dd, *J* = 8.6, 1.7 Hz, H27), 7.85 (1H, dd, *J* = 7.9, 1.7 Hz, H30), 7.68 (1H, dd, *J* = 8.0, 1.3 Hz, H32), 7.48 (1H, ddd, *J* = 8.6, 6.7, 1.7 Hz, H28), 7.45 (1H, ddd, *J* = 7.9, 6.7, 1.7 Hz, H29), 7.44 (1H, dd, *J* = 8.0, 7.2 Hz, H33), 7.38 (1H, dd, *J* = 7.2, 1.3 Hz, H34), 3.61 (1H, dq, *J* = 8.4, 6.9 Hz, H23), 2.05 (1H, dqd, *J* = 8.4, 6.8, 4.2 Hz, H21), 1.67 (1H, qdd, *J* = 6.8, 6.7, 6.2 Hz, H5), 1.57 (1H, dqd, *J* = 8.9, 6.8, 4.4 Hz, H17), 1.54 – 1.43 (3H, m, 3 × CH), 1.42 – 1.34 (2H, m, 2 × CH), 1.31 (3H, d, *J* = 6.9 Hz, H24), 1.25 (1H, dqd, *J* = 8.9, 6.8, 4.2 Hz, H19), 1.24 (6H, s, H1), 1.23 (6H, s, H1'), 1.16 (1H, qd, *J* = 7.3, 6.2 Hz, H3), 0.90 (3H, d, *J* = 6.8 Hz, H22), 0.87 (3H, d, *J* = 7.3 Hz, H4), 0.79 (3H, d, *J* = 6.8 Hz, H6), 0.73 (3H, d, *J* = 6.5 Hz, CH₃), 0.71 – 0.66 (12H, m, 4 × CH₃), 0.62 (3H, d, *J* = 6.8 Hz, H18), 0.45 (3H, d, *J* = 6.7 Hz, CH₃) ppm

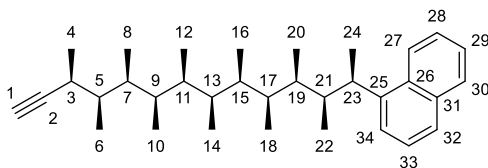
¹³C NMR: (126 MHz, Chloroform-*d*) δ 144.1 (C25), 134.1 (C31), 132.0 (C26), 129.1 (C30), 126.2 (C32), 125.6 (2 × CH_{Ar}), 125.2 (CH_{Ar}), 124.2 (C34), 123.4 (C27), 82.9 (C2), 39.9 (C21), 37.3 (CH), 36.8 (C23), 36.3 (C17), 36.2 (C19), 36.1 (CH), 36.0 (C5), 35.8 (CH), 35.5 (CH), 35.4 (CH), 25.1 (C1), 24.8 (C1'), 20.3 (C3), 19.1 (C24), 14.4 (C6), 12.3 (3 × CH₃), 12.0(4) (CH₃), 12.0(3) (CH₃), 11.9 (CH₃), 11.8 (CH₃), 11.7 (CH₃), 10.8 (C4) ppm

HRMS (*m/z*): (MALDI⁺) calc'd for C₃₈H₆₃BNaO₂ [M+Na]⁺: 585.4820; found: 585.4828

IR (*ν*_{max}): 2966, 2876, 1450, 1381, 1362, 1307, 1149, 1077, 1016, 965 cm⁻¹

[α]_D²³: +22 (CHCl₃, *c* = 1.0)

1-((2R,3S,4R,5S,6R,7S,8S,9R,10S,11R,12S)-3,4,5,6,7,8,9,10,11,12-Decamethyltetradec-13-yn-2-yl)naphthalene (172)



Part A: In a flame-dried Schlenk tube, boronic ester **171** (47 mg, 0.08 mmol, 1.00 equiv.) and vinyl carbamate **15** (18 mg, 0.11 mmol, 1.33 equiv.) were dissolved in anhydrous THF (0.50 mL) at $-78\text{ }^{\circ}\text{C}$ under an atmosphere of nitrogen. A freshly prepared solution of LDA (0.86 M in THF, 0.12 mL, 0.11 mmol, 1.33 equiv.) was added and the reaction mixture was stirred at the same temperature for 1 h. The acetone/dry ice bath was replaced with an acetonitrile/dry ice bath and the reaction mixture was stirred at $-40\text{ }^{\circ}\text{C}$ for 1 h. After cooling the reaction mixture back to $-78\text{ }^{\circ}\text{C}$, a freshly prepared solution of iodine (27 mg, 0.11 mmol, 1.33 equiv.) in MeOH (0.40 mL) was added dropwise at *via* syringe. After the addition, the reaction mixture was allowed to stir at room temperature for 1 h. A saturated aqueous solution of NH_4Cl was added and the biphasic mixture was extracted 3 times with Et_2O . The organic layers were combined, washed with brine, dried over MgSO_4 , filtered through silica (2 cm depth of dry silica, using a filter frit connected directly to a flame-dried receiving vessel), concentrated under reduced pressure and dried under high vacuum for (at least) 1 h. **Part B:** The dried crude residue was dissolved in anhydrous Et_2O (0.80 mL) at $-78\text{ }^{\circ}\text{C}$ under an atmosphere of nitrogen. A solution of *tert*-BuLi (1.70 M in *n*-pentane, 0.12 mL, 0.20 mmol, 2.50 equiv.) was added and the reaction mixture was allowed to stir at room temperature for 1 h. A saturated aqueous solution of NH_4Cl was added *via* syringe and the biphasic mixture was extracted 3 times with Et_2O . The organic layers were combined, washed with brine, dried over MgSO_4 , filtered and concentrated under reduced pressure. The residue was purified by flash column chromatography (pure *n*-pentane) to give **172** (24 mg, 65%) as a colourless liquid.

TLC: $R_f = 0.46$ (*n*-pentane: CH_2Cl_2 80:20)

^1H NMR: (500 MHz, Chloroform-*d*) δ 8.16 (1H, dd, $J = 8.3, 1.5$ Hz, H27), 7.85 (1H, dd, $J = 7.9, 1.8$ Hz, H30), 7.69 (1H, dd, $J = 8.1, 1.3$ Hz, H32), 7.48 (1H, ddd, $J = 8.3, 6.8, 1.8$ Hz, H28), 7.45 (1H, ddd, $J = 7.9, 6.8, 1.5$ Hz, H29), 7.44 (1H, dd, $J = 8.1, 7.3$ Hz, H33), 7.38 (1H, dd, $J = 7.3, 1.3$ Hz, H34), 3.63 (1H, dq, $J = 7.9, 6.9$ Hz, H23), 2.49 (1H, dqd, $J = 6.9, 6.8, 2.4$ Hz, H3), 2.03 (1H, d, $J = 2.4$ Hz, H1), 2.02 (1H, dqd, $J = 7.9, 6.8, 4.6$ Hz, H21), 1.71 (1H, qdd, $J = 6.8, 6.0, 5.8$ Hz, H7), 1.61 (1H, qdd, $J = 6.8, 6.9, 5.8$ Hz, H5), 1.58 (1H, dqd, $J = 7.0, 6.8, 5.1$ Hz, H17), 1.54 – 1.43 (2H, m, H11 & H15), 1.40 (1H, qdd, $J = 6.8, 6.3, 6.0$ Hz, H9), 1.35 (1H, qdd, $J = 6.8, 6.5, 6.0$ Hz, H13), 1.32 (3H, d, $J = 6.9$ Hz, H24), 1.29 (1H, dqd, $J = 7.0, 6.8, 4.6$ Hz, H19), 1.11 (3H, d, $J = 6.9$ Hz, H4), 0.90 (3H, d, $J = 6.8$ Hz, H22), 0.85 (3H, d, $J = 6.9$ Hz, H6), 0.74 – 0.71

(6H, m, $2 \times \text{CH}_3$), 0.71 – 0.67 (9H, m, $3 \times \text{CH}_3$), 0.65 (3H, d, $J = 6.8$ Hz, H18), 0.47 (3H, d, $J = 6.8$ Hz, CH_3) ppm

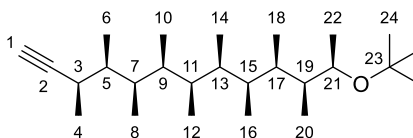
^{13}C NMR: (126 MHz, Chloroform- d) δ 144.0 (C25), 134.1 (C31), 132.0 (C26), 129.1 (C30), 126.2 (C32), 125.6(0) (C28), 125.5(6) (C29), 125.2 (C33), 124.3 (C34), 123.4 (C27), 89.6 (C2), 68.6 (C1), 40.1 (C21), 39.3 (C5), 36.8 (C23), 36.5 (C17), 36.2 (C19), 36.0(8) (C7), 35.9(8) (C9 & C13), 35.4(8) (C11 or C15), 35.4(6) (C15 or C11), 28.7 (C3), 18.8 (C24), 16.9 (C4), 12.5 (CH_3), 12.4(1) (CH_3), 12.3(9) (CH_3), 12.3(8) (CH_3), 12.0 (CH_3), 11.9 (CH_3), 11.7(0) (CH_3), 11.6(8) (CH_3), 11.6(7) (CH_3) ppm

HRMS (m/z): (MALDI $^+$) calc'd for $\text{C}_{34}\text{H}_{52}\text{Na}$ $[\text{M}+\text{Na}]^+$: 483.3961; found: 483.3968

IR (ν_{max}): 3309, 3047, 2969, 2923, 2878, 2111, 1451, 1382, 1081, 777 cm^{-1}

$[\alpha]_D^{23}$: +24 (CHCl_3 , $c = 1.0$)

(3R,4S,5R,6S,7S,8R,9S,10R,11S,12R)-12-(tert-Butoxy)-3,4,5,6,7,8,9,10,11-nonamethyltridec-1-yne (174)



Part A: Boronic ester **163** (29 mg, 0.07 mmol, 1.00 equiv.) was oxidised according to **GP1** to give crude intermediate **173**. **Part B:** Freshly-dried $\text{Mg}(\text{ClO}_4)_2$ (1 mg, 5 μmol , 0.10 equiv.) (WARNING: shock sensitive!) was charged in a separated flask at room temperature, under an atmosphere of nitrogen. A solution of alcohol **173** in anhydrous CH_2Cl_2 (0.10 mL) was added, followed by Boc_2O (23 mg, 0.11 mmol, 2.30 equiv.). The reaction mixture was stirred at 40 $^\circ\text{C}$ for 48 h. Water (5.00 mL) was added and the biphasic mixture was extracted with Et_2O (3×5.00 mL). The organic layers were combined, washed with brine, dried over MgSO_4 , filtered and concentrated. The residue was purified by flash column chromatography (n -pentane: Et_2O 95:5) to give ether **174** (9 mg, 36% over 2 steps) as a colourless liquid.

TLC: $R_f = 0.57$ (n -pentane: Et_2O 95:5)

^1H NMR (500 MHz, Chloroform- d): δ 3.47 (1H, *app.* pent, $J^{\text{app.}} = 6.2$ Hz, H21), 2.32 (1H, dqd, $J = 7.9, 6.9, 2.4$ Hz, H3), 1.97 (1H, dqd, $J = 7.6, 6.8, 4.5$ Hz, H7), 1.84 (1H, d, $J = 2.4$ Hz, H1), 1.78 (1H, dqd, $J = 7.6, 6.8, 4.8$ Hz, H17), 1.73 – 1.66 (2H, m, H5 & H19), 1.65 – 1.58 (3H, m, H11, H13 & H15), 1.50 (1H, dqd, $J = 7.6, 6.8, 4.0$ Hz, H9), 1.14 (9H, s, H24), 1.11 – 1.08 (6H, m, H4 & H22), 0.87 – 0.83 (12H, m, $4 \times \text{CH}_3$), 0.81 – 0.78 (9H, m, $3 \times \text{CH}_3$), 0.77 (3H, d, $J = 6.8$ Hz, H8) ppm

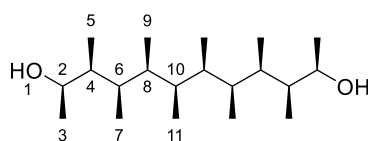
¹³C NMR (126 MHz, Chloroform-*d*): δ 88.8 (C2), 72.8 (C23), 69.5 (C1), 68.9 (C21), 41.4 (C19 or C5), 39.2 (C19 or C5), 36.7 (C7), 36.2 (CH), 36.2 (CH), 35.9 (CH), 35.7 (CH), 35.1 (C17), 29.6 (C3), 29.0 (C24), 20.1 (C4 or C22), 18.0 (C22 or C4), 12.7 (CH₃), 12.1 (CH₃), 12.1 (CH₃), 12.0 (CH₃), 12.0 (CH₃), 11.8 (CH₃), 11.8 (CH₃), 11.0 (CH₃) ppm

HRMS (*m/z*): (ESI⁺) calc'd. for C₂₆H₅₀NaO [M+Na]⁺: 401.3754; found 401.3753

IR (ν_{\max}): 3312, 2971, 2931, 2879, 1454, 1383, 1197, 1080, 1018 cm⁻¹

[α]_D²²: -4 (CHCl₃, *c* = 1.0)

(2*R*,3*S*,4*R*,5*S*,6*R*,7*R*,8*S*,9*R*,10*S*,11*R*)-3,4,5,6,7,8,9,10-Octamethyldodecane-2,11-diol (175)



Boronic ester **154** (70 mg, 0.13 mmol, 1.00 equiv.) was oxidised according to **GP1**. The crude residue was purified by flash column chromatography (CH₂Cl₂:Et₂O 90:10) to give diol **175** (39 mg, 95%) as a white solid.

TLC: *R_f* = 0.26 (CH₂Cl₂:Et₂O 90:10)

m.p.: 136 – 140 °C (*n*-hexane)

¹H NMR (400 MHz, Chloroform-*d*): δ 3.65 (2H, dq, *J* = 8.1, 6.1 Hz, H2), 1.75 (2H, dqd, *J* = 8.5, 6.8, 3.4 Hz, H6), 1.57 (2H, dqd, *J* = 8.1, 7.0, 3.4 Hz, H4), 1.55 – 1.39 (4H, m, H8 & H10), 1.28 (2H, br. s, H1), 1.19 (6H, d, *J* = 6.1 Hz, H3), 0.77 (6H, d, *J* = 6.8 Hz, H7), 0.76 – 0.73 (12H, m, H9 & H11), 0.72 (6H, d, *J* = 7.0 Hz, H5) ppm

¹³C NMR (126 MHz, Chloroform-*d*): δ 70.0 (C2), 41.1 (C4), 35.5 (CH), 35.2 (CH), 34.7 (C6), 21.6 (C3), 12.0 (CH₃), 11.9 (CH₃), 11.8 (CH₃), 10.5 (CH₃) ppm

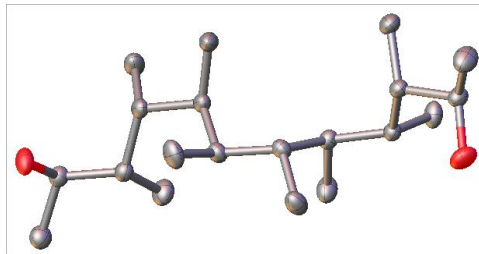
HRMS (*m/z*): (ESI⁺) calc'd. for C₂₀H₄₂NaO₂ [M+Na]⁺: 337.3077; found 337.3088

IR (ν_{\max}): 3307, 2968, 2919, 2879, 1454, 1382, 1084, 1053, 918 cm⁻¹

[α]_D²³: -5 (CHCl₃, *c* = 1.0)

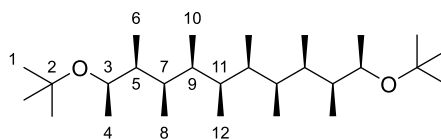
X-ray: Absolute configuration not determined. The molecule is a weak anomalous scatterer and therefore the absolute structure parameter is meaningless and has been removed from the .cif file. Hydrogen atoms on the oxygen atoms were found by difference map, disorder was present and these hydrogen atoms were both modelled in two positions with a constrained occupancy of 0.5. Due to the disorder, rotating group refinement was used. All other hydrogens were geometrically

placed and refined using a riding model. Density is slightly lower than expected (0.9978 g cm^{-3}) and solvent accessible voids (41 \AA^3) are present. Only water is small enough to fit in these voids and there is no electron density visible within these voids. The space group was checked and the slightly low density is believed to be due to the voids.



Identification code	175
Empirical formula	$\text{C}_{20}\text{H}_{42}\text{O}_2$
Formula weight	314.53
Temperature/K	100
Crystal system	trigonal
Space group	$P3_121$
$a/\text{\AA}$	16.3491(3)
$b/\text{\AA}$	16.3491(3)
$c/\text{\AA}$	13.5683(3)
$\alpha/^\circ$	90
$\beta/^\circ$	90
$\gamma/^\circ$	120
Volume/ \AA^3	3140.82(13)
Z	6
$\rho_{\text{calc}}/\text{g cm}^{-3}$	0.998
μ/mm^{-1}	0.061
$F(000)$	1068.0
Crystal size/ mm^3	$0.524 \times 0.17 \times 0.102$
Radiation	$\text{MoK}\alpha$ ($\lambda = 0.71073$)
2θ range for data collection/ $^\circ$	2.876 to 54.312
Index ranges	$-20 \leq h \leq 20, -20 \leq k \leq 20, -17 \leq l \leq 17$
Reflections collected	53962
Independent reflections	4647 [$R_{\text{int}} = 0.0890, R_{\text{sigma}} = 0.0416$]
Data/restraints/parameters	4647/0/213
Goodness-of-fit on F^2	1.046
Final R indexes [$I \geq 2\sigma(I)$]	$R_1 = 0.0407, wR_2 = 0.0827$
Final R indexes [all data]	$R_1 = 0.0625, wR_2 = 0.0928$
Largest diff. peak/hole / e \AA^{-3}	0.14/-0.16

(2R,3S,4R,5S,6R,7R,8S,9R,10S,11R)-2,11-Di-tert-butoxy-3,4,5,6,7,8,9,10-octamethyldodecane (176)



In a flame-dried vial, $\text{Mg}(\text{ClO}_4)_2$ (2 mg, 0.01 mmol, 0.20 equiv.) (WARNING: shock sensitive!) was dried under high vacuum at 130 °C for 2 h without magnetic stirrer. The solid was allowed to cool down under nitrogen and a solution of alcohol **175** (15 mg, 0.05 mmol, 1.00 equiv.) in anhydrous CH_2Cl_2 (0.10 mL) was added, followed by Boc_2O (48 mg, 0.22 mmol, 4.60 equiv.) and a small magnetic stirred. The vial was capped and the reaction mixture was stirred at 45 °C for 18 h before being diluted with Et_2O (5.00 mL) and water (5.00 mL). The layers were separated and the aqueous phase was extracted with Et_2O (2×5.00 mL). The organic layers were combined, washed with brine, dried over MgSO_4 , filtered and concentrated. The crude residue was purified by flash column chromatography (*n*-hexane: Et_2O 97:3) to give ether **176** (8 mg, 39%) as a colourless liquid.

TLC: $R_f = 0.47$ (*n*-hexane: Et_2O 95:5)

^1H NMR (500 MHz, Toluene- d_8): δ 3.60 (2H, dq, $J = 5.8, 6.1$ Hz, H3), 1.77 – 1.58 (8H, m, $8 \times \text{CH}$), 1.14 (18H, s, H1), 1.10 (6H, d, $J = 6.1$ Hz, H4), 0.92 (6H, d, $J = 6.7$ Hz, CH_3), 0.87 (6H, d, $J = 5.1$ Hz, CH_3), 0.86 (6H, d, $J = 4.8$ Hz, H12), 0.81 (6H, d, $J = 6.5$ Hz, CH_3) ppm

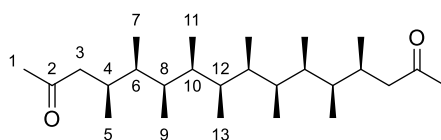
^{13}C NMR (126 MHz, Toluene- d_8): δ 72.8 (C2), 68.3 (C3), 41.9 (CH), 36.3 (CH), 36.0 (CH), 35.3 (CH), 28.9 (C1), 19.0 (C4), 12.4 (CH_3), 12.2 (CH_3), 12.1 (CH_3), 11.3 (CH_3) ppm

HRMS (m/z): (ESI $^+$) calc'd. for $\text{C}_{28}\text{H}_{58}\text{NaO}_2$ [$\text{M}+\text{Na}$] $^+$: 449.4329; found 449.4324

IR (ν_{max}): 2970, 2924, 2878, 1457, 1382, 1198, 1077, 1019, 804 cm^{-1}

$[\alpha]_D^{25}$: +13 (CHCl_3 , $c = 1.0$)

(4S,5R,6S,7R,8S,9S,10R,11S,12R,13S)-4,5,6,7,8,9,10,11,12,13-Decamethylhexadecane-2,15-dione (177)



Alkyne **179** (38 mg, 0.11 mmol, 1.00 equiv.) was charged in a flame-dried vial at room temperature under an atmosphere of nitrogen. A solution of 9-BBN-H (0.50 M in THF, 42 μL , 0.02 mmol, 0.20 equiv.) was added, followed by catechol borane (25 μL , 0.23 mmol,

2.20 equiv.). The vial was capped and the reaction mixture was stirred at 75 °C for 18 h. The reaction mixture was diluted with THF (2.00 mL) and the pale-yellow solution was transferred to a round-bottom flask containing a mixture of NaOH (2.00 M in water, 2.00 mL) and H₂O₂ (30% in water, 1.00 mL) at 0 °C. The biphasic mixture was vigorously stirred at 0 °C for 4 h. The layers were separated and the aqueous phase was extracted with Et₂O (3 × 5.00 mL). The organic layers were combined, washed with brine, dried over MgSO₄, filtered and concentrated. The crude residue was purified by flash column chromatography (*n*-pentane:EtOAc 95:5) to give ketone **177** (25 mg, 60%) as a colourless liquid.

TLC: *R*_f = 0.44 (*n*-pentane:EtOAc 90:10)

¹H NMR (500 MHz, Toluene-*d*₈): δ 2.29 (2H, dqdd, *J* = 7.5, 6.8, 6.1, 4.1 Hz, H₄), 2.08 (2H, dd, *J* = 16.3, 6.1 Hz, H₃), 1.91 (2H, dd, *J* = 16.3, 7.5 Hz, H_{3'}), 1.71 (6H, s, H₁), 1.67 (2H, dqd, *J* = 7.8, 6.7, 4.0 Hz, H₁₀), 1.61 (2H, m, H₁₂), 1.53 (2H, dqd, *J* = 7.8, 6.8, 4.0 Hz, H₈), 1.31 (2H, dqd, *J* = 7.8, 6.9, 4.1 Hz, H₆), 0.83 (6H, d, *J* = 6.7 Hz, H₁₁), 0.81 (6H, d, *J* = 6.3 Hz, H₁₃), 0.78 (6H, d, *J* = 6.8 Hz, H₉), 0.76 (6H, d, *J* = 6.8 Hz, H₅), 0.70 (6H, d, *J* = 6.9 Hz, H₇) ppm

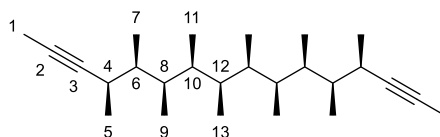
¹³C NMR (126 MHz, Toluene-*d*₈): δ 205.6 (C₂), 49.6 (C₃), 39.1 (C₆), 36.0(1) (C₈ or C₁₀), 36.0(2) (C₁₀ or C₈), 35.8 (C₁₂), 29.8 (C₁), 29.7 (C₄), 14.6 (C₅), 12.2(0) (CH₃), 12.1(7) (CH₃), 11.9 (CH₃), 11.8 (C₇) ppm

HRMS (*m/z*): (ESI⁺) calc'd. for C₂₆H₅₀NaO₂ [M+Na]⁺: 417.3703; found 417.3702

IR (*ν*_{max}): 2967, 2922, 2879, 1715, 1452, 1382, 1357, 1166, 1077, 803 cm⁻¹

[α]_D²⁵: +8 (CHCl₃, *c* = 1.0)

(4*R*,5*S*,6*R*,7*S*,8*R*,9*R*,10*S*,11*R*,12*S*,13*R*)-4,5,6,7,8,9,10,11,12,13-Decamethylhexadeca-2,14-diyne (179**)**



In a flame-dried Schlenk tube, alkyne **C10** (38 mg, 0.11 mmol, 1.00 equiv.) was dissolved in anhydrous THF (1.10 mL) at -78 °C under an atmosphere of nitrogen. A solution of *n*-BuLi (1.58 M in *n*-hexane, 0.29 mL, 0.46 mmol, 4.00 equiv.) was added dropwise and the reaction was stirred at -78 °C for 20 min. Methyl iodide (0.07 mL, 1.15 mmol, 10.00 equiv.) was added *via* syringe and the acetone/dry ice bath was removed. The reaction mixture was allowed to stir at room temperature for 3 h and a saturated aqueous solution of NH₄Cl (2.00 mL) was added. The biphasic mixture was extracted with Et₂O (3 × 2.00 mL). The organic layers were combined,

washed with brine, dried over MgSO₄, filtered and concentrated to give alkyne **179** (40 mg, quant.) as a colourless liquid.

TLC: R_f = 0.47 (*n*-pentane:CH₂Cl₂ 95:5)

¹H NMR (400 MHz, Chloroform-*d*): δ 2.27 (2H, dqq, J = 8.8, 6.9, 2.4 Hz, H4), 1.86 (2H, dqd, J = 8.8, 6.9, 3.6 Hz, H8), 1.79 (6H, d, J = 2.4 Hz), 1.57 (2H, dqd, J = 8.8, 6.8, 3.6 Hz, H6), 1.51 (2H, m, H12), 1.44 (2H, m, H10), 1.11 (6H, d, J = 6.9 Hz, H5), 0.80 – 0.67 (24H, m, 8 \times CH₃) ppm

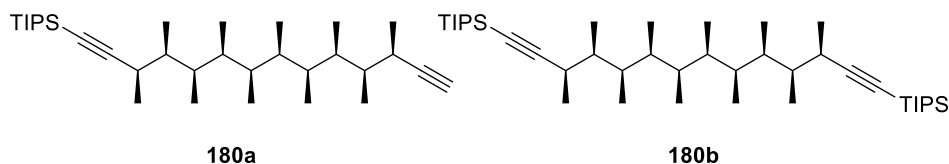
¹³C NMR (101 MHz, Chloroform-*d*): δ 84.2 (C3), 76.1 (C2), 39.2 (C6), 36.8 (C8), 35.5 (C12), 35.4 (C10), 30.0 (C4), 19.0 (C5), 12.0 (CH₃), 11.9 (CH₃), 11.7(4) (CH₃), 11.6(8) (CH₃), 3.7 (C1) ppm

HRMS (m/z): (MALDI⁺) calc'd. for C₂₆H₄₆Na [M+Na]⁺: 381.3492; found 381.3484

IR (ν_{\max}): 2968, 2919, 2878, 1451, 1382, 1309, 1081, 1058, 1022, 936 cm⁻¹

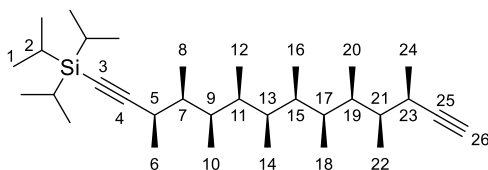
$[\alpha]_D^{20}$: +10 (CHCl₃, c = 1.0)

((**3*R*,4*S*,5*R*,6*S*,7*R*,8*R*,9*S*,10*R*,11*S*,12*R***)-3,4,5,6,7,8,9,10,11,12-Decamethyltetradeca-1,13-diyn-1-yl)triisopropylsilane (**180a**) and ((**3*R*,4*S*,5*R*,6*S*,7*R*,8*R*,9*S*,10*R*,11*S*,12*R***)-3,4,5,6,7,8,9,10,11,12-Decamethyltetradeca-1,13-diyn-1,14-diyl)bis(triisopropylsilane) (**180b**)



In a flame-dried Schlenk tube, alkyne **C10** (94 mg, 0.28 mmol, 1.00 equiv.) was dissolved in anhydrous THF (3.00 mL) at –78 °C under an atmosphere of nitrogen. A solution of *n*-BuLi (1.50 M in *n*-hexane, 0.19 mL, 0.28 mmol, 1.00 equiv.) was added dropwise and the reaction mixture was stirred at the same temperature for 30 min. After the dropwise addition of TIPSCl (0.06 mL, 0.28 mmol, 1.00 equiv.), the acetone/dry ice bath was removed and the reaction mixture was stirred at room temperature for 1 h. A saturated aqueous solution of NH₄Cl (2.00 mL) and water (2.00 mL) were successively added and the biphasic mixture was extracted with Et₂O (3 \times 5.00 mL). The organic layers were combined, washed with brine, dried over MgSO₄, filtered and concentrated. The residue was purified by flash column chromatography (pure *n*-pentane) to give mono-protected alkyne **180a** (61 mg, 44%) and bis-protected **180b** (34 mg, 19%) as colourless liquids.

((3*R*,4*S*,5*R*,6*S*,7*R*,8*R*,9*S*,10*R*,11*S*,12*R*)-3,4,5,6,7,8,9,10,11,12-Decamethyltetradeca-1,13-diyn-1-yl)triisopropylsilane (180a)



TLC: R_f = 0.60 (*n*-pentane:CH₂Cl₂ 90:10)

¹H NMR (500 MHz, Chloroform-*d*): δ 2.41 – 2.28 (2H, m, H5 & H23), 2.05 (1H, d, J = 2.4 Hz, H26), 1.97 (1H, m, H9), 1.88 (1H, m, H19), 1.69 – 1.56 (2H, m, H7 & H21), 1.53 – 1.39 (4H, m, H11, H13, H15 & H17), 1.20 – 1.17 (6H, m, H6 & H24), 1.08 – 1.00 (21H, m, H1 & H2), 0.79 – 0.71 (24H, m, 8 \times CH₃) ppm

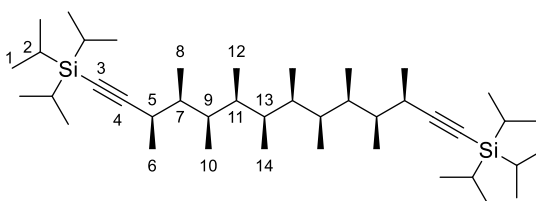
¹³C NMR (126 MHz, Chloroform-*d*): δ 113.5 (C4), 89.2 (C25), 80.7 (C3), 69.0 (C26), 38.6 (C7 or C21), 38.6 (C21 or C7), 37.4 (C9), 37.1 (C19), 35.6 (CH), 35.4 (CH), 35.4 (CH), 35.4 (CH), 31.4 (C5 or C23), 29.9 (C23 or C5), 19.4 (C6 or C24), 18.9 (C24 or C6), 18.8 (C1), 12.0 (CH₃), 12.0 (CH₃), 11.9 (CH₃), 11.9 (CH₃), 11.9 (CH₃), 11.7 (CH₃), 11.6 (CH₃), 11.6 (CH₃), 11.5 (C2) ppm

HRMS (m/z): (MALDI⁺) calc'd. for C₃₃H₆₂NaSi [M+Na]⁺: 509.4513; found 509.4519

IR (ν_{\max}): 3312, 2967, 2940, 2865, 2162, 1453, 1383, 1083, 995, 883 cm⁻¹

$[\alpha]_D^{23}$: +15 (CHCl₃, c = 1.0)

((3*R*,4*S*,5*R*,6*S*,7*R*,8*R*,9*S*,10*R*,11*S*,12*R*)-3,4,5,6,7,8,9,10,11,12-Decamethyltetradeca-1,13-diyne-1,14-diyl)bis(triisopropylsilane) (180b)



TLC: R_f = 0.74 (*n*-pentane:CH₂Cl₂ 90:10)

¹H NMR (500 MHz, Chloroform-*d*): δ 2.35 (2H, dq, J = 9.2, 6.8 Hz, H5), 1.97 (2H, dqd, J = 8.8, 6.8, 3.4 Hz, H9), 1.58 (2H, dqd, J = 9.2, 7.0, 3.4 Hz, H7), 1.50 – 1.39 (4H, m, H11 & H13), 1.19 (6H, d, J = 6.8 Hz, H6), 1.13 – 0.84 (42H, m, H1 & H2), 0.80 – 0.68 (24H, m, H8, H10, H12 & H14) ppm

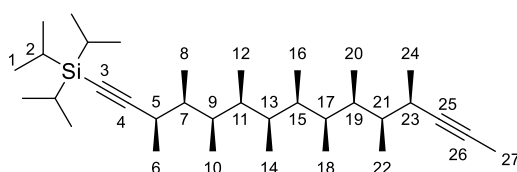
¹³C NMR (126 MHz, Chloroform-*d*): δ 113.5 (C4), 80.7 (C3), 38.5 (C7), 37.5 (C9), 35.5 (C11 or C13), 35.4 (C13 or C11), 31.5 (C5), 19.6 (C6), 18.8 (CH₃), 12.1 (CH₃), 11.9 (CH₃), 11.9 (CH₃), 11.6 (CH₃), 11.5 (CH₃) ppm

HRMS (*m/z*): (MALDI⁺) calc'd. for C₄₂H₈₂Si₂ [M+Na]⁺: 665.5847; found 665.5855

IR (ν_{\max}): 2964, 2941, 2865, 2163, 1461, 1383, 1086, 996, 883 cm⁻¹

[α]_D²³: +13 (CHCl₃, *c* = 1.0)

((3*R*,4*S*,5*R*,6*S*,7*R*,8*R*,9*S*,10*R*,11*S*,12*R*)-3,4,5,6,7,8,9,10,11,12-Decamethylpentadeca-1,13-diyn-1-yl)triisopropylsilane (181**)**



In a flame-dried Schlenk tube, alkyne **180a** (26 mg, 0.05 mmol, 1.00 equiv.) was dissolved in anhydrous THF (0.50 mL) at -78 °C under an atmosphere of nitrogen. A solution of *n*-BuLi (1.50 M in *n*-hexane, 0.07 mL, 0.11 mmol, 2.00 equiv.) was added and the reaction mixture was stirred at the same temperature for 20 min. After the dropwise addition of MeI (0.02 mL, 0.27 mmol, 5.00 equiv.), the acetone/dry ice bath was removed and the reaction was stirred at room temperature for 2 h. A saturated aqueous solution of NH₄Cl (2.00 mL) and water (2.00 mL) were successively added and the biphasic mixture was extracted with Et₂O (3 × 5.00 mL). The organic layers were combined, washed with brine, dried over MgSO₄, filtered and concentrated. The residue was purified by flash column chromatography (pure *n*-pentane) to give alkyne **181** (25 mg, 93%).

TLC: *R*_f = 0.41 (*n*-pentane:CH₂Cl₂ 95:5)

m.p.: 75 – 79 °C (acetonitrile)

¹H NMR (500 MHz, Chloroform-*d*): δ 2.37 (1H, dq, *J* = 9.3, 6.8 Hz, H5), 2.25 (1H, dq, *J* = 9.3, 6.8, 2.3 Hz, H23), 1.96 (1H, m, H9), 1.88 (1H, m, H19), 1.79 (3H, d, *J* = 2.3 Hz, H27), 1.63 – 1.55 (2H, m, H7 & H21), 1.52 – 1.39 (4H, m, H11, H13, H15 & H17), 1.19 (3H, d, *J* = 6.8 Hz, H6), 1.12 (3H, d, *J* = 6.8 Hz, H24), 1.08 – 0.98 (21H, m, H1 & H2), 0.80 – 0.69 (24H, m, 8 × CH₃) ppm

¹³C NMR (126 MHz, Chloroform-*d*): δ 113.6 (C4), 84.2 (C25), 80.6 (C3), 76.1 (C26), 39.1 (C7 or C21), 38.6 (C21 or C7), 37.4 (C9), 37.0 (C19), 35.5 (CH), 35.5 (CH), 35.4 (CH), 35.3 (CH),

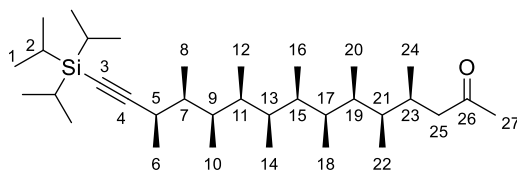
31.4 (C5), 30.1 (C23), 19.4 (C6), 19.2 (C24), 18.8 (C1), 12.0 (CH₃), 12.0 (CH₃), 12.0 (CH₃), 11.9 (CH₃), 11.9 (CH₃), 11.7 (CH₃), 11.7 (CH₃), 11.6 (CH₃), 11.5 (C2), 3.7 (C27) ppm

HRMS (*m/z*): (MALDI⁺) calc'd. for C₃₄H₆₄NaSi [M+Na]⁺: 523.4669; found 523.4661

IR (ν_{\max}): 2967, 2941, 2865, 2162, 1457, 1382, 1260, 1079, 1017, 883, 803 cm⁻¹

[α]_D²⁴: +10 (CHCl₃, *c* = 1.0)

(4*S*,5*R*,6*S*,7*R*,8*S*,9*R*,10*S*,11*R*,12*S*,13*R*)-4,5,6,7,8,9,10,11,12,13-Decamethyl-15-(triisopropylsilyl)pentadec-14-yn-2-one (182)



In a vial were successively charged alkyne **181** (24 mg, 0.05 mmol, 1.00 equiv.), catecholborane (6 μ L, 0.05 mmol, 1.10 equiv.) and a solution of 9-BBN (0.50 M in THF, 10 μ L, 5 μ mol, 0.10 equiv.). The vial was capped and the reaction mixture was stirred at 80 °C for 16 h. The pale-yellow solution was cooled down to 0 °C and diluted with THF (0.30 mL). An aqueous solution of NaOH (2.00 M, 0.20 mL) was added, followed by an aqueous solution of H₂O₂ (30%, 0.10 mL). The biphasic mixture was stirred at 0 °C for 2 h. A saturated aqueous solution of NH₄Cl (1.00 mL) was added and the biphasic mixture was extracted with Et₂O (3 \times 2.00 mL). The organic layers were combined, washed with brine, dried over MgSO₄, filtered and concentrated. The residue was purified by flash column chromatography (*n*-pentane:Et₂O 98:2) to give ketone **182** (13 mg, 52% over 2 steps) as a colourless liquid.

TLC: *R*_f = 0.38 (*n*-pentane:Et₂O 90:10)

¹H NMR (500 MHz, Chloroform-*d*): δ 2.49 (1H, dd, *J* = 15.5, 4.5 Hz, H25), 2.45 (1H, dq, *J* = 7.3, 6.8 Hz, H5), 2.18 (1H, dd, *J* = 15.5, 9.1 Hz, H25'), 2.13 (3H, s, H27), 2.07 (1H, ddqd, *J* = 9.1, 6.8, 6.7, 4.5 Hz, H23), 1.85 (1H, dqd, *J* = 7.1, 6.9, 4.8 Hz, H9), 1.59 (1H, dqd, *J* = 7.3, 6.8, 4.8 Hz, H7), 1.52 – 1.38 (5H, m, 5 \times CH), 1.31 (1H, m), 1.14 (3H, d, *J* = 6.8 Hz, H6), 1.10 – 0.96 (21H, m, H1 & H2), 0.84 – 0.81 (6H, m, H8 & H24), 0.76 – 0.70 (21H, m, 7 \times CH₃) ppm

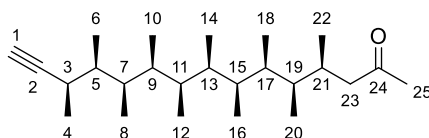
¹³C NMR (126 MHz, Chloroform-*d*): δ 209.5 (C26), 113.8 (C4), 80.4 (C3), 50.0 (C25), 39.0 (C7), 38.5 (CH), 36.7 (C9), 36.4 (CH), 36.0 (CH), 35.7 (CH), 35.5 (CH), 35.4 (CH), 31.4 (C23), 30.7 (C5), 30.6 (C27), 18.8 (C1), 18.3 (C6), 16.6 (C24), 12.2 (CH₃), 12.1(3) (2 \times CH₃), 12.0(9) (CH₃), 11.8(4) (CH₃), 11.8(2) (CH₃), 11.8(0) (CH₃), 11.7 (CH₃), 11.5 (C2) ppm

HRMS (*m/z*): (MALDI⁺) calc'd. for C₃₄H₆₆NaOSi [M+Na]⁺: 541.4775; found 541.4779

IR (ν_{\max}): 2966, 2941, 2866, 2162, 1719, 1460, 1383, 1082, 883, 676 cm^{-1}

$[\alpha]_D^{23}$: +6 (CHCl_3 , $c = 1.0$)

(4*S*,5*R*,6*S*,7*R*,8*S*,9*R*,10*S*,11*R*,12*S*,13*R*)-4,5,6,7,8,9,10,11,12,13-Decamethylpentadec-14-yn-2-one (183)



Alkyne **182** (10 mg, 0.02 mmol, 1.00 equiv.) was deprotected with TBAF (1.00 M in THF, 0.02 mL, 0.02 mmol, 1.10 equiv.) according to **GP5**. The residue was purified by flash column chromatography (*n*-pentane:Et₂O 100:0→95:5) to give ketone **183** (3 mg, 43%) as a colourless liquid.

TLC: $R_f = 0.44$ (*n*-pentane:Et₂O 90:10)

¹H NMR (500 MHz, Chloroform-*d*): δ 2.48 (1H, dd, $J = 15.6, 4.8$ Hz, H23), 2.44 (1H, dqd, $J = 7.0, 6.9, 2.4$ Hz, H3), 2.20 (1H, dd, $J = 15.6, 8.9$ Hz, H23'), 2.13 (3H, s, H25), 2.09 (1H, dqdd, $J = 8.9, 6.8, 5.9, 4.8$ Hz, H21), 2.04 (1H, d, $J = 2.4$ Hz, H1), 1.77 (1H, m, H7), 1.61 (1H, dqd, $J = 7.0, 6.9, 6.3$ Hz, H5), 1.55 – 1.39 (5H, m, 5 \times CH), 1.32 (1H, dqd, $J = 7.0, 6.6, 5.9$ Hz, H19), 1.13 (3H, d, $J = 6.9$ Hz, H4), 0.83 (3H, d, $J = 6.9$ Hz, H6), 0.82 (3H, d, $J = 6.8$ Hz, H22), 0.77 – 0.69 (21H, m, 7 \times CH₃) ppm

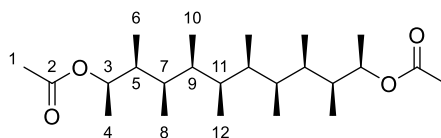
¹³C NMR (126 MHz, Chloroform-*d*): δ 209.5 (C24), 89.5 (C2), 68.7 (C1), 50.0 (C23), 39.2 (C5), 38.6 (C19), 36.3 (CH), 36.2 (CH), 36.0 (CH), 35.7 (CH), 35.5 (CH), 35.4 (CH), 31.1 (C21), 30.6 (C25), 29.0 (C3), 17.5 (C4), 16.2 (C22), 12.1(9) (CH₃), 12.1(5) (CH₃), 12.1 (CH₃), 12.0 (CH₃), 11.8 (CH₃), 11.7(5) (CH₃), 11.7(4) (CH₃), 11.6(9) (CH₃) ppm

HRMS (m/z): (ESI⁺) calc'd. for C₂₅H₄₆NaO [M+Na]⁺: 385.3441; found 385.3446

IR (ν_{\max}): 3311, 2969, 2926, 2879, 1717, 1453, 1383, 1083 cm^{-1}

$[\alpha]_D^{26}$: +13 (CHCl_3 , $c = 1.0$)

(2*R*,3*S*,4*R*,5*S*,6*R*,7*R*,8*S*,9*R*,10*S*,11*R*)-3,4,5,6,7,8,9,10-Octamethyldodecane-2,11-diyl diacetate (184)



In a vial, alcohol **175** (33 mg, 0.10 mmol, 1.00 equiv.) was suspended in anhydrous CH₂Cl₂ (1.00 mL). Acetic anhydride (30 μ L, 0.31 mmol, 3.00 equiv.) was added, followed by triethylamine (43 μ L, 0.31 mmol, 3.00 equiv.) and DMAP (3 mg, 0.02 mmol, 0.20 equiv.). The colourless solution was stirred at room temperature for 4 h. The reaction mixture was diluted with Et₂O (10.00 mL), sequentially washed with an aqueous solution of HCl (0.50 M, 10.00 mL), a saturated aqueous solution of NaHCO₃ (10.00 mL) and brine, dried over MgSO₄, filtered and concentrated. The crude residue was purified by flash column chromatography (*n*-pentane:Et₂O 90:10) to give diacetate **184** (40 mg, quantitative yield) as a colourless liquid.

TLC: *R*_f = 0.30 (*n*-pentane:Et₂O 90:10)

¹H NMR (400 MHz, Toluene-*d*₈): δ 5.00 (2H, dq, *J* = 7.8, 6.3 Hz, H3), 1.83 (2H, dqd, *J* = 7.8, 7.0, 4.2 Hz, H5), 1.73 (6H, s, H1), 1.60 (2H, dqd, *J* = 7.8, 6.7, 4.2 Hz, H7), 1.59 – 1.48 (4H, m, H9 & H11), 1.09 (6H, d, *J* = 6.3 Hz, H4), 0.80 (6H, d, *J* = 6.6 Hz, H10), 0.79 (6H, d, *J* = 6.2 Hz, H12), 0.76 (6H, d, *J* = 6.7 Hz, H8), 0.70 (6H, d, *J* = 7.0 Hz, H6) ppm

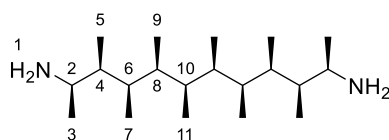
¹³C NMR (101 MHz, Toluene-*d*₈): δ 169.8 (C2), 72.5 (C3), 39.2 (C5), 36.3 (C9 or C11), 36.0 (C11 or C9), 35.6 (C7), 21.2 (C1), 17.8 (C4), 12.4(0) (CH₃), 12.3(6) (CH₃), 12.2 (C10 or C12), 11.0 (C6) ppm

HRMS (*m/z*): (MALDI⁺) calc'd. for C₂₄H₄₆NaO₄ [M+Na]⁺: 421.3288; found 421.3295

IR (ν_{max}): 2972, 2925, 2881, 1732, 1453, 1384, 1241, 1078, 1048, 1021, 946 cm⁻¹

$[\alpha]_D^{22}$: +9 (CHCl₃, *c* = 1.0)

(2*R*,3*S*,4*R*,5*S*,6*R*,7*R*,8*S*,9*R*,10*S*,11*R*)-3,4,5,6,7,8,9,10-Octamethyldodecane-2,11-diamine (185)



Carbamate **187** (50 mg, 0.09 mmol, 1.00 equiv.) was dissolved in a mixture of MeOH and EtOAc (50:50, 4.00 mL) at room temperature under argon atmosphere. Palladium on activated charcoal (10% w/w, 9 mg, 0.01 mmol, 0.10 equiv.) was added and the black suspension was purged with argon for 20 min. The inert atmosphere was purged with hydrogen and the reaction mixture was stirred at room temperature for 4 h. Hydrogen was replaced with argon and the catalyst was removed by filtration over Celite[®]. The filtrate was concentrated to give diamine **185** (23 mg, 81%) as a white solid.

TLC: *R*_f = 0.05 (CH₂Cl₂:MeOH 80:20 + aq. NH₃ 35% [1 drop/10.00 mL])

m.p.: 238 – 245 °C (dichloromethane/methanol)

¹H NMR (500 MHz, Toluene-*d*₈): δ 2.59 (2H, dq, J = 7.9, 6.3 Hz, H2), 1.75 (2H, dqd, J = 8.3, 6.8, 3.7 Hz, H6), 1.63 (2H, m, H10), 1.56 (2H, dqd, J = 8.3, 6.8, 3.3 Hz, H8), 1.35 (2H, dqd, J = 7.9, 6.9, 3.7 Hz, H4), 0.93 (6H, d, J = 6.3 Hz, H3), 0.84 – 0.79 (12H, m, H9 & H11), 0.75 (6H, d, J = 6.8 Hz, H7), 0.74 (6H, d, J = 6.9 Hz, H5) ppm

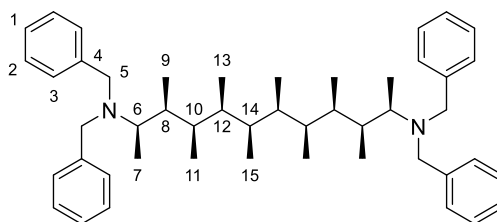
¹³C NMR (126 MHz, Toluene-*d*₈): δ 49.2 (C2), 41.7 (C4), 35.7 (C8 or C10), 35.6 (C10 or C8), 35.4 (C6), 22.2 (C3), 12.2 (CH₃), 11.9(3) (CH₃), 11.8(8) (CH₃), 11.1 (CH₃) ppm

HRMS (m/z): (ESI⁺) calc'd. for C₂₀H₄₅N₂ [M+H]⁺: 313.3577; found 313.3581

IR (ν_{max}): 3457, 3369, 3279, 3176, 2966, 2921, 2878, 1580, 1452, 1382, 1080, 1014, 817 cm⁻¹

$[\alpha]_D^{26}$: –2 (MeOH, c = 1.0)

(2*R*,3*S*,4*R*,5*S*,6*R*,7*R*,8*S*,9*R*,10*S*,11*R*)-*N*²,*N*²,*N*¹¹,*N*¹¹-Tetrabenzyl-3,4,5,6,7,8,9,10-octamethyl-dodecane-2,11-diamine (186**)**



Potassium carbonate (19 mg, 0.14 mmol, 4.00 equiv.) was charged in a flame-dried vial under an atmosphere of nitrogen. A solution of diamine **185** (11 mg, 0.04 mmol, 1.00 equiv.) in anhydrous acetonitrile (0.20 mL) was added, followed by benzyl bromide (17 μ L, 0.14 mmol, 4.00 equiv.). The vial was capped and the white suspension was stirred at 80 °C for 18 h. The reaction mixture was allowed to cool to room temperature, diluted with water (1.00 mL) and extracted with Et₂O (3 \times 1.00 mL). The organic layers were combined, washed with brine, dried over MgSO₄, filtered and concentrated. The residue was purified by flash column chromatography (*n*-pentane:Et₂O 99:1) to give diamine **186** (15 mg, 64%) as a colourless liquid.

TLC: R_f = 0.67 (*n*-pentane:Et₂O 90:10)

¹H NMR (500 MHz, Chloroform-*d*): δ 7.37 (8H, m, H3), 7.29 (8H, m, H2), 7.19 (4H, m, H1), 3.73 (4H, d, J = 13.6 Hz, H5), 3.26 (4H, d, J = 13.6 Hz, H5'), 2.48 (2H, dq, J = 10.0, 6.5 Hz, H6), 2.04 (2H, dqd, J = 9.9, 6.8, 2.4 Hz, H10), 1.73 (2H, dqd, J = 10.0, 6.8, 2.4 Hz, H8), 1.42 – 1.33 (4H, m, H12 & H14), 1.01 (6H, d, J = 6.5 Hz, H7), 0.63 (6H, d, J = 6.8 Hz, H13), 0.57 (6H, d, J = 6.8 Hz, H9), 0.56 (6H, m, H15), 0.22 (6H, d, J = 6.8 Hz, H11) ppm

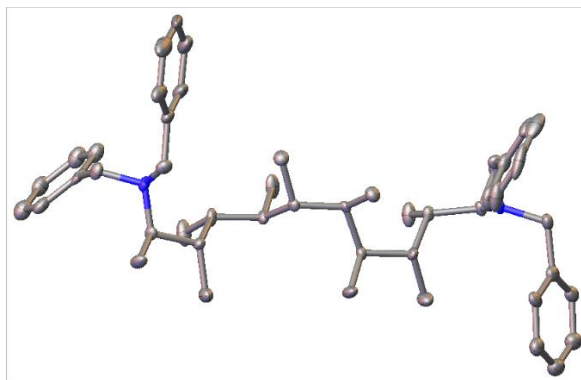
^{13}C NMR (126 MHz, Chloroform-*d*): δ 140.5 (C4), 129.2 (C3), 128.1 (C2), 126.8 (C1), 54.8 (C6), 53.7 (C5), 36.5 (C8), 36.0 (C12 or C14), 35.4 (C14 or C12), 34.4 (C10), 12.5 (C9 or C15), 12.2 (C13), 11.7 (C11), 11.6 (C15 or C9), 9.9 (C7) ppm

HRMS (*m/z*): (MALDI⁺) calc'd. for $\text{C}_{48}\text{H}_{68}\text{N}_2\text{Na}$ [$\text{M}+\text{Na}$]⁺: 695.5275; found 695.5282

IR (ν_{max}): 3085, 3063, 3027, 2968, 2929, 2876, 2801, 1945, 1873, 1801, 1740, 1603, 1494, 1453, 1381, 1028, 744, 730, 697 cm^{-1}

$[\alpha]_D^{24}$: +11 (CHCl_3 , $c = 1.0$)

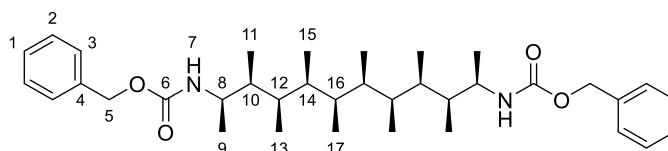
X-ray: Absolute configuration not determined. Occupancies of the disordered phenyl groups refined with their sum set to equal 1. Restraints and constraints were applied to maintain sensible thermal and geometric parameters. The disordered diethyl ether occupancies were necessarily fixed at 0.5 as the disorder was across a symmetry element. Restraints and constraints were applied to maintain sensible thermal and geometric parameters.



Identification code	186
Empirical formula	$\text{C}_{52}\text{H}_{78}\text{N}_2\text{O}$
Formula weight	747.16
Temperature/K	100(2)
Crystal system	orthorhombic
Space group	$\text{P2}_1\text{2}_1\text{2}$
$a/\text{\AA}$	13.2858(3)
$b/\text{\AA}$	16.2747(4)
$c/\text{\AA}$	10.7159(3)
$\alpha/^\circ$	90
$\beta/^\circ$	90
$\gamma/^\circ$	90
Volume/ \AA^3	2317.02(10)
Z	2
$\rho_{\text{calc}}/\text{g cm}^{-3}$	1.071
μ/mm^{-1}	0.062
$F(000)$	824.0
Crystal size/ mm^3	$0.557 \times 0.295 \times 0.251$

Radiation	MoK α (λ = 0.71073)
2 θ range for data collection/ $^{\circ}$	3.8 to 52.742
Index ranges	-16 \leq h \leq 16, -20 \leq k \leq 20, -13 \leq l \leq 13
Reflections collected	38291
Independent reflections	4758 [R_{int} = 0.0668, R_{sigma} = 0.0409]
Data/restraints/parameters	4758/242/309
Goodness-of-fit on F^2	1.223
Final R indexes [$I \geq 2\sigma(I)$]	R_1 = 0.0782, wR_2 = 0.1619
Final R indexes [all data]	R_1 = 0.0829, wR_2 = 0.1640
Largest diff. peak/hole / e \AA^{-3}	0.26/-0.26

Dibenzyl ((2*R*,3*S*,4*R*,5*S*,6*R*,7*R*,8*S*,9*R*,10*S*,11*R*)-3,4,5,6,7,8,9,10-octamethyldodecane-2,11-diyl)dicarbamate (187**)**



Part A: In a flame-dried vial, potassium *tert*-butoxide (185 mg, 1.65 mmol, 11.00 equiv.) was dried under high vacuum at 100 $^{\circ}\text{C}$ for 4 h. The solid was allowed to cool to room temperature under argon atmosphere and a mixed solution of boronic ester **154** (80 mg, 0.15 mmol, 1.00 equiv.) and freshly distilled methoxyamine (93 μL , 1.80 mmol, 12.00 equiv.) in anhydrous toluene (1.00 mL) was added. The vial was capped and the white suspension was stirred at 105 $^{\circ}\text{C}$ for 24 h. The reaction mixture was allowed to cool to room temperature before an aqueous solution of NaOH (3.00 M, 2.00 mL) was added. The biphasic mixture was vigorously stirred for 30 min at room temperature and Na_2SO_4 (614 mg) was added. The white suspension was stirred for 30 min, layers were separated and the aqueous phase was extracted with EtOAc (5 \times 2.00 mL). The organic layers were combined, sequentially washed with an aqueous solution of NaOH (3.00 M, 5.00 mL) and with brine, dried over MgSO_4 , filtered and concentrated. **Part B:** The crude residue was dissolved in anhydrous THF (0.50 mL) at 0 $^{\circ}\text{C}$ under an atmosphere of nitrogen. Diisopropylethylamine (0.105 mL, 0.60 mmol, 4.00 equiv.) was added, followed by benzyl chloroformate (44 μL , 0.32 mmol, 2.10 equiv.). The ice bath was removed and the suspension was stirred at room temperature for 18 h. The reaction mixture was diluted with a saturated aqueous solution of NH_4Cl (2.00 mL) and extracted with Et_2O (3 \times 2.00 mL). The organic layers were combined, washed with brine, dried over MgSO_4 , filtered and concentrated. The residue was purified by flash column chromatography (*n*-pentane: Et_2O 90:10 \rightarrow 80:20) to give carbamate **187** (54 mg, 62% over 2 steps) as a colourless liquid.

TLC: R_f = 0.17 (*n*-pentane:Et₂O 70:30)

¹H NMR (500 MHz, Toluene-*d*₈): δ 7.23 (4H, m, H3), 7.12 (4H, m, H2), 7.06 (2H, m, H1), 5.08 (2H, d, J = 12.4 Hz, H5), 5.02 (2H, d, J = 12.4 Hz, H5'), 4.25 (2H, *app.* d, $J^{app.}$ = 8.8 Hz, H7), 3.82 (2H, *app.* pent, $J^{app.}$ = 7.1 Hz, H8), 1.61 – 1.40 (8H, m, 8 \times CH), 0.86 – 0.79 (12H, m, 4 \times CH₃), 0.79 – 0.70 (12H, m, 4 \times CH₃), 0.60 (6H, d, J = 6.3 Hz, CH₃) ppm

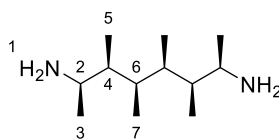
¹³C NMR (126 MHz, Toluene-*d*₈): δ 155.6 (C6), 137.7 (C4), 128.5(3) (C2 or C3), 128.4(8) (C3 or C2), 128.0 (C1), 66.4 (C5), 48.7 (C8), 39.9 (CH), 35.9 (CH), 35.8 (CH), 35.6 (CH), 17.0 (CH₃), 12.1 (CH₃), 12.0 (CH₃), 11.9 (CH₃), 11.3 (CH₃) ppm

HRMS (m/z): (MALDI⁺) calc'd. for C₃₆H₅₆N₂NaO₄ [M+Na]⁺: 603.4138; found 603.4132

IR (ν_{max}): 3332, 3066, 3033, 2970, 2939, 2879, 2479, 1693, 1532, 1452, 1420, 1383, 1327, 1237, 1072, 733, 696 cm⁻¹

$[\alpha]_D^{25}$: +1 (MeOH, c = 1.0)

(2*R*,3*S*,4*R*,5*R*,6*S*,7*R*)-3,4,5,6-Tetramethyloctane-2,7-diamine (188)



Carbamate **190** (66 mg, 0.14 mmol, 1.00 equiv.) was dissolved in a mixture of MeOH and EtOAc (50:50, 4.00 mL) at room temperature under argon atmosphere. Palladium on activated charcoal (10% w/w, 15 mg, 0.01 mmol, 0.10 equiv.) was added and the black suspension was purged with argon for 20 min. The inert atmosphere was purged with hydrogen and the reaction mixture was stirred at room temperature for 4 h. Hydrogen was replaced with argon and the catalyst was removed by filtration over Celite®. The filtrate was concentrated to give diamine **188** (22 mg, 78%) as a colourless wax.

TLC: R_f = 0.05 (CH₂Cl₂:MeOH 80:20 + aq. NH₃ 35% [1 drop/10.00 mL])

¹H NMR (500 MHz, Toluene-*d*₈): δ 2.58 (2H, dq, J = 8.0, 6.3 Hz, H2), 1.64 (2H, m, H6), 1.28 (2H, dqd, J = 8.0, 6.9, 3.4 Hz, H4), 0.91 (6H, d, J = 6.3 Hz, H3), 0.73 (6H, m, H7), 0.71 (6H, d, J = 6.9 Hz, H5) ppm

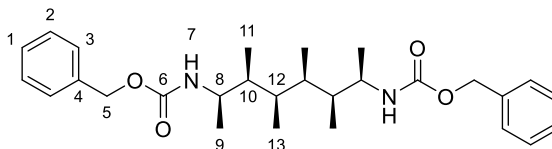
¹³C NMR (126 MHz, Toluene-*d*₈): δ 49.0 (C2), 41.6 (C4), 35.2 (C6), 22.1 (C3), 11.8 (C7), 10.8 (C5) ppm

HRMS (m/z): (ESI⁺) calc'd. for C₁₂H₂₉N₂ [M+H]⁺: 201.2325; found 201.2332

IR (ν_{max}): 3315, 2968, 2923, 2879, 2585, 2157, 1663, 1574, 1447, 1380, 1307, 1081, 817 cm⁻¹

$[\alpha]_D^{26}$: -6 (MeOH, $c = 1.0$)

Dibenzyl ((2*R*,3*S*,4*R*,5*R*,6*S*,7*R*)-3,4,5,6-tetramethyloctane-2,7-diyl)dicarbamate (190**)**



Part A: In a flame-dried vial, potassium *tert*-butoxide (293 mg, 2.61 mmol, 11.00 equiv.) was dried under high vacuum at 100 °C for 4 h. The solid was allowed to cool to room temperature under argon atmosphere and a mixed solution of boronic ester **152** (100 mg, 0.24 mmol, 1.00 equiv.) and freshly distilled methoxyamine (0.15 mL, 2.84 mmol, 12.00 equiv.) in anhydrous toluene (2.00 mL) was added. The vial was capped and the white suspension was stirred at 105 °C for 24 h. The reaction mixture was allowed to cool to room temperature before an aqueous solution of NaOH (3.00 M, 2.00 mL) was added. The biphasic mixture was vigorously stirred for 30 min at room temperature and Na₂SO₄ (614 mg) was added. The white suspension was stirred for 30 min, layers were separated and the aqueous phase was extracted with EtOAc (5 × 2.00 mL). The organic layers were combined, sequentially washed with an aqueous solution of NaOH (3.00 M, 5.00 mL) and brine, dried over MgSO₄, filtered and concentrated. **Part B:** The crude residue was dissolved in anhydrous THF (2.00 mL) and the solution was transferred to a flame-dried vial under an atmosphere of nitrogen. Diisopropylethylamine (0.17 mL, 0.96 mmol, 4.00 equiv.) was added, followed by benzyl chloroformate (0.07 mL, 0.50 mmol, 2.10 equiv.). After the addition, the suspension was stirred at room temperature for 18 h. The reaction mixture was diluted with a saturated aqueous solution of NH₄Cl (2.00 mL) and extracted with Et₂O (3 × 2.00 mL). The organic layers were combined, washed with brine, dried over MgSO₄, filtered and concentrated. The crude residue was purified by flash column chromatography (*n*-pentane:Et₂O 100:0→60:40) to give carbamate **190** (66 mg, 59% over 2 steps) as a colourless liquid.

TLC: $R_f = 0.15$ (*n*-pentane:Et₂O 70:30)

¹H NMR (500 MHz, Chloroform-*d*): δ 7.42 – 7.29 (10H, m, H1, H2 & H3), 5.11 (2H, d, $J = 12.2$ Hz, H5), 5.05 (2H, d, $J = 12.2$ Hz, H5'), 4.49 (2H, m, H7), 3.71 (2H, m, H8), 1.56 (2H, m, H10), 1.48 (2H, m, H12), 1.05 (6H, d, $J = 6.7$ Hz, H9), 0.84 (6H, m, H13), 0.76 (6H, d, $J = 6.9$ Hz, H11) ppm

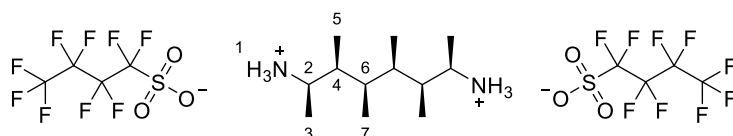
¹³C NMR (126 MHz, Chloroform-*d*): δ 155.8 (C6), 136.8 (C4), 128.7 (CH_{Ar}), 128.3 (2 × CH_{Ar}), 66.7 (C5), 48.6 (C8), 39.3 (C10), 35.6 (C12), 17.0 (C9), 11.7 (C13), 11.4 (C11) ppm

HRMS (m/z): (MALDI⁺) calc'd. for C₂₈H₄₀N₂NaO₄ [M+Na]⁺: 491.2880; found 491.2889

IR (ν_{max}): 3426, 3325, 3063, 3034, 2973, 2880, 1696, 1532, 1454, 1337, 1239, 1070, 697 cm^{-1}

$[\alpha]_D^{24}$: -7 (CHCl_3 , $c = 1.0$)

(2*R*,3*S*,4*R*,5*R*,6*S*,7*R*)-3,4,5,6-Tetramethyloctane-2,7-diaminium 1,1,2,2,3,3,4,4,4-nonafluorobutane-1-sulfonate (191)



Diamine **188** (2 mg, 0.01 mmol, 1.00 equiv.) was dissolved in methanol- d_4 in an NMR tube. Nonfluorobutanesulfonic acid (3 μL , 0.02 mmol, 2.00 equiv.) was added, the tube was capped and vigorously shaken to give **191** as a solution in methanol- d_4 .

^1H NMR (500 MHz, Methanol- d_4) δ 3.25 (2H, qd, $J = 6.6, 6.3$ Hz, H2), 1.71 (2H, qdd, $J = 6.9, 6.3, 5.0$ Hz, H4), 1.52 (2H, m, H6), 1.19 (6H, d, $J = 6.6$ Hz, H3), 0.88 (6H, d, $J = 6.9$ Hz, H5), 0.86 (6H, m, H7) ppm

^{13}C NMR (126 MHz, Methanol- d_4) δ 50.3 (C2), 39.8 (C4), 36.4 (C6), 16.1 (C3), 11.7 (C7), 10.7 (C5) ppm

3.3. Supplementary materials – Chapter 2

3.3.1. General procedures

General procedure 6 (GP6): In a round-bottomed flask, *N*-hydroxyphthalimide (1.0 or 2.00 equiv.) or tetrachloro-*N*-hydroxyphthalimide (1.00 equiv.) or methyl-substituted *N*-hydroxyphthalimide **369** (1.00 equiv.) was suspended in ethanol-free CH_2Cl_2 (0.10 M) at room temperature. Carboxylic acid (1.00 equiv.) was added, followed by diisopropylcarbodiimide (DIC) (1.0 or 2.00 equiv.) and dimethylaminopyridine (DMAP) (0.00–0.40 equiv.). The reaction mixture was stirred at room temperature for 16 h. The white suspension was concentrated under reduced pressure and the crude residue was purified by flash column chromatography and/or recrystallisation to give the desired product.

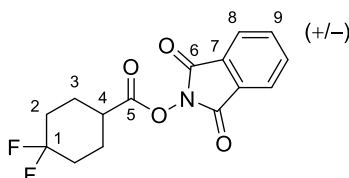
General procedure 7 (GP7): In a round-bottomed flask, *N*-hydroxyphthalimide (1.00 equiv.) and carboxylic acid (1.00 equiv.) were suspended in THF (0.40 M) at room temperature. A solution of dicyclohexylcarbodiimide (DCC) (1.00 equiv.) in THF (0.40 M) was added and the reaction mixture was stirred at room temperature for 48 h. The white suspension stored at -20 $^\circ\text{C}$ for

1 h and the white solid was removed by filtration. The filtrate was concentrated under reduced pressure and the crude residue was purified by flash column chromatography and/or recrystallisation to give the desired product.

General procedure 8 (GP8): Activated ester (1.00 equiv.) and B₂cat₂ (1.25 or 2.50 equiv.) were carefully weighed into a flame-dried 7-mL vial containing a small magnetic stirrer bar. DMAc (0.10 M) was added and the headspace of the vial was purged with a gentle stream of argon for approximately 10 seconds. The vial was tightly sealed and stirred under blue LED irradiation for 14 h. Pinacol (4.0 or 8.00 equiv.) was added, followed by Et₃N (0.45 mL) and the reaction mixture was stirred for 1 h. The reaction mixture was transferred into a vial containing EtOAc (15 mL), water (3.00 mL) and a saturated aqueous solution of NH₄Cl (3.00 mL). After vigorously shaking and allowing the two layers to separate, the top organic layer was carefully removed with a pipette. This was repeated twice more with EtOAc (5.00 mL). The organic layers were combined and concentrated under reduced pressure. The crude residue was directly purified using a short silica gel column to yield the desired boronic ester.

3.3.2. Experimental procedures and characterisation data

1,3-Dioxoisindolin-2-yl 4,4-difluorocyclohexane-1-carboxylate (**305**)



Carboxylic acid **304** (250 mg, 1.52 mmol, 1.00 equiv.) was activated with *N*-hydroxyphthalimide (248 mg, 1.52 mmol, 1.00 equiv.), DIC (0.24 mL, 1.52 mmol, 1.00 equiv.) and DMAP (18 mg, 0.15 mmol, 0.10 equiv.) according to **GP6**. The crude residue was purified by flash column chromatography (*n*-pentane:Et₂O 75:25) to give activated ester **305** (417 mg, 89%) as a white solid.

TLC: *R*_f = 0.19 (*n*-pentane:EtOAc 90:10)

m.p.: 109 – 112 °C (dichloromethane/methanol)

¹H NMR: (400 MHz, Chloroform-*d*) δ 7.89 (2H, m, H8 or H9), 7.80 (2H, m, H9 or H8), 2.89 (1H, m, H4), 2.26 – 2.04 (6H, m, 2 × CH^aH^b & 2 × CH₂), 1.97 – 1.84 (2H, m, 2 × CH^aH^b) ppm

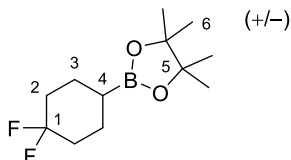
¹³C NMR: (126 MHz, Chloroform-*d*) δ 170.6 (C5), 162.0 (C6), 135.0 (C8 or C9), 129.0 (C7), 124.1 (C9 or C8), 122.3 (t, *J* = 241.3 Hz, C1), 37.9 (C4), 32.2 (t, *J* = 24.8 Hz, C2), 25.1 (t, *J* = 5.1 Hz, C3) ppm

¹⁹F NMR: (377 MHz, Chloroform-*d*) δ -95.6 (*app.* d, $J^{app.} = 239.8$ Hz), -98.4 (*app.* d, $J^{app.} = 239.8$ Hz) ppm

HRMS (*m/z*): (ESI⁺) calc'd for C₁₅H₁₃F₂NNaO₄ [M+Na]⁺: 332.0705; found: 332.0708

IR (ν_{max}): 2973, 2948, 1809, 1782, 1740, 1374, 1360, 1147, 1114, 1115, 1079, 981, 947 cm⁻¹

2-(4,4-Difluorocyclohexyl)-4,4,5,5-tetramethyl-1,3,2-dioxaborolane (306)



Activated ester **305** (40 mg, 0.13 mmol, 1.00 equiv.) was borylated with B₂cat₂ (40 mg, 0.16 mmol, 1.25 equiv.), and pinacol (63 mg, 0.53 mmol, 4.00 equiv.) according to **GP8**. The crude residue was purified by flash column chromatography (*n*-pentane:Et₂O 95:5) to give boronic ester **306** (21 mg, 66%) as a colourless liquid.

TLC: *R*_f = 0.51 (*n*-pentane:Et₂O 85:15)

¹H NMR: (400 MHz, Chloroform-*d*) δ 1.99 (2H, m, 2 × CH^aH^b), 1.85 – 1.52 (6H, m, 2 × CH^aH^b & 2 × CH₂), 1.23 (12H, s, H₆), 0.97 (1H, m, H₄) ppm

¹³C NMR: (101 MHz, Chloroform-*d*) δ 123.9 (t, $J = 240.5$ Hz, C₁), 83.4 (C₅), 34.5 (t, $J = 23.2$ Hz, C₂), 24.9 (C₆), 24.4 (m, C₃) ppm

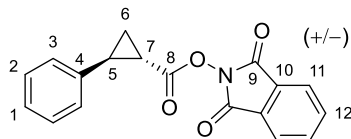
The signal corresponding to C₄ was not observed due to quadrupolar relaxation.

¹⁹F NMR: (377 MHz, Chloroform-*d*) δ -91.6 (*app.* d, $J^{app.} = 234.0$ Hz), -98.7 (*app.* d, $J^{app.} = 234.0$ Hz) ppm

HRMS (*m/z*): *Despite repeated attempts, a HRMS could not be obtained.*

IR (ν_{max}): 2878, 2938, 2870, 1414, 1388, 1369, 1320, 1145, 1108, 1093, 958, 852 cm⁻¹

1,3-Dioxoisindolin-2-yl *trans*-2-phenylcyclopropane-1-carboxylate (308)



Carboxylic acid **307** (1.00 g, 6.17 mmol, 1.00 equiv.) was activated with *N*-hydroxyphthalimide (1.01 g, 6.17 mmol, 1.00 equiv.), DIC (0.95 mL, 6.17 mmol, 1.00 equiv.) and DMAP (75 mg,

0.62 mmol, 0.10 equiv.) according to **GP6**. The crude residue was purified by flash column chromatography (*n*-pentane:Et₂O 80:20→60:40) to give activated ester **308** (1.55 g, 82%) as a white solid.

TLC: *R*_f = 0.34 (*n*-pentane:Et₂O 70:30)

m.p.: 116 – 119 °C (diethyl ether)

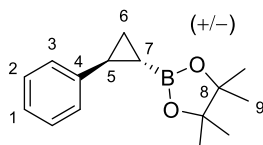
¹H NMR: (400 MHz, Chloroform-*d*) δ 7.90 (2H, m, H11 or H12), 7.79 (2H, m, H12 or H11), 7.34 (2H, m, H2 or H3), 7.27 (1H, m, H1), 7.28 (2H, m, H3 or H2), 2.79 (1H, ddd, *J* = 9.1, 6.9, 4.0 Hz, H5), 2.23 (1H, ddd, *J* = 8.4, 5.2, 4.0 Hz, H7), 1.83 (1H, ddd, *J* = 9.1, 5.2, 4.9 Hz, H6), 1.64 (1H, ddd, *J* = 8.4, 6.9, 4.9 Hz, H6') ppm

¹³C NMR: (101 MHz, Chloroform-*d*) δ 169.8 (C8), 162.1 (C9), 138.6 (C4), 134.8 (C11 or C12), 129.1 (C10), 128.8 (C2 or C3), 127.3 (C1), 126.5 (C3 or C2), 124.1 (C12 or C11), 28.4 (C5), 21.1 (C7), 18.6 (C6) ppm

HRMS (*m/z*): (ESI⁺) calc'd for C₁₈H₁₃NNaO₄ [M+Na]⁺: 330.0737; found: 330.0748

IR (*ν*_{max}): 3518, 3065, 3031, 1806, 1778, 1738, 1401, 1360, 1186, 1100, 1072, 878, 757 cm⁻¹

4,4,5,5-Tetramethyl-2-(*trans*-2-phenylcyclopropyl)-1,3,2-dioxaborolane (**309**)



Activated ester **308** (40 mg, 0.13 mmol, 1.00 equiv.) was borylated with B₂cat₂ (40 mg, 0.16 mmol, 1.25 equiv.), and pinacol (63 mg, 0.53 mmol, 4.00 equiv.) according to **GP8**. The crude residue was purified by flash column chromatography (*n*-pentane:Et₂O 95:5) to give boronic ester **309** (19 mg, 60%, 98:2 *d.r.*) as a colourless liquid.

TLC: *R*_f = 0.35 (*n*-pentane:Et₂O 95:5)

¹H NMR: (400 MHz, Chloroform-*d*) δ 7.24 (2H, m, H2 or H3), 7.14 (1H, m, H1), 7.08 (2H, m, H3 or H2), 2.11 (1H, ddd, *J* = 8.1, 5.5, 5.2 Hz, H5), 1.26 (6H, s, H9), 1.24 (6H, s, H9'), 1.16 (1H, ddd, *J* = 8.1, 6.8, 3.7 Hz, H6), 1.01 (1H, ddd, *J* = 9.5, 5.2, 3.7 Hz, H6'), 0.31 (1H, ddd, *J* = 9.5, 6.8, 5.5 Hz, H7) ppm

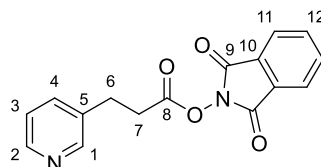
¹³C NMR: (101 MHz, Chloroform-*d*) δ 143.5 (C4), 128.4 (C2 or C3), 125.8 (C3 or C2), 125.7 (C1), 83.3 (C8), 24.9 (C9), 24.8 (C9'), 22.0 (C5), 15.2 (C6) ppm

The signal corresponding to C7 was not observed due to quadrupolar relaxation.

HRMS (*m/z*): (EI⁺) calc'd for C₁₅H₂₁BO₂ [M]⁺: 244.1635; found: 244.1634

IR (ν_{max}): 3518, 3065, 3031, 1806, 1778, 1738, 1467, 1401, 1360, 1186, 1100, 1072, 878 cm^{-1}

1,3-Dioxoisindolin-2-yl 3-(pyridin-3-yl)propanoate (311)



Carboxylic acid **310** (500 mg, 3.31 mmol, 1.00 equiv.) was activated with *N*-hydroxyphthalimide (540 mg, 3.31 mmol, 1.00 equiv.) and DCC (682 mg, 3.31 mmol, 1.00 equiv.) according to **GP7**. The crude residue was purified by recrystallisation from EtOAc to afford activated ester **311** (447 mg, 46%) as a pale yellow solid.

TLC: R_f = 0.21 (*n*-pentane:acetone 30:70)

m.p.: 111 – 115 °C (ethyl acetate)

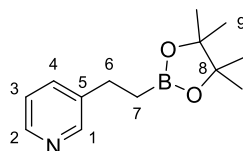
^1H NMR: (400 MHz, Chloroform-*d*) δ 8.54 (1H, d, J = 2.3 Hz, H1), 8.50 (1H, dd, J = 4.9, 1.6 Hz, H2), 7.87 (2H, m, H11 or H12), 7.78 (2H, m, H12 or H11), 7.60 (1H, ddd, J = 7.8, 2.3, 1.6 Hz, H4), 7.26 (1H, dd, J = 7.8, 4.9 Hz, H3), 3.11 (2H, t, J = 7.4 Hz, H6), 2.99 (2H, t, J = 7.4 Hz, H7) ppm

^{13}C NMR: (101 MHz, Chloroform-*d*) δ 168.6 (C8), 161.9 (C9), 149.9 (C1), 148.4 (C2), 136.0 (C4), 134.9 (C11 or C12), 134.6 (C5), 129.0 (C10), 124.1 (C12 or C11), 123.7 (C3), 32.4 (C7), 27.9 (C6) ppm

HRMS (m/z): (ESI⁺) calc'd for $\text{C}_{16}\text{H}_{12}\text{N}_2\text{NaO}_4$ [$\text{M}+\text{Na}$]⁺: 319.0689; found: 319.0692

IR (ν_{max}): 3055, 2943, 2324 (br.), 1812, 1783, 1741, 1714, 1188, 1135, 1079, 970, 876 cm^{-1}

3-(2-(4,4,5,5-Tetramethyl-1,3,2-dioxaborolan-2-yl)ethyl)pyridine (312)



Activated ester **311** (77 mg, 0.26 mmol, 1.00 equiv.) was borylated with B_2cat_2 (40 mg, 0.16 mmol, 1.25 equiv.), and pinacol (63 mg, 0.53 mmol, 4.00 equiv.) according to **GP8**. The crude residue was purified by flash column chromatography (*n*-hexane:acetone 90:10) to give boronic ester **312** (10 mg, 16%) as a colourless liquid.

TLC: R_f = 0.54 (*n*-pentane:acetone 80:20)

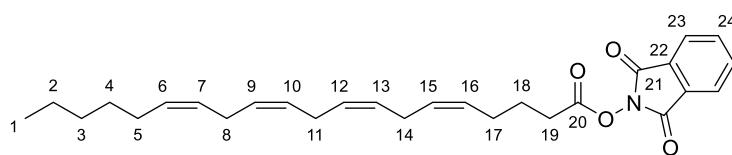
¹H NMR: (500 MHz, Chloroform-*d*) δ 8.48 (1H, *app.* br. s, H1), 8.41 (1H, *app.* d, $J^{app.} = 4.8$ Hz, H2), 7.52 (1H, *app.* d, $J^{app.} = 7.7$ Hz, H4), 7.18 (1H, dd, $J = 7.7, 4.8$ Hz, H3), 2.74 (2H, t, $J = 8.0$ Hz, H6), 1.21 (12H, s, H9 & H9'), 1.14 (2H, t, $J = 8.0$ Hz, H7) ppm

¹³C NMR: (101 MHz, Chloroform-*d*) δ 149.9 (C1), 147.2 (C2), 139.6 (C5), 135.6 (C4), 123.3 (C3), 83.4 (C8), 29.8 (C7), 27.3 (C6), 24.9 (C9) ppm

HRMS (m/z): (ESI⁺) calc'd for C₁₃H₂₀BNNaO₂ [M+Na]⁺: 256.1482; found: 256.1480

IR (ν_{max}): 2978, 2929, 1575, 1479, 1422, 1372, 1311, 1144, 968, 849, 714 cm⁻¹

1,3-Dioxoisindolin-2-yl (5Z,8Z,11Z,14Z)-icosa-5,8,11,14-tetraenoate (314)



Carboxylic acid **313** (100 mg, 0.33 mmol, 1.00 equiv.) was activated with *N*-hydroxyphthalimide (54 mg, 0.33 mmol, 1.00 equiv.), DIC (0.05 mL, 0.33 mmol, 1.00 equiv.) and DMAP (4 mg, 0.03 mmol, 0.10 equiv.) according to **GP6**. The crude residue was purified by flash column chromatography (*n*-pentane:Et₂O 90:10) to give activated ester **314** (110 mg, 74%) as a colourless liquid.

TLC: $R_f = 0.15$ (*n*-pentane:Et₂O 90:10)

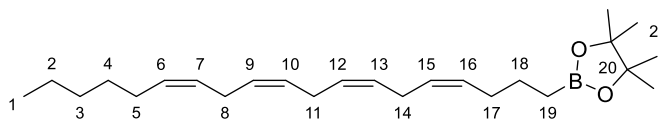
¹H NMR: (400 MHz, Chloroform-*d*) δ 7.88 (2H, m, H23 or H24), 7.78 (2H, m, H24 or H23), 5.50 – 5.29 (8H, m, 8 \times CH), 2.87 – 2.80 (6H, m, H8, H11 & H14), 2.68 (2H, t, $J = 7.4$ Hz, H19), 2.24 (2H, td, $J = 7.3, 7.1$ Hz, H17), 2.05 (2H, td, $J = 7.0, 6.9$ Hz, H5), 1.87 (2H, tt, $J = 7.4, 7.3$ Hz, H18), 1.40 – 1.22 (6H, m, H2, H3 & H4), 0.88 (3H, t, $J = 6.8$ Hz, H1) ppm

¹³C NMR: (101 MHz, Chloroform-*d*) δ 169.6 (C20), 162.0 (C21), 134.8 (C23 or C24), 130.6 (CH), 129.8 (CH), 129.1 (C22), 128.7 (CH), 128.5 (CH), 128.3 (CH), 128.2 (CH), 128.0 (CH), 127.7 (CH), 124.1 (C24 or C23), 31.6 (CH₂), 30.5 (C19), 29.5 (CH₂), 27.3 (C5), 26.3 (C17), 25.8 (C8, C11 & C14), 24.7 (C18), 22.7 (CH₂), 14.2 (C1) ppm

HRMS (m/z): (ESI⁺) calc'd for C₂₈H₃₅NNaO₄ [M+Na]⁺: 472.2458; found: 472.2460

IR (ν_{max}): 3525, 3012, 2927, 2856, 1816, 1789, 1743, 1467, 1367, 1185, 1081, 969, 878 cm⁻¹

4,4,5,5-Tetramethyl-2-((4Z,7Z,10Z,13Z)-nonadeca-4,7,10,13-tetraen-1-yl)-1,3,2-dioxaborolane (315)



Activated ester **314** (58 mg, 0.13 mmol, 1.00 equiv.) was borylated with B_2cat_2 (40 mg, 0.16 mmol, 1.25 equiv.), and pinacol (63 mg, 0.53 mmol, 4.00 equiv.) according to **GP8**. The crude residue was purified by flash column chromatography (*n*-pentane:Et₂O 95:5) to give boronic ester **315** (29 mg, 58%) as a colourless liquid.

TLC: R_f = 0.50 (*n*-pentane:Et₂O 95:5)

¹H NMR: (400 MHz, Chloroform-*d*) δ 5.48 – 5.24 (8H, m, 8 \times CH), 2.92 – 2.73 (6H, m, H8, H11 & H14), 2.06 (4H, *app.* q, $J^{app.}$ = 7.0 Hz, H5 & H17), 1.48 (2H, tt, J = 7.8, 7.7 Hz, H18), 1.41 – 1.27 (6H, m, H2, H3 & H4), 1.24 (12H, s, H21), 0.89 (3H, t, J = 6.8 Hz, H1), 0.80 (2H, t, J = 7.9 Hz, H19) ppm

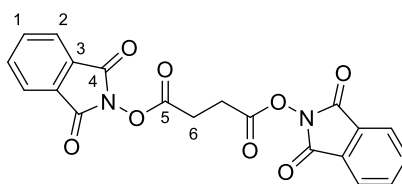
¹³C NMR: (101 MHz, Chloroform-*d*) δ 130.5 (CH), 130.2 (CH), 128.6 (CH), 128.5 (CH), 128.0 (CH), 128.0 (CH), 127.9 (CH), 127.6 (CH), 82.9 (C20), 31.5 (CH₂), 29.8 (C5 or C17), 29.3 (CH₂), 27.2 (C17 or C5), 25.6 (C8, C11 & C14), 24.8 (C21), 24.1 (C18), 22.6 (CH₂), 14.1 (C1) ppm

The signal corresponding to C19 was not observed due to quadrupolar relaxation.

HRMS (m/z): (EI⁺) calc'd for C₂₅H₄₃BO₂ [M]⁺: 386.3356; found: 386.3338

IR (ν_{max}): 3012, 2977, 2958, 2927, 2858, 1459, 1371, 1316, 969, 846 cm⁻¹

Bis(1,3-dioxoisindolin-2-yl) succinate (317)



Succinic acid **316** (500 mg, 4.23 mmol, 1.00 equiv.) was activated with *N*-hydroxyphthalimide (1.38 g, 8.46 mmol, 2.00 equiv.), DIC (2.64 mL, 8.46 mmol, 2.00 equiv.) and DMAP (102 mg, 0.84 mmol, 0.20 equiv.) according to **GP6**. The crude residue was purified by flash column chromatography (CH₂Cl₂:Et₂O 98:2) to give activated ester **317** (1.02 g, 59%) as a colourless wax.

TLC: R_f = 0.21 (CH₂Cl₂:Et₂O 98:2)

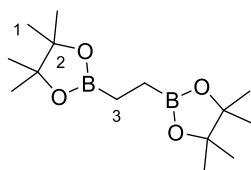
¹H NMR: (400 MHz, Dimethyl sulfoxide-*d*₆) δ 8.00 – 7.93 (8H, m, H1 & H2), 3.21 (4H, s, H6) ppm

¹³C NMR: (101 MHz, Dimethyl sulfoxide-*d*₆) δ 168.8 (C5), 161.6 (C4), 135.5 (C1 or C2), 128.1 (C3), 124.0 (C2 or C1), 25.3 (C6) ppm

HRMS (*m/z*): (ESI⁺) calc'd for C₂₀H₁₂N₂NaO₈ [M+Na]⁺: 431.0486, found: 431.0484

IR (ν_{max}): 3058, 2939, 1788, 1732, 1467, 1375, 1301, 1186, 1140, 1076, 972, 882, 789, 728, 694, 601, 519 cm⁻¹

1,2-Bis(4,4,5,5-tetramethyl-1,3,2-dioxaborolan-2-yl)ethane (318)



Activated ester **317** (53 mg, 0.13 mmol, 1.00 equiv.) was borylated with B₂cat₂ (80 mg, 0.32 mmol, 2.50 equiv.), and pinacol (126 mg, 1.06 mmol, 8.00 equiv.) according to **GP8**. The crude residue was purified by flash column chromatography (*n*-pentane:Et₂O 100:0→90:10) to give boronic ester **318** (15 mg, 41%) as a colourless liquid.

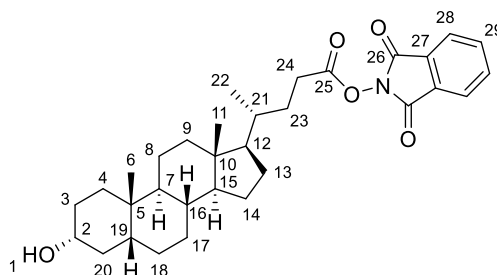
TLC: *R*_f=0.37 (*n*-pentane:Et₂O 85:15)

¹H NMR: (400 MHz, Chloroform-*d*) δ 1.23 (24H, s, H1), 0.84 (4H, s, H3) ppm

¹³C NMR: (101 MHz, Chloroform-*d*) δ 83.0 (C2), 25.0 (C1), 4.6 (C3) ppm

Spectral data were in accordance with that reported in the literature.²⁹³

1,3-Dioxoisindolin-2-yl (*R*)-4-((3*R*,5*R*,8*R*,9*S*,10*S*,13*R*,14*S*,17*R*)-3-hydroxy-10,13-dimethylhexadecahydro-1*H*-cyclopenta[*a*]phenanthren-17-yl)pentanoate (320)



Carboxylic acid **319** (1.00 g, 2.66 mmol, 1.00 equiv.) was activated with *N*-hydroxyphthalimide (433 mg, 2.66 mmol, 1.00 equiv.), DIC (0.41 mL, 2.66 mmol, 1.00 equiv.) and DMAP (32 mg, 0.27 mmol, 0.10 equiv.) according to **GP6**. The crude residue was purified by flash column chromatography (*n*-pentane:EtOAc 80:20→60:40) to give activated ester **320** (418 mg, 30%) as a white solid.

TLC: R_f = 0.42 (*n*-pentane:EtOAc 50:50)

m.p.: 161 – 163 °C (ethyl acetate)

^1H NMR: (400 MHz, Chloroform-*d*) δ 7.88 (2H, m, H28 or H29), 7.78 (2H, m, H29 or H28), 3.62 (1H, dddd, J = 11.1, 11.0, 4.7, 4.6 Hz, H2), 2.71 (1H, ddd, J = 15.9, 9.6, 4.8 Hz, H24), 2.58 (1H, ddd, J = 15.9, 9.0, 6.9 Hz, H24'), 2.05 – 1.93 (2H, m), 1.91 – 1.83 (2H, m), 1.81 – 1.70 (2H, m), 1.66 (1H, m), 1.61 – 1.46 (4H, m), 1.44 – 1.36 (5H, m), 1.35 – 1.21 (4H, m), 1.19 – 1.02 (5H, m), 1.01 – 0.95 (4H, m), 0.92 (3H, s, CH₃), 0.67 (3H, s, CH₃) ppm

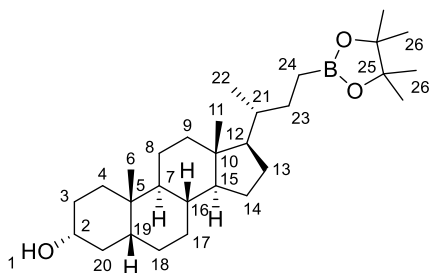
^{13}C NMR: (101 MHz, Chloroform-*d*) δ 170.2 (C25), 162.1 (C26), 134.8 (C28 or C29), 129.1 (C27), 124.1 (C29 or C28), 72.0 (C2), 56.6 (CH), 56.0 (CH), 43.0 (C^{IV}), 42.2 (CH), 40.6 (CH), 40.3 (CH₂), 36.6 (CH₂), 36.0 (CH), 35.5 (CH₂), 35.4 (CH), 34.7 (C^{IV}), 30.9 (CH₂), 30.7 (CH₂), 28.3 (CH₂), 28.2 (CH₂), 27.3 (CH₂), 26.6 (CH₂), 24.3 (CH₂), 23.5 (CH₃), 21.0 (CH₂), 18.4 (C21), 12.2 (CH₃) ppm

HRMS (m/z): (ESI⁺) calc'd for C₃₂H₄₃NNaO₅ [M+Na]⁺: 544.3033; found: 544.3032

IR (ν_{max}): 3366 (br.), 2929, 2863, 1816, 1788, 1741, 1467, 1365, 1186, 1067, 878, 732 cm⁻¹

$[\alpha]_D^{24}$: +18 (CHCl₃, c = 1.0)

(3*R*,5*R*,8*R*,9*S*,10*S*,13*R*,14*S*,17*R*)-10,13-Dimethyl-17-((*R*)-4-(4,4,5,5-tetramethyl-1,3,2-dioxaborolan-2-yl)butan-2-yl)hexadecahydro-1*H*-cyclopenta[*a*]phenanthren-3-ol (321)



Activated ester **320** (68 mg, 0.13 mmol, 1.00 equiv.) was borylated with B₂cat₂ (40 mg, 0.16 mmol, 1.25 equiv.), and pinacol (63 mg, 0.53 mmol, 4.00 equiv.) according to **GP8**. The crude residue was purified by flash column chromatography (*n*-pentane:Et₂O 60:40) to give boronic ester **321** (52 mg, 87%) as a white solid.

TLC: R_f = 0.24 (*n*-pentane:Et₂O 50:50)

m.p.: 159 – 161 °C (diethyl ether)

^1H NMR: (400 MHz, Chloroform-*d*) δ 3.61 (1H, dddd, J = 11.1, 11.0, 4.7, 4.6 Hz, H2), 1.96 (1H, m), 1.91 – 1.70 (4H, m), 1.65 (1H, m), 1.60 – 1.46 (3H, m), 1.45 – 1.28 (7H, m), 1.28 – 1.17

(15H, m), 1.17 – 0.94 (7H, m), 0.91 (3H, s, CH₃), 0.88 (3H, d, *J* = 6.5 Hz, H₂₂), 0.79 (1H, ddd, *J* = 15.8, 10.7, 5.1 Hz, H₂₄), 0.68 – 0.56 (4H, m, CH₃ & H_{24'}) ppm

¹³C NMR: (101 MHz, Chloroform-*d*) δ 82.9 (C₂₅), 72.0 (C₂), 56.7 (CH), 56.1 (CH), 42.8 (C^{IV}), 42.3 (CH), 40.6 (CH), 40.4 (CH₂), 37.8 (CH), 36.7 (CH₂), 36.0 (CH), 35.5 (CH₂), 34.7 (C^{IV}), 30.7 (CH₂), 29.9 (CH₂), 28.4 (CH₂), 27.4 (CH₂), 26.6 (CH₂), 25.0 (C₂₆), 24.9 (C_{26'}), 24.4 (CH₂), 23.5 (CH₃), 21.0 (CH₂), 18.2 (C₂₂), 12.2 (CH₃) ppm

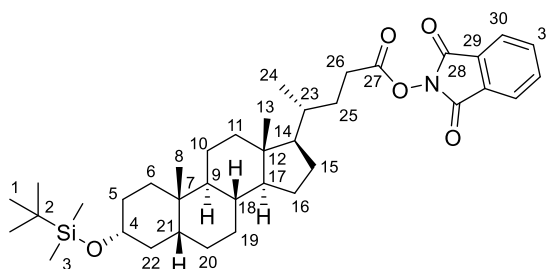
The signal corresponding to C₂₄ was not observed due to quadrupolar relaxation.

HRMS (*m/z*): (ESI⁺) calc'd for C₂₉H₅₁BNaO₃ [M+Na]⁺: 481.3829; found: 481.3827

IR (ν_{max}): 3346, 2975, 2929, 2864, 1448, 1369, 1311, 1144, 1040, 966, 909, 848, 732 cm⁻¹

[α]_D²⁶: +21 (CHCl₃, *c* = 1.0)

1,3-Dioxoisindolin-2-yl (*R*)-4-((3*R*,5*R*,8*R*,9*S*,10*S*,13*R*,14*S*,17*R*)-3-((*tert*-butyldimethylsilyloxy)-10,13-dimethylhexadecahydro-1*H*-cyclopenta[*a*]phenanthren-17-yl)pentanoate (323)



Part A: To a 100-mL round-bottom flask was added lithocholic acid **322** (1.88 g, 5.00 mmol, 1.00 equiv.) and dry DMF (13.00 mL) under nitrogen. To the stirring solution was added TBSCl (3.01 g, 20.00 mmol, 4.00 equiv.), followed by the portion-wise addition of imidazole (2.72 g, 40.00 mmol, 8.00 equiv.). The suspension was heated to 50 °C for 4 hours and then cooled to room temperature. Brine (50.00 mL) was added and the crude reaction mixture was extracted with *n*-hexane (2 × 50.00 mL). The combined organic extracts were washed with cold 1.00 M HCl (20.00 mL), dried over MgSO₄, filtered, and concentrated under reduced pressure to afford a viscous oil. The crude material was dissolved in a mixture of THF and MeOH (50:50, 34 mL), and an aqueous solution of K₂CO₃ (1.00 M, 17 mL) was added. The reaction was stirred at room temperature overnight, diluted with brine (30.00 mL), acidified to pH = 4 with an aqueous solution of KHSO₄ (1.00 M), and extracted with CH₂Cl₂ (3 × 50.00 mL). The combined organic extracts were dried over MgSO₄, filtered, and concentrated under reduced pressure. **Part B:** The intermediate was activated with *N*-hydroxyphthalimide (816 mg, 5.00 mmol, 1.00 equiv.), DIC (0.77 mL, 5.00 mmol, 1.00 equiv.) and DMAP (61 mg, 0.50 mmol, 0.10 equiv.) according to

GP6. The crude residue was purified by flash column chromatography (*n*-hexane:EtOAc 95:5) to give activated ester **323** (1.37 g, 43% over 2 steps) as a white solid.

TLC: R_f = 0.55 (*n*-hexane:EtOAc 90:10)

m.p.: 194 – 198 °C (dichloromethane/methanol)

^1H NMR: (400 MHz, Chloroform-*d*) δ 7.91 – 7.86 (2H, m, H30 or H31), 7.80 – 7.76 (2H, m, H31 or H30), 3.58 (1H, *app.* tt, $J^{app.}$ = 11.0, 4.7 Hz, H4), 2.71 (1H, m, H26), 2.59 (1H, m, H26'), 1.98 – 1.72 (6H, m), 1.58 – 0.86 (23H, m), 0.90 (3H, s, CH₃), 0.89 (9H, s, H1), 0.67 (3H, s, CH₃), 0.06 (6H, s, H3) ppm

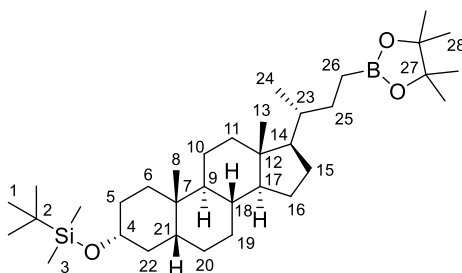
^{13}C NMR: (101 MHz, Chloroform-*d*) δ 170.2 (C27), 162.1 (C28), 134.8 (C30 or C31), 129.1 (C29), 124.1 (C31 or C30), 73.0 (C4), 56.5 (CH), 56.1 (CH), 42.9 (C^{IV}), 42.4 (CH), 40.4 (CH), 40.3 (CH₂), 37.1 (CH₂), 36.0 (CH), 35.7 (CH₂), 35.4 (CH), 34.7 (C^{IV}), 31.2 (CH₂), 30.9 (CH₂), 28.3 (CH₂), 28.2 (CH₂), 27.5 (CH₂), 26.5 (CH₂), 26.1 (C1), 24.4 (CH₂), 23.5 (CH₃), 21.0 (CH₂), 18.5 (C2), 18.4 (C23), 12.2 (CH₃), –4.4 (C3) ppm

HRMS (m/z): (ESI⁺) calc'd for C₃₈H₅₇BNO₅SiNa [M+Na]⁺: 658.3898, found: 658.3888

IR (ν_{max}): 2930, 2860, 1744, 1065, 835, 781 cm^{–1}

$[\alpha]_D^{24}$: +20 (CHCl₃, *c* = 1.0)

***tert*-Butyl(((3*R*,5*R*,8*R*,9*S*,10*S*,13*R*,14*S*,17*R*)-10,13-dimethyl-17-((*R*)-4-(4,4,5,5-tetramethyl-1,3,2-dioxaborolan-2-yl)butan-2-yl)hexadecahydro-1*H*-cyclopenta[*a*]phenanthren-3-yl)oxy)dimethylsilane (324)**



Activated ester **323** (83 mg, 0.13 mmol, 1.00 equiv.) was borylated with B₂cat₂ (40 mg, 0.16 mmol, 1.25 equiv.), and pinacol (63 mg, 0.53 mmol, 4.00 equiv.) according to **GP8**. The crude residue was purified by flash column chromatography (*n*-pentane:Et₂O 95:5) to give boronic ester **324** (54 mg, 72%) as a viscous solid.

TLC: R_f = 0.38 (*n*-pentane:Et₂O 95:5)

m.p.: 159 – 161 °C (diethyl ether)

¹H NMR: (400 MHz, Chloroform-*d*) δ 3.57 (1H, dddd, J = 10.9, 10.7, 4.7, 4.5 Hz, H4), 1.95 (1H, m), 1.90 – 1.70 (4H, m), 1.59 – 1.50 (3H, m), 1.48 – 1.28 (8H, m), 1.28 – 1.17 (15H, m), 1.16 – 0.98 (6H, m), 0.98 – 0.75 (17H, m), 0.69 – 0.54 (4H, m), 0.05 (6H, s, C3) ppm

¹³C NMR: (101 MHz, Chloroform-*d*) δ 82.9 (C27), 73.0 (C4), 56.6 (CH), 56.2 (CH), 42.9 (C^{IV}), 42.5 (CH), 40.4 (CH), 40.3 (CH₂), 37.8 (CH), 37.1 (CH₂), 36.1 (CH), 35.8 (CH₂), 34.8 (C^{IV}), 31.2 (CH₂), 29.9 (CH₂), 28.4 (CH₂), 27.5 (CH₂), 26.6 (CH₂), 26.2 (C1), 25.0 (C28), 24.9 (C28'), 24.4 (CH₂), 23.6 (CH₃), 21.0 (CH₂), 18.5 (CH), 18.2 (CH₃), 12.2 (CH₃), –4.4 (C3) ppm

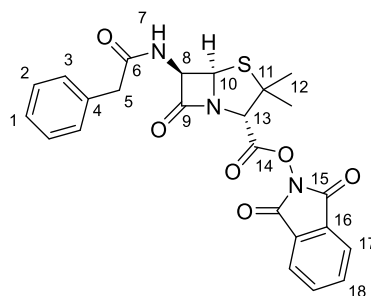
The signal corresponding to C26 was not observed due to quadrupolar relaxation.

HRMS (m/z): (ESI⁺) calc'd for C₃₅H₆₅BNaO₃Si [M+Na]⁺: 595.4695; found: 595.4690

IR (ν_{\max}): 2927, 2856, 1470, 1370, 1312, 1251, 1146, 1095, 1080, 871, 835, 774 cm^{–1}

$[\alpha]_D^{24}$: +17 (CHCl₃, c = 1.0)

1,3-Dioxoisindolin-2-yl (2*S*,5*R*,6*R*)-3,3-dimethyl-7-oxo-6-(2-phenylacetamido)-4-thia-1-azabicyclo[3.2.0]heptane-2-carboxylate (326**)**



Penicillin **325** (437 mg, 1.31 mmol, 1.00 equiv.) was activated with *N*-hydroxyphthalimide (213 mg, 1.31 mmol, 1.00 equiv.) and DCC (270 mg, 1.31 mmol, 1.00 equiv.) according to **GP7**. The crude residue was recrystallised from EtOAc/*n*-pentane to give activated ester **326** (182 mg, 29%) as a white solid.

TLC: R_f = 0.38 (*n*-pentane:acetone 50:50)

m.p.: decomp. 185 – 189 °C (ethyl acetate)

¹H NMR: (400 MHz, Chloroform-*d*) δ 7.87 (2H, m, H17 or H18), 7.79 (2H, m, H18 or H17), 7.36 (2H, m, H2), 7.30 (1H, m, H1), 7.25 (2H, m, H3), 6.14 (1H, m, H7), 5.67 (1H, dd, J = 9.0, 4.3 Hz, H8), 5.51 (1H, d, J = 4.3 Hz, H10), 4.69 (1H, s, H13), 3.62 (2H, s, H5), 1.71 (3H, s, H12), 1.53 (3H, s, H12') ppm

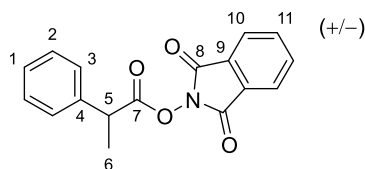
¹³C NMR: (101 MHz, Chloroform-*d*) δ 173.5 (C9), 170.5 (C6), 164.3 (C14), 161.4 (C15), 135.1 (C17 or C18), 133.9 (C4), 129.6 (C3), 129.3 (C2), 128.7 (C16), 127.8 (C1), 124.3 (C18 or C17), 68.8 (C13), 68.4 (C10), 65.0 (C11), 59.0 (C8), 43.4 (C5), 31.4 (C12), 26.9 (C12') ppm

HRMS (m/z): (ESI⁺) calc'd for C₂₄H₂₁N₃NaO₆S [M+Na]⁺: 502.1043; found: 502.1041

IR (ν_{\max}): 3531, 3363, 3295, 3032, 2972, 2934, 1788, 1745, 1666, 1517, 1293, 1133, 967 cm⁻¹

$[\alpha]_D^{24}$: +103 (CHCl₃, c = 1.0)

(+/-)-1,3-dioxoisindolin-2-yl 2-phenylpropanoate (329**)**



Carboxylic acid **328** (1.00 g, 6.66 mmol, 1.00 equiv.) was activated with *N*-hydroxyphthalimide (1.09 g, 6.66 mmol, 1.00 equiv.), DIC (1.03 mL, 6.66 mmol, 1.00 equiv.) and DMAP (81 mg, 0.67 mmol, 0.10 equiv.) according to **GP6**. The crude residue was purified by flash column chromatography (*n*-pentane:EtOAc 90:10) to give activated ester **329** (1.79 mg, 91%) as a colourless liquid.

TLC: R_f = 0.16 (*n*-pentane:Et₂O 90:10)

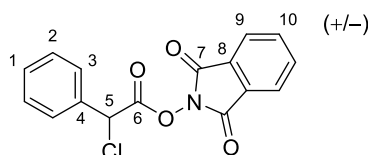
¹H NMR: (400 MHz, Chloroform-*d*) δ 7.86 (2H, m, H10 or H11), 7.77 (2H, m, 2H, H11 or H10), 7.44 – 7.37 (4H, m, H2 & H3), 7.33 (1H, m, H1), 4.13 (1H, q, J = 7.2 Hz, H5), 1.68 (3H, d, J = 7.2 Hz, H6) ppm

¹³C NMR: (126 MHz, Chloroform-*d*) δ 170.9 (C7), 162.0 (C8), 138.5 (C4), 134.9 (C10 or C11), 129.07 (C9), 129.06 (C2 or C3), 128.0 (C1), 127.7 (C3 or C2), 124.1 (C11 or C10), 43.1 (C5), 19.1 (C6) ppm

HRMS (m/z): (ESI⁺) calc'd for C₁₇H₁₃NNaO₄ [M+Na]⁺: 318.0737, found: 318.0748

IR (ν_{\max}): 2993, 2944, 1781, 1736, 1353, 1185, 1041, 875, 854, 792, 738, 692, 512 cm⁻¹

1,3-Dioxoisindolin-2-yl 2-chloro-2-phenylacetate (332**)**



In a flame-dried Schlenk tube, 2-chloro-2-phenylacetic acid **331** (486 mg, 2.85 mmol, 1.00 equiv.) was dissolved in anhydrous CH₂Cl₂ (10.00 mL) at 0 °C under an atmosphere of nitrogen. One drop of DMF was added to the reaction mixture, followed by oxalyl chloride (0.27 mL, 3.13 mmol, 1.10 equiv.). After the addition, the ice bath was removed and the reaction

mixture was stirred at room temperature. The colourless solution turned yellow. After 1.5 h, gas evolution ceased and volatiles were removed under reduced pressure to afford a bright yellow liquid. In parallel, *N*-hydroxyphthalimide (465 mg, 2.85 mmol, 1.00 equiv.) and DIPEA (0.75 mL, 4.27 mmol, 1.50 equiv.) were dissolved in a second flame-dried Schlenk tube in anhydrous CH₂Cl₂ (10.00 mL) at 0 °C under an atmosphere of nitrogen. Freshly prepared acyl chloride as a solution in anhydrous CH₂Cl₂ (2.00 mL) was then carefully added to the reaction mixture *via* syringe. After the addition, the ice bath was removed and the reaction mixture was stirred at room temperature for 16 h. The orange solution was then washed with water (4 × 10.00 mL), dried over MgSO₄, filtered and concentrated to afford a yellow solid. The crude residue was purified by flash column chromatography (*n*-pentane:CH₂Cl₂ 50:50→0:100) to give activated ester **332** (404 mg, 45%) as a white solid.

TLC: *R*_f = 0.29 (*n*-pentane:CH₂Cl₂ 50:50)

m.p.: 59 – 61 °C (*n*-hexane)

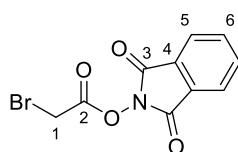
¹H NMR: (400 MHz, Chloroform-*d*) δ 7.88 (2H, m, H9 or H10), 7.80 (2H, m, H10 or H9), 7.61 (2H, m, H2 or H3), 7.54 – 7.36 (3H, m, (H3 or H2) & H1), 5.74 (1H, s, H5) ppm

¹³C NMR: (101 MHz, Chloroform-*d*) δ 165.4 (C6), 161.4 (C7), 135.1 (C9 or C10), 134.2 (C4), 130.1 (C1), 129.3 (C2 or C3), 128.9 (C8), 128.3 (C3 or C2), 124.3 (C10 or C9), 56.3 (C5) ppm

HRMS (*m/z*): (ESI⁺) calc'd for C₁₆H₁₀ClNNaO₄ [M+Na]⁺: 338.0191; found: 338.0190

IR (*ν*_{max}): 3523, 3066, 2998, 1819, 1788, 1740, 1467, 1349, 1183, 1079, 964, 873, 737 cm⁻¹

1,3-Dioxoisindolin-2-yl 2-bromoacetate (**335**)



In a flame-dried Schlenk tube, *N*-hydroxyphthalimide (808 mg, 4.95 mmol, 1.00 equiv.) and DIPEA (0.86 mL, 4.95 mmol, 1.00 equiv.) were dissolved in anhydrous CH₂Cl₂ (20.00 mL) at 0 °C under an atmosphere of nitrogen. Bromoacetyl bromide **334** (0.43 mL, 4.95 mmol, 1.00 equiv.) was slowly added *via* syringe. After the addition, the red solution turned colorless. The ice bath was removed and the reaction mixture was stirred at room temperature for 16 h. The reaction mixture was quenched with water (20.00 mL). The organic layer was separated, washed with water (3 × 15 mL), dried over MgSO₄, filtered and concentrated under reduced pressure to afford a yellow solid. The product was recrystallised from EtOAc/*n*-pentane to give activated ester **335** (1.18 g, 84%) as an off-white solid.

TLC: R_f = 0.43 (*n*-pentane:Et₂O 50:50)

m.p.: 92 – 95 °C (*n*-hexane)

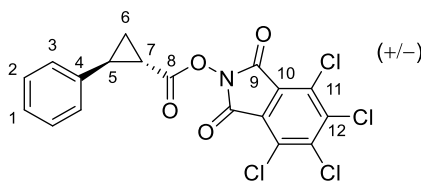
¹H NMR: (400 MHz, Chloroform-*d*) δ 7.90 (2H, m, H5 or H6), 7.81 (2H, m, H6 or H5), 4.16 (2H, s, H1) ppm

¹³C NMR: (101 MHz, Chloroform-*d*) δ 164.0 (C2), 161.4 (C3), 135.1 (C5 or C6), 128.9 (C10), 124.3 (C6 or C5), 21.4 (C1) ppm

HRMS (*m/z*): *Despite repeated attempts, a HRMS could not be obtained.*

IR (ν_{\max}): 3516, 3042, 3004, 2979, 1808, 1782, 1740, 1466, 1372, 1184, 1068, 973, 877 cm⁻¹

4,5,6,7-Tetrachloro-1,3-dioxoisindolin-2-yl *trans*-2-phenylcyclopropane-1-carboxylate (337)



Carboxylic acid **307** (1.00 g, 6.17 mmol, 1.00 equiv.) was activated with tetrachloro-*N*-hydroxyphthalimide (1.86 g, 6.17 mmol, 1.00 equiv.), DIC (0.95 mL, 6.17 mmol, 1.00 equiv.) and DMAP (75 mg, 0.62 mmol, 0.10 equiv.) according to **GP6**. The crude residue was purified by flash column chromatography (*n*-pentane:EtOAc 100:0→0:100) to give activated ester **337** (118 mg, 4%) as a white solid. **Note:** Product unstable on silica gel.

TLC: R_f = 0.43 (*n*-pentane:Et₂O 80:20)

m.p.: 211 – 214 °C (ethyl acetate)

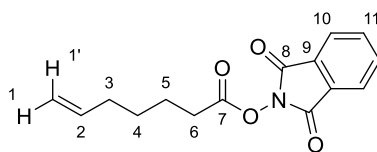
¹H NMR: (400 MHz, Chloroform-*d*) δ 7.35 (2H, m, H2 or H3), 7.26 (1H, m, H1), 7.16 (2H, m, H3 or H2), 2.79 (1H, ddd, J = 9.3, 7.0, 4.1 Hz, H5), 2.22 (1H, ddd, J = 8.4, 5.2, 4.1, H7), 1.84 (1H, ddd, J = 9.3, 5.2, 4.9 Hz, H6), 1.67 (1H, ddd, J = 8.4, 7.0, 4.9 Hz, H6') ppm

¹³C NMR: (101 MHz, Chloroform-*d*) δ 169.4 (C8), 157.7 (C9), 141.2 (2 × C_{Ar}), 138.3 (C4), 130.6 (2 × C_{Ar}), 128.9 (C2 or C3), 127.4 (C1), 126.6 (C3 or C2), 124.9 (2 × C_{Ar}), 28.8 (C5), 21.0 (C7), 18.5 (C6) ppm

HRMS (*m/z*): (EI⁺) calc'd for C₁₈H₉Cl₄NO₄ [M]⁺: 442.9286; found: 442.9293

IR (ν_{\max}): 3510, 3061, 3029, 1810, 1785, 1748, 1402, 1379, 1099, 1071, 1039, 731 cm⁻¹

1,3-Dioxoisindolin-2-yl hept-6-enoate (**339**)



Carboxylic acid **338** (150 mg, 1.17 mmol, 1.00 equiv.) was activated with *N*-hydroxyphthalimide (191 mg, 1.17 mmol, 1.00 equiv.), DIC (0.18 mL, 1.17 mmol, 1.00 equiv.) and DMAP (15 mg, 0.12 mmol, 0.10 equiv.) according to **GP6**. The crude residue was purified by flash column chromatography (*n*-hexane:acetone 90:10) to give activated ester **339** (215 mg, 67%) as a colourless liquid.

TLC: R_f = 0.27 (*n*-hexane:acetone 80:20)

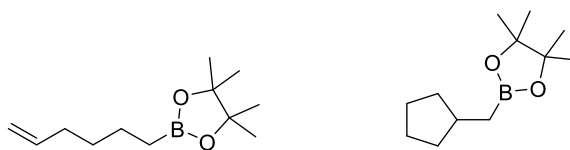
^1H NMR: (400 MHz, Chloroform-*d*) δ 7.88 (2H, m, H10 or H11), 7.78 (2H, m, H11 or H10), 5.81 (1H, ddt, J = 17.0, 10.2, 6.7 Hz, H2), 5.04 (1H, ddt, J = 17.0, 2.2, 1.7 Hz, H1'), 4.98 (1H, ddt, J = 10.2, 2.2, 1.2 Hz, H1), 2.67 (2H, t, J = 7.4 Hz, H6), 2.12 (2H, dddt, J = 7.4, 6.7, 1.7, 1.2 Hz, H3), 1.81 (2H, *app.* pent, $J^{app.}$ = 7.4 Hz, H5), 1.55 (2H, *app.* pent, $J^{app.}$ = 7.4 Hz, H4) ppm

^{13}C NMR: (101 MHz, Chloroform-*d*) δ 169.6 (C7), 162.1 (C8), 138.2 (C2), 134.9 (C10 or C11), 129.1 (C9), 124.1 (C11 or C10), 115.2 (C1), 33.3 (C3), 31.0 (C6), 28.1 (C4), 24.2 (C5) ppm

HRMS (m/z): (ESI⁺) calc'd for C₁₅H₁₅NNaO₄ [M+Na]⁺: 296.0893; found: 296.0883

IR (ν_{max}): 3522, 3076, 2934, 2865, 1815, 1787, 1738, 1467, 1362, 1185, 1133, 1081, 877 cm⁻¹

2-(Hex-5-en-1-yl)-4,4,5,5-tetramethyl-1,3,2-dioxaborolane (**341a**) and 2-(Cyclopentylmethyl)-4,4,5,5-tetramethyl-1,3,2-dioxaborolane (**341b**)



341a

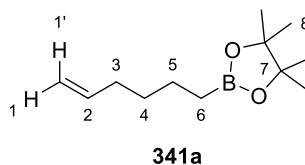
341b

Activated ester **339** (36 mg, 0.13 mmol, 1.00 equiv.) was borylated with B₂cat₂ (40 mg, 0.16 mmol, 1.25 equiv.), and pinacol (63 mg, 0.53 mmol, 4.00 equiv.) according to **GP8**. The crude residue was purified by flash column chromatography (*n*-pentane:Et₂O 100:0→90:10) to give a mixture of linear boronic ester **341a** and cyclized boronic ester **341b** (57:43, 21 mg, 77%) as a colourless liquid. **Note:** Both products are volatile.

TLC: R_f = 0.55 (*n*-pentane:Et₂O 95:5)

HRMS (*m/z*): Despite repeated attempts, a HRMS could not be obtained.

2-(Hex-5-en-1-yl)-4,4,5,5-tetramethyl-1,3,2-dioxaborolane (341a)

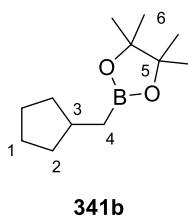


¹H NMR: (400 MHz, Chloroform-*d*) δ 5.81 (1H, ddt, J = 17.1, 10.1, 6.6 Hz, H2), 4.98 (1H, d, J = 17.1 Hz, H1'), 4.91 (1H, d, J = 10.1 Hz, H1), 2.04 (2H, td, J = 7.0, 6.6 Hz, H3), 1.45 – 1.34 (4H, m, H4 & H5), 1.24 (12H, s, H8), 0.77 (2H, t, J = 7.3 Hz, H6) ppm

¹³C NMR: (101 MHz, Chloroform-*d*) δ 139.3 (C2), 114.2 (C1), 83.0 (C7), 33.7 (C3), 31.8 (C4 or C5), 25.0 (C8), 23.7 (C5 or C4) ppm

The signal corresponding to C6 was not observed due to quadrupolar relaxation.

2-(Cyclopentylmethyl)-4,4,5,5-tetramethyl-1,3,2-dioxaborolane (341b)

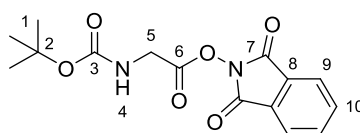


¹H NMR: (400 MHz, Chloroform-*d*) δ 1.95 (1H, m, H3), 1.76 (2H, m), 1.60 (2H, m), 1.50 (2H, m), 1.05 (2H, m), 0.83 (2H, d, J = 7.4 Hz, H4) ppm

¹³C NMR: (101 MHz, Chloroform-*d*) δ 82.9 (C5), 36.3 (C3), 35.2 (C2), 25.3 (C1), 25.0 (C6) ppm

The signal corresponding to C4 was not observed due to quadrupolar relaxation.

1,3-Dioxoisindolin-2-yl (*tert*-butoxycarbonyl)glycinate (353)



(*tert*-Butoxycarbonyl)glycine **352** (2.50 g, 14.27 mmol, 1.00 equiv.) was activated with *N*-hydroxyphthalimide (2.33 g, 14.27 mmol, 1.00 equiv.) and DCC (2.94 g, 14.27 mmol, 1.00 equiv.)

according to **GP7**. The crude residue was purified by recrystallisation from EtOAc to give, after 4 crops, activated ester **353** (1.81 g, 40%) as a white solid.

TLC: R_f = 0.59 (*n*-pentane:EtOAc 50:50)

m.p.: 184 – 188 °C (ethyl acetate)

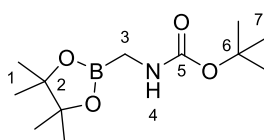
¹H NMR: (500 MHz, Dimethyl sulfoxide-*d*₆) δ 8.03 – 7.90 (4H, m, H9 & H10), 7.51 (1H, t, J = 6.1 Hz, H4), 4.17 (2H, d, J = 6.1 Hz, H5), 1.38 (9H, s, H1) ppm

¹³C NMR: (126 MHz, Dimethyl sulfoxide-*d*₆) δ 168.4 (C6), 162.1 (C7), 156.2 (C3), 136.1 (C9 or C10), 128.5 (C8), 124.5 (C10 or C9), 79.4 (C2), 40.3 (C5), 28.5 (C1) ppm

HRMS (*m/z*): (ESI⁺) calc'd for C₁₅H₁₆N₂NaO₆ [M+Na]⁺: 343.0901; found: 343.0905

IR (ν_{\max}): 3295, 2979, 2930, 2850, 1840, 1825, 1788, 1738, 1686, 1532, 1365, 1289, 1144, 1071, 970, 878, 693 cm⁻¹

***tert*-Butyl ((4,4,5,5-tetramethyl-1,3,2-dioxaborolan-2-yl)methyl)carbamate (**354**)**



In a flame-dried Schlenk tube was diluted a solution of NaHMDS (1.00 M in THF, 1.00 mL, 1.00 mmol, 1.00 equiv.) with anhydrous THF (5.00 mL) at –78 °C under an atmosphere of nitrogen. A solution of boronic ester **385** (176 mg, 1.00 mmol, 1.00 equiv.) in anhydrous THF (1.00 mL) was added dropwise and the reaction mixture was stirred at –78 °C for 20 min. The acetone/dry ice bath was removed and the reaction mixture was stirred at room temperature for 2 h. The suspension was cooled to 0 °C and MeOH (81 μ L, 2.00 mmol, 2.00 equiv.) was added. The reaction mixture was stirred at 0 °C for 1 h and Boc₂O (262 mg, 1.20 mmol, 1.20 equiv.) was added. After the addition, the reaction mixture was stirred at room temperature for 3 days under an atmosphere of nitrogen. The suspension was concentrated and the crude residue was purified by flash column chromatography (oven-dried silica; petroleum ether 40–60:Et₂O 80:20→0:100) to give boronic ester **354** (97 mg, 38%) as a pale yellow liquid.

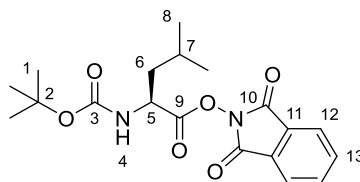
TLC: R_f = 0.31 (*n*-pentane:EtOAc 50:50)

¹H NMR: (400 MHz, Chloroform-*d*) δ 4.63 (1H, s, H4), 2.77 (2H, d, J = 4.3 Hz, H3), 1.44 (9H, s, H7), 1.27 (12H, s, H1) ppm

¹³C NMR: (101 MHz, Chloroform-*d*) δ 157.0 (C5), 84.1 (C2), 79.1 (C6), 28.4 (C3), 24.8 (C1) ppm

Spectral data were in accordance with that reported in the literature.²⁷⁴

1,3-Dioxoisindolin-2-yl (*tert*-butoxycarbonyl)-*L*-leucinate ((*S*)-356)



Protected leucine (**(S)-355**) (500 mg, 2.16 mmol, 1.00 equiv.) was activated with *N*-hydroxyphthalimide (353 mg, 2.16 mmol, 1.00 equiv.) and DCC (446 mg, 2.16 mmol, 1.00 equiv.) according to **GP7**. The crude residue was triturated in cold EtOAc. The solid was removed by filtration, the filtrate was concentrated under reduced pressure and the resulting waxy solid was dried under high vacuum to afford activated ester (**(S)-356**) (415 mg, 51%) as a colourless wax.

TLC: R_f = 0.10 (*n*-hexane:EtOAc 90:10)

¹H NMR: (500 MHz, Chloroform-*d*) δ 7.89 (2H, m, H12 or H13), 7.79 (2H, m, H13 or H12), 4.94 (1H, m, H4), 4.62 (1H, m, H5), 1.97 – 1.80 (2H, m, H6 & H7), 1.72 (1H, m, H6'), 1.48 (9H, m, H1), 1.02 (6H, m, H8) ppm

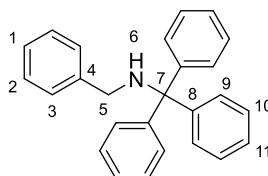
¹³C NMR: (126 MHz, Chloroform-*d*) δ 170.1 (C9), 161.7 (C10), 155.1 (C3), 134.9 (C12 or C13), 129.0 (C11), 124.1 (C13 or C12), 80.7 (C2), 50.8 (C5), 42.0 (C6), 28.4 (C1), 24.9 (C7), 22.9 (C8) ppm

HRMS (m/z): (ESI⁺) calc'd for C₁₉H₂₄N₂NaO₆ [M+Na]⁺: 399.1527; found: 399.1537

IR (ν_{\max}): 3375, 2961, 2934, 2873, 1819, 1789, 1744, 1713, 1367, 1163, 1080, 697 cm⁻¹

$[\alpha]_D^{24}$: -33 (CHCl₃, *c* = 1.0)

N-Benzyl-1,1,1-triphenylmethanamine (358)



In a round-bottomed flask, benzylamine (0.20 mL, 1.87 mmol, 1.00 equiv.) was dissolved in anhydrous CH₂Cl₂ (6.00 mL) at room temperature. Ph₃CCl (572 mg, 2.05 mmol, 1.10 equiv.) was added, followed by DMAP (23 mg, 0.19 mmol, 0.10 equiv.) and the reaction mixture was stirred at room temperature for 16 h. A saturated aqueous solution of NaHCO₃ (9.00 mL) was added,

followed by water (1.00 mL). The aqueous layer was extracted with Et₂O (3 × 5 mL). The organic phases were combined, washed with brine, dried over MgSO₄, filtered and concentrated. The crude residue was purified by flash column chromatography (*n*-pentane:CH₂Cl₂ 80:20→60:40) to give amine **358** (317 mg, 49%) as a white solid.

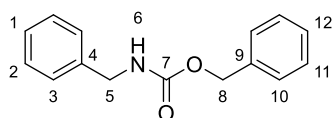
TLC: *R*_f = 0.38 (*n*-pentane:Et₂O 80:20)

¹H NMR: (500 MHz, Chloroform-*d*) δ 7.58 (6H, m, H₉ or H₁₀), 7.41 (2H, m, H₂ or H₃), 7.37 – 7.27 (9H, m, H₁ & 8 × H_{Ar}), 7.22 (3H, m, H₁₁), 3.36 (2H, s, H₅), 1.87 (1H, s, H₆) ppm

¹³C NMR: (126 MHz, Chloroform-*d*) δ 146.2 (C₈), 141.2 (C₄), 128.8 (C_{Ar}), 128.5 (C_{Ar}), 128.0 (2 × C_{Ar}), 126.9 (C_{Ar}), 126.5 (C₁₁), 71.1 (C₇), 48.0 (C₅) ppm

Spectral data were in accordance with that reported in the literature.²⁹⁴

Benzyl benzylcarbamate (**359**)



In a round-bottomed flask, benzylamine (0.20 mL, 1.87 mmol, 1.00 equiv.) was dissolved in MeOH (4.00 mL) at room temperature. CbzCl (0.32 mL, 2.24 mmol, 1.20 equiv.) was added, followed by iodine (10 mg, 0.04 mmol, 0.02 equiv.) and the reaction mixture was stirred at room temperature for 16 h. The reaction mixture was diluted with Et₂O (10.00 mL) and successively washed with a saturated aqueous solution of Na₂S₂O₃ (5.00 mL), a saturated aqueous solution of NaHCO₃ (5.00 mL) and brine. The organic layer was dried over MgSO₄, filtered and concentrated. The crude residue was purified by flash column chromatography (*n*-pentane:Et₂O 80:20) to give carbamate **359** (217 mg, 48%) as a white solid.

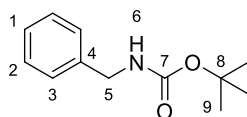
TLC: *R*_f = 0.22 (*n*-pentane:Et₂O 80:20)

¹H NMR: (500 MHz, Chloroform-*d*) δ 7.42 – 7.26 (10H, m, 10 × H_{Ar}), 5.14 (2H, s, H₈), 5.08 (1H, br. s, H₆), 4.39 (2H, d, *J* = 6.0 Hz, H₅) ppm

¹³C NMR: (126 MHz, Chloroform-*d*) δ 156.5 (C₇), 138.5 (C₄), 136.6 (C₉), 128.8 (C_{Ar}), 128.7 (2 × C_{Ar}), 128.3 (2 × C_{Ar}), 127.7 (C_{Ar}), 67.0 (C₈), 45.3 (C₅) ppm

Spectral data were in accordance with that reported in the literature.²⁹⁵

***tert*-Butyl benzylcarbamate (360)**



In a round-bottomed flask, benzylamine (0.20 mL, 1.87 mmol, 1.00 equiv.) was dissolved in EtOH (4.00 mL) at room temperature. Boc₂O (448 mg, 2.05 mmol, 1.10 equiv.) was added and the reaction mixture was stirred at 30 °C for 4 h and at room temperature for 16 h. A saturated aqueous solution of NH₄Cl (3.00 mL) was added, followed by water (1.00 mL). The layers were separated and the aqueous phase was extracted with Et₂O (3 × 5 mL). The organic layers were combined, washed with brine, dried over MgSO₄, filtered and concentrated. The crude residue was purified by flash column chromatography (*n*-pentane:CH₂Cl₂ 80:20→60:40) to give carbamate **360** (340 mg, 88%) as a white solid.

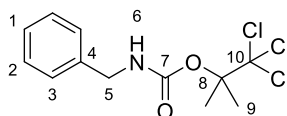
TLC: *R*_f = 0.38 (*n*-pentane:Et₂O 80:20)

¹H NMR: (500 MHz, Chloroform-*d*) δ 7.33 (2H, m, H₂), 7.30 – 7.24 (3H, m, H₁ & H₃), 4.83 (1H, m, H₆), 4.32 (2H, d, *J* = 5.9 Hz, H₅), 1.46 (9H, s, H₉) ppm

¹³C NMR: (126 MHz, Chloroform-*d*) δ 156.0 (C₇), 139.0 (C₄), 128.7 (C₂), 127.6 (C₁), 127.4 (C₃), 79.6 (C₈), 44.8 (C₅), 28.5 (C₉) ppm

Spectral data were in accordance with that reported in the literature.²⁹⁶

1,1,1-Trichloro-2-methylpropan-2-yl benzylcarbamate (361)



In a round-bottomed flask, benzylamine (0.20 mL, 1.87 mmol, 1.00 equiv.) and Et₃N (0.52 mL, 3.73 mmol, 2.00 equiv.) were dissolved in CH₂Cl₂ (4.00 mL) at 0 °C. DMTrOcCl (448 mg, 1.87 mmol, 1.00 equiv.) was added portionwise. After the addition, the ice bath was removed and the reaction mixture was stirred at room temperature for 16 h. The reaction mixture was diluted with EtOAc (10.00 mL) and a saturated aqueous solution of NH₄Cl (10.00 mL) was added. The aqueous phase was extracted with EtOAc (3 × 5 mL). The organic layers were combined, washed with brine, dried over MgSO₄, filtered and concentrated. The crude residue was purified by flash column chromatography (*n*-pentane:CH₂Cl₂ 80:20→60:40) to give carbamate **361** (174 mg, 30%) as a pale yellow solid.

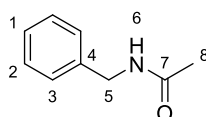
TLC: *R*_f = 0.43 (*n*-pentane:Et₂O 80:20)

¹H NMR: (500 MHz, Chloroform-*d*) δ 7.35 (2H, m, H2), 7.32 – 7.27 (3H, m, H1 & H3), 5.15 (1H, br. s, H6), 4.36 (2H, d, J = 5.9 Hz, H5), 1.95 (6H, s, H9) ppm

¹³C NMR: (126 MHz, Chloroform-*d*) δ 154.2 (C7), 138.2 (C4), 128.9 (C2), 127.8 (C3), 127.3 (C1), 106.7 (C10), 88.3 (C8), 45.1 (C5), 21.8 (C9) ppm

Spectral data were in accordance with that reported in the literature.²⁹⁷

***N*-Benzylacetamide (362)**



In a round-bottomed flask, benzylamine (0.20 mL, 1.87 mmol, 1.00 equiv.) and Et₃N (0.52 mL, 3.73 mmol, 2.00 equiv.) were dissolved in anhydrous CH₂Cl₂ (4.00 mL) at 0 °C. Ac₂O (0.18 mL, 1.87 mmol, 1.00 equiv.) was added, followed by DMAP (23 mg, 0.19 mmol, 0.10 equiv.). After 5 min, the ice bath was removed and the reaction mixture was stirred at room temperature for 16 h. The reaction mixture was diluted with Et₂O (4.00 mL) and an aqueous solution of HCl (0.20 M, 10.00 mL) was added. The aqueous phase was extracted with Et₂O (3 × 5 mL). The organic layers were combined, washed with brine, dried over MgSO₄, filtered and concentrated. The crude residue was purified by flash column chromatography (*n*-pentane:EtOAc 50:50→25:75) to give acetamide **362** (206 mg, 74%) as a white solid.

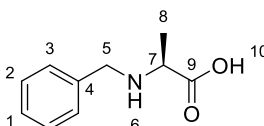
TLC: R_f = 0.16 (*n*-pentane:EtOAc 50:50)

¹H NMR: (500 MHz, Chloroform-*d*) δ 7.33 (2H, m, H2), 7.30 – 7.26 (3H, m, H1 & H3), 5.79 (1H, br. s, H6), 4.43 (2H, d, J = 5.7 Hz, H5), 2.02 (3H, s, H8) ppm

¹³C NMR: (126 MHz, Chloroform-*d*) δ 170.0 (C7), 138.3 (C4), 128.9 (C2), 128.0 (C3), 127.7 (C1), 43.9 (C5), 23.4 (C8) ppm

Spectral data were in accordance with that reported in the literature.²⁹⁸

Benzyl-*L*-alanine ((*S*)-365)



Alanine (*S*)-**364** (1.00 g, 11.22 mmol, 1.00 equiv.) was dissolved in an aqueous solution of NaOH (2.00 M, 6.00 mL) at room temperature. Benzaldehyde (1.15 mL, 11.22 mmol, 1.00 equiv.) was added, and the biphasic mixture was stirred at room temperature for 1 h. The colourless solution

was cooled to 0 °C and NaBH₄ (212 mg, 5.61 mmol, 0.50 equiv.) was added portionwise. After the addition, the reaction mixture was stirred at room temperature for 30 min before benzaldehyde (1.15 mL, 11.22 mmol, 1.00 equiv.) and NaBH₄ (212 mg, 5.61 mmol, 0.50 equiv.) were added. The reaction mixture was stirred for 1 h and Et₂O (10.00 mL) was added. The biphasic mixture was vigorously stirred for 16 h. The layers were separated and the aqueous phase was washed with Et₂O (2 × 10.00 mL), acidified to pH 7 and concentrated under reduced pressure. The white precipitate was triturated in cold water, collected by filtration and dried under high vacuum to give benzylalanine (**(S)**-**365**) (738 mg, 37%) as a white solid.

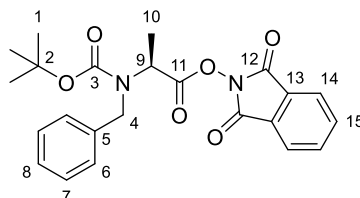
TLC: R_f = 0.10 (CH₂Cl₂:MeOH 80:20)

¹H NMR: (500 MHz, Deuterium Oxide) δ 7.56 – 7.42 (5H, m, H1, H2 & H3), 4.26 (1H, d, J = 13.0 Hz, H5), 4.22 (1H, d, J = 13.0 Hz, H5'), 3.71 (1H, q, J = 7.2 Hz, H7), 1.51 (3H, d, J = 7.2 Hz, H8) ppm

¹³C NMR: (126 MHz, Deuterium Oxide) δ 174.7 (C9), 130.9 (C4), 129.8 (C2), 129.6 (C1), 129.2 (C3), 57.3 (C7), 49.8 (C5), 15.2 (C8) ppm

Spectral data were in accordance with that reported in the literature.²⁹⁹

1,3-Dioxoisindolin-2-yl *N*-benzyl-*N*-(*tert*-butoxycarbonyl)-*L*-alaninate ((**(S)**)-**366**)



Part A: Benzylalanine (**(S)**-**365**) (695 mg, 3.88 mmol, 1.00 equiv.) was dissolved in a mixture of water and dioxane (50:50, 12.00 mL) by addition of Et₃N (1.62 mL, 11.63 mmol, 3.00 equiv.) at room temperature. Boc₂O (846 mg, 3.88 mmol, 1.00 equiv.) was added, and the reaction mixture was stirred at room temperature for 16 h. The colourless solution was cooled to 0 °C and an aqueous solution of HCl (2.00 M) was carefully added to bring pH to 4. The solution was extracted with EtOAc (3 × 10.00 mL), washed with brine, dried over MgSO₄, filtered and concentrated. **Part B:** The crude residue was coupled with *N*-hydroxyphthalimide (542 mg, 3.32 mmol, 1.00 equiv.), DIC (0.51 mL, 3.32 mmol, 1.00 equiv.) and DMAP (41 mg, 0.33 mmol, 0.10 equiv.) according to **GP6**. The crude residue was purified by flash column chromatography (*n*-pentane:Et₂O 80:20→50:50) to give activated ester (**(S)**-**366**) (1.08 g, 76% over 2 steps) as a colourless wax.

TLC: R_f = 0.30 (*n*-pentane:Et₂O 70:30)

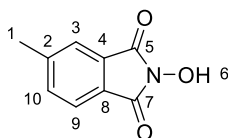
¹H NMR: (400 MHz, Chloroform-*d*) δ 7.88 (2H, m, H14 or H15), 7.78 (2H, m, H15 or H14), 7.38 – 7.27 (5H, m, H6, H7 & H8), 5.07 – 4.29 (3H, m, H4 & H9), 1.67 – 1.36 (12H, m, H1 & H10) ppm

¹³C NMR: (101 MHz, Chloroform-*d*) δ 168.9 (C11), 161.7 (C12), 155.2 (C3), 138.1 (C5), 134.9 (C14 or C15), 129.1 (C13), 128.7 (C7), 128.0 (C6), 127.6 (C8), 124.1 (C15 or C14), 82.2 (C2), 54.1 (C9), 51.0 (C4), 28.3 (C1), 16.4 (C10) ppm

HRMS (*m/z*): (ESI⁺) calc'd for C₂₃H₂₄N₂NaO₆ [M+Na]⁺: 447.1527; found: 447.1534

IR (ν_{\max}): 3065, 2977, 2933, 1816, 1789, 1742, 1697, 1367, 1153, 1052, 876, 733 cm⁻¹

2-Hydroxy-5-methylisoindoline-1,3-dione (369)



In a microwave vial, 5-methylisobenzofuran-1,3-dione **368** (4.00 g, 24.67 mmol, 1.00 equiv.) and hydroxylamine hydrochloride (3.40 g, 48.93 mmol, 2.00 equiv.) were dissolved in pyridine (20.00 mL) at room temperature. After stirring at room temperature for 5 min, the vial was sealed and the reaction mixture was stirred at 100 °C under microwave irradiation for 5 min. The yellow solution was allowed to cool to room temperature and was poured onto an aqueous solution of HCl (1.00 M, 40.00 mL) at 0 °C. The white precipitate was collected by filtration, washed with water and dried under high vacuum for 16 h to give compound **369** (3.80 g, 87%) as a white solid.

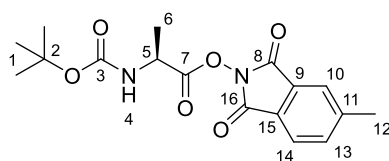
TLC: R_f = 0.33 (*n*-hexane:EtOAc 50:50)

¹H NMR: (500 MHz, Dimethyl sulfoxide-*d*₆) δ 10.83 (1H, br. s, H6), 7.70 (1H, d, J = 7.5 Hz, H9), 7.64 (1H, br. s, H3), 7.61 (1H, d, J = 7.5 Hz, H10), 2.45 (3H, s) ppm

¹³C NMR: (126 MHz, Dimethyl sulfoxide-*d*₆) δ 164.5 (C5 or C7), 164.4 (C7 or C5), 145.7 (C2), 134.9 (C10), 129.1 (C4 or C8), 126.1 (C8 or C4), 123.7 (C3), 123.1 (C9), 21.6 (C1) ppm

Spectral data were in accordance with that reported in the literature.²⁷³

5-Methyl-1,3-dioxoisindolin-2-yl (*tert*-butoxycarbonyl)-*L*-alaninate ((*S*)-371)



Carboxylic acid **328** (500 mg, 2.64 mmol, 1.00 equiv.) was activated with methyl-substituted *N*-hydroxyphthalimide **369** (468 mg, 2.64 mmol, 1.00 equiv.) and DIC (0.41 mL, 2.64 mmol, 1.00 equiv.) (no DMAP) according to **GP6**. The crude residue was purified by flash column chromatography (*n*-pentane:Et₂O 50:50) to give activated ester (**S**)-**371** (681 mg, 74%) as a colourless liquid.

TLC: *R*_f = 0.28 (*n*-pentane:Et₂O 50:50)

Compound (S)-371 exists as a 50:50 mixture of rotamers.

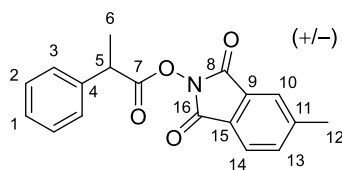
¹H NMR: (500 MHz, Dimethyl sulfoxide-*d*₆) δ 7.84 (0.5H, d, *J* = 7.7 Hz, H14), 7.79 (0.5H, s, H10), 7.74 (0.5H, d, *J* = 7.7 Hz, H13), 7.70 (0.5H, d, *J* = 7.6 Hz, H14), 7.65 (0.5H, s, H10), 7.62 (0.5H, d, *J* = 7.6 Hz, H13), 7.27 (0.5H, d, *J* = 6.5 Hz, H4), 7.07 (0.5H, d, *J* = 7.6 Hz, H4), 4.46 (0.5H, *app.* pent, *J*^{*app.*} = 7.3 Hz, H5), 3.90 (0.5H, *app.* pent, *J*^{*app.*} = 7.4 Hz, H5), 2.50 (1.5H, s, H12), 2.45 (1.5H, s, H12), 1.45 (1.5H, d, *J* = 7.4 Hz, H6), 1.39 (4.5H, s, H1), 1.36 (4.5H, s, H1), 1.21 (1.5H, d, *J* = 7.4 Hz, H6) ppm

¹³C NMR: (126 MHz, Dimethyl sulfoxide-*d*₆) δ 174.9 (C7), 170.7 (C7), 164.4 (C8 or C16), 164.4 (C16 or C8), 162.0 (C8 or C16), 161.9 (C16 or C8), 155.5 (C3), 155.3 (C3), 147.0 (C11), 145.7 (C11), 136.0 (C13), 135.0 (C13), 129.1 (C9 or C15), 128.6 (C9 or C15), 126.1 (C15 or C9), 125.6 (C15 or C9), 124.6 (C10), 124.2 (C14), 123.7 (C10), 123.1 (C14), 79.0 (C2), 78.2 (C2), 49.0 (C5), 47.7 (C5), 28.4 (C1), 28.3 (C1), 21.7 (C12), 21.6 (C12), 17.2 (C6), 17.1 (C6) ppm

HRMS (*m/z*): (ESI⁺) calc'd for C₁₇H₂₀N₂NaO₆ [M+Na]⁺: 371.1214; found: 371.1225

IR (ν_{max}): 3675, 3384, 2988, 2972, 2901, 1731, 1452, 1406, 1394, 1230, 1057, 869 cm⁻¹

(+/-)-5-Methyl-1,3-dioxoisindolin-2-yl 2-phenylpropanoate (**373**)



Carboxylic acid **328** (500 mg, 3.33 mmol, 1.00 equiv.) was activated with methyl-substituted *N*-hydroxyphthalimide **369** (590 mg, 3.33 mmol, 1.00 equiv.) and DIC (0.52 mL, 3.33 mmol, 1.00 equiv.) (no DMAP) according to **GP6**. The crude residue was purified by flash column chromatography (*n*-pentane:Et₂O 80:20) to give activated ester **373** (811 mg, 79%) as a colourless liquid.

TLC: *R*_f = 0.51 (*n*-pentane:Et₂O 50:50)

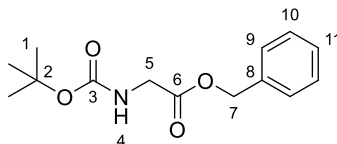
¹H NMR: (500 MHz, Chloroform-*d*) δ 7.69 (1H, d, J = 7.7 Hz, H14), 7.61 (1H, s, H10), 7.52 (1H, d, J = 7.7 Hz, H13), 7.39 – 7.32 (4H, m, H2 & H3), 7.28 (1H, m, H1), 4.07 (1H, q, J = 7.2 Hz, H5), 2.47 (3H, s, H12), 1.62 (3H, d, J = 7.2 Hz, H6) ppm

¹³C NMR: (126 MHz, Chloroform-*d*) δ 170.9 (C7), 162.2 (C8 or C16), 162.0 (C16 or C8), 146.3 (C11), 138.4 (C4), 135.3 (C13), 129.2 (C9 or C15), 128.9 (C2 or C3), 127.8 (C1), 127.6 (C3 or C2), 126.2 (C15 or C9), 124.5 (C10), 123.9 (C14), 43.0 (C5), 22.2 (C12), 19.0 (C6) ppm

HRMS (m/z): (ESI⁺) calc'd for C₁₈H₁₆NO₄ [M+H]⁺: 310.1074; found: 310.1077

IR (ν_{\max}): 3675, 2988, 2972, 2901, 1807, 1780, 1734, 1702, 1407, 1394, 1224, 1066, 1047 cm⁻¹

Benzyl (*tert*-butoxycarbonyl)glycinate (374)



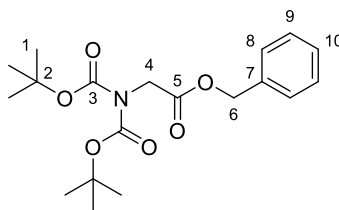
(*tert*-Butoxycarbonyl)-glycine **352** (200 mg, 1.14 mmol, 1.00 equiv.) and Cs₂CO₃ (371 mg, 1.14 mmol, 1.00 equiv.) were suspended in DMF (2.00 mL) at room temperature. Benzyl bromide (0.14 mL, 1.14 mmol, 1.00 equiv.) was added and the reaction mixture was stirred for 16 h. Water (7.00 mL) was added and the resulting suspension was extracted with a mixture *n*-hexane:EtOAc (50:50, 2.00 mL), then with pure *n*-hexane (3 × 2.00 mL). The organic layers were combined, washed with water (7.00 mL) and brine, dried over MgSO₄, filtered and concentrated to give ester **374** (275 mg, 91%) as a colourless liquid.

TLC: R_f = 0.14 (*n*-hexane:EtOAc 90:10)

¹H NMR: (500 MHz, Chloroform-*d*) δ 7.42 – 7.30 (5H, m, H9, H10 & H11), 5.18 (2H, s, H7), 4.73 (1H, m, H4), 3.90 (2H, m, H5), 1.45 (9H, s, H1) ppm

¹³C NMR: (126 MHz, Chloroform-*d*) δ 170.4 (C6), 155.8 (C3), 135.4 (C8), 128.8 (C10), 128.6 (C11), 128.5 (C9), 80.2 (C2), 67.2 (C7), 42.7 (C5), 28.5 (C1) ppm

Spectral data were in accordance with that reported in the literature.³⁰⁰

Benzyl (*N,N*-bis(*tert*-butoxycarbonyl))glycinate (375)

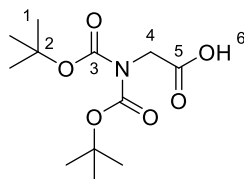
Benzyl ester **374** (275 mg, 1.04 mmol, 1.00 equiv.) was dissolved in anhydrous MeCN (2.00 mL) at room temperature under an atmosphere of nitrogen. DMAP (25 mg, 0.21 mmol, 0.20 equiv.) was added, followed by Boc₂O (227 mg, 1.04 mmol, 1.00 equiv.). The yellow solution was stirred at room temperature for 16 h and was concentrated under reduced pressure. The crude residue was purified by flash column chromatography (petroleum ether 40–60:EtOAc 95:5) to give compound **375** (372 mg, 98%) as a colourless liquid.

TLC: R_f = 0.30 (*n*-hexane:EtOAc 90:10)

¹H NMR: (500 MHz, Chloroform-*d*) δ 7.40 – 7.29 (5H, m, H8, H9 & H10), 5.18 (2H, s, H6), 4.37 (2H, s, H4), 1.46 (18H, s, H1) ppm

¹³C NMR: (126 MHz, Chloroform-*d*) δ 169.2 (C5), 152.0 (C3), 135.6 (C7), 128.7 (C9), 128.5 (C10), 128.5 (C8), 83.3 (C2), 67.0 (C6), 47.5 (C2), 28.1 (C1) ppm

Spectral data were in accordance with that reported in the literature.³⁰¹

***N,N*-Bis(*tert*-butoxycarbonyl))glycine (376)**

Benzyl ester **375** (370 mg, 1.01 mmol, 1.00 equiv.) and palladium on activated charcoal (10% w/w, 99 mg, 0.10 mmol, 0.10 equiv.) were suspended in MeOH (10.00 mL) at room temperature under argon atmosphere. The black suspension was purged with argon for 20 min. The inert atmosphere was purged with hydrogen and the reaction mixture was stirred for 4 h. The hydrogen atmosphere was replaced with argon and the black solid was removed by filtration over Celite®. The filtrate was concentrated and the residue was dried under high vacuum to give compound **376** (207 mg, 74%) as a white solid.

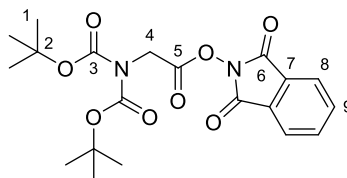
TLC: R_f = 0.13 (CH₂Cl₂:MeOH 95:5)

¹H NMR: (500 MHz, Chloroform-*d*) δ 4.39 (2H, s, H4), 1.50 (18H, s, H1) ppm

^{13}C NMR: (126 MHz, Chloroform-*d*) δ 174.5 (C5), 152.0 (C3), 83.5 (C2), 47.2 (C4), 28.1 (C1) ppm

Spectral data were in accordance with that reported in the literature.³⁰²

1,3-Dioxoisindolin-2-yl (*N,N*-bis(*tert*-butoxycarbonyl))glycinate (377**)**



Carboxylic acid **376** (207 mg, 0.75 mmol, 1.00 equiv.) was activated with *N*-hydroxyphthalimide (122 mg, 0.75 mmol, 1.00 equiv.) and DCC (155 mg, 0.75 mmol, 1.00 equiv.) according to **GP7**. The crude residue was purified by flash column chromatography (petroleum ether 40–60:EtOAc 80:20) to give activated ester **377** (296 mg, 94%) as a white solid.

TLC: R_f = 0.64 (*n*-hexane:EtOAc 50:50)

m.p.: 124 – 128 °C (diethyl ether)

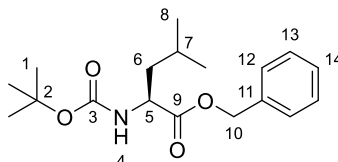
^1H NMR: (500 MHz, Chloroform-*d*) δ 7.96 – 7.85 (2H, m, H8 or H9), 7.85 – 7.73 (2H, m, H9 or H8), 4.75 (2H, s, H4), 1.54 (18H, s, H1) ppm

^{13}C NMR: (126 MHz, Chloroform-*d*) δ 166.1 (C5), 161.6 (C6), 150.9 (C3), 135.0 (C8 or C9), 129.0 (C7), 124.2 (C9 or C8), 84.2 (C2), 45.5 (C4), 28.0 (C1) ppm

HRMS (m/z): (ESI⁺) calc'd for C₂₀H₂₄N₂NaO₈ [M+Na]⁺: 443.1425; found: 443.1437

IR (ν_{max}): 2980, 2934, 1832, 1794, 1747, 1369, 1343, 1228, 1145, 1116, 1092, 697 cm⁻¹

Benzyl (*tert*-butoxycarbonyl)-*L*-leucinate ((*S*)-379**)**



(*tert*-Butoxycarbonyl)-*L*-leucine (**S**)-**355** (200 mg, 0.86 mmol, 1.00 equiv.) and Cs₂CO₃ (282 mg, 0.86 mmol, 1.00 equiv.) were suspended in DMF (2.00 mL) at room temperature. Benzyl bromide (0.10 mL, 0.86 mmol, 1.00 equiv.) was added and the reaction mixture was stirred for 4 h. Water (7.00 mL) was added and the resulting suspension was extracted with *n*-hexane

(4 × 2.00 mL). The organic layers were combined, washed with water (7.00 mL) and brine, dried over MgSO₄, filtered and concentrated to give ester (**S**)-**379** (250 mg, 90%) as a colourless liquid.

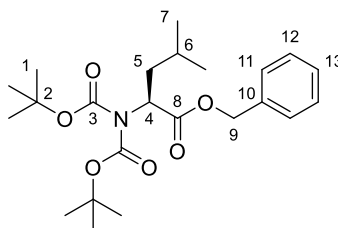
TLC: R_f = 0.33 (*n*-pentane:EtOAc 90:10)

¹H NMR: (500 MHz, Chloroform-*d*) δ 7.43 – 7.29 (5H, m, H12, H13 & H14), 5.19 (1H, d, J = 12.4 Hz, H10), 5.13 (1H, d, J = 12.4 Hz, H10'), 4.75 (1H, m, H4), 4.25 (1H, m, H5), 1.70 (1H, m, H7), 1.62 (1H, m, H6), 1.49 (1H, ddd, J = 13.5, 9.2, 5.7 Hz, H6'), 1.43 (9H, s, H1), 0.92 (6H, m, H8) ppm

¹³C NMR: (126 MHz, Chloroform-*d*) δ 173.5 (C9), 155.5 (C3), 135.7 (C11), 128.7 (C_{Ar}), 128.5 (C_{Ar}), 128.3 (C_{Ar}), 80.0 (C2), 67.0 (C10), 52.3 (C5), 41.9 (C6), 28.5 (C1), 24.9 (C7), 23.0 (C8), 22.0 (C8') ppm

Spectral data were in accordance with that reported in the literature.³⁰³

Benzyl (*N,N*-bis(*tert*-butoxycarbonyl))-*L*-leucinate ((*S*)-380**)**



Benzyl ester (**S**)-**379** (250 mg, 0.78 mmol, 1.00 equiv.) was dissolved in anhydrous MeCN (1.00 mL) at room temperature under an atmosphere of nitrogen. DMAP (19 mg, 0.16 mmol, 0.20 equiv.) was added, followed by Boc₂O (188 mg, 0.86 mmol, 1.10 equiv.). The orange solution was stirred at room temperature for 16 h. Boc₂O (94 mg, 0.43 mmol, 0.50 equiv.) was added and the reaction mixture was stirred at room temperature for 16 h. The orange solution was concentrated and the crude residue was purified by flash column chromatography (*n*-hexane:Et₂O 95:5) to give compound (**S**)-**380** (267 mg, 81%) as a colourless liquid.

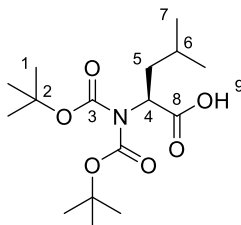
TLC: R_f = 0.39 (*n*-hexane:EtOAc 90:10)

¹H NMR: (500 MHz, Chloroform-*d*) δ 7.36 – 7.27 (5H, m, H11, H12 & H13), 5.16 (1H, d, J = 12.5 Hz, H9), 5.13 (1H, d, J = 12.5 Hz, H9'), 4.96 (1H, dd, J = 9.6, 5.1 Hz, H4), 1.92 (1H, ddd, J = 14.3, 9.2, 5.1 Hz, H5), 1.86 (1H, ddd, J = 14.3, 9.6, 4.8 Hz, H5'), 1.63 (1H, d, J = 9.2, 6.7, 4.8 Hz, H6), 1.44 (18H, s, H1), 0.91 (6H, m, H7) ppm

¹³C NMR: (126 MHz, Chloroform-*d*) δ 171.4 (C8), 152.4 (C3), 135.9 (C10), 128.6 (C12), 128.2 (C13), 128.1 (C11), 83.1 (C2), 66.8 (C9), 56.8 (C4), 38.5 (C5), 28.1 (C1), 25.2 (C6), 23.4 (C7), 21.9 (C7') ppm

Spectral data were in accordance with that reported in the literature.³⁰¹

***N,N*-Bis(*tert*-butoxycarbonyl)-*L*-leucine ((*S*)-**381**)**



Benzyl ester (**S**)-**380** (265 mg, 0.63 mmol, 1.00 equiv.) and palladium on activated charcoal (10% w/w, 335 mg, 0.32 mmol, 0.51 equiv.) were suspended in MeOH (10.00 mL) at room temperature under argon atmosphere. The black suspension was purged with argon for 20 min. The inert atmosphere was purged with hydrogen and the reaction mixture was stirred for 6 h. The hydrogen atmosphere was replaced with argon and the black solid was removed by filtration over Celite®. The filtrate was concentrated and the residue was dried under high vacuum to give compound (**S**)-**381** (192 mg, 92%) as a white solid.

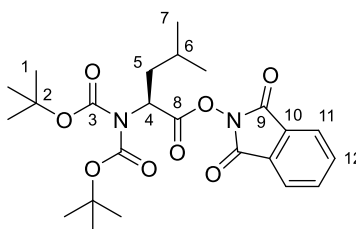
TLC: R_f = 0.16 (CH₂Cl₂:MeOH 95:5)

¹H NMR: (500 MHz, Chloroform-*d*) δ 4.96 (1H, dd, J = 9.4, 5.2 Hz, H4), 1.88 (1H, ddd, J = 14.2, 9.1, 5.2 Hz, H5), 1.83 (1H, ddd, J = 14.2, 9.4, 4.8 Hz, H5'), 1.62 (1H, dheptd, J = 9.1, 6.7, 4.8 Hz, H6), 1.50 (18H, s, H1), 0.93 (6H, m, H7) ppm

¹³C NMR: (126 MHz, Chloroform-*d*) δ 176.7 (C8), 152.4 (C3), 83.4 (C2), 56.7 (C4), 38.7 (C5), 28.1 (C1), 25.2 (C6), 23.3 (C7), 22.0 (C7') ppm

Spectral data were in accordance with that reported in the literature.³⁰¹

1,3-Dioxoisindolin-2-yl (*N,N*-bis(*tert*-butoxycarbonyl))-*L*-leucinate ((*S*)-382**)**



Carboxylic acid (**S**)-**381** (190 mg, 0.57 mmol, 1.00 equiv.) was activated with *N*-hydroxyphthalimide (94 mg, 0.57 mmol, 1.00 equiv.) and DCC (118 mg, 0.57 mmol, 1.00 equiv.) according to **GP7**. The crude residue was concentrated and triturated in cold EtOAc. The solid was removed by filtration and the filtrate was concentrated under reduced pressure. The resulting

residue was dried under high vacuum to give activated ester (**S**)-**382** (215 mg, 79%) as a pale yellow solid.

TLC: R_f = 0.25 (*n*-hexane:EtOAc 80:20)

m.p.: 96 – 98 °C (diethyl ether)

¹H NMR: (500 MHz, Chloroform-*d*) δ 7.87 (2H, m, H11 or H12), 7.78 (2H, m, H12 or H11), 5.37 (1H, m, H4), 1.99 (2H, m, H5), 1.70 (1H, m, H6), 1.55 (18H, s, H1), 0.98 (6H, m, H7) ppm

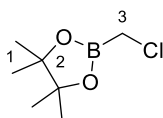
¹³C NMR: (126 MHz, Chloroform-*d*) δ 167.9 (C8), 161.7 (C9), 151.4 (C3), 134.8 (C11 or C12), 129.1 (C10), 124.0 (C12 or C11), 84.2 (C2), 55.1 (C4), 38.9 (C5), 28.0 (C1), 25.0 (C6), 23.3 (C7), 21.9 (C7') ppm

HRMS (m/z): (ESI⁺) calc'd for C₂₄H₃₂N₂NaO₈ [M+Na]⁺: 499.2051; found: 499.2057

IR (ν_{\max}): 3511, 3211, 2981, 2937, 1757, 1732, 1699, 1368, 1338, 1228, 1144, 1111, 965, 853, 787 cm⁻¹

$[\alpha]_D^{24}$: +1 (CHCl₃, *c* = 2.0)

2-(Chloromethyl)-4,4,5,5-tetramethyl-1,3,2-dioxaborolane (**385**)



In a flame-dried Schlenk tube, 2-isopropoxy-4,4,5,5-tetramethyl-1,3,2-dioxaborolane (4.08 mL, 20.00 mmol, 1.00 equiv.) and bromochloromethane (1.43 mL, 22.00 mmol, 1.10 equiv.) were dissolved in anhydrous THF (20.00 mL) at –78 °C under an atmosphere of nitrogen. A solution of *n*-BuLi (1.54 M in *n*-hexane, 14.29 mL, 22.00 mmol, 1.10 equiv.) was added dropwise and the reaction mixture was stirred at –78 °C for 30 min. TMSCl (3.05 mL, 24.00 mmol, 1.20 equiv.) was added and the reaction mixture was stirred at –78 °C for 10 min. The acetone/dry ice bath was removed and the reaction mixture was stirred at room temperature for 16 h. Water (25 mL) was added, layers were separated and the aqueous phase was extracted with Et₂O (3 × 10.00 mL). The organic layers were combined, washed with brine, dried over MgSO₄, filtered and concentrated. The crude residue was purified by distillation (60 mbar; 95–100 °C at the top of the column) to obtain boronic ester **385** (1.88 g, 53%) as a colourless liquid.

TLC: *Unstable on silica.*

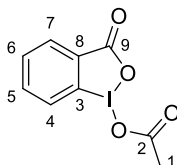
¹H NMR: (400 MHz, Chloroform-*d*) δ 2.95 (2H, s, H3), 1.28 (12H, s, H1) ppm

¹³C NMR: (101 MHz, Chloroform-*d*) δ 84.8 (C2), 24.8 (C1), 23.8* (C3) ppm

**shift value determined by HSQC correlation.*

Spectral data were in accordance with that reported in the literature.³⁰⁴

3-Oxo-1 λ^3 -benzo[d][1,2]iodaoxol-1(3*H*)-yl acetate (**387**)



In a round-bottomed flask, 2-iodobenzoic acid **404** (1.24 g, 5.00 mmol, 1.00 equiv.) was dissolved in a mixture of AcOH and Ac₂O (50:50, 40.00 mL) at room temperature. *m*-CPBA (77% w/w, 1.23 g, 5.50 mmol, 1.10 equiv.) was added and the reaction mixture was stirred at 60 °C for 48 h. The yellow solution was allowed to cool to room temperature and Et₂O (40.00 mL) was added, followed by *n*-pentane (40.00 mL). The suspension was stored at –20 °C for 16 h and the white precipitate was collected by filtration to obtain compound **387** (742 mg, 48%) as a pale yellow solid.

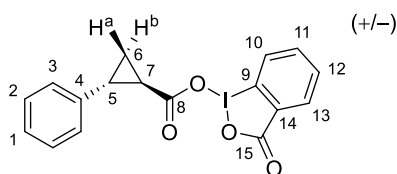
TLC: *Unstable on silica.*

¹H NMR: (400 MHz, Dimethyl sulfoxide-*d*₆) δ 8.01 (1H, dd, J = 7.5, 1.5 Hz, H4 or H7), 7.96 (1H, ddd, J = 8.2, 7.2, 1.5 Hz, H5 or H6), 7.83 (1H, dd, J = 8.2, 1.0 Hz, H7 or H4), 7.70 (1H, ddd, J = 7.5, 7.2, 1.0 Hz, H6 or H5), 1.90 (3H, s, H1) ppm

¹³C NMR: (126 MHz, Dimethyl sulfoxide-*d*₆) δ 172.3 (C2), 168.1 (C9), 134.8 (C5 or C6), 131.5 (C3 or C8), 131.3 (C4 or C7), 130.6 (C6 or C5), 126.4 (C7 or C4), 120.6 (C8 or C3), 21.2 (C1) ppm

Spectral data were in accordance with that reported in the literature.²⁷⁶

3-Oxo-1 λ^3 -benzo[d][1,2]iodaoxol-1(3*H*)-yl *trans*-2-phenylcyclopropane-1-carboxylate (**405**)



In a round-bottomed flask, acetate **387** (200 mg, 0.65 mmol, 1.00 equiv.) and *trans*-2-phenylcyclopropane-1-carboxylic acid **307** (106 mg, 0.65 mmol, 1.00 equiv.) were suspended in xylenes (7.00 mL) at room temperature. The suspension was heated at 75 °C under reduced pressure (~200 mbar). After complete removal of the solvent, the white residual powder was suspended

in petroleum ether 40–60 (4.00 mL), collected by filtration, washed with *n*-pentane and dried under high vacuum to obtain compound **405** (97 mg, 37%) as a white solid.

TLC: *Unstable on silica.*

m.p.: 201 – 205 °C (xylenes)

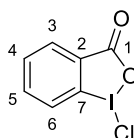
¹H NMR: (500 MHz, Dimethyl sulfoxide-*d*₆) δ 8.01 (1H, dd, *J* = 7.5, 1.4 Hz, H10 or H13), 7.96 (1H, ddd, *J* = 8.2, 7.2, 1.4 Hz, H11 or H12), 7.83 (1H, dd, *J* = 8.2, 1.0 Hz, H13 or H10), 7.70 (1H, ddd, *J* = 7.5, 7.4, 1.0 Hz, H12 or H11), 7.26 (2H, m, H2 or H3), 7.18 (1H, m, H1), 7.14 (2H, m, H3 or H2), 2.36 (1H, ddd, *J* = 9.3, 6.4, 4.2 Hz, H5), 1.78 (1H, ddd, *J* = 8.4, 5.3, 4.2 Hz, H7), 1.41 (1H, ddd, *J* = 9.3, 5.3, 4.4 Hz, H6^b), 1.32 (1H, ddd, *J* = 8.4, 6.4, 4.4 Hz, H6^a) ppm

¹³C NMR: (126 MHz, Dimethyl sulfoxide-*d*₆) δ 174.2 (C8), 168.1 (C15), 140.4 (C4), 134.8 (C11 or C12), 131.5 (C9 or C14), 131.3 (C10 or C13), 130.6 (C12 or C11), 128.6 (C2 or C3), 126.5 (C13 or C10 or C1), 126.4 (C1 or C13 or C10), 126.1 (C3 or C2), 120.6 (C14 or C9), 25.5 (C5), 24.4 (C7), 16.8 (C6) ppm

HRMS (*m/z*): *Despite repeated attempts, a HRMS could not be obtained.*

IR (*ν*_{max}): 3670, 3085, 3059, 2989, 2903, 2756, 2647, 2547, 2414, 1688, 1620, 1442, 1341, 1230, 1117, 742, 696, 546 cm⁻¹

1-Chloro-1λ³-benzo[*d*][1,2]iodaoxol-3(1*H*)-one (**412**)



In a round-bottomed flask, 2-iodobenzoic acid **404** (2.00 g, 7.90 mmol, 1.00 equiv.) was dissolved in anhydrous MeCN (75.00 mL) at 75 °C under an atmosphere of nitrogen. A solution of trichloroisocyanuric acid (637 mg, 2.67 mmol, 0.34 equiv.) in anhydrous MeCN (3.00 mL) was added dropwise and the reaction mixture was stirred at 75 °C for 5 min. The white precipitate was removed by filtration over Celite® in a pre-heated sintered funnel and the filtrate was concentrated to afford a yellow suspension, which was allowed to cool to room temperature. The resulting white solid was collected by filtration and dried under high vacuum to give, after two crops, compound **412** (1.25 g, 56%) as a white solid.

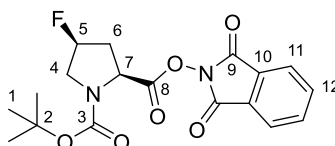
TLC: *Unstable on silica.*

¹H NMR: (500 MHz, Dimethyl sulfoxide-*d*₆) δ 7.96 (1H, d, *J* = 7.9 Hz, H3 or H6), 7.69 (1H, d, *J* = 7.7 Hz, H6 or H3), 7.47 (1H, dd, *J* = 7.7, 7.5 Hz, H4 or H5), 7.22 (1H, dd, *J* = 7.9, 7.5 Hz, H5 or H4) ppm

^{13}C NMR: (126 MHz, Dimethyl sulfoxide- d_6) δ 168.4 (C1), 140.7 (C3 or C6), 137.1 (C2 or C7), 132.7 (C4 or C5), 130.2 (C6 or C3), 128.4 (C5 or C4), 94.2 (C7 or C2) ppm

Spectral data were in accordance with that reported in the literature.²⁷⁷

1-(*tert*-Butyl) 2-(1,3-dioxoisindolin-2-yl) (2*S*,4*S*)-4-fluoropyrrolidine-1,2-dicarboxylate (414)



Carboxylic acid **413** (117 mg, 0.50 mmol, 1.00 equiv.) was activated with *N*-hydroxyphthalimide (82 mg, 0.50 mmol, 1.00 equiv.), DIC (0.08 mL, 0.50 mmol, 1.00 equiv.) and DMAP (6 mg, 0.05 mmol, 0.10 equiv.) according to **GP6**. The crude residue was purified by flash column chromatography (*n*-hexane:EtOAc 70:30) to give activated ester **414** (175 mg, 93%) as a white solid.

TLC: R_f = 0.37 (*n*-hexane:EtOAc 50:50)

m.p.: 126 – 128 °C (diethyl ether)

^1H NMR: (400 MHz, Chloroform- d) δ 7.88 (2H, m, H11 or H12), 7.78 (2H, m, H12 or H11), 5.29 (1H, *app.* dt, $J^{app.}$ = 52.1, 4.0 Hz, H5), 4.80 (1H, dd, J = 10.1, 1.5 Hz, H7), 3.94 (1H, ddd, J = 25.3, 13.1, 1.9 Hz, H4), 3.70 (1H, ddd, J = 35.2, 13.1, 4.2 Hz, H4'), 2.82 (1H, m, H6), 2.60 (1H, dddd, J = 39.8, 14.6, 10.1, 4.0 Hz, H6'), 1.51 (9H, m, H1) ppm

^{13}C NMR: (101 MHz, Chloroform- d) δ 168.3 (C8), 161.7 (C9), 153.4 (C3), 134.9 (C11 or C12), 129.1 (C10), 124.1 (C12 or C11), 90.9 (d, J = 179.2 Hz, C5), 81.8 (C2), 56.0 (C7), 53.1 (d, J = 24.4 Hz, C4), 37.8 (d, J = 22.6 Hz, C6), 28.2 (C1) ppm

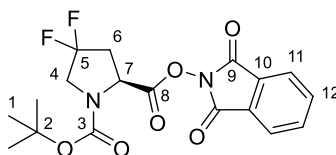
^{19}F NMR (377 MHz, Chloroform- d) δ -173.0 (ddddd, J = 52.1, 39.8, 35.2, 25.3, 18.4 Hz) ppm

HRMS (m/z): (ESI⁺) calc'd for C₁₈H₁₉FN₂NaO₆ [M+Na]⁺: 401.1119; found: 401.1136

IR (ν_{max}): 2977, 1828, 1791, 1742, 1701, 1392, 1366, 1040, 877, 697 cm⁻¹

$[\alpha]_D^{23}$: -45 (CHCl₃, c = 1.0)

1-(*tert*-Butyl) 2-(1,3-dioxisoindolin-2-yl) (*S*)-4,4-difluoropyrrolidine-1,2-dicarboxylate ((*S*)-417)



Carboxylic acid (**S**)-**416** (125 mg, 0.50 mmol, 1.00 equiv.) was activated with *N*-hydroxyphthalimide (82 mg, 0.50 mmol, 1.00 equiv.), DIC (0.08 mL, 0.50 mmol, 1.00 equiv.) and DMAP (6 mg, 0.05 mmol, 0.10 equiv.) according to **GP6**. The crude residue was purified by flash column chromatography (*n*-hexane:EtOAc 70:30) to give activated ester (**S**)-**417** (169 mg, 85%) as a white solid.

TLC: R_f = 0.61 (*n*-hexane:EtOAc 50:50)

m.p.: 116 – 119 °C (diethyl ether)

^1H NMR: (400 MHz, Chloroform-*d*) δ 7.89 (2H, m, H11 or H12), 7.80 (2H, m, H12 or H11), 4.85 (1H, m, H7), 4.02 – 3.78 (2H, m, H4 & H4'), 2.95 (1H, m, H6), 2.82 (1H, m, H6'), 1.51 (9H, m, H1) ppm

^{13}C NMR: (101 MHz, Chloroform-*d*) δ 167.9 (C8), 161.6 (C9), 152.8 (C3), 135.1 (C11 or C12), 129.0 (C10), 124.2 (C12 or C11), 82.7 (C2), 55.4 (C7), 52.9 (t, J = 31.8 Hz, C4), 39.0 (t, J = 26.5 Hz, C6), 28.1 (C1) ppm

Due to its low intensity, the expected triplet corresponding to C5 could not be distinguished from the baseline.

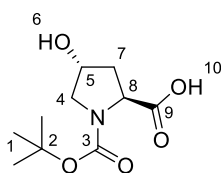
^{19}F NMR: (377 MHz, Chloroform-*d*) δ –99.8 (2F, m) ppm

HRMS (m/z): (ESI⁺) calc'd for C₁₈H₁₈F₂N₂NaO₆ [M+Na]⁺: 419.1040; found: 419.1025

IR (ν_{max}): 2979, 1824, 1792, 1745, 1710, 1394, 1369, 1153, 1104, 1079, 697 cm^{–1}

$[\alpha]_D^{23}$: –55 (CHCl₃, c = 1.0)

(2*S*,4*R*)-1-(*tert*-Butoxycarbonyl)-4-hydroxypyrrolidine-2-carboxylic acid (419)



(2*S*,4*R*)-4-hydroxypyrrolidine-2-carboxylic acid (131 mg, 1.00 mmol, 1.00 equiv.) was suspended in a mixture of THF and water (2:1, 3.00 mL) at room temperature. An aqueous solution

of NaOH (10% w/w, 0.50 mL) was added, followed by Boc₂O (327 mg, 1.50 mmol, 1.50 equiv.). The reaction mixture was stirred at room temperature for 2 days and pH was brought to 3 by addition of an aqueous solution of HCl (2.00 M) and the reaction mixture was extracted with EtOAc (3 × 3.00 mL). The organic layers were combined, washed with brine, dried over MgSO₄, filtered and concentrated. The crude residue was purified by flash column chromatography (*n*-hexane:Et₂O 80:20) to give compound **419** (229 mg, 99%) as a white solid.

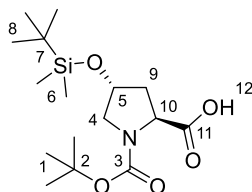
TLC: *R*_f = 0.12 (CH₂Cl₂:MeOH 90:10)

¹H NMR: (400 MHz, Chloroform-*d*) δ 4.51 – 4.27 (2H, m, H5 & H8), 3.65 – 3.34 (2H, m, H4), 2.38 – 2.05 (2H, m, H7), 1.41 (9H, m, H1) ppm

¹³C NMR: (101 MHz, Chloroform-*d*) δ 176.1 (C9), 154.3 (C3), 80.5 (C2), 69.3 (C5 or C8), 58.0 (C8 or C5), 54.6 (C4), 39.2 (C7), 28.4 (C1) ppm

Spectral data were in accordance with that reported in the literature.³⁰⁵

(2*S*,4*R*)-1-(*tert*-Butoxycarbonyl)-4-((*tert*-butyldimethylsilyl)oxy)pyrrolidine-2-carboxylic acid (420**)**



Proline derivative **419** (229 mg, 0.99 mmol, 1.00 equiv.) and imidazole (297 mg, 4.36 mmol, 4.40 equiv.) were dissolved in DMF (3.00 mL) at room temperature. TBSCl (328 mg, 2.18 mmol, 2.20 equiv.) was added portionwise and the resulting mixture was stirred at room temperature for 16 h. Water (3.00 mL) was added and the pH was brought to 3 by addition of an aqueous solution of citric acid (10% w/w). The reaction mixture was extracted with EtOAc (3 × 5.00 mL). The organic layers were combined, washed with water (3 × 5.00 mL) and brine, dried over MgSO₄, filtered and concentrated. The residue was purified by flash column chromatography (*n*-hexane:EtOAc 80:20→50:50) to give compound **420** (265 mg, 77%) as a colourless liquid.

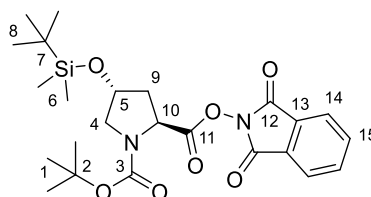
TLC: *R*_f = 0.28 (CH₂Cl₂:MeOH 90:10)

¹H NMR: (400 MHz, Chloroform-*d*) δ 9.78 (1H, br. s, H12), 4.55 – 4.27 (2H, m, H5 & H10), 3.67 – 3.26 (2H, m, H4), 2.40 – 1.99 (2H, m, H9), 1.44 (9H, m, H1), 0.86 (9H, s, H8), 0.06 (6H, s, H6) ppm

^{13}C NMR: (101 MHz, Chloroform-*d*) δ 179.1 (C11), 154.0 (C3), 80.7 (C2), 69.9 (C5 or C10), 58.1 (C10 or C5), 55.1 (C4), 39.9 (C9), 28.5 (C1), 25.8 (C8), 18.0 (C7), -4.6 (C6), -4.8 (C6') ppm

Spectral data were in accordance with that reported in the literature.³⁰⁶

1-(*tert*-Butyl) 2-(1,3-dioxoisindolin-2-yl) (2*S*,4*R*)-4-((*tert*-butyldimethylsilyl)oxy)pyrrolidine-1,2-dicarboxylate (421**)**



Carboxylic acid **420** (265 mg, 0.77 mmol, 1.00 equiv.) was activated with *N*-hydroxyphthalimide (125 mg, 0.77 mmol, 1.00 equiv.), DIC (0.12 mL, 0.77 mmol, 1.00 equiv.) and DMAP (9 mg, 0.08 mmol, 0.10 equiv.) according to **GP6**. The crude residue was purified by flash column chromatography (*n*-hexane:EtOAc 80:20) to give activated ester **421** (332 mg, 88%) as a white solid.

TLC: R_f = 0.57 (*n*-hexane:EtOAc 50:50)

m.p.: 142 – 145 °C (diethyl ether)

^1H NMR: (400 MHz, Chloroform-*d*) δ 7.88 (2H, m, H14 or H15), 7.77 (2H, m, H15 or H14), 4.70 (1H, m, H10), 4.51 (1H, m, H5), 3.62 (1H, m, H4), 3.13 (1H, m, H4'), 2.49 – 2.32 (3H, m, H9), 1.49 (9H, m, H1), 0.87 (9H, m, H8), 0.08 (6H, m, H6) ppm

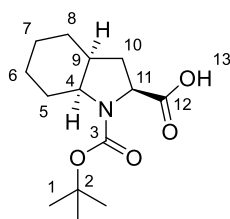
^{13}C NMR: (101 MHz, Chloroform-*d*) δ 169.8 (C11), 161.8 (C12), 153.8 (C3), 134.9 (C14 or C15), 129.0 (C13), 124.1 (C15 or C14), 81.5 (C2), 69.7 (C5), 56.4 (C10), 54.5 (C4), 40.4 (C9), 28.2 (C1), 25.8 (C8), 18.1 (C7), -4.7 (C6) ppm

HRMS (m/z): (ESI⁺) calc'd for C₂₄H₃₄N₂NaO₇Si [M+Na]⁺: 513.2027; found: 513.2010

IR (ν_{max}): 2954, 2931, 2886, 2858, 1820, 1791, 1745, 1707, 1392, 1367, 1254, 1161, 1119, 1080, 877, 836, 778, 696 cm⁻¹

$[\alpha]_D^{22}$: -41 (CHCl₃, *c* = 1.0)

(2*S*,3*aS*,7*aS*)-1-(*tert*-Butoxycarbonyl)octahydro-1*H*-indole-2-carboxylic acid (423**)**



(2*S*,3*aS*,7*aS*)-octahydro-1*H*-indole-2-carboxylic acid (102 mg, 0.60 mmol, 1.00 equiv.) was dissolved in CH₂Cl₂ (2.00 mL) by addition of Et₃N (0.17 mL, 1.20 mmol, 2.00 equiv.) at room temperature. Boc₂O (144 mg, 0.66 mmol, 1.10 equiv.) was added and the reaction mixture was stirred at room temperature for 2 days. CH₂Cl₂ (3.00 mL) was added and the reaction mixture was washed with an aqueous solution of HCl (1.00 M, 6.00 mL). The layers were separated and the aqueous phase was extracted with CH₂Cl₂ (3 × 5.00 mL). The organic layers were combined, dried over MgSO₄, filtered and concentrated. The crude residue was purified by flash column chromatography (*n*-hexane:Et₂O 90:10, then CH₂Cl₂:MeOH 95:5) to give compound **423** (147 mg, 91%) as a white solid.

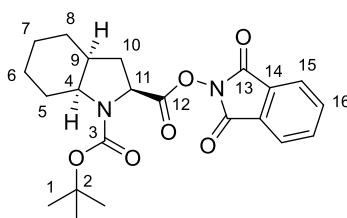
TLC: *R*_f = 0.49 (CH₂Cl₂:MeOH 90:10)

¹H NMR: (400 MHz, Chloroform-*d*) δ 9.81 (1H, br. s, H13), 4.27 (1H, br. s, H11), 3.80 (1H, br. s, H4), 2.43 – 1.82 (4H, m 4 × CH), 1.77 – 1.56 (3H, m, 3 × CH), 1.52 – 1.37 (10H, m, H1 & CH), 1.36 – 1.21 (2H, m, 2 × CH), 1.20 – 1.04 (1H, m, CH) ppm

¹³C NMR: (101 MHz, Chloroform-*d*) δ 176.0 (C12), 156.1 (C3), 81.2 (C2), 59.2 (C11), 58.0 (C4), 36.6 (C9), 30.7 (CH₂), 28.5 (C1), 28.0 (CH₂), 25.9 (CH₂), 23.8 (CH₂), 20.6 (CH₂) ppm

Spectral data were in accordance with that reported in the literature.³⁰⁷

1-(*tert*-Butyl) 2-(1,3-dioxoisindolin-2-yl) (2*S*,3*aS*,7*aS*)-octahydro-1*H*-indole-1,2-dicarboxylate (424**)**



Carboxylic acid **423** (147 mg, 0.55 mmol, 1.00 equiv.) was activated with *N*-hydroxyphthalimide (89 mg, 0.55 mmol, 1.00 equiv.), DIC (0.08 mL, 0.55 mmol, 1.00 equiv.) and DMAP (7 mg,

0.06 mmol, 0.10 equiv.) according to **GP6**. The crude residue was purified by flash column chromatography (*n*-hexane:EtOAc 80:20) to give activated ester **424** (168 mg, 74%) as a colourless wax.

TLC: R_f = 0.22 (*n*-hexane:EtOAc 80:20)

^1H NMR: (400 MHz, Chloroform-*d*) δ 7.88 (2H, m, H15 or H16), 7.77 (2H, m, H16 or H15), 4.59 (1H, m, H11), 3.86 (1H, m, H4), 2.48 – 2.22 (3H, m, H9 & CH₂), 2.04 (1H, m, CH), 1.78 (1H, m, CH), 1.72 – 1.62 (2H, m, 2 \times CH), 1.53 – 1.44 (10H, m, H1 & CH), 1.43 – 1.28 (2H, m, 2 \times CH), 1.15 (1H, m, CH) ppm

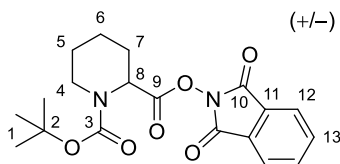
^{13}C NMR: (101 MHz, Chloroform-*d*) δ 170.3 (C12), 161.9 (C13), 153.2 (C3), 134.9 (C15 or C16), 129.1 (C14), 124.0 (C16 or C15), 81.1 (C2), 57.4 (C4), 57.2 (C11), 36.7 (C9), 33.3 (C10), 28.3 (C1), 27.7 (CH₂), 25.9 (CH₂), 23.7 (CH₂), 20.6 (CH₂) ppm

HRMS (m/z): (ESI⁺) calc'd for C₂₂H₂₆N₂NaO₆ [M+Na]⁺: 437.1683; found: 437.1689

IR (ν_{max}): 2974, 2930, 1819, 1790, 1742, 1697, 1391, 1366, 1163, 1081, 972, 877, 696 cm⁻¹

$[\alpha]_D^{22}$: –38 (CHCl₃, *c* = 1.0)

(+/-)-1-(*tert*-Butyl) 2-(1,3-dioxoisindolin-2-yl) piperidine-1,2-dicarboxylate (427**)**



Carboxylic acid **426** (229 mg, 1.00 mmol, 1.00 equiv.) was activated with *N*-hydroxyphthalimide (163 mg, 1.00 mmol, 1.00 equiv.), DIC (0.15 mL, 1.00 mmol, 1.00 equiv.) and DMAP (12 mg, 0.10 mmol, 0.10 equiv.) according to **GP6**. The crude residue was purified by flash column chromatography (*n*-hexane:EtOAc 80:20) to give activated ester **427** (328 mg, 88%) as a white solid.

TLC: R_f = 0.24 (*n*-hexane:EtOAc 80:20)

m.p.: 96 – 99 °C (diethyl ether)

^1H NMR: (400 MHz, Chloroform-*d*) δ 7.88 (2H, m, H12 or H13), 7.78 (2H, m, H13 or H12), 5.26 (1H, m, H8), 4.02 (1H, m, H4), 3.07 (1H, m, H4'), 2.36 (1H, m, CH), 1.94 – 1.64 (3H, m, 3 \times CH), 1.57 – 1.39 (11H, m, H1 & 2 \times CH) ppm

^{13}C NMR: (101 MHz, Chloroform-*d*) δ 168.9 (C9), 161.8 (C10), 155.3 (C3), 134.9 (C12 or C13), 129.1 (C11), 124.1 (C13 or C12), 81.2 (C2), 53.7 (C8), 41.3 (C5), 28.3 (C1), 27.3 (CH₂), 24.5 (CH₂), 20.4 (CH₂) ppm

HRMS (m/z): (ESI⁺) calc'd for C₁₉H₂₂N₂NaO₆ [M+Na]⁺: 397.1370; found: 397.1379

IR (ν_{max}): 2974, 2941, 2867, 1815, 1787, 1745, 1704, 1367, 1162, 1066, 877, 697 cm⁻¹

REFERENCES

1. Burns, M.; Essafi, S.; Bame, J. R.; Bull, S. P.; Webster, M. P.; Balieu, S.; Dale, J. W.; Butts, C. P.; Harvey, J. N.; Aggarwal, V. K. *Nature* **2014**, *513*, 183.
2. Fawcett, A.; Pradeilles, J.; Wang, Y.; Mutsuga, T.; Myers, E. L.; Aggarwal, V. K. *Science* (80-.). **2017**, *357*, 283.
3. Brown, H. C.; Zweifel, G. *J. Am. Chem. Soc.* **1961**, *83*, 486.
4. Collins, B. S. L.; Wilson, C. M.; Myers, E. L.; Aggarwal, V. K. *Angew. Chemie Int. Ed.* **2017**, *56*, 11700.
5. Sandford, C.; Aggarwal, V. K. *Chem. Commun.* **2017**, *53*, 5481.
6. Aggarwal, V. K.; Fang, G. Y.; Ginesta, X.; Howells, D. M.; Zaja, M. *Pure Appl. Chem.* **2006**, *78*, 215.
7. Beckmann, E.; Desai, V.; Hoppe, D. *Synlett* **2004**, 2275.
8. Bottoni, A.; Lombardo, M.; Neri, A.; Trombini, C. *J. Org. Chem.* **2003**, *68*, 3397.
9. Brown, H. C.; Zweifel, G. *J. Am. Chem. Soc.* **1961**, *83*, 2544.
10. Lennox, A. J. J.; Lloyd-Jones, G. C. *Chem. Soc. Rev.* **2014**, *43*, 412.
11. Matteson, D. S. *J. Organomet. Chem.* **1999**, *581*, 51.
12. Zweifel, G.; Arzoumanian, H.; Whitney, C. C. *J. Am. Chem. Soc.* **1967**, *89*, 3652.
13. Matteson, D. S.; Jesthi, P. K. *J. Organomet. Chem.* **1976**, *110*, 25.
14. Matteson, D. S. *Synthesis (Stuttg.)* **1975**, *1975*, 147.
15. Evans, D. A.; Thomas, R. C.; Walker, J. A. *Tetrahedron Lett.* **1976**, *17*, 1427.
16. Evans, D. A.; Crawford, T. C.; Thomas, R. C.; Walker, J. A. *J. Org. Chem.* **1976**, *41*, 3947.
17. Wang, Y.; Noble, A.; Myers, E. L.; Aggarwal, V. K. *Angew. Chemie Int. Ed.* **2016**, *55*, 4270.
18. Bonet, A.; Odachowski, M.; Leonori, D.; Essafi, S.; Aggarwal, V. K. *Nat. Chem.* **2014**, *6*, 584.
19. Llaveria, J.; Leonori, D.; Aggarwal, V. K. *J. Am. Chem. Soc.* **2015**, *137*, 10958.
20. Odachowski, M.; Bonet, A.; Essafi, S.; Conti-Ramsden, P.; Harvey, J. N.; Leonori, D.; Aggarwal, V. K. *J. Am. Chem. Soc.* **2016**, *138*, 9521.
21. Wang, Y.; Noble, A.; Sandford, C.; Aggarwal, V. K. *Angew. Chemie Int. Ed.* **2017**, *56*, 1810.
22. Ganesh, V.; Odachowski, M.; Aggarwal, V. K. *Angew. Chemie Int. Ed.* **2017**, *56*, 9752.
23. Aichhorn, S.; Bigler, R.; Myers, E. L.; Aggarwal, V. K. *J. Am. Chem. Soc.* **2017**, *139*, 9519.
24. Wilson, C. M.; Ganesh, V.; Noble, A.; Aggarwal, V. K. *Angew. Chemie Int. Ed.* **2017**, *56*, 16318.
25. Bigler, R.; Aggarwal, V. K. *Angew. Chemie Int. Ed.* **2018**, *57*, 1082.
26. Ganesh, V.; Noble, A.; Aggarwal, V. K. *Org. Lett.* **2018**, *20*, 6144.
27. Mlynarski, S. N.; Karns, A. S.; Morken, J. P. *J. Am. Chem. Soc.* **2012**, *134*, 16449.
28. Edelstein, E.; Grote, A.; Palkowitz, M.; Morken, J. P. *Synlett* **2018**, *29*, 1749.
29. Matteson, D. S.; Mah, R. W. H. *J. Am. Chem. Soc.* **1963**, *85*, 2599.
30. Matteson, D. S.; Majumdar, D. *J. Am. Chem. Soc.* **1980**, *102*, 7588.
31. Matteson, D. S.; Majumdar, D. *Organometallics* **1983**, *2*, 1529.
32. Matteson, D. S.; Ray, R.; Rocks, R. R.; Tsai, D. J. S. *Organometallics* **1983**, *2*, 1536.
33. Matteson, D. S.; Ray, R. *J. Am. Chem. Soc.* **1980**, *102*, 7590.
34. Aggarwal, V. K.; Richardson, J. *Chem. Commun.* **2003**, 2644.
35. Aggarwal, V. K.; Fang, G. Y.; Schmidt, A. T. *J. Am. Chem. Soc.* **2005**, *127*, 1642.
36. Fang, G. Y.; Wallner, O. A.; Blasio, N. Di; Ginesta, X.; Harvey, J. N.; Aggarwal, V. K. *J. Am. Chem. Soc.* **2007**, *129*, 14632.
37. Blakemore, P. R.; Marsden, S. P.; Vater, H. D. *Org. Lett.* **2006**, *8*, 773.
38. Blakemore, P. R.; Burge, M. S. *J. Am. Chem. Soc.* **2007**, *129*, 3068.

39. Hoppe, D.; Carstens, A.; Krámer, T.; Krámer, T. *Angew. Chemie Int. Ed.* **1990**, 29, 1424.
40. Hoppe, D.; Hense, T. *Angew. Chemie Int. Ed.* **1997**, 36, 2282.
41. Hoppe, D.; Hintze, F.; Tebben, P. *Angew. Chemie Int. Ed.* **1990**, 29, 1422.
42. Hoppe, D.; Hintze, F.; Tebben, P.; Paetow, M.; Ahrens, H.; Schwerdtfeger, J.; Sommerfeld, P.; Haller, J.; Guarnieri, W.; Kolczewski, S.; Hense, T.; Hoppe, I. *Pure Appl. Chem.* **1994**, 66, 1479.
43. Besong, G.; Jarowicki, K.; Kocienski, P. J.; Sliwinski, E.; Boyle, F. T. *Org. Biomol. Chem.* **2006**, 4, 2193.
44. Stymiest, J. L.; Dutheuil, G.; Mahmood, A.; Aggarwal, V. K. *Angew. Chemie Int. Ed.* **2007**, 46, 7491.
45. Bagutski, V.; French, R. M.; Aggarwal, V. K. *Angew. Chemie Int. Ed.* **2010**, 49, 5142.
46. Kapeller, D. C.; Hammerschmidt, F. *J. Org. Chem.* **2009**, 74, 2380.
47. Beak, P.; Carter, L. G. *J. Org. Chem.* **1981**, 46, 2363.
48. Larouche-Gauthier, R.; Fletcher, C. J.; Couto, I.; Aggarwal, V. K. *Chem. Commun.* **2011**, 47, 12592.
49. Hoffmann, R. W.; Sander, T.; Brumm, M. *Chem. Ber.* **1992**, 125, 2319.
50. Hoffmann, R. W. *Angew. Chemie Int. Ed.* **1992**, 31, 1124.
51. Hoffmann, R. W.; Kahrs, B. C.; Schiffer, J.; Fleischhauer, J. *J. Chem. Soc. Perkin Trans. 2* **1996**, 2407.
52. Göttlich, R.; Fäcke, T.; Rolle, U.; Hoffmann, R. W. *J. Chem. Soc., Perkin Trans. 2* **1996**, 2059.
53. Göttlich, R.; Schopfer, U.; Stahl, M.; Hoffmann, R. W. *Liebigs Ann.* **1997**, 1997, 1757.
54. Göttlich, R.; Colin Kahrs, B.; Krüger, J.; Hoffmann, R. W. *Chem. Commun.* **1997**, 247.
55. Hoffmann, R. W.; Göttlich, R. *Liebigs Ann.* **1997**, 1997, 2103.
56. Stahl, M.; Schopfer, U. *J. Chem. Soc. Perkin Trans. 2* **1997**, 2, 905.
57. Gil de Oliveira Santos, A.; Klute, W.; Torode, J.; Böhm, V. P. W.; Cabrita, E.; Runsink, J.; Hoffmann, R. W. *New J. Chem.* **1998**, 22, 993.
58. Hoffmann, R. W.; Stahl, M.; Schopfer, U.; Frenking, G. *Chem. - A Eur. J.* **1998**, 4, 559.
59. Hoffmann, R. W.; Stenkamp, D.; Trieselmann, T.; Göttlich, R. *European J. Org. Chem.* **1999**, 1999, 2915.
60. Hoffmann, R. W.; Stenkamp, D. *Tetrahedron* **1999**, 55, 7169.
61. Stenkamp, D.; Hoffmann, R. W.; Göttlich, R. *European J. Org. Chem.* **1999**, 1999, 2929.
62. Hoffmann, R. W.; Kahrs, B. C.; Reiß, P.; Trieselmann, T.; Stiasny, H.-C.; Massa, W. *European J. Org. Chem.* **2001**, 2001, 1857.
63. Hoffmann, R. W.; Menzel, K. *European J. Org. Chem.* **2001**, 2001, 2749.
64. Hoffmann, R. W.; Göttlich, R.; Schopfer, U. *European J. Org. Chem.* **2001**, 2001, 1865.
65. Hoffmann, R. W.; Menzel, K.; Harms, K. *European J. Org. Chem.* **2002**, 2002, 2603.
66. Hoffmann, R. W.; Mas, G.; Brandl, T. *European J. Org. Chem.* **2002**, 2002, 3455.
67. Brandl, T.; Hoffmann, R. W. *European J. Org. Chem.* **2002**, 2002, 2613.
68. Trieselmann, T.; Hoffmann, R. W.; Menzel, K. *European J. Org. Chem.* **2002**, 2002, 1292.
69. Brandl, T.; Hoffmann, R. W. *European J. Org. Chem.* **2004**, 2004, 4373.
70. Tsuzuki, S.; Schafer, L.; Goto, H.; Jemmis, E. D.; Hosoya, H.; Siam, K.; Tanabe, K.; Osawa, E. *J. Am. Chem. Soc.* **1991**, 113, 4665.
71. Abe, A.; Jernigan, R. L.; Flory, P. J. *J. Am. Chem. Soc.* **1966**, 88, 631.
72. Hehre, W. J. In *A Guide to Molecular Mechanics and Quantum Chemical Calculations*; Wavefunction, Inc.: Irvine, USA, 2003.
73. Young, D. In *Computational Chemistry: A Practical Guide for Applying Techniques to Real World Problems*; John Wiley & Sons, Inc.: Canada, 2001.
74. Hill, D. J.; Mio, M. J.; Prince, R. B.; Hughes, T. S.; Moore, J. S. *Chem. Rev.* **2001**, 101, 3893.
75. Cheng, R. P.; Gellman, S. H.; DeGrado, W. F. *Chem. Rev.* **2001**, 101, 3219.
76. Schmuck, C. *Angew. Chemie Int. Ed.* **2003**, 42, 2448.
77. Huc, I. *European J. Org. Chem.* **2004**, 2004, 17.

78. Licini, G.; Prins, L. J.; Scrimin, P. *European J. Org. Chem.* **2005**, 2005, 969.
79. Appella, D. H.; Christianson, L. A.; Karle, I. L.; Powell, D. R.; Gellman, S. H. *J. Am. Chem. Soc.* **1999**, 121, 6206.
80. Jiang, H.; Dolain, C.; Léger, J.-M.; Gornitzka, H.; Huc, I. *J. Am. Chem. Soc.* **2004**, 126, 1034.
81. Dolain, C.; Jiang, H.; Léger, J.-M.; Guionneau, P.; Huc, I. *J. Am. Chem. Soc.* **2005**, 127, 12943.
82. Gillies, E. R.; Dolain, C.; Léger, J.-M.; Huc, I. *J. Org. Chem.* **2006**, 71, 7931.
83. Glättli, A.; Daura, X.; Seebach, D.; van Gunsteren, W. F. *J. Am. Chem. Soc.* **2002**, 124, 12972.
84. Sugiura, H.; Nigorikawa, Y.; Saiki, Y.; Nakamura, K.; Yamaguchi, M. *J. Am. Chem. Soc.* **2004**, 126, 14858.
85. Tanatani, A.; Yokoyama, A.; Azumaya, I.; Takakura, Y.; Mitsui, C.; Shiro, M.; Uchiyama, M.; Muranaka, A.; Kobayashi, N.; Yokozawa, T. *J. Am. Chem. Soc.* **2005**, 127, 8553.
86. Nafie, L. A.; Dukor, R. K.; Freedman, T. B. In *Handbook of Vibrational Spectroscopy, Volume 1*; John Wiley & Sons, Inc.: Chichester, UK, 2002.
87. Stephens, P. J.; Devlin, F. J. *Chirality* **2000**, 12, 172.
88. Freedman, T. B.; Cao, X.; Dukor, R. K.; Nafie, L. A. *Chirality* **2003**, 15, 743.
89. Buffeteau, T.; Ducasse, L.; Brizard, A.; Huc, I.; Oda, R. *J. Phys. Chem. A* **2004**, 108, 4080.
90. Su, C. N.; Keiderling, T. A. *J. Am. Chem. Soc.* **1980**, 102, 511.
91. Polavarapu, P. L.; Ewig, C. S.; Chandramouly, T. *J. Am. Chem. Soc.* **1987**, 109, 7382.
92. Zhang, P.; Polavarapu, P. L. *J. Phys. Chem. A* **2007**, 111, 858.
93. Abbate, S.; Castiglione, F.; Lebon, F.; Longhi, G.; Longo, A.; Mele, A.; Panzeri, W.; Ruggirello, A.; Liveri, V. T. *J. Phys. Chem. B* **2009**, 113, 3024.
94. Feynman, R. P. In *Miniaturization*; Reinhold: New York, USA, 1961.
95. Feynman, R. P. *Eng. Sci.* **1960**, 23, 22.
96. Drexler, K. E. In *Unbounding the Future: The Nanotechnology Revolution*; Morrow: New York, USA, 1991.
97. Drexler, K. E. In *Nanosystems: Molecular Machinery, Manufacturing and Computation*; Wiley Interscience: New York, USA, 1992.
98. Ball, P. In *Designing the Molecular World: Chemistry at the Frontier*; Princeton University Press: Princeton, USA, 1996.
99. Lehn, J.-M. In *Supramolecular Chemistry: Concepts and Perspectives*; VCH Verlagsgesellschaft mbH: Weinheim, Germany, 1995.
100. Ball, P.; Garwin, L. *Nature* **1992**, 355, 761.
101. Sanders, J. K. M. *Angew. Chemie Int. Ed.* **1995**, 34, 2563.
102. Ashton, P. R.; Brown, G. R.; Hayes, W.; Menzer, S.; Philp, D.; Stoddart, J. F.; Williams, D. J. *Adv. Mater.* **1996**, 8, 564.
103. Michl, J.; Sun, Y.-P. *Electronic Structure, Photophysics, and Photochemistry of Polysilanes* 1993; p 131.
104. Vögtle, F. In *Supramolecular Chemistry: An Introduction*; John Wiley & Sons, Ltd.: New York, USA, 1993.
105. Shinkai, S. *Pure Appl. Chem.* **1987**, 59, 425.
106. Willner, I.; Marx, S.; Eichen, Y. *Angew. Chemie Int. Ed.* **1992**, 31, 1243.
107. Junge, D. M.; McGrath, D. V. *Chem. Commun.* **1997**, 857.
108. Jiang, D.-L.; Aida, T. *Nature* **1997**, 388, 454.
109. Archut, A.; Vögtle, F.; De Cola, L.; Azzellini, G. C.; Balzani, V.; Ramanujam, P. S.; Berg, R. H. *Chem. - A Eur. J.* **1998**, 4, 699.
110. Würthner, F.; Rebek, J. *Angew. Chemie Int. Ed.* **1995**, 34, 446.
111. Würthner, F.; Rebek, J. *J. Chem. Soc., Perkin Trans. 2* **1995**, 1727.
112. Tachibana, H.; Nakamura, T.; Matsumoto, M.; Komizu, H.; Manda, E.; Niino, H.; Yabe, A.; Kawabata, Y. *J. Am. Chem. Soc.* **1989**, 111, 3080.
113. Tachibana, H.; Azumi, R.; Nakamura, T.; Matsumoto, M.; Kawabata, Y. *Chem. Lett.* **1992**, 173.

114. Yamazaki, I.; Ohta, N. *Pure Appl. Chem.* **1995**, 67, 209.
115. Tanida, J.; Ichioka, Y. *Appl. Opt.* **1988**, 27, 2926.
116. Ahuja, R. C.; Maack, J.; Tachibana, H. *J. Phys. Chem.* **1995**, 99, 9221.
117. Maack, J.; Ahuja, R. C.; Tachibana, H. *J. Phys. Chem.* **1995**, 99, 9210.
118. Lahav, M.; Ranjit, K. T.; Katz, E.; Willner, I. *Chem. Commun.* **1997**, 259.
119. Bissell, R. A.; Córdova, E.; Kaifer, A. E.; Stoddart, J. F. *Nature* **1994**, 369, 133.
120. Anelli, P. L.; Spencer, N.; Stoddart, J. F. *J. Am. Chem. Soc.* **1991**, 113, 5131.
121. Ashton, P. R.; Pérez-García, L.; Stoddart, J. F.; White, A. J. P.; Williams, D. J. *Angew. Chemie Int. Ed.* **1995**, 34, 571.
122. Livoreil, A.; Dietrich-Buchecker, C. O.; Sauvage, J.-P. *J. Am. Chem. Soc.* **1994**, 116, 9399.
123. Livoreil, A.; Sauvage, J.-P.; Armaroli, N.; Balzani, V.; Flamigni, L.; Ventura, B. *J. Am. Chem. Soc.* **1997**, 119, 12114.
124. Credi, A.; Balzani, V.; Langford, S. J.; Stoddart, J. F. *J. Am. Chem. Soc.* **1997**, 119, 2679.
125. Martínez-Díaz, M.-V.; Spencer, N.; Stoddart, J. F. *Angew. Chemie Int. Ed.* **1997**, 36, 1904.
126. Kelly, T. R.; Bowyer, M. C.; Bhaskar, K. V.; Bebbington, D.; Garcia, A.; Lang, F.; Kim, M. H.; Jette, M. P. *J. Am. Chem. Soc.* **1994**, 116, 3657.
127. Bedard, T. C.; Moore, J. S. *J. Am. Chem. Soc.* **1995**, 117, 10662.
128. Kelly, T. R.; Tellitu, I.; Sestelo, J. P. *Angew. Chemie Int. Ed.* **1997**, 36, 1866.
129. Nagasaki, T.; Tamagaki, S.; Ogino, K. *Chem. Lett.* **1997**, 26, 717.
130. Bissell, R. A.; de Silva, A. P.; Gunaratne, H. Q. N.; Lynch, P. L. M.; Maguire, G. E. M.; Sandanayake, K. R. A. S. *Chem. Soc. Rev.* **1992**, 21, 187.
131. James, T. D.; Samankumara Sandanayake, K. R. A.; Shinkai, S. *Nature* **1995**, 374, 345.
132. Willner, I. *Acc. Chem. Res.* **1997**, 30, 347.
133. Hoch, H. C.; Jelinski, L.; Craighead, H. G. In *Nanofabrication and biosystems : integrating materials science, engineering, and biology*; Cambridge University Press: Cambridge, UK, 1996.
134. Kawai, S. H.; Gilat, S. L.; Lehn, J.-M. *J. Chem. Soc., Chem. Commun.* **1994**, 1011.
135. Gómez-López, M.; Preece, J. A.; Stoddart, J. F. *Nanotechnology* **1996**, 7, 183.
136. Ulman, A. In *An Introduction to Ultrathin Organic Films: from Langmuir-Blodgett to Self-Assembly*; Academic Press: New York, USA, 1991.
137. Ulman, A. *Chem. Rev.* **1996**, 96, 1533.
138. Kaifer, A. E. *Isr. J. Chem.* **1996**, 36, 389.
139. Kumar, A.; Biebuyck, H. A.; Abbott, N. L.; Whitesides, G. M. *J. Am. Chem. Soc.* **1992**, 114, 9188.
140. Prime, K.; Whitesides, G. *Science* **1991**, 252, 1164.
141. Böltau, M.; Walheim, S.; Mlynek, J.; Krausch, G.; Steiner, U. *Nature* **1998**, 391, 877.
142. Ozin, G. A. *Adv. Mater.* **1992**, 4, 612.
143. Schneider, H.-J.; Dürr, H. In *Frontiers in supramolecular organic chemistry and photochemistry*; VCH Verlagsgesellschaft mbH: Weinheim, Germany, 1991.
144. Whitesides, G.; Mathias, J.; Seto, C. *Science* **1991**, 254, 1312.
145. Wagner, R. W.; Brown, P. A.; Johnson, T. E.; Lindsey, J. S. *J. Chem. Soc., Chem. Commun.* **1991**, 1463.
146. Lawrence, D. S.; Jiang, T.; Levett, M. *Chem. Rev.* **1995**, 95, 2229.
147. Philp, D.; Stoddart, J. F. *Angew. Chemie Int. Ed.* **1996**, 35, 1154.
148. Amabilino, D. B.; Stoddart, J. F. *Chem. Rev.* **1995**, 95, 2725.
149. Gibson, H. W.; Bheda, M. C.; Engen, P. T. *Prog. Polym. Sci.* **1994**, 19, 843.
150. Philp, D.; Stoddart, J. F. *Synlett* **1991**, 1991, 445.
151. Whitesides, G. M.; Simanek, E. E.; Mathias, J. P.; Seto, C. T.; Chin, D.; Mammen, M.; Gordon, D. M. *Acc.*

- Chem. Res.* **1995**, 28, 37.
152. Irie, M. In *Photo-reactive materials for ultrahigh density optical memory : MITI research and development program on basic technologies for future industries*; Elsevier: New York, USA, 1994.
 153. Balzani, V.; Scandola, F. In *Supramolecular photochemistry*; Ellis Horwood: New York, USA, 1991.
 154. Carter, F. L.; Siatkowski, R. E.; Wohltjen, H. In *Molecular electronic devices : proceedings of the 3rd International Symposium on Molecular Electronic Devices, Arlington, Virginia, 6-8 October 1986*; Elsevier: New York, USA, 1988.
 155. Feringa, B. L.; Jager, W. F.; de Lange, B. *Tetrahedron* **1993**, 49, 8267.
 156. Willner, I.; Rubin, S. *Angew. Chemie Int. Ed.* **1996**, 35, 367.
 157. Emmelius, M.; Pawlowski, G.; Vollmann, H. W. *Angew. Chemie Int. Ed.* **1989**, 28, 1445.
 158. Dürr, H.; Bouas-Laurent, H. In *Photochromism : molecules and systems*; Elsevier: Amsterdam, Netherlands, 2003.
 159. El'Tsov, A. V. In *Organic Photochromes*; Plenum Press: New York, USA, 2012.
 160. Brown, G. H. In *Photochromism (Techniques of Chemistry)*; John Wiley & Sons Inc.: New York, USA, 1971.
 161. Wasielewski, M. R. *Chem. Rev.* **1992**, 92, 435.
 162. Gosztola, D.; Niemczyk, M. P.; Wasielewski, M. R. *J. Am. Chem. Soc.* **1998**, 120, 5118.
 163. Debreczeny, M. P.; Svec, W. A.; Wasielewski, M. R. *Science* **1996**, 274, 584.
 164. De Poli, M.; Zawodny, W.; Quinonero, O.; Lorch, M.; Webb, S. J.; Clayden, J. *Science* **2016**, 352, 575.
 165. Pauling, L.; Corey, R. B.; Branson, H. R. *Proc. Natl. Acad. Sci.* **1951**, 37, 205.
 166. Watson, J. D.; Crick, F. H. C. *Nature* **1953**, 171, 737.
 167. Natta, G.; Pino, P.; Corradini, P.; Danusso, F.; Mantica, E.; Mazzanti, G.; Moraglio, G. *J. Am. Chem. Soc.* **1955**, 77, 1708.
 168. Yashima, E.; Maeda, K.; Iida, H.; Furusho, Y.; Nagai, K. *Chem. Rev.* **2009**, 109, 6102.
 169. Nishikawa, T.; Nagata, Y.; Sugimoto, M. *ACS Macro Lett.* **2017**, 6, 431.
 170. Shen, Y.; Chen, C.-F. *Chem. Rev.* **2012**, 112, 1463.
 171. Megens, R. P.; Roelfes, G. *Chem. - A Eur. J.* **2011**, 17, 8514.
 172. Miyake, H.; Tsukube, H. *Chem. Soc. Rev.* **2012**, 41, 6977.
 173. Nakano, T.; Okamoto, Y. *Chem. Rev.* **2001**, 101, 4013.
 174. Lv, Z.; Chen, Z.; Shao, K.; Qing, G.; Sun, T. *Polymers* **2016**, 8, 310.
 175. Le Bailly, B. A. F.; Clayden, J. *Chem. Commun.* **2014**, 50, 7949.
 176. De Poli, M.; Byrne, L.; Brown, R. A.; Solà, J.; Castellanos, A.; Boddaert, T.; Wechsel, R.; Beadle, J. D.; Clayden, J. *J. Org. Chem.* **2014**, 79, 4659.
 177. Nagata, Y.; Nishikawa, T.; Sugimoto, M. *ACS Macro Lett.* **2016**, 5, 519.
 178. Yashima, E.; Maeda, K.; Nishimura, T. *Chem. - A Eur. J.* **2004**, 10, 42.
 179. Zhang, D.-W.; Wang, H.; Li, Z.-T. *Macromol. Rapid Commun.* **2017**, 38, 1700179.
 180. Andrews, M. J. I.; Tabor, A. B. *Tetrahedron* **1999**, 55, 11711.
 181. Hunter, L.; Kirsch, P.; Slawin, A. M. Z.; O'Hagan, D. *Angew. Chemie Int. Ed.* **2009**, 48, 5457.
 182. Scarso, A.; Trembleau, L.; Rebek, J. *Angew. Chemie Int. Ed.* **2003**, 42, 5499.
 183. Trembleau, L. *Science* **2003**, 301, 1219.
 184. Hoffmann, R. W. *Angew. Chemie Int. Ed.* **2000**, 39, 2054.
 185. Millán, A.; Grigol Martinez, P. D.; Aggarwal, V. K. *Chem. - A Eur. J.* **2018**, 24, 730.
 186. Pulis, A. P.; Fackler, P.; Aggarwal, V. K. *Angew. Chemie Int. Ed.* **2014**, 53, 4382.
 187. Varela, A.; Garve, L. K. B.; Leonori, D.; Aggarwal, V. K. *Angew. Chemie Int. Ed.* **2017**, 56, 2127.
 188. Wu, J.; Lorenzo, P.; Zhong, S.; Ali, M.; Butts, C. P.; Myers, E. L.; Aggarwal, V. K. *Nature* **2017**, 547, 436.
 189. Leonori, D.; Aggarwal, V. K. *Acc. Chem. Res.* **2014**, 47, 3174.

190. Rasappan, R.; Aggarwal, V. K. *Nat. Chem.* **2014**, *6*, 810.
191. Blair, D. J.; Tanini, D.; Bateman, J. M.; Scott, H. K.; Myers, E. L.; Aggarwal, V. K. *Chem. Sci.* **2017**, *8*, 2898.
192. Morgan, J. B.; Miller, S. P.; Morken, J. P. *J. Am. Chem. Soc.* **2003**, *125*, 8702.
193. Trudeau, S.; Morgan, J. B.; Shrestha, M.; Morken, J. P. *J. Org. Chem.* **2005**, *70*, 9538.
194. Lim, Y.-K.; Lee, K.-S.; Cho, C.-G. *Org. Lett.* **2003**, *5*, 979.
195. Tait, K. M.; Parkinson, J. A.; Bates, S. P.; Ebenezer, W. J.; Jones, A. C. *J. Photochem. Photobiol. A Chem.* **2003**, *154*, 179.
196. Ke, Y.-Z.; Nagata, Y.; Yamada, T.; Suginome, M. *Angew. Chemie Int. Ed.* **2015**, *54*, 9333.
197. Yamamoto, T.; Akai, Y.; Suginome, M. *Angew. Chemie Int. Ed.* **2014**, *53*, 12785.
198. Hu, G.; Chen, W.; Fu, T.; Peng, Z.; Qiao, H.; Gao, Y.; Zhao, Y. *Org. Lett.* **2013**, *15*, 5362.
199. Li, Y.; Das, S.; Zhou, S.; Junge, K.; Beller, M. *J. Am. Chem. Soc.* **2012**, *134*, 9727.
200. Noh, D.; Yoon, S. K.; Won, J.; Lee, J. Y.; Yun, J. *Chem. - An Asian J.* **2011**, *6*, 1967.
201. Sadhu, K. M.; Matteson, D. S. *Organometallics* **1985**, *4*, 1687.
202. Glasspoole, B. W.; Ghazati, K.; Moir, J. W.; Crudden, C. M. *Chem. Commun.* **2012**, *48*, 1230.
203. Mykura, R. C.; Veth, S.; Varela, A.; Dewis, L.; Farndon, J. J.; Myers, E. L.; Aggarwal, V. K. *J. Am. Chem. Soc.* **2018**, *140*, 14677.
204. Essafi, S.; Tomasi, S.; Aggarwal, V. K.; Harvey, J. N. *J. Org. Chem.* **2014**, *79*, 12148.
205. Balieu, S.; Hallett, G. E.; Burns, M.; Bootwicha, T.; Studley, J.; Aggarwal, V. K. *J. Am. Chem. Soc.* **2015**, *137*, 4398.
206. Karplus, M. *J. Am. Chem. Soc.* **1963**, *85*, 2870.
207. Webb, N. J.; Marsden, S. P.; Raw, S. A. *Org. Lett.* **2014**, *16*, 4718.
208. Zhong, S. Ph.D. Dissertation: Combining Computational Modelling, NMR Spectroscopy, and Assembly-Line Synthesis for Studying Molecular Conformations. 2018.
209. Alder, R. W.; Allen, P. R.; Anderson, K. R.; Butts, C. P.; Khosravi, E.; Martín, A.; Maunder, C. M.; Orpen, A. G.; St. Pourçain, C. B. *J. Chem. Soc. Perkin Trans. 2* **1998**, 2083.
210. Alder, R. W.; Maunder, C. M.; Guy Orpen, A. *Tetrahedron Lett.* **1990**, *31*, 6717.
211. Bartoli, G.; Bosco, M.; Locatelli, M.; Marcantoni, E.; Melchiorre, P.; Sambri, L. *Org. Lett.* **2005**, *7*, 427.
212. Hirsch, J. A. Table of Conformational Energies—1967 In *Topics in Stereochemistry, Volume 1*; John Wiley & Sons, Inc.: New York, USA, 1967; p 199.
213. Jensen, F. R.; Bushweller, C. H. Conformational Preferences in Cyclohexanes and Cyclohexenes In *Advances in Alicyclic Chemistry, Volume 3*; Academic Press: New York, 1971; p 139.
214. Fawcett, A. Ph.D. Dissertation: New Developments in Organoboron Incorporation, Homologation and Functionalization. 2018.
215. Lienhard, G. E.; Koehler, K. A. *Biochemistry* **1971**, *10*, 2477.
216. Wolfenden, R. *Acc. Chem. Res.* **1972**, *5*, 10.
217. Antonov, V. K.; Ivanina, T. V.; Ivanova, A. G.; Berezin, I. V.; Levashov, A. V.; Martinek, K. *FEBS Lett.* **1972**, *20*, 37.
218. Philipp, M.; Bender, M. L. *Proc. Natl. Acad. Sci.* **1971**, *68*, 478.
219. Rawn, J. D.; Lienhard, G. E. *Biochemistry* **1974**, *13*, 3124.
220. Bauer, C.-A.; Pettersson, G. *Eur. J. Biochem.* **1974**, *45*, 473.
221. Matthews, D. A.; Alden, R. A.; Birktoft, J. J.; Freer, S. T.; Kraut, J. *J. Biol. Chem.* **1975**, *250*, 7120.
222. Nakatani, H.; Uehara, Y.; Hiromi, K. *J. Biochem.* **1975**, *78*, 611.
223. Trippier, P. C.; McGuigan, C. *MedChemComm* **2010**, *1*, 183.
224. Baker, S. J.; Tomsho, J. W.; Benkovic, S. J. *Chem. Soc. Rev.* **2011**, *40*, 4279.
225. Smoum, R.; Rubinstein, A.; Dembitsky, V. M.; Srebnik, M. *Chem. Rev.* **2012**, *112*, 4156.
226. Powers, J. C.; Harper, J. W. In *Proteinase Inhibitors*; Elsevier: Amstersam, Netherlands, 1986.

227. Hiratake, J.; Oda, J. *Biosci. Biotechnol. Biochem.* **1997**, *61*, 211.
228. Knott, K.; Fishovitz, J.; Thorpe, S. B.; Lee, I.; Santos, W. L. *Org. Biomol. Chem.* **2010**, *8*, 3451.
229. Matteson, D. S.; Sadhu, K. M.; Lienhard, G. E. *J. Am. Chem. Soc.* **1981**, *103*, 5241.
230. Molander, G. A.; Ham, J. *Org. Lett.* **2006**, *8*, 2031.
231. Shiro, T.; Schuhmacher, A.; Jackl, M. K.; Bode, J. W. *Chem. Sci.* **2018**, *9*, 5191.
232. Beenen, M. A.; An, C.; Ellman, J. A. *J. Am. Chem. Soc.* **2008**, *130*, 6910.
233. Buesking, A. W.; Bacauanu, V.; Cai, I.; Ellman, J. A. *J. Org. Chem.* **2014**, *79*, 3671.
234. Wen, K.; Chen, J.; Gao, F.; Bhadury, P. S.; Fan, E.; Sun, Z. *Org. Biomol. Chem.* **2013**, *11*, 6350.
235. Wen, K.; Wang, H.; Chen, J.; Zhang, H.; Cui, X.; Wei, C.; Fan, E.; Sun, Z. *J. Org. Chem.* **2013**, *78*, 3405.
236. Chen, J.; Chen, L.-Y.; Zheng, Y.; Sun, Z. *RSC Adv.* **2014**, *4*, 21131.
237. Zhang, S.-S.; Zhao, Y.-S.; Tian, P.; Lin, G.-Q. *Synlett* **2013**, *24*, 437.
238. Hong, K.; Morken, J. P. *J. Am. Chem. Soc.* **2013**, *135*, 9252.
239. Schwamb, C. B.; Fitzpatrick, K. P.; Brueckner, A. C.; Richardson, H. C.; Cheong, P. H.-Y.; Scheidt, K. A. *J. Am. Chem. Soc.* **2018**, *140*, 10644.
240. Wang, D.; Cao, P.; Wang, B.; Jia, T.; Lou, Y.; Wang, M.; Liao, J. *Org. Lett.* **2015**, *17*, 2420.
241. Mann, G.; John, K. D.; Baker, R. T. *Org. Lett.* **2000**, *2*, 2105.
242. Hu, N.; Zhao, G.; Zhang, Y.; Liu, X.; Li, G.; Tang, W. *J. Am. Chem. Soc.* **2015**, *137*, 6746.
243. López, A.; Clark, T. B.; Parra, A.; Tortosa, M. *Org. Lett.* **2017**, *19*, 6272.
244. Chen, L.; Zou, X.; Zhao, H.; Xu, S. *Org. Lett.* **2017**, *19*, 3676.
245. Nishikawa, D.; Hirano, K.; Miura, M. *J. Am. Chem. Soc.* **2015**, *137*, 15620.
246. Okada, K.; Okamoto, K.; Oda, M. *J. Am. Chem. Soc.* **1988**, *110*, 8736.
247. Okada, K.; Okamoto, K.; Morita, N.; Okubo, K.; Oda, M. *J. Am. Chem. Soc.* **1991**, *113*, 9401.
248. Okada, K.; Okubo, K.; Morita, N.; Oda, M. *Tetrahedron Lett.* **1992**, *33*, 7377.
249. Okada, K.; Okubo, K.; Morita, N.; Oda, M. *Chem. Lett.* **1993**, *22*, 2021.
250. Murarka, S. *Adv. Synth. Catal.* **2018**, *360*, 1735.
251. Wang, J.; Qin, T.; Chen, T.-G.; Wimmer, L.; Edwards, J. T.; Cornella, J.; Vokits, B.; Shaw, S. A.; Baran, P. S. *Angew. Chemie Int. Ed.* **2016**, *55*, 9676.
252. Yasu, Y.; Koike, T.; Akita, M. *Adv. Synth. Catal.* **2012**, *354*, 3414.
253. Tellis, J. C.; Kelly, C. B.; Primer, D. N.; Jouffroy, M.; Patel, N. R.; Molander, G. A. *Acc. Chem. Res.* **2016**, *49*, 1429.
254. Lima, F.; Kabeshov, M. A.; Tran, D. N.; Battilocchio, C.; Sedelmeier, J.; Sedelmeier, G.; Schenkel, B.; Ley, S. V. *Angew. Chemie Int. Ed.* **2016**, *55*, 14085.
255. Zhang, L.; Jiao, L. *J. Am. Chem. Soc.* **2017**, *139*, 607.
256. Zhang, L.; Jiao, L. *Chem. Sci.* **2018**, *9*, 2711.
257. Jiang, M.; Yang, H.; Fu, H. *Org. Lett.* **2016**, *18*, 5248.
258. Kanaoka, Y. *Acc. Chem. Res.* **1978**, *11*, 407.
259. Yoon, U. C.; Mariano, P. S. *Acc. Chem. Res.* **2001**, *34*, 523.
260. Oelgemöller, M.; Griesbeck, A. G. *J. Photochem. Photobiol. C Photochem. Rev.* **2002**, *3*, 109.
261. Jin, Y.; Yang, H.; Fu, H. *Chem. Commun.* **2016**, *52*, 12909.
262. Foster, R. *J. Phys. Chem.* **1980**, *84*, 2135.
263. Rosokha, S. V.; Kochi, J. K. *Acc. Chem. Res.* **2008**, *41*, 641.
264. Lima, C. G. S.; de M. Lima, T.; Duarte, M.; Jurberg, I. D.; Paixão, M. W. *ACS Catal.* **2016**, *6*, 1389.
265. Davidson, R. S.; Lewis, A. *J. Chem. Soc., Perkin Trans. 2* **1979**, 900.
266. Yan, G.; Huang, D.; Wu, X. *Adv. Synth. Catal.* **2018**, *360*, 1040.

267. Xu, L. *European J. Org. Chem.* **2018**, 2018, 3884.
268. Li, C.; Wang, J.; Barton, L. M.; Yu, S.; Tian, M.; Peters, D. S.; Kumar, M.; Yu, A. W.; Johnson, K. A.; Chatterjee, A. K.; Yan, M.; Baran, P. S. *Science* **2017**, 356, 1045.
269. Wang, J.; Shang, M.; Lundberg, H.; Feu, K. S.; Hecker, S. J.; Qin, T.; Blackmond, D. G.; Baran, P. S. *ACS Catal.* **2018**, 8, 9537.
270. Hu, D.; Wang, L.; Li, P. *Org. Lett.* **2017**, 19, 2770.
271. Candish, L.; Teders, M.; Glorius, F. *J. Am. Chem. Soc.* **2017**, 139, 7440.
272. Cheng, W.-M.; Shang, R.; Zhao, B.; Xing, W.-L.; Fu, Y. *Org. Lett.* **2017**, 19, 4291.
273. Sugamoto, K.; Matsushita, Y.-I.; Kameda, Y.-H.; Suzuki, M.; Matsui, T. *Synth. Commun.* **2005**, 35, 67.
274. Lima, F.; Sharma, U. K.; Grunenber, L.; Saha, D.; Johannsen, S.; Sedelmeier, J.; Van der Eycken, E. V.; Ley, S. V. *Angew. Chemie Int. Ed.* **2017**, 56, 15136.
275. Huang, H.; Jia, K.; Chen, Y. *Angew. Chemie Int. Ed.* **2015**, 54, 1881.
276. Iinuma, M.; Moriyama, K.; Togo, H. *Synlett* **2012**, 23, 2663.
277. Matoušek, V.; Pietrasiak, E.; Schwenk, R.; Togni, A. *J. Org. Chem.* **2013**, 78, 6763.
278. Mohamadi, F.; Richards, N. G. J.; Guida, W. C.; Liskamp, R.; Lipton, M.; Caufield, C.; Chang, G.; Hendrickson, T.; Still, W. C. *J. Comput. Chem.* **1990**, 11, 440.
279. Maestro, version 9.2, Schrödinger, LLC, New York, USA, 2011.
280. Gaussian 09, Revision D.01, Frisch, M. J.; Trucks, G. W.; Schlegel, H. B.; Scuseria, G. E.; M. A. Robb, J. R. C.; G. Scalmani, V. B.; Mennucci, B.; Petersson, G. A.; Nakatsuji, H.; Caricato, M. et al., Gaussian, Inc., Wallingford, USA, 2009.
281. Pangborn, A. B.; Giardello, M. A.; Grubbs, R. H.; Rosen, R. K.; Timmers, F. J. *Organometallics* **1996**, 15, 1518.
282. Nikolic, N. A.; Beak, P. *Org. Synth.* **1997**, 74, 23.
283. Burchat, A. F.; Chong, J. M.; Nielsen, N. J. *Organomet. Chem.* **1997**, 542, 281.
284. Bruker, SAINT+ v8.38A Integration Engine, Data Reduction Software, Bruker Analytical X-ray Instruments Inc., Madison, USA, 2015.
285. Bruker, SADABS, Bruker AXS area detector scaling and absorption correction, Bruker Analytical X-ray Instruments Inc., Madison, USA, 2001.
286. Palatinus, L.; Chapuis, G. *J. Appl. Crystallogr.* **2007**, 40, 786.
287. Palatinus, L.; Prathapa, S. J.; van Smaalen, S. *J. Appl. Crystallogr.* **2012**, 45, 575.
288. Sheldrick, G. M. *Acta Crystallogr. Sect. A Found. Crystallogr.* **2008**, 64, 112.
289. Sheldrick, G. M. *Acta Crystallogr. Sect. A Found. Adv.* **2015**, 71, 3.
290. Dolomanov, O. V.; Bourhis, L. J.; Gildea, R. J.; Howard, J. A. K.; Puschmann, H. *J. Appl. Crystallogr.* **2009**, 42, 339.
291. Luo, A.-Y.; Bao, Y.; Cheng, X.-F.; Wang, X.-S. *Synthesis.* **2017**, 49, 3962.
292. Brondani, P. B.; Dudek, H.; Reis, J. S.; Fraaije, M. W.; Andrade, L. H. *Tetrahedron: Asymmetry* **2012**, 23, 703.
293. Bose, S. K.; Brand, S.; Omereghe, H. O.; Haehnel, M.; Maier, J.; Bringmann, G.; Marder, T. B. *ACS Catal.* **2016**, 6, 8332.
294. Beckendorf, S.; Asmus, S.; Mück-Lichtenfeld, C.; García Mancheño, O. *Chem. - A Eur. J.* **2013**, 19, 1581.
295. Yang, R.-F.; Huang, P.-Q. *Chem. - A Eur. J.* **2010**, 16, 10319.
296. Chankeshwara, S. V.; Chakraborti, A. K. *Org. Lett.* **2006**, 8, 3259.
297. Lebel, H.; Huard, K. *Org. Lett.* **2007**, 9, 639.
298. Bi, N.-M.; Ren, M.-G.; Song, Q.-H. *Synth. Commun.* **2010**, 40, 2617.
299. Huy, P. H.; Koskinen, A. M. P. *Org. Lett.* **2013**, 15, 5178.
300. Wiles, C.; Watts, P.; Haswell, S. J.; Pombo-Villar, E. *Tetrahedron* **2003**, 59, 10173.
301. Gunnarsson, K.; Ragnarsson, U.; Halme, M. H.; Lopenen, J. M.; Euranto, E. K.; Pettersson, T. *Acta Chem.*

- Scand.* **1990**, *44*, 944.
302. Gunnarsson, K.; Grehn, L.; Ragnarsson, U. *Angew. Chemie* **1988**, *100*, 411.
303. Thalluri, K.; Nadimpally, K. C.; Chakravarty, M. P.; Paul, A.; Mandal, B. *Adv. Synth. Catal.* **2013**, *355*, 448.
304. Dutheuil, G.; Webster, M. P.; Worthington, P. A.; Aggarwal, V. K. *Angew. Chemie Int. Ed.* **2009**, *48*, 6317.
305. Zhang, S.; Fu, X.; Fu, S. *Tetrahedron Lett.* **2009**, *50*, 1173.
306. Watts, J.; Luu, L.; McKee, V.; Carey, E.; Kelleher, F. *Adv. Synth. Catal.* **2012**, *354*, 1035.
307. Liégault, B.; Tang, X.; Bruneau, C.; Renaud, J.-L. *European J. Org. Chem.* **2008**, *2008*, 934.

